BioMed Research International

Prooxidant Mechanisms in Toxicology

Guest Editors: Afaf K. El-Ansary, Malak Kotb, Maha Zaki Rizk, and Nikhat J. Siddiqi

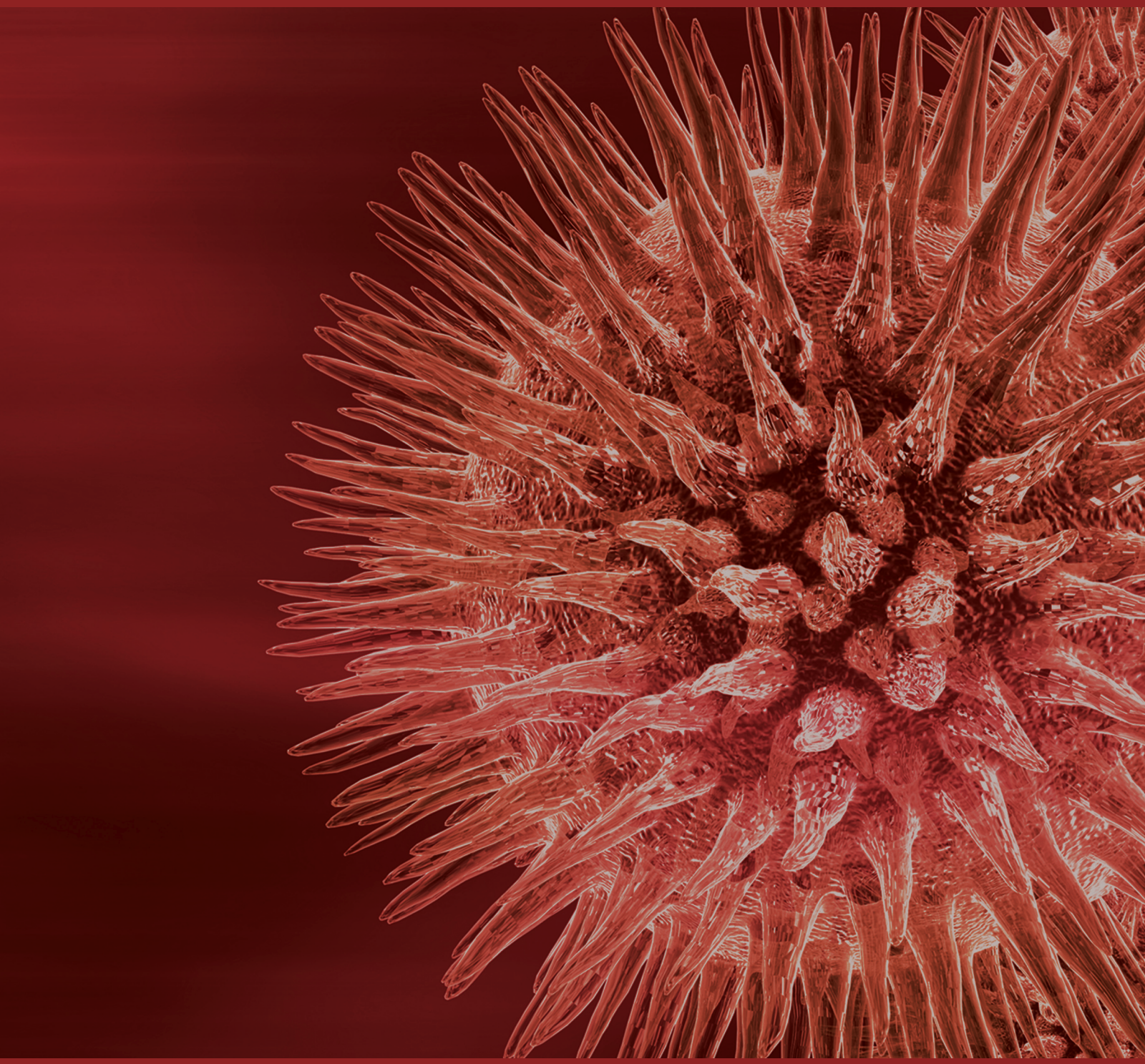

Prooxidant Mechanisms in Toxicology

BioMed Research International

Prooxidant Mechanisms in Toxicology

Guest Editors: Afaf K. El-Ansary, Malak Kotb,
Maha Zaki Rizk, and Nikhat J. Siddiqi

Contents

Hindawi Publishing Corporation
BioMed Research International
Volume 2014, Article ID 308625, 2 pages
http://dx.doi.org/10.1155/2014/308625

Editorial

Prooxidant Mechanisms in Toxicology

Afaf K. El-Ansary,[1] Malak Kotb,[2] Maha Zaki Rizk,[3] and Nikhat J. Siddiqi[1]

[1] *Biochemistry Department, College of Science, King Saud University, P.O. Box 22452, Riyadh 11495, Saudi Arabia*
[2] *Department of Molecular Genetics, Biochemistry and Microbiology, University of Cincinnati College of Medicine, Cincinnati, OH, USA*
[3] *Therapeutic Chemistry Department, National Research Center, Dokki, Cairo, Egypt*

Correspondence should be addressed to Nikhat J. Siddiqi; niksiddiqi@gmail.com

Received 20 January 2014; Accepted 20 January 2014; Published 20 March 2014

Oxidative stress is an important aspect of toxicology and therefore of considerable interest. It can be traced back to 1954 when Gerschman et al. propounded the free radical theory which for the first time implicated partially reduced forms of oxygen in its toxic mechanism [1]. This was followed by Harman in 1956 proposing the concept of free radicals playing a role in the ageing process [2]. The discovery of superoxide dismutase by McCord and Fridovich in 1969 [3] was a second landmark in the role of free radicals in biological systems [4]. The third era of free radicals in biological systems dates back to 1977 when Mittal and Murad [5] provided evidence that the hydroxyl radicals, $^{\bullet}$OH, stimulate activation of guanylate cyclase and formation of the "second messenger" cyclic guanosine monophosphate [4]. Since then a large body of evidence indicates that living systems not only generate free radicals but also have developed mechanisms for simultaneous coexistence and optimal use of free radicals to their advantage. The cellular defenses include low molecular weight free radical scavengers such as reduced glutathione, α-tocopherol, thioredoxins, and ascorbic acid, as well as enzymatic defenses such as superoxide dismutase, catalase, and glutathione peroxidase. Biological sources of free radicals include mitochondrial electron transport chain, enzymes like cytochrome P450, xanthine oxidase, and phagocytosis. Reactive oxygen species (ROS) and reactive nitrogen species (RNS) are well known for playing a dual role as both deleterious and beneficial species, since they can be either harmful or beneficial to living systems [4]. Beneficial effects of ROS occuring at low/moderate concentrations involve physiological roles in cellular responses to anoxia, in defense against infectious agents and in the function of a number of cellular signaling systems. One further beneficial example of ROS at low/moderate concentrations is the induction of a mitogenic response [4]. The harmful effect of free radicals causing potential biological damage is termed oxidative stress and nitrosative stress [4]. This occurs in biological systems when there is an overproduction of ROS/RNS on one hand and a deficiency of enzymatic and nonenzymatic antioxidants on the other hand. Therefore oxidative stress represents a disturbance in the equilibrium status of prooxidant/antioxidant reactions in living organisms. Excess of ROS can damage cellular lipids, proteins, nucleic acids, and other macromolecules inhibiting their normal functions.

In addition to disease states, oxidative stress has been implicated in the mechanisms of drug-induced toxicity [6], chemical toxicity [7], and more recently in nanoparticles-induced toxicity. Metals like iron, copper, chromium, vanadium, and cobalt undergo redox-cycling reactions and thus participate in free radical generation. Other metals like mercury, cadmium, and nickel are toxic by their ability to deplete glutathione and bind to sulfhydryl groups of proteins [8]. Toxicants cause tissue damage via diverse mechanisms, many of which involve activation of cell survival and apoptotic pathways. One of the key areas of recent interest is the role that oxidative stress and nitrative stress play in mediating the response to toxicants via this cytotoxic pathway [9]. However the question whether uncontrolled formation of ROS is a primary cause or a downstream consequence of the pathological process remains to be answered [4]. Therefore in this special issue an attempt has been made to include reviews and research papers which update our knowledge about the role of free radicals in the toxicological processes

and identify gaps in knowledge which would lead to a better understanding of toxicological pathogenesis.

Afaf K. El-Ansary
Malak Kotb
Maha Zaki Rizk
Nikhat J. Siddiqi

References

[1] R. Gerschman, D. L. Gilbert, S. W. Nye, P. Dwyer, and W. O. Fenn, "Oxygen poisoning and X-irradiation: a mechanism in common," *Science*, vol. 119, no. 3097, pp. 623–626, 1954.

[2] D. Harman, "Aging: a theory based on free radical and radiation chemistry," *Journal of Gerontology*, vol. 11, no. 3, pp. 298–300, 1956.

[3] J. M. McCord and I. Fridovich, "Superoxide dismutase. An enzymic function for erythrocuprein (hemocuprein)," *Journal of Biological Chemistry*, vol. 244, no. 22, pp. 6049–6055, 1969.

[4] M. Valko, D. Leibfritz, J. Moncol, M. T. D. Cronin, M. Mazur, and J. Telser, "Free radicals and antioxidants in normal physiological functions and human disease," *International Journal of Biochemistry and Cell Biology*, vol. 39, no. 1, pp. 44–84, 2007.

[5] C. K. Mittal and F. Murad, "Activation of guanylate cyclase by superoxide dismutase and hydroxyl radical: a physiological regulator of guanosine 3′,5′-monophosphate formation," *Proceedings of the National Academy of Sciences of the United States of America*, vol. 74, no. 10, pp. 4360–4364, 1977.

[6] D. G. Deavall, E. A. Martin, J. M. Horner, and R. Roberts, "Drug-induced oxidative stress and toxicity," *Journal of Toxicology*, vol. 2012, Article ID 645460, 13 pages, 2012.

[7] K. Rashid, K. Sinha, and P. C. Sil, "An update on oxidative stress-mediated organ pathophysiology," *Food and Chemical Toxicology*, vol. 62, pp. 584–600, 2013.

[8] M. Valko, H. Morris, and M. T. D. Cronin, "Metals, toxicity and oxidative stress," *Current Medicinal Chemistry*, vol. 12, no. 10, pp. 1161–1208, 2005.

[9] R. A. Roberts, D. L. Laskin, C. V. Smith et al., "Nitrative and oxidative stress in toxicology and disease," *Toxicological Sciences*, vol. 112, no. 1, pp. 4–16, 2009.

Hindawi Publishing Corporation
BioMed Research International
Volume 2014, Article ID 878062, 14 pages
http://dx.doi.org/10.1155/2014/878062

Research Article

Prooxidant Effects of Verbascoside, a Bioactive Compound from Olive Oil Mill Wastewater, on *In Vitro* Developmental Potential of Ovine Prepubertal Oocytes and Bioenergetic/Oxidative Stress Parameters of Fresh and Vitrified Oocytes

M. E. Dell'Aquila,[1] L. Bogliolo,[2] R. Russo,[1] N. A. Martino,[1] M. Filioli Uranio,[1] F. Ariu,[2] F. Amati,[3] A. M. Sardanelli,[3,4] V. Linsalata,[5] M. G. Ferruzzi,[6] A. Cardinali,[5] and F. Minervini[5]

[1] *Section of Veterinary Clinics and Animal Production, Department of Emergency and Organ Transplantation (DETO), University of Bari "Aldo Moro", Strada Provincial Casamassima Km 3, Valenzano, 70010 Bari, Italy*
[2] *Obstetric and Gynecological Section, Department of Veterinary Medicine, Via Vienna 2, 07100 Sassari, Italy*
[3] *Department of Basic Medical Sciences, Neurosciences and Sense Organs, University of Bari "Aldo Moro", Piazza Giulio Cesare, 70124 Bari, Italy*
[4] *Institute of Translational Pharmacology (IFT), National Research Council (CNR), Via Fosso del Cavaliere No. 100, 00133 Rome, Italy*
[5] *Institute of Sciences of Food Production (ISPA), National Research Council (CNR), Via G. Amendola 122/O, 70126 Bari, Italy*
[6] *Department of Food Science, 745 Agriculture Mall Drive, West Lafayette, IN 47907, USA*

Correspondence should be addressed to M. E. Dell'Aquila; mariaelena.dellaquila@uniba.it

Received 10 June 2013; Revised 3 December 2013; Accepted 8 December 2013; Published 25 February 2014

Academic Editor: Maha Zaki Rizk

Verbascoside (VB) is a bioactive polyphenol from olive oil mill wastewater with known antioxidant activity. Oxidative stress is an emerging problem in assisted reproductive technology (ART). Juvenile ART is a promising topic because, in farm animals, it reduces the generation gap and, in human reproductive medicine, it helps to overcome premature ovarian failure. The aim of this study was to test the effects of VB on the developmental competence of ovine prepubertal oocytes and the bioenergetic/oxidative stress status of fresh and vitrified oocytes. In fresh oocytes, VB exerted prooxidant short-term effects, that is, catalase activity increase and uncoupled increases of mitochondria and reactive oxygen species (ROS) fluorescence signals, and long-term effects, that is, reduced blastocyst formation rate. In vitrified oocytes, VB increased ROS levels. Prooxidant VB effects in ovine prepubertal oocytes could be related to higher VB accumulation, which was found as almost one thousand times higher than that reported in other cell systems in previous studies. Also, long exposure times of oocytes to VB, throughout the duration of *in vitro* maturation culture, may have contributed to significant increase of oocyte oxidation. Further studies are needed to identify lower concentrations and/or shorter exposure times to figure out VB antioxidant effects in juvenile ARTs.

1. Introduction

Verbascoside (VB) or acteoside is a phenylpropanoid glycoside structurally characterized by the caffeic acid linked by a β-(D)-glucopyranoside to 4,5-hydroxyphenylethanol (hydroxytyrosol) bound through ester and glycosidic links, with a rhamnose in sequence (1–3) to the glucose molecule. Verbascoside can be extracted, as other phenolic compounds, from primary plants, such as olives, but it is also present in a good amount in olive oil mill wastewater (OMWW), a phytotoxic material discarded during olive oil production [1]. For long time, OMWW has been regarded as a hazardous waste with negative impact on the environment and an economic burden on olive oil industry. However, this view has recently changed to recognise OMWW as a potential low cost starting material rich in bioactive compounds, particularly phenolic

compounds, which can be used as natural antioxidants in various systems [2]. Anti-inflammatory activity of VB has also been demonstrated by *in vitro* tests performed on cell cultures of primary human keratinocytes [3], on the inflammatory bowel disease in a mouse model [4], and on glioma cell line (G6) [5]. Other studies demonstrate that VB prevents reactive oxygen species (ROS) related damages in different ways, such as by interfering with initial ROS generating reactions, by scavenging the free oxygen molecules required to begin ROS production, by chelating metals that speed up oxidative processes, and by inducing glutathione transferase (GST) activity [6, 7]. In a recent study, VB antioxidant activity has been evidenced by using two different bioassays: a cell-free system, based on *in vitro* copper (Cu^+) induced low density lipoproteins (LDL) peroxidation, and an *in vitro* cultured cell system (HT-29 intestinal cell line), based on the observation of VB effects on intracellular ROS levels [2].

Oxidative stress occurs if disequilibrium between ROS production and the antioxidative capacity of the cell takes place [8]. Reactive oxygen species, such as superoxide anion (O_2^-) inactivated by the superoxide dismutase (SOD), hydrogen peroxide (H_2O_2) inactivated by catalase (CAT), and hydroxyl radical (OH^-) inactivated by glutathione peroxidase (GPX), are oxygen-derived molecules which have the ability to react with any molecule and modify it oxidatively, resulting in structural and functional alterations. They are not just damaging by-products of respiration but, at low concentration, are also important molecules for cell signalling within intracellular compartments [9]. Reactive oxygen species have also been implicated in the aetiology of some forms of female infertility [10]. The effects of ROS on oocytes can be clearly evidenced in assisted reproductive techniques (ARTS) setting, due to the reduction or lack in the culture environment of physiological defence mechanisms available in the female reproductive tract, such as the follicular and oviductal fluids and cumulus oophorus matrix [11].

A major source for ROS production is the mitochondrion, in which they are produced during oxidative phosphorylation [12–14]. Mitochondria are essential organelles in all eukaryotic cell systems, as the powerhouse to provide ATP for a multitude of cellular processes. They are the hub of metabolic pathways, primary sources of ROS, regulators of apoptosis as well as signal transduction regulators, and buffers of intracellular calcium [15, 16]. Increasing evidences show the essential role of mitochondria as determinants for developmental competence for human and mammalian oocytes [17–19]. Mitochondrial (mt) dysfunctions or abnormalities may compromise developmental processes, by inducing chromosomal segregation disorders, maturation and fertilization failures, or embryonic cell fragmentation resulting in mitochondria-driven apoptosis. Mitochondrial distribution and activity and oxidative stress status have been analyzed by confocal laser scanning microscopy (CLSM) in oocytes of several species [20].

In vitro embryo production (IVP) using oocytes derived from prepubertal subjects in conjunction with *in vitro* embryo transfer, termed as juvenile *in vitro* embryo transfer (JIVET), is pursued with the aim of increasing the rate of genetic gain through a reduction of the generation gap [21, 22]. Moreover, this technology could be employed in human ART to preserve female fertility of young adolescent or paediatric premenarcheal patients affected by cancer or by different forms of premature ovarian failure [23–25]. A widely used animal model for the JIVET research field is the ovine species, but despite considerable research and great interest in this technology, the efficiency of JIVET remains low mainly due to reduced meiotic and developmental competence of prepubertal oocytes [22, 26]. In addition to biological concerns, JIVET technology has the need of oocyte cryopreservation which still strictly affects prepubertal oocyte fertilization and developmental competence. Among cryopreservation procedures, vitrification, that is, the solidification of a solution at low temperature, a process achieved by a combination of a high concentration of cryoprotectants and an extremely high cooling rate, is an alternative approach to slow freezing, because it avoids the formation of ice crystals in the intracellular and extracellular spaces [27–31]. Few papers have been published to date on vitrification of prepubertal farm animal oocytes [32–34] as well as in human pediatric oocytes [35]. Also, few studies on mt bioenergetic potential of fresh or vitrified prepubertal oocytes have been reported in farm animals to date [36, 37] but no studies in humans. Lastly, no data on oxidative stress parameters of prepubertal oocytes are available in the literature in any species. In this context, studies aimed to evaluate the potentially antioxidant activity of natural bioactive compounds, such as phenolic compounds and polyphenols, present in plant-derived by products would be beneficial to improve cryopreservation and *in vitro* culture protocols of prepubertal oocytes.

The aim of the present study was to test the effects of VB, added during *in vitro* maturation (IVM) culture, on oocyte maturation, cleavage, and blastocyst formation rates of fresh oocytes and on bioenergetic/oxidative status of fresh and vitrified oocytes. Moreover, the stability of VB in the IVM culture system and its absorptive potential by the oocyte-cumulus complex (OCC) were also assessed.

2. Materials and Methods

All chemicals were purchased from Sigma-Aldrich (Milano, Italy) unless otherwise indicated.

2.1. Verbascoside Extraction and Purification and HPLC Analysis. Verbascoside was recovered from OMWW following the protocol described by Cardinali et al. [1]. Verbascoside was purified by low-pressure gel filtration chromatography on a Sephadex LH-20 column (40 cm × 1.6 cm, Pharmacia) and quantified by High Performance Liquid Chromatography with diode array detection (HPLC-DAD) analysis. Analytical-scale HPLC analyses of VB were performed using a Thermo Scientific HPLC Spectra System equipped with a P2000 gradient pump, an SCM1000 vacuum membrane degasser, a UV6000LP diode array UV-VIS detector, an AS3000 autosampler, and ThermoQuest software. The ChromQuest Chromatography data system 4.1 version was used for spectra and data processing. For the HPLC analysis, an analytical Phenomenex (Torrance, CA) Luna C18 (5 μm)

column (4.6 × 250 mm) was used throughout this work. The solvent system consisted of (A) methanol and (B) acetic acid/water (5 : 95, v/v). The elution profile was 0–25 min 15–40% A in B (linear), 25–30 min 40% A in B (isocratic), 30–45 min 40–63% A in B (linear), 45–47 min 63% A in B (isocratic), and 47–51 min 63–100% A in B (linear). The flow rate was 1 mL/min. Samples of 25 μL were applied to the column by means of a 25 μL loop valve.

2.2. Oocyte Collection. Ovaries from juvenile (less than 6 months of age) sheep, recovered at two local slaughterhouses, located at a maximum distance of 20 km (30 min) from the laboratory, were processed by the slicing procedure [38]. Only OCCs with intact cumulus cells layers and a homogeneous cytoplasm were selected.

2.3. Oocyte In Vitro Maturation. In vitro maturation was performed following the procedures currently in use in the two laboratories (Bari and Sassari). Experiments performed in Sassari aimed to assess the effect of VB exposure during IVM on oocyte nuclear maturation, cleavage and blastocyst developmental rates and on the viability of vitrified/warmed metaphase II (MII) oocytes. Oocytes were cultured in the conditions described by Bogliolo et al. (Medium 1; [39]). *In vitro* maturation was performed in TCM-199, buffered with 249 mM sodium bicarbonate and supplemented with 1.8 μM sodium pyruvate, 10% Oestrus Sheep Serum (OSS), 0.1 IU/mL FSH, 0.1 IU/mL LH, 100 μM cysteamine, 0.1 g/L penicillin, and 0.1 g/L streptomycin. Oocyte-cumulus complexes were cultured in four-well Petri dishes (Nunclon; Nalge Nunc International, Roskilde, Denmark) covered with 300 μL preequilibrated mineral oil for 24 h under 5% CO_2 in air at 38.5°C. Experiments conducted in Bari aimed to perform confocal microscopy and biochemical analyses of bioenergetic/oxidative status of fresh and vitrified/warmed MII oocytes exposed to VB during IVM culture and to perform the stability and uptake assays. Oocytes were cultured as reported by Martino et al. [40] with some modifications (Medium 2). Medium TCM-199 with Earle's salts, buffered with 4.43 mM 4-(2-hydroxyethyl)-1-piperazineethanesulfonic acid (HEPES) and 33.9 mM sodium bicarbonate and supplemented with 0.1 g/L L-glutamine, 2 mM sodium pyruvate, 2.92 mM calcium-L-lactate pentahydrate (Fluka 21175; Serva Feinbiochem), 50 μg/mL gentamicin, 10% (v/v) Fetal Calf Serum (FCS), 10 μg/mL ovine FSH and 20 μg/mL ovine LH, and 1 μg/mL 17 beta estradiol was used. Oocyte-cumulus complexes were placed in 400 μL of medium/well of a four-well dish (Nunc Intermed, Roskilde, Denmark) covered with preequilibrated lightweight paraffin oil and cultured for 24 h at 38.5°C under 5% CO_2 in air. After IVM culture, oocytes underwent cumulus and corona cells removal by incubation in TCM-199 with 20% FCS containing 80 IU hyaluronidase/mL and aspiration in and out of finely drawn glass pipettes. Verbascoside stock solution (100 μM) was prepared on the day of use by dissolving VB in distilled water and added in the maturation medium for the whole duration of IVM culture at three increasing concentrations (1.03, 2.06, and 4.11 μM) which were reported as being effective as ROS scavenger [2].

2.4. Oocyte Vitrification. Oocyte vitrification was performed with the method of minimum essential volume (MEV), as described by Bogliolo et al. [41]. Briefly, groups of five MII oocytes were initially equilibrated at 38.5°C for 1 min in holding medium (HM) consisting of 20 mM HEPES-buffered TCM-199 supplemented with 20% (v/v) FCS. After equilibration, the oocytes were incubated in 10% (v/v) ethylene glycol (EG) + 10% (v/v) dimethylsulfoxide (DMSO) in HM for 30 sec and then transferred to 20% (v/v) EG and 20% (v/v) DMSO and 0.25 M sucrose in HM for 20 s. The oocytes were then loaded on cryotops (Kitazato Ltd., Tokyo, Japan) and immediately plunged into liquid nitrogen (LN_2) for storage. For warming, cryotops were directly inserted in HM supplemented with 1.25 M sucrose for 1 min. Oocytes were transferred into HM at decreasing sucrose concentrations (0.62 M and 0.31 M) and then washed in HM. Warmed oocytes were cultured for 1 h in TCM-199 supplemented with 10% OSS and their viability was assessed by observation under a Nikon SMZ 1500 stereomicroscope (60–110x magnification).

2.5. In Vitro Fertilization (IVF) and In Vitro Embryo Development. As described by Berlinguer et al. [42], *in vitro* matured oocytes were fertilized in Synthetic Oviductal Fluid (SOF, [43]) + 2% OSS + 1 μg/mL heparin + 1 μg/mL hypotaurine for 22 h at 38.5°C and under a 5% CO_2, 5% O_2, and 90% N_2 atmosphere in four-well Petri dishes with frozen-thawed spermatozoa selected by swim-up technique (1×10^6 spermatozoa/mL^{-1}). Presumptive zygotes were cultured for 8 days in four-well Petri dishes in SOF + essential and nonessential amino acids at oviductal concentration [44] + 0.4% Bovine Serum Albumin (BSA) under mineral oil, in maximum humidified atmosphere with 5% CO_2, 5% O_2, and 90% N_2 at 38.5°C.

2.6. Nuclear Chromatin Evaluation of Oocytes and Embryos. To evaluate nuclear chromatin, at the end of IVM and IVP, oocytes and embryos were stained with 2.5 μg/mL Hoechst 33258 in 3 : 1 (v/v) glycerol/PBS and mounted on microscope slides covered with cover slips, sealed with nail polish, and kept at 4°C in the dark until observation. Oocytes were evaluated in relation to their meiotic stage under an epifluorescence microscope (Nikon Eclipse 600, 400x magnification) equipped with the B-2 A (346 nm excitation/460 nm emission) filter, as the germinal vesicle (GV), metaphase to telophase I (MI to TI), MII with 1st polar body (PB) extruded and degenerated [45]. Embryos were classified as normal when the presence of a regular shaped nucleus inside each blastomere was observed [39, 46].

2.7. Oocyte Mitochondria and ROS Staining. After IVM, additional oocytes showing the 1st PB extruded (MII stage oocytes) were washed three times in PBS with 3% BSA and incubated for 30 min in the same medium containing 280 nM MitoTracker Orange CMTM Ros (Molecular Probes M-7510, Oregon, USA) at 38.5°C under 5% CO_2 [20, 40, 47]. The cell-permeant probe contains a thiol-reactive chloromethyl moiety. Once the MitoTracker probe accumulates in the

mitochondria, it can react with accessible thiol groups on peptides and proteins to form an aldehyde-fixable conjugate. This cell-permeant probe is readily sequestered only by active mitochondria [48, 49]. The organelle specificity of the probe was assessed, as reported by Valentini et al. [50], in control oocytes which were imaged after incubation in MitoTracker Orange and further incubation for 5 min in the presence of 5 μM of the mt membrane potential (Delta Psi) collapsing uncoupler carbonyl cyanide 3-chloro phenyl hydrazone (CCCP; Molecular Probes), which inhibits mt respiratory activity, thus reducing fluorescence intensity. After incubation with mt probe, oocytes were washed three times in PBS with 0.3% BSA and incubated for 15 min in the same media containing 10 μM 2′,7′-dichlorodihydrofluorescein diacetate (H_2DCF-DA) [51, 52] in order to detect and localize intracellular sources of ROS. The principle underlying this procedure may be described briefly as follows: nonionized H_2DCF-DA is membrane permeant and therefore is able to diffuse readily into cells. Once within the cell, the acetate groups are hydrolysed by intracellular esterase activity forming 2′,7′-dichlorodihydrofluorescein (H_2DCF) which is polar and thus trapped within the cell. H_2DCF fluoresces when it is oxidized by H_2O_2 or lipid peroxides to yield 2′,7′-dichlorofluorescein (DCF). The level of DCF produced within the cells is related linearly to that of peroxides present and thus its fluorescent emission provides a measure of the peroxide levels [51]. After incubation, oocytes were washed three times in prewarmed PBS without BSA and fixed overnight at 4°C with 2% paraformaldehyde solution in PBS.

2.8. Assessment of Oocyte Mitochondrial Distribution Pattern and Intracellular ROS Localization. For mt distribution pattern evaluation, MII oocytes were selected among those having regular ooplasmic size and texture (no vacuoles). Oocytes were observed at 600x magnification in oil immersion with Nikon C1/TE2000-U laser scanning confocal microscope. A helium/neon laser ray at 543 nm and the G-2 A filter (551 nm exposure and 576 nm emission) were used to point out the MitoTracker Orange CMTM Ros. An argon ions laser ray at 488 nm and the B-2 A filter (495 nm exposure and 519 nm emission) were used to point out the DCF. Scanning was conducted with 25 optical series from the top to the bottom of the oocyte with a step size of 0.45 μm to allow three-dimensional distribution analysis. General criteria for oocyte mt patterns definition were adopted on the basis of previous studies in other species [20, 40, 47, 50]. Homogeneous/even distribution of small mt aggregates throughout the cytoplasm was considered as indication of immature cytoplasmic condition, whereas heterogeneous/uneven distribution of small and/or large aggregates within the cytoplasm indicated a metabolically active ooplasm. In particular, accumulation of mitochondria in the peripheral cytoplasm and around the nucleus was considered as aspects of the developmental program of cytoplasmic maturation [53]. Oocytes showing irregular distribution of large mt clusters unrelated to the specific cell compartments were classified as abnormal. To our knowledge, few studies are reported to date on intracellular ROS localization in mammalian oocytes. Recent studies performed in mouse [54], equine [47], and ovine [40] oocytes from adult females reported mt/ROS colocalization as a biomarker of healthy oocytes.

2.9. Quantification of MitoTracker Orange CMTM Ros and DCF Fluorescence Intensity. Measurements of fluorescence intensities were performed in MII oocytes having either heterogeneous (perinuclear and/or pericortical) or homogeneous (small aggregates) mt distribution pattern. Oocytes showing abnormal mt distribution pattern were excluded from this analysis. In each individual oocyte, MitoTracker and DCF fluorescence intensities were measured at the equatorial plane, as in previous studies from our unit performed in human [55] and animal oocytes [20, 40, 47, 50], with the aid of the EZ-C1 Gold Version 3.70 image analysis software platform for Nikon C1 (Nikon Instruments) confocal microscope. A circle of an area = 100 in diameter (arbitrary value) was drawn to measure only the cytoplasmic area (512 × 512 pixels). The fluorescence intensity encountered within the programmed scan area was recorded and plotted against the conventional pixel unit scale (0–255). Fluorescence intensity was expressed as arbitrary densitometric units (ADU). Parameters related to fluorescence intensity were maintained at constant values for all measurements. In detail, images were taken under fixed scanning conditions with respect to laser energy, signal detection (gain), and pinhole size.

2.10. Oocyte Mitochondria/ROS Colocalization Analysis. Colocalization analysis of mitochondria and ROS was performed by using the EZC1 Gold Version 3.70 software. Degree of colocalization was reported as Pearson's correlation coefficient quantifying the overlap degree between MitoTraker Orange CMTM Ros and DCF fluorescence signals [40].

2.11. Measurement of the Total CAT Activity in Single Oocytes. Additional MII oocytes were washed in SB buffer (TRIS/HCl 60 mM pH 6.8, Glycerol 40%) and individually solubilized for one hour at 4°C in the presence of 1.0% Triton X-100. The protein concentration was assessed by the method of Bradford [56]. Each test was performed on 7 μg of proteins from a single solubilized oocyte. The CAT activity was determined following the Beers and Sizer method [57]. A spectrophotometer Varian Cary WinUV50 was used to follow the absorbance decrease at 240 nm in the presence of H_2O_2 for time unit, in potassium-phosphate 50 mM, EDTA 1 mM pH 7.0, at 25°C, in a final volume of 1 mL. After determining the baseline with the measure mixture, 3.5 mM H_2O_2 was added. Reaching stability, the reactions with protein extract started. Since H_2O_2 molar extinction coefficient (ε = 40 $M^{-1} * cm^{-1}$) is known, CAT activity was calculated as μmoles of H_2O_2 converted in H_2O per minute. Specific activities were calculated by dividing enzymatic activities per total protein concentration expressed in mg.

2.12. Measurement of the Total SOD Activity in Single Oocytes. Additional MII oocytes were washed in SB buffer (TRIS/ HCl 60 mM pH 6.8, Glycerol 40%) and individually solubilized for one hour at 4°C in the presence of 1.0% Triton X-100. The protein concentration was assessed by the

method of Bradford [56]. Each test was performed on 7 μg of proteins of a single solubilized oocyte. SOD activity was determined with the Fluka analytical assay kit using a multiplate reader Victor X, Perkin Elmer at λ = 440 nm. Total SOD activity (SOD, EC 1.15.1.1) was assayed by its ability to inhibit the reduction of a novel tetrazolium salt, WST-1[2-(4-Iodophenyl)-3-(4-nitrophenyl)-5-(2,4-disulfophenyl)-2H-tetrazolium, monosodium salt] by superoxide anions generated with the xanthine/xanthine oxidase method [58, 59]. One unit of SOD activity was defined as the amount of the enzyme causing half maximum inhibition of WST-1 reduction. It was measured with high sensitivity (0.01 pmol) and expressed as U/mg proteins. A nine-point standard curve was routinely included in each assay.

2.13. Verbascoside Stability in Oocyte-Free Culture Medium and Its Uptake by the OCC. Verbascoside stability in the IVM culture medium was assessed in the same conditions as that used in IVM experiments. In particular, VB (10 μM) was added to the maturation medium in the absence of oocytes for 24 h at 38.5°C. After 0, 4, 12, and 24 h, aliquots of the mixed solutions were analyzed by HPLC-DAD as described in HPLC analysis section. For accumulation experiments, OCCs were cultured in maturation medium containing 100 μM VB. Oocytes were then incubated at 38.5°C for 30 and 60 min. Following incubation, media were aspirated and stored at −80°C until analysis; oocytes were washed 3 times with PBS (pH 7.4) then were collected and stored at −80°C until analysis. Protein values for each tested oocyte pool (n = 2 pools of 36 OCCs each) were assessed by Bio-Rad protein assay method [56] and were found to be 0.504 ± 0.05 mg of total protein/pool. Verbascoside was extracted from sonicated OCCs with 3 mL of ethyl acetate (0.01% butylated hydroxytoluene) for three times. Ethyl acetate layers were pooled, dried under vacuum, and resolubilized in 300 μL of HPLC mobile phase. HPLC analysis was performed following the protocol as described before.

2.14. Statistical Analysis. Oocyte nuclear maturation rates, cleavage and blastocyst developmental rates, and the percentages of oocytes showing different mt and intracellular ROS distribution patterns were compared between treated and control groups by Chi-square test with the Yates correction for continuity. The effects of VB on nuclear maturation rates were also assessed by multifactor ANOVA, taking into account the use of the two IVM media. Fisher's exact test was applied in all cases in which at least one cell contained a value less than 5. For confocal quantification analysis of mt activity and intracellular ROS levels, the least-square means of the dependent variable (MitoTracker CMTM Ros and DCF fluorescence intensity) were calculated in examined samples and the statistical significance of the least-square means between treated and control groups was calculated by one-way ANOVA followed by Multiple Comparison Dunn's method (SigmaPlot software). For mt/ROS colocalization, mean values of Pearson's correlation coefficient were compared between treated and control groups by one-way ANOVA followed by Multiple Comparison Dunn's method (SigmaPlot software). CAT and SOD activities were compared between treated and control groups by Student's t test. Differences with $P < 0.05$ were considered as statistically significant.

3. Results

3.1. Verbascoside Extraction and Purification and HPLC Analysis. Verbascoside was purified from OMWW by using a laboratory scale system to remove solid particles from the fluid and to fractionate molecules with different molecular weight. From the two permeate fractions obtained, microfiltrate (MF) and ultrafiltrate (UF), UF was considered to be around 50% of the initial volume of OMWW (5 L of UF from 10 L of OMWW). This fraction was subsequently separated by low-pressure gel filtration chromatography on a Sephadex LH-20 column to give a highly purified VB fraction. The concentration of VB obtained was on average 3.25 mg/30 mL of UF giving a final yield of around 54 mg of VB from each liter of OMWW. Purification degree for VB, calculated on peak area, was around 95% as demonstrated by HPLC analysis.

3.2. Verbascoside Did Not Affect the Nuclear Maturation Rate of Fresh Prepubertal Lamb Oocytes. One thousand and twenty-nine oocytes were recovered, 850 of which were surrounded by a healthy cumulus and were selected for IVM culture. Oocytes were cultured in IVM medium 1 or in IVM medium 2. For each medium, five consecutive trials were performed. In Table 1, separated and pooled data obtained with both culture media are presented. Verbascoside did not affect the maturation rate of prepubertal lamb oocytes neither when added in medium 1 nor when added in medium 2. No effects were also noticed in pooled data of oocytes matured in medium 1 + medium 2.

On the other hand, within each medium and at specific tested VB concentrations (2.06 and 4.11 μM), an indirect beneficial influence of medium 1 composition on the VB effects on oocyte meiosis resumption and progression to the MII stage was noticed. In oocytes cultured in presence of 2.06 μM VB, a significantly higher rate of those cultured in medium 1 resumed meiosis (significantly lower rate of GV oocytes; $P < 0.001$) and reached the metaphase stages ($P < 0.001$) compared with those cultured in medium 2. In oocytes cultured in presence of 4.11 μM, a significantly lower rate of GV oocytes ($P < 0.001$) was found and the maturation rate to the MII stage tended to be higher ($P = 0.054$) compared with those cultured in medium 2. Thus, possibly, the VB effects may differ in oocytes primed by different media. The multifactor ANOVA analysis confirmed Chi-square based significances.

3.3. Verbascoside Impaired the Blastocyst Formation Rate of Fresh Prepubertal Lamb Oocytes. Nine hundred MII oocytes were used for IVF and *in vitro* embryo culture experiments. Early cleavage and blastocyst formation rates were recorded as resumed in Table 2. After IVF, for each condition, the number of cleaved oocytes at 24 and 30 hours after fertilization and the number of embryos reaching the blastocyst stage at

Table 1: Effects of verbascoside on the *in vitro* meiotic maturation of prepubertal lamb oocytes.

Verbascoside concentration (μM)	Number of cultured oocytes	IVM medium type	Nuclear chromatin configuration number (%)			
			GV	MI to TI	MII + PB	Degenerated
0	93	1	9 (9.7)[c]	6 (6.5)	59 (63.4)	19 (20.4)[a]
	111	2	27 (24.3)[d]	17 (15.3)	60 (54.1)	7 (6.3)[b]
	204	(∗)	**36 (17.6)**	**23 (11.3)**	**119 (58.3)**	**26 (12.7)**
1.03	79	1	11 (13.9)	12 (15.2)	44 (55.7)	12 (15.2)
	118	2	27 (22.9)	21 (17.8)	61 (51.7)	9 (7.6)
	197	(∗)	**38 (19.3)**	**33 (16.8)**	**105 (53.3)**	**21 (10.7)**
2.06	98	1	12 (12.2)[c]	6 (6.1)[a]	67 (68.4)[c]	13 (13.3)
	116	2	33 (28.4)[d]	21 (18.1)[b]	50 (43.1)[d]	12 (10.3)
	214	(∗)	**45 (21)**	**27 (12.6)**	**117 (54.7)**	**25 (11.7)**
4.11	98	1	11 (11.2)[c]	13 (13.3)	58 (59.2)	16 (16.3)
	137	2	36 (26.3)[d]	23 (16.8)	63 (46)	15 (10.9)
	235	(∗)	**47 (20)**	**36 (15.3)**	**121 (51.5)**	**31 (13.2)**

GV: germinal vesicle, M: metaphase, T: telophase, and PB: polar body. *Pooled data of oocytes cultured in medium 1 + medium 2. Chi-square test and multifactor ANOVA test: within each medium type and pooled data, VB-treated versus controls: NS; between media, within each VB concentration: [a,b] $P < 0.05$; [c,d] $P < 0.001$.

Table 2: Effects of verbascoside on cleavage and blastocyst developmental rates of prepubertal lamb oocytes after IVF and IVP.

Verbascoside concentration (μM)	Number of MII oocytes	Number of cleaved embryos (%)		Number of blastocysts (%)	
		24 h after-IVF	30 h after-IVF	At day 7	At day 8
0	200	76 (38)	150 (75)	28 (18.7)[a]	36 (24)[a]
1.03	240	103 (42.9)	189 (78.7)	38 (20.1)	59 (31.2)
2.06	220	77 (35)	156 (70.9)	18 (11.5)	18 (11.5)[b]
4.11	240	93 (38.7)	185 (77.1)	11 (5.9)[b]	22 (11.9)[b]

Chi-square test: [a,b] $P < 0.05$.

Table 3: Effects of verbascoside on the mitochondrial distribution pattern of *in vitro* matured prepubertal lamb oocytes.

Verbascoside concentration (μM)	Number of MII oocytes	Mitochondrial distribution number (%)					
		Homogeneous	Heterogeneous				Abnormal
			Total (1 + 2 + 3)	Perinuclear/ pericortical (1)	Peri-nuclear (2)	Peri-cortical (3)	
0	30	16 (53.3)	14 (46.7)	0 (0)	2 (6.7)	12 (40)	0 (0)
1.03	29	15 (51.7)	12 (41.4)	1 (3.4)	2 (6.9)	9 (31)	2 (6.9)
2.06	25	16 (64)	9 (36.0)	1 (4)	2 (8)	6 (24)	0 (0)
4.11	29	13 (44.8)	16 (55.2)	0 (0)	2 (6.9)	14 (48.3)	0 (0)

Chi-square test: NS.

day 7 and day 8 were recorded. No significant differences in the early cleavage rate were found between VB-treated and control groups. Significant reductions of the blastocyst formation rate were found in the group of oocytes exposed to 2.06 and 4.11 μM VB compared with controls (Table 2; $P < 0.05$).

3.4. Verbascoside Did Not Affect mt Distribution Pattern and Intracellular ROS Localization of Fresh MII Stage Prepubertal Lamb Oocytes. One hundred and thirteen fresh oocytes matured *in vitro* and found at the MII stage were analyzed. No significant effects of VB on mt distribution pattern of fresh prepubertal lamb MII stage oocytes was found (Table 3). Intracellular ROS localization was also unaffected by VB and data concerning this parameter corresponded to data of mt distribution pattern presented in Table 3.

3.5. Verbascoside, at the Highest Tested Concentration, Increased mt Activity and ROS Levels in MII Fresh Prepubertal Lamb Oocytes. A significant increase in mt activity was found in oocytes treatment groups exposed to the highest VB concentration (4.11 μM) compared with controls (Figure 1(a), $P < 0.05$). No variations were found, at the lower concentrations assessed. As well, in the 4.11 μM VB exposed group, a significant increase in intracellular ROS levels was found compared with controls (Figure 1(b), $P < 0.001$). The mt/ROS

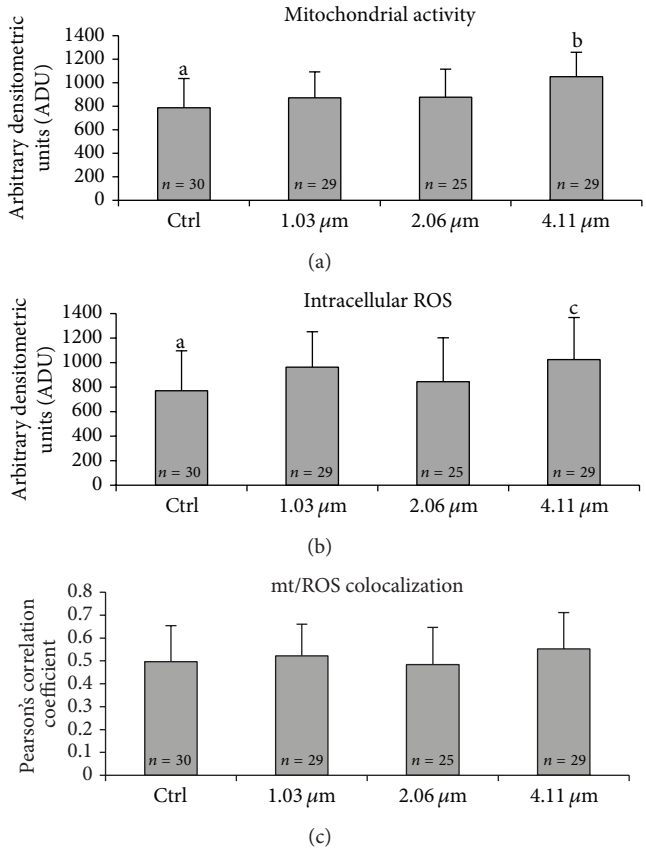

Figure 1: Dose response curve of the *in vitro* effects of VB on mt activity and intracellular ROS levels in single fresh prepubertal lamb MII stage oocytes, expressed as MitoTracker Orange CMTM Ros (panel (a)) and DCF (panel (b)) fluorescence intensities. Oocytes treated with 4.11 μM VB showed significantly higher mt activity and intracellular ROS levels compared with controls. Values are expressed as ADU (arbitrary densitometric units). Pearson's correlation coefficients of MitoTracker Orange CMTM Ros and DCF fluorescent labelling colocalization of treated versus control MII oocytes (panel (c)). Numbers of analyzed oocytes per group are indicated at the bottom of each histogram. (a) One-way ANOVA: a, b: $P < 0.05$; (b) one-way ANOVA: a, c: $P < 0.001$; and (c) one-way ANOVA: NS (not significant).

colocalization, expressed as Pearson's correlation coefficient, was not affected by VB addition (Figure 1(c), NS). Figure 2 shows mt distribution pattern and activity, intracellular ROS localization and levels, and mt/ROS colocalization of a representative control MII oocyte (Figure 2(a)) and a MII oocyte representative of those cultured in presence of 4.11 μM VB (Figure 2(b)). Increased MitoTracker and DCF fluorescence intensities, indicating mt activity and ROS levels, are evident in the VB-treated oocyte compared with the control one.

3.6. Verbascoside Affected CAT but Not Total SOD Activity in MII Fresh Prepubertal Lamb Oocytes. Scavenging enzymes, CAT and SOD, activities were evaluated on fresh MII oocytes. CAT activity assay was conducted on individual oocytes ($n = 64$) that showed the 1st PB extruded after IVM. For SOD activity assay, 41 individual MII oocytes were evaluated.

Table 4: Postvitrification/warming viability of prepubertal lamb oocytes matured *in vitro* in presence of verbascoside.

Verbascoside concentration (μM)	Number of MII oocytes vitrified/warmed	Viability number (%)
0	55	28 (50.9)
1.03	41	28 (68.3)
2.06	55	37 (67.3)
4.11	58	29 (50.0)

Chi-square test: NS.

Results are reported in Figure 3. Significant increase of CAT activity in VB-treated groups was observed compared with controls (Figure 3(a); $P < 0.05$). On the contrary, SOD activity was not affected by VB addition and constant levels were found at any tested concentration (Figure 3(b), NS).

3.7. Verbascoside Did Not Affect Oocyte Viability in MII Vitrified/Warmed Prepubertal Lamb Oocytes. Oocytes cultured *in vitro* in presence of different VB concentrations and found at the MII stage were vitrified/warmed and analyzed for cell viability. Oocyte viability assessment, expressed as the percentage of oocytes showing zona pellucida and oolemma integrity and absence of ooplasmic cyto-fragmentation, was conducted on 209 vitrified/warmed oocytes. No significant effects of VB on oocyte viability after vitrification/warming were observed (Table 4).

3.8. Verbascoside Did Not Affect mt Distribution Pattern and ROS Intracellular Localization in MII Vitrified/Warmed Prepubertal Lamb Oocytes. Oocytes cultured *in vitro* in presence of different VB concentrations and found at the MII stage were vitrified/warmed and analyzed for confocal parameters expressing the bioenergetic/oxidative status. Sixty-six vitrified/warmed oocytes were analyzed. Verbascoside did not affect the mt distribution pattern in MII vitrified/warmed prepubertal lamb oocytes (Table 5). Intracellular ROS localization also did not vary upon VB addition in vitrified samples and data concerning this parameter corresponded to those presented in Table 5, as previously observed for fresh oocytes.

3.9. Verbascoside Did Not Affect mt Activity but Increased ROS Levels in MII Vitrified/Warmed Prepubertal Lamb Oocytes. Concerning mt activity, no significant difference was observed in the comparisons between treated and control groups (Figure 4(a), NS). Intracellular ROS levels increased in the group of oocytes treated with the low VB concentration (1.03 μM) compared with controls (Figure 4(b), $P < 0.001$). In vitrified/warmed oocytes, mt/ROS colocalization, expressed as Pearson's correlation coefficient, was not affected by VB addition (Figure 4(c)).

3.10. Low Verbascoside Stability in Oocyte IVM Culture Medium. As shown in Figure 5, after 4 hours of exposure, VB concentration decreased about 55.6% with respect to the initial amount; moreover, the presence of an isomerisation

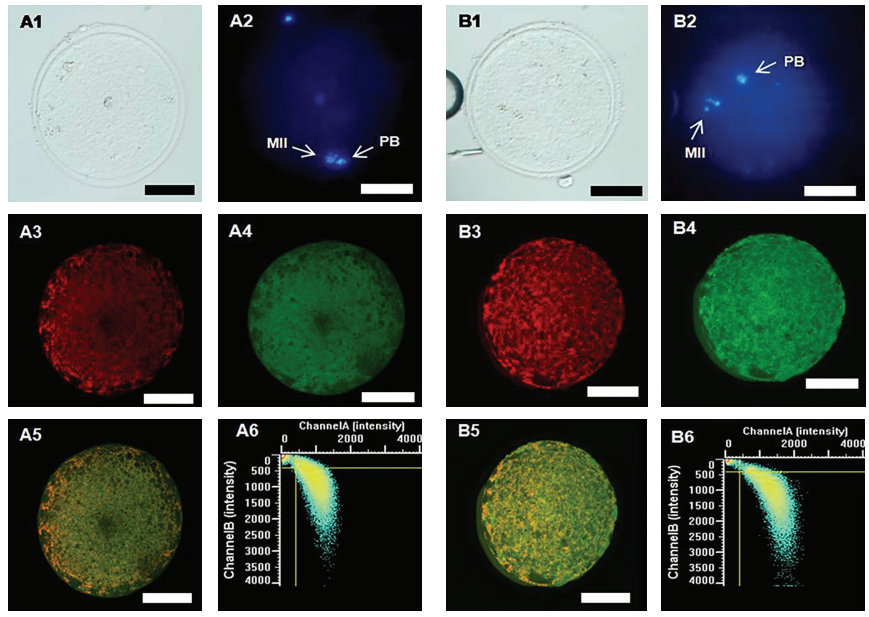

(a) (b)

Figure 2: Mitochondrial distribution pattern and activity, intracellular ROS localization and levels, and mt/ROS colocalization of a representative prepubertal lamb control MII oocyte (panel (a)) and a MII oocyte representative of those cultured in presence of 4.11 μM VB (panel (b)). Both oocytes show heterogeneous mt pattern. For each culture condition, corresponding bright-field (A1, B1), UV light (A2, B2), and confocal laser scanning images of mt distribution pattern (A3, B3), intracellular ROS localization (A4, B4), mt/ROS merge (A5, B5), and colocalization scatterplot graph (A6, B6) are shown. Increased mt activity, expressed as MitoTracker Orange CMTM Ros fluorescence intensity, and intracellular ROS levels, expressed as DCF fluorescent intensity (B4), can be seen in the oocyte exposed to 4.11 μM VB compared with the control oocyte (B3 versus A3 and B4 versus A4, resp.). Scale bars represent 50 μM.

Table 5: Post vitrification/warming mitochondrial distribution pattern of prepubertal lamb MII oocytes obtained after IVM in presence of verbascoside.

Verbascoside concentration	Number of MII oocytes	Mitochondrial distribution pattern number (%)					
		Homogeneous	Heterogeneous				Abnormal
			Total (1 + 2 + 3)	Peri-nuclear/peri-cortical (1)	Peri-nuclear (2)	Peri-cortical (3)	
0 (control)	15	8 (53.3)	7 (46.7)	0 (0)	2 (13.3)	5 (33.3)	0 (0)
1.03	18	11 (61.1)	6 (33.3)	2 (11.1)	1 (5.6)	3 (16.7)	1 (5.6)
2.06	19	14 (73.7)	5 (26.3)	0 (0)	0 (0)	5 (26.3)	0 (0)
4.11	14	10 (71.4)	4 (28.6)	0 (0)	2 (14.3)	2 (14.3)	0 (0)

Chi-square test: NS.

product was recorded. In fact, at this time point, its positional isomer, isoverbascoside (isoVB) of occurred in the proportion of 20% to the total. After 12 h with exposure in oocyte-free medium, further reduction of VB concentration, by 80% with respect to the initial amount, was found. Verbascoside and its positional isomer isoVB, at this time, were present with the same proportions. After 24 hours, no traces of both polyphenols were recovered. No specific degradation products were characterized beyond isoVB.

3.11. Rapid Verbascoside Uptake in Prepubertal Lamb OCCs. To evaluate absorptive potential of the OCC, VB accumulation experiments were conducted on two groups of 36 OCCs each, one examined at 30 min and the other examined at 60 min after the start of exposure. Uptake of VB was found to be time dependent and reached the maximum at 30 min after start of exposure. At 100 μM, OCCs accumulated 79.4 nmol of VB/mg of OCCs proteins. It represents approximately 0.2% of absorption of the tested VB. At 60 min, VB accumulated by the OCCs decreased to 19.05 nmol of VB/mg of OCCs proteins.

4. Discussion

The highly purified VB from OMWW was previously analyzed for assessing its antioxidant activity and, after brief incubation in HT-29 cell line, it showed antioxidant properties [2]. However, at the typical conditions used in the present study, VB showed an opposite behavior. In fact, this compound had no effect on oocyte nuclear maturation rate.

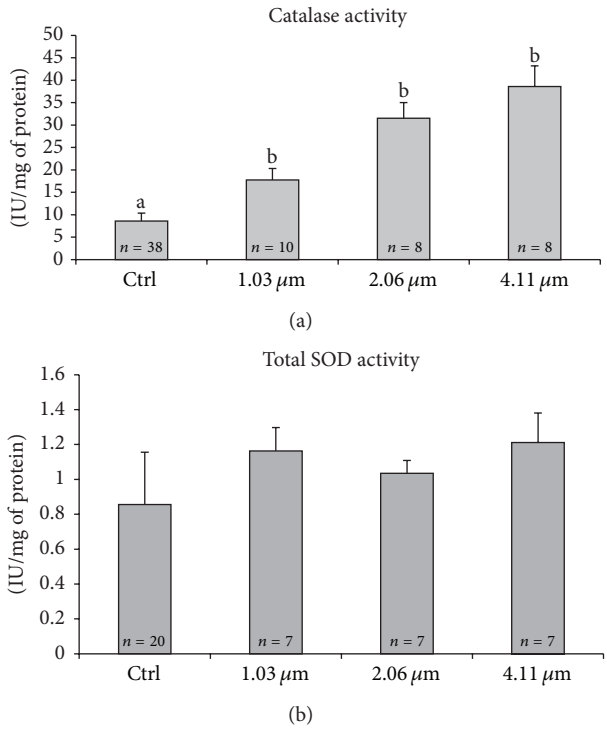

Figure 3: Catalase (CAT) and total superoxide dismutase (SOD) activities in individual prepubertal lamb MII oocytes matured *in vitro* in presence of VB. Numbers of analyzed oocytes per group are indicated at the bottom of each histogram. Values are expressed as IU/mg protein. Treatment with VB induced a significant increase in CAT activity compared to controls (panel (a); Student's *t*-test: a, b; $P < 0.001$). Total SOD activity did not vary between treated and control groups (panel (b); Student's *t*-test: NS).

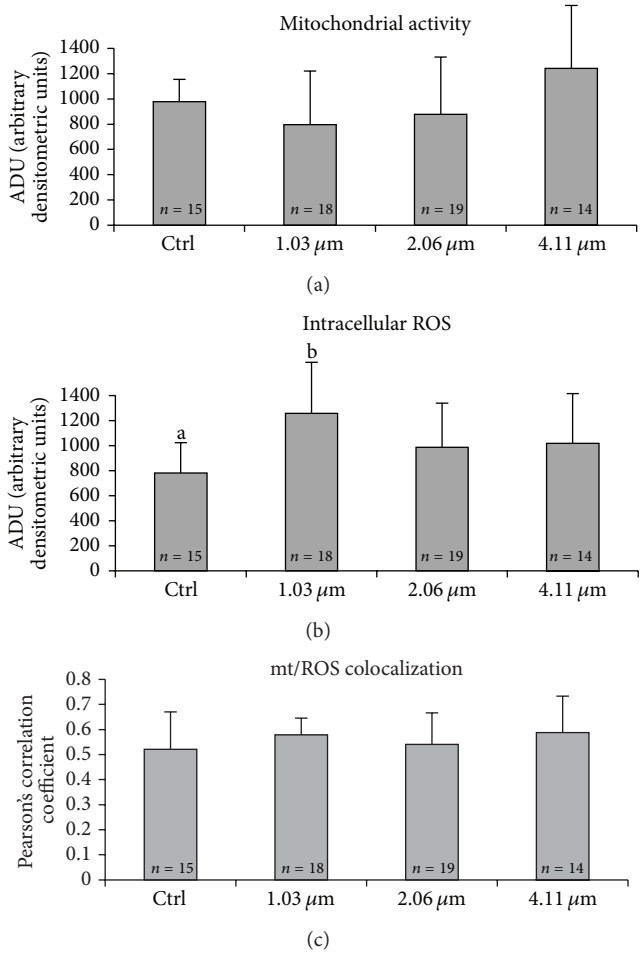

Figure 4: Dose response curve of the *in vitro* effects of VB, added during IVM culture, on mt activity and intracellular ROS levels in single prepubertal lamb MII stage oocytes vitrified/warmed, expressed as MitoTracker Orange CMTM Ros (panel (a)) and DCF (panel (b)) fluorescence intensities. Oocytes treated with 1.03 μM VB showed significantly higher intracellular ROS levels compared with controls. Values are expressed as ADU (arbitrary densitometric units). Pearson's correlation coefficients of MitoTracker Orange CMTM Ros and DCF fluorescent labelling colocalization in MII oocytes obtained after IVM culture in presence of VB and vitrified/warmed (panel (c)). Numbers of analyzed oocytes per group are indicated at the bottom of each histogram. (a) One-way ANOVA: NS. (b) One-way ANOVA: a,b: $P < 0.001$. (c) One-way ANOVA: NS.

IVM data obtained with media 1 and 2 were kept separated in order to avoid misinterpretation due to the effects of different culture conditions. In both tested media, no significant differences were noticed between VB-treated and control oocytes. Moreover, a reduction of the blastocyst formation rate after exposure to intermediate and high VB doses was found. This result can be considered as a long-term effect of VB or VB derived products on oocyte cytoplasmic competence and consequently on embryo development. These findings lead us to hypothesize that, in our cell system, VB had an oxidatively stressful and toxic effect probably as a consequence of a prolonged exposure time at the tested concentrations or toxicity resulting from oxidative degradation of VB and subsequent generation of H_2O_2 as reported for oxidation of phenolic compounds in culture media [60]. This observation is interesting considering that the concentrations used in these studies were reported as being effective in modulating oxidative stress in HT29 cell line after brief (30 min) *in vitro* exposure [2].

In order to investigate the reasons of the observed compromised embryo development, we investigated the bioenergetic potential and oxidative status of oocytes exposed to VB. The supplementation of the IVM medium with VB did not change mt distribution pattern and intracellular ROS localization in prepubertal lamb oocytes. However, in the group of oocytes exposed to the highest VB concentration, it increased mt activity and intracellular ROS levels without affecting mt/ROS colocalization. This finding allowed us to consider that the two fluorescence signals were not overlapping; thus observed ROS increase could be not only due to mt ROS generation, rather it could be also of cytosolic origin, thus indicating a stressed/toxic cytoplasmic condition. In fact, high levels of mt/ROS colocalization were reported as a reliable marker of healthy MII oocytes [40]. In the culture conditions (VB exposure times and tested concentrations) of this study, the ooplasmic bioenergetic/redox status was not improved by VB addition, as confocal analysis stated that VB,

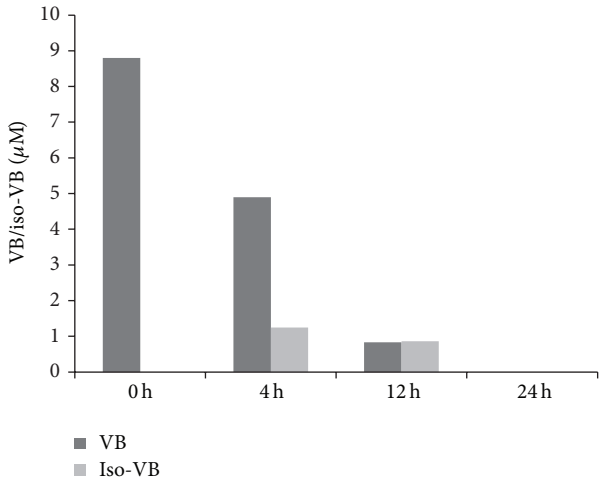

Figure 5: Stability test of VB in oocyte-free IVM medium, incubated at 38.5°C under 5% CO_2 in air. The figure shows the decrease of VB versus time. isoVB appears after 4 hours of incubation. After 24 hours, both VB and isoVB are not detected.

at the tested concentrations, failed to behave as an antioxidant compound, a role which was previously demonstrated in other cell line system [2, 3, 6, 7]; rather it demonstrated a prooxidant effect.

To provide further information about the effects of VB on oocyte cytoplasm oxidative status, the activities of two scavenging enzymes, CAT and SOD, in VB exposed oocytes were tested. The assays demonstrated that while SOD activity was not affected, CAT activity significantly increased upon VB addition. This increase could be due to the potential formation of H_2O_2 during oxidation of phenolics in cell culture media. Verbascoside stability was observed to be poor in the conditions tested (Figure 5). Oxidative degradation of phenolic compounds has been reported to proceed through auto-oxidative mechanism involving formation of H_2O_2 [61, 62]. This increase in peroxides would explain the subsequent increase in CAT activity without an increase in SOD activity. The observed lack of variation of SOD activity may also be related to the fact that, in our experiments, total SOD activity was investigated. It cannot be excluded that the relative ratio between cytosolic and mt SOD could be varied upon VB addition, but further studies are necessary to address this hypothesis. The stimulating effect of VB on CAT activity may also be related to the observed increase in intracellular ROS levels. Moreover, it can be interpreted under the light of current literature. In fact, recent *in vivo* and *in vitro* studies report different effects of VB on the antioxidant enzyme network [6, 63–65]. Other studies show that VB increased the expression of the transcription factor peroxisome proliferator activated receptor α (PPAR-α) in nuclear extracts of colon cells [4]. Another member of PPARs family, PPARγ, has been shown to activate genes with a peroxisome proliferator response element (PPRE) in their promoter regions [66]. Indeed, the CAT promoter gene is known to contain functional PPAR-γ responsive elements, so it is possible that the CAT activity could be regulated by PPAR-γ agonists [67, 68]. Based on our results and these observations, it is possible to hypothesize that VB may act by increasing oocyte intracellular ROS levels, both by generating H_2O_2 through its own oxidative degradation and by increasing CAT expression levels through multiple mechanisms.

As a further step of the JIVET technology and due to the particular interest of establishing suitable cryopreservation procedures allowing the prepubertal oocyte to be protected against cryodamage, the effects of VB added during IVM on the viability and bioenergetic/oxidative status of MII vitrified/warmed oocytes were evaluated. Exposure to high cryoprotectant concentrations and subphysiological temperature generates in the oocyte a widespread oxidative stress, as reported by Zhao et al. [69]. Moreover, Succu et al. [34] demonstrated that prepubertal oocytes are more susceptible than adult counterparts to cryoinjury during vitrification performing. No effects of VB on cell viability parameters of vitrified/warmed oocytes were found. In order to provide additional information on cytoplasmic condition after vitrification/warming, we investigated the effects of VB on the bioenergy/oxidative status of vitrified/warmed oocytes. Just like in fresh oocytes, VB did not affect mt distribution pattern, ROS localization, and mt activity of vitrified oocytes. However, when used at the lowest tested concentration (1.03 μM) during IVM, it increased ROS levels without affecting mt/ROS colocalization. This finding can be explained considering that, in the case of vitrified oocytes (a more stressed cell system compared to their fresh counterpart), the prooxidant toxic effect of VB could have been strengthened, as supported by the comparison between fresh and vitrified oocytes at 1.03 μM VB ($P = 0.002$).

In the light of obtained results and considering that it is well known that, for every drug, the line between benefit and toxicity is represented by the administered dose, differences in the cellular metabolism, dimension, and number of cells per dish between oocytes and cultured cell lines leading to differences in drug uptake which may result as a beneficial or toxic concentration to the cell were hypothesized. For these reasons, we performed experiments to test (1) VB stability in our culture conditions and (2) its uptake by the OCCs. Determinations of VB stability in an oocyte-free IVM medium at 38.5°C indicated that VB was unstable under our IVM culture conditions, as previously reported [70], also for other polyphenols such as catechin, chlorogenic acid [60, 71–73]. After 4 hours of incubation, an isomerization process occurred, with the appearance of the positional isomer, isoVB. This process is probably related to the medium pH (7.2–7.4) and culture temperature (38.5°C) or to the deacetylation and VB caffeoyl moiety migration under hydrolytic environment of harsh extraction conditions [74]. After 12 hours, the residual percentage of VB and isoVB was 20% and reached zero after 24 hours of incubation. Probably, other products derived from oxidation activity were present but, at this point of the research, no information about these products is available. These data are in agreement with the results obtained from other polyphenols that were also unstable under the incubation conditions used [71]. Moreover, VB uptake experiments demonstrated that the compound was rapidly incorporated into the OCCs in a

time-dependent manner with an accumulation efficiency of about 0.2% after 30 min. This observed low level of VB uptake was similar to that reported for HT-29 and Caco-2 human intestinal cells [2, 75] and for other polyphenols such as catechins [76–78] and is consistent with poor *in vivo* VB bioavailability, as reported by Funes et al. [79] following oral administration of lemon verbena extract in rodents and by Cardinali et al., [80] with *ex vivo* experiments. The uptake experiments by OCCs also demonstrated that the amount of VB in our cells was one thousand times higher (in the order of nmol/mg proteins) than that found in the Caco-2 and HT 29 human intestinal cell lines (in the order of pmol/mg proteins) by Cardinali et al. [2, 75]. This result could be consistent with the observed prooxidant activity of VB in the current model. Future experiments should consider lower levels of VB exposure to better emulate intracellular concentrations observed in other cell models and to better understand if lower levels may be able to deliver differential protection against oxidative stress.

Taken together, our data demonstrated that VB, at the conditions used in this study, exerted toxic effects (as it was shown by reduced blastocyst formation) which could be induced by its prooxidant activity. This prooxidant activity could be due to an excessively high tested concentration as observed by uptake data, by prolonged incubation time in culture media (24 hours) used in the present study, in which H_2O_2 production is probably induced. Hydrogen peroxide production was already demonstrated in previous studies in which other polyphenols have been used in different cell systems [61, 62, 81]. The H_2O_2 production was assessed by Odiatou et al. [81] on the two main olive polyphenols (hydroxytyrosol and oleuropein) incubated in the culture media and was observed as being dependent upon the presence of sodium bicarbonate in the medium. Therefore, polyphenols, normally considered as antioxidant, work as prooxidants, when they are added in the commonly used media, in standard culture conditions at high concentrations, thus producing significant amounts of H_2O_2. Even for VB, in the culture medium conditions used in this study, it could be possible to speculate the same behaviour. In addition, the possible presence of H_2O_2 in the culture medium could justify the increased oocyte intracellular ROS levels and CAT activity.

5. Conclusions

In conclusion, VB, added at μ-molar concentrations in a continuative 24 hours IVM exposure protocol, acts as a prooxidant molecule, by impairing oocyte bioenergetic potential and oxidative status and embryo developmental competence of prepubertal lamb oocytes. Applications of this compound in oocyte or embryo culture systems could be developed by evaluating its use at lower concentrations and reduced exposure times.

Conflict of Interests

The authors declare that there is no conflict of interests regarding the publication of this paper.

Authors' Contribution

M. E. Dell'Aquila and L. Bogliolo contributed equally to this work, and A. Cardinali and F. Minervini contributed equally to this work. M. E. Dell'Aquila, L. Bogliolo, A. Cardinali, and F. Minervini designed the study, analyzed data, and wrote the paper. R. Russo, N. A. Martino, M. Filioli Uranio, F. Ariu, F. Amati, and V. Linsalata conducted experimental procedures of the study and collaborated in analyzing data and drafting the paper. R. Russo, F. Ariu, and M. Filioli Uranio performed *in vitro* culture and vitrification experiments under the guidance of L. Bogliolo. N. A. Martino performed confocal analysis. F. Amati performed scavenger enzyme tests under the guidance of A. M. Sardanelli. V. Linsalata performed HPLC analysis. A. Cardinal performed stability and uptake tests. M. E. Dell'Aquila, L. Bogliolo, A. Cardinali, F. Minervini, A. M. Sardanelli, and M. G. Ferruzzi supervised experiments and performed critical reading of the paper. All authors read and approved the paper.

Acknowledgments

This work was supported by: Regione Autonoma della Sardegna (LR 7, Agosto 2007, no. 7); CEGBA project University of Bari Aldo Moro, Italy; ONEV project MIUR PONa3 00134-no. 254/R&C 18/05/2011; Regione Puglia: PIF MIS 124: Tracciabilità dell'olio extravergine di oliva e valorizzazione dei sottoprodotti dell'industria olearia Filiera Olivicola 100% Pugliese Federiciano.

References

[1] A. Cardinali, N. Cicco, V. Linsalata et al., "Biological activity of high molecular weight phenolics from olive mill wastewater," *Journal of Agricultural and Food Chemistry*, vol. 58, no. 15, pp. 8585–8590, 2010.

[2] A. Cardinali, S. Pati, F. Minervini, I. D'Antuono, V. Linsalata, and V. Lattanzio, "Verbascoside, isoverbascoside, and their derivatives recovered from olive mill wastewater as possible food antioxidants," *Journal of Agricultural and Food Chemistry*, vol. 60, no. 7, pp. 1822–1829, 2012.

[3] L. G. Korkina, E. V. Mikhal'chik, M. V. Suprun, S. Pastore, and R. Dal Toso, "Molecular mechanisms underlying wound healing and anti-inflammatory properties of naturally occurring biotechnologically produced phenylpropanoid glycosides," *Cellular and Molecular Biology*, vol. 53, no. 5, pp. 84–91, 2007.

[4] E. Esposito, E. Mazzon, I. Paterniti et al., "PPAR-contributes to the anti-inflammatory activity of verbascoside in a model of inflammatory bowel disease in mice," *PPAR Research*, vol. 2010, Article ID 917312, 10 pages, 2010.

[5] E. Esposito, R. Dal Toso, G. Pressi, P. Bramanti, R. Meli, and S. Cuzzocrea, "Protective effect of verbascoside in activated C6 glioma cells: possible molecular mechanisms," *Naunyn-Schmiedeberg's Archives of Pharmacology*, vol. 381, no. 1, pp. 93–105, 2010.

[6] L. Speranza, S. Franceschelli, M. Pesce et al., "Antiinflammatory effects in THP-1 cells treated with verbascoside," *Phytotherapy Research*, vol. 24, no. 9, pp. 1398–1404, 2010.

[7] V. A. Kostyuk, A. I. Potapovich, T. O. Suhan, C. De Luca, and L. G. Korkina, "Antioxidant and signal modulation properties

of plant polyphenols in controlling vascular inflammation," *European Journal of Pharmacology*, vol. 658, no. 2-3, pp. 248–256, 2011.

[8] T. Finkel and N. J. Holbrook, "Oxidants, oxidative stress and the biology of ageing," *Nature*, vol. 408, no. 6809, pp. 239–247, 2000.

[9] P. S. Brookes, A.-L. Levonen, S. Shiva, P. Sarti, and V. M. Darley-Usmar, "Mitochondria: regulators of signal transduction by reactive oxygen and nitrogen species," *Free Radical Biology and Medicine*, vol. 33, no. 6, pp. 755–764, 2002.

[10] A. Agarwal and S. S. R. Allamaneni, "Role of free radicals in female reproductive diseases and assisted reproduction," *Reproductive BioMedicine Online*, vol. 9, no. 3, pp. 338–347, 2004.

[11] A. Agarwal, T. M. Said, M. A. Bedaiwy, J. Banerjee, and J. G. Alvarez, "Oxidative stress in an assisted reproductive techniques setting," *Fertility and Sterility*, vol. 86, no. 3, pp. 503–512, 2006.

[12] E. Cadenas and K. J. A. Davies, "Mitochondrial free radical generation, oxidative stress, and aging," *Free Radical Biology and Medicine*, vol. 29, no. 3-4, pp. 222–230, 2000.

[13] E. Cadenas, "Mitochondrial free radical production and cell signaling," *Molecular Aspects of Medicine*, vol. 25, no. 1-2, pp. 17–26, 2004.

[14] P. G. Winyard, C. J. Moody, and C. Jacob, "Oxidative activation of antioxidant defence," *Trends in Biochemical Sciences*, vol. 30, no. 8, pp. 453–461, 2005.

[15] P. S. Brookes, Y. Yoon, J. L. Robotham, M. W. Anders, and S.-S. Sheu, "Calcium, ATP, and ROS: a mitochondrial love-hate triangle," *American Journal of Physiology: Cell Physiology*, vol. 287, no. 4, pp. C817–C833, 2004.

[16] R. Dumollard, J. Carroll, M. R. Duchen, K. Campbell, and K. Swann, "Mitochondrial function and redox state in mammalian embryos," *Seminars in Cell and Developmental Biology*, vol. 20, no. 3, pp. 346–353, 2009.

[17] L.-Y. Wang, D.-H. Wang, X.-Y. Zou, and C.-M. Xu, "Mitochondrial functions on oocytes and preimplantation embryos," *Journal of Zhejiang University B*, vol. 10, no. 7, pp. 483–492, 2009.

[18] U. Eichenlaub-Ritter, M. Wieczorek, S. Lüke, and T. Seidel, "Age related changes in mitochondrial function and new approaches to study redox regulation in mammalian oocytes in response to age or maturation conditions," *Mitochondrion*, vol. 11, no. 5, pp. 783–796, 2011.

[19] J. Van Blerkom, "Mitochondrial function in the human oocyte and embryo and their role in developmental competence," *Mitochondrion*, vol. 11, no. 5, pp. 797–813, 2011.

[20] B. Ambruosi, G. M. Lacalandra, A. I. Iorga et al., "Cytoplasmic lipid droplets and mitochondrial distribution in equine oocytes: implications on oocyte maturation, fertilization and developmental competence after ICSI," *Theriogenology*, vol. 71, no. 7, pp. 1093–1104, 2009.

[21] F. W. Nicholas, "Genetic improvement through reproductive technology," *Animal Reproduction Science*, vol. 42, no. 1–4, pp. 205–214, 1996.

[22] K. M. Morton, "Developmental capabilities of embryos produced *in vitro* from prepubertal lamb oocytes," *Reproduction in Domestic Animals*, vol. 43, pp. 137–143, 2008.

[23] L. Ayensu-Coker, D. Bauman, S. R. Lindheim, and L. Breech, "Fertility preservation in pediatric, adolescent and young adult female cancer patients," *Pediatrics Endocrinology Review*, vol. 10, no. 1, pp. 174–187, 2012.

[24] D. E. Reichman, O. K. Davis, N. Zaninovic, Z. Rosenwaks, and D. E. Goldschlag, "Fertility preservation using controlled ovarian hyperstimulation and oocyte cryopreservation in a premenarcheal female with myelodysplastic syndrome," *Fertility and Sterility*, vol. 98, no. 5, pp. 1225–1228, 2012.

[25] K. E. Dillon and C. R. Gracia, "Pediatric and young adult patients and oncofertility," *Current Treatment Options in Oncology*, vol. 13, no. 2, pp. 1–13, 2012.

[26] D. Dorji, Y. Ohkubo, K. Miyoshi, and M. Yoshida, "Gene expression profile differences in embryos derived from prepubertal and adult Japanese Black cattle during *in vitro* development," *Reproduction, Fertility and Development*, vol. 24, no. 2, pp. 370–381, 2012.

[27] W. F. Rall and G. M. Fahy, "Ice-free cryopreservation of mouse embryos at −196°C by vitrification," *Nature*, vol. 313, no. 6003, pp. 573–575, 1985.

[28] W. F. Rall, "Factors affecting the survival of mouse embryos cryopreserved by vitrification," *Cryobiology*, vol. 24, no. 5, pp. 387–402, 1987.

[29] G. Vajta, "Vitrification of the oocytes and embryos of domestic animals," *Animal Reproduction Science*, vol. 60-61, pp. 357–364, 2000.

[30] J. Liebermann, F. Nawroth, V. Isachenko, E. Isachenko, G. Rahimi, and M. J. Tucker, "Potential importance of vitrification in reproductive medicine," *Biology of Reproduction*, vol. 67, no. 6, pp. 1671–1680, 2002.

[31] B. Fuller, S. Paynter, and P. Watson, "Cryopreservation of human gametes and embryos," in *Life in the Frozen State*, B. Fuller, N. Lane, and E. Benson, Eds., pp. 505–541, CRC Press, Boca Raton, Fla, USA, 2004.

[32] J. L. Albarracín, R. Morató, C. Rojas, and T. Mogas, "Effects of vitrification in open pulled straws on the cytology of *in vitro* matured prepubertal and adult bovine oocytes," *Theriogenology*, vol. 63, no. 3, pp. 890–901, 2005.

[33] F. Berlinguer, S. Succu, F. Mossa et al., "Effects of trehalose co-incubation on *in vitro* matured prepubertal ovine oocyte vitrification," *Cryobiology*, vol. 55, no. 1, pp. 27–34, 2007.

[34] S. Succu, G. G. Leoni, F. Berlinguer et al., "Effect of vitrification solutions and cooling upon *in vitro* matured prepubertal ovine oocytes," *Theriogenology*, vol. 68, no. 1, pp. 107–114, 2007.

[35] G. Fasano, F. Moffa, J. Dechène, Y. Englert, and I. Demeestere, "Vitrification of *in vitro* matured oocytes collected from antral follicles at the time of ovarian tissue cryopreservation," *Reproductive Biology and Endocrinology*, vol. 9, article 150, 2011.

[36] M. G. Catalá, D. Izquierdo, S. Uzbekova et al., "Brilliant Cresyl Blue stain selects largest oocytes with highest mitochondrial activity, maturation-promoting factor activity and embryo developmental competence in prepubertal sheep," *Reproduction*, vol. 142, no. 4, pp. 517–527, 2011.

[37] P. Pawlak, A. Cieslak, E. Warzych et al., "No single way to explain cytoplasmic maturation of oocytes from prepubertal and cyclic gilts," *Theriogenology*, vol. 78, no. 9, pp. 2020–2030, 2012.

[38] S. Ledda, L. Bogliolo, G. Leoni, and S. Naitana, "Cell coupling and maturation-promoting factor activity in *in vitro*-matured prepubertal and adult sheep oocytes," *Biology of Reproduction*, vol. 65, no. 1, pp. 247–252, 2001.

[39] L. Bogliolo, F. Ariu, G. Leoni, S. Uccheddu, and D. Bebbere, "High hydrostatic pressure treatment improves the quality of *in vitro*-produced ovine blastocysts," *Reproduction, Fertility and Development*, vol. 23, no. 6, pp. 809–817, 2011.

[40] N. A. Martino, G. M. Lacalandra, M. Filioli Uranio et al., "Oocyte mitochondrial bioenergy potential and oxidative

stress: within-/between-subject, *in vivo* versus *in vitro* maturation, and age-related variations in a sheep model," *Fertility and Sterility*, vol. 97, no. 3, pp. 720–728, 2012.

[41] L. Bogliolo, F. Ariu, S. Fois et al., "Morphological and biochemical analysis of immature ovine oocytes vitrified with or without cumulus cells," *Theriogenology*, vol. 68, no. 8, pp. 1138–1149, 2007.

[42] F. Berlinguer, G. G. Leoni, S. Succu et al., "Exogenous melatonin positively influences follicular dynamics, oocyte developmental competence and blastocyst output in a goat model," *Journal of Pineal Research*, vol. 46, no. 4, pp. 383–391, 2009.

[43] H. R. Tervit, D. G. Whittingham, and L. E. Rowson, "Successful culture *in vitro* of sheep and cattle ova," *Journal of Reproduction and Fertility*, vol. 30, no. 3, pp. 493–497, 1972.

[44] S. K. Walker, J. L. Hill, D. O. Kleemann, and C. D. Nancarrow, "Development of ovine embryos in synthetic oviductal fluid containing amino acids at oviductal fluid concentrations," *Biology of Reproduction*, vol. 55, no. 3, pp. 703–708, 1996.

[45] S. Ledda, L. Bogliolo, P. Calvia, G. Leoni, and S. Naitana, "Meiotic progression and developmental competence of oocytes collected from juvenile and adult ewes," *Journal of Reproduction and Fertility*, vol. 109, no. 1, pp. 73–78, 1997.

[46] J. Liu, S. Tang, W. Xu, Y. Wang, B. Yin, and Y. Zhang, "Detrimental effects of antibiotics on mouse embryos in chromatin integrity, apoptosis and expression of zygotically activated genes," *Zygote*, vol. 19, no. 2, pp. 137–145, 2011.

[47] B. Ambruosi, M. Uranio, A. M. Sardanelli et al., "*in vitro* acute exposure to DEHP affects oocyte meiotic maturation, energy and oxidative stress parameters in a large animal model," *PLoS One*, vol. 6, no. 11, Article ID e27452, 2011.

[48] M. Poot, Y.-Z. Zhang, J. A. Krämer et al., "Analysis of mitochondrial morphology and function with novel fixable fluorescent stains," *Journal of Histochemistry and Cytochemistry*, vol. 44, no. 12, pp. 1363–1372, 1996.

[49] H. Torner, K.-P. Brüssow, H. Alm et al., "Mitochondrial aggregation patterns and activity in porcine oocytes and apoptosis in surrounding cumulus cells depends on the stage of preovulatory maturation," *Theriogenology*, vol. 61, no. 9, pp. 1675–1689, 2004.

[50] L. Valentini, A. I. Iorga, T. De Santis et al., "Mitochondrial distribution patterns in canine oocytes as related to the reproductive cycle stage," *Animal Reproduction Science*, vol. 117, no. 1-2, pp. 166–177, 2010.

[51] H. W. Yang, K. J. Hwang, H. C. Kwon, H. S. Kim, K. W. Choi, and K. S. Oh, "Detection of reactive oxygen species (ROS) and apoptosis in human fragmented embryos," *Human Reproduction*, vol. 13, no. 4, pp. 998–1002, 1998.

[52] A. V. Kuznetsov, I. Kehrer, A. V. Kozlov et al., "Mitochondrial ROS production under cellular stress: comparison of different detection methods," *Analytical and Bioanalytical Chemistry*, vol. 400, no. 8, pp. 2383–2390, 2011.

[53] H. Torner, H. Alm, W. Kanitz et al., "Effect of initial cumulus morphology on meiotic dynamic and status of mitochondria in horse oocytes during IVM," *Reproduction in Domestic Animals*, vol. 42, no. 2, pp. 176–183, 2007.

[54] S. L. Wakefield, M. Lane, S. J. Schulz, M. L. Hebart, J. G. Thompson, and M. Mitchell, "Maternal supply of omega-3 polyunsaturated fatty acids alter mechanisms involved in oocyte and early embryo development in the mouse," *American Journal of Physiology: Endocrinology and Metabolism*, vol. 294, no. 2, pp. E425–E434, 2008.

[55] M. E. Dell'Aquila, B. Ambruosi, T. De Santis, and Y. S. Cho, "Mitochondrial distribution and activity in human mature oocytes: gonadotropin-releasing hormone agonist versus antagonist for pituitary down-regulation," *Fertility and Sterility*, vol. 91, no. 1, pp. 249–255, 2009.

[56] M. M. Bradford, "A rapid and sensitive method for the quantitation of microgram quantities of protein utilizing the principle of protein dye binding," *Analytical Biochemistry*, vol. 72, no. 1-2, pp. 248–254, 1976.

[57] R. F. Beers Jr. and I. W. Sizer, "A spectrophotometric method for measuring the breakdown of hydrogen peroxide by catalase," *The Journal of biological chemistry*, vol. 195, no. 1, pp. 133–140, 1952.

[58] H. Ukeda, D. Kawana, S. Maeda, and M. Sawamura, "Spectrophotometric assay for superoxide dismutase based on the reduction of highly water-soluble tetrazolium salts by xanthine-xanthine oxidase," *Bioscience, Biotechnology and Biochemistry*, vol. 63, no. 3, pp. 485–488, 1999.

[59] J. M. McCord and I. Fridovich, "Superoxide dismutase. An enzymic function for erythrocuprein (hemocuprein)," *Journal of Biological Chemistry*, vol. 244, no. 22, pp. 6049–6055, 1969.

[60] J. Hong, H. Lu, X. Meng, J.-H. Ryu, Y. Hara, and C. S. Yang, "Stability, cellular uptake, biotransformation, and efflux of tea polyphenol (−)-epigallocatechin-3-gallate in HT-29 human colon adenocarcinoma cells," *Cancer Research*, vol. 62, no. 24, pp. 7241–7246, 2002.

[61] P. Bellion, M. Olk, F. Will et al., "Formation of hydrogen peroxide in cell culture media by apple polyphenols and its effect on antioxidant biomarkers in the colon cell line HT-29," *Molecular Nutrition and Food Research*, vol. 53, no. 10, pp. 1226–1236, 2009.

[62] L. H. Long, A. Hoi, and B. Halliwell, "Instability of, and generation of hydrogen peroxide by, phenolic compounds in cell culture media," *Archives of Biochemistry and Biophysics*, vol. 501, no. 1, pp. 162–169, 2010.

[63] Z. Qiusheng, Z. Yuntao, Z. Rongliang, G. Dean, and L. Changling, "Effects of verbascoside and luteolin on oxidative damage in brain of heroin treated mice," *Pharmazie*, vol. 60, no. 7, pp. 539–543, 2005.

[64] L. Lenoir, A. Rossary, J. Joubert-Zakeyh et al., "Lemon verbena infusion consumption attenuates oxidative stress in dextran sulfate sodium-induced colitis in the rat," *Digestive Diseases and Sciences*, vol. 56, no. 12, pp. 3534–3545, 2011.

[65] A. Mestre-Alfaro, M. D. Ferrer, A. Sureda et al., "Phytoestrogens enhance antioxidant enzymes after swimming exercise and modulate sex hormone plasma levels in female swimmers," *European Journal of Applied Physiology*, vol. 111, no. 9, pp. 2281–2294, 2011.

[66] M. B. Crosby, J. Svenson, G. S. Gilkeson, and T. K. Nowling, "A novel PPAR response element in the murine iNOS promoter," *Molecular Immunology*, vol. 42, no. 11, pp. 1303–1310, 2005.

[67] G. D. Girnun, F. E. Domann, S. A. Moore, and M. E. C. Robbins, "Identification of a functional peroxisome proliferator-activated receptor response element in the rat catalase promoter," *Molecular Endocrinology*, vol. 16, no. 12, pp. 2793–2801, 2002.

[68] E. Gray, M. Ginty, K. Kemp, N. Scolding, and A. Wilkins, "The PPAR-gamma agonist pioglitazone protects cortical neurons from inflammatory mediators via improvement in peroxisomal function," *Journal of Neuroinflammation*, vol. 9, article 63, 2012.

[69] X.-M. Zhao, W.-H. Du, D. Wang et al., "Recovery of mitochondrial function and endogenous antioxidant systems in vitrified bovine oocytes during extended *in vitro* culture," *Molecular Reproduction and Development*, vol. 78, no. 12, pp. 942–950, 2011.

[70] S. Vertuani, E. Beghelli, E. Scalambra et al., "Activity and stability studies of verbascoside, a novel antioxidant, in dermocosmetic and pharmaceutical topical formulations," *Molecules*, vol. 16, no. 8, pp. 7068–7080, 2011.

[71] H. Bergmann, D. Rogoll, W. Scheppach, R. Melcher, and E. Richling, "The Ussing type chamber model to study the intestinal transport and modulation of specific tight-junction genes using a colonic cell line," *Molecular Nutrition and Food Research*, vol. 53, no. 10, pp. 1211–1225, 2009.

[72] S. Sang, I. Yang, B. Buckley, C.-T. Ho, and C. S. Yang, "Autoxidative quinone formation *in vitro* and metabolite formation *in vivo* from tea polyphenol (−)-epigallocatechin-3-gallate: studied by real-time mass spectrometry combined with tandem mass ion mapping," *Free Radical Biology and Medicine*, vol. 43, no. 3, pp. 362–371, 2007.

[73] A. P. Neilson, B. J. Song, T. N. Sapper, J. A. Bomser, and M. G. Ferruzzi, "Tea catechin auto-oxidation dimers are accumulated and retained by Caco-2 human intestinal cells," *Nutrition Research*, vol. 30, no. 5, pp. 327–340, 2010.

[74] T. Kawada, R. Asano, K. Makino, and T. Sakuno, "Synthesis of isoacteoside, a dihydroxyphenylethyl glycoside," *Journal of Wood Science*, vol. 48, no. 6, pp. 512–515, 2002.

[75] A. Cardinali, V. Linsalata, V. Lattanzio, and M. G. Ferruzzi, "Verbascosides from olive mill waste water: assessment of their bioaccessibility and Intestinal uptake using an *in vitro* digestion/Caco-2 model system," *Journal of Food Science*, vol. 76, no. 2, pp. H48–H54, 2011.

[76] J. B. Vaidyanathan and T. Walle, "Cellular uptake and efflux of the tea favonoid (−)-epicatechin-3-gallate in the human intestinal cell Line caco-2," *Journal of Pharmacology and Experimental Therapeutics*, vol. 307, no. 2, pp. 745–752, 2003.

[77] A. P. Neilson, J. C. George, E. M. Janle et al., "Influence of chocolate matrix composition on cocoa flavan-3-ol bioaccessibility *in vitro* and bioavailability in humans," *Journal of Agricultural and Food Chemistry*, vol. 57, no. 20, pp. 9418–9426, 2009.

[78] C. M. Peters, R. J. Green, E. M. Janle, and M. G. Ferruzzi, "Formulation with ascorbic acid and sucrose modulates catechin bioavailability from green tea," *Food Research International*, vol. 43, no. 1, pp. 95–102, 2010.

[79] L. Funes, S. Fernández-Arroyo, O. Laporta et al., "Correlation between plasma antioxidant capacity and verbascoside levels in rats after oral administration of lemon verbena extract," *Food Chemistry*, vol. 117, no. 4, pp. 589–598, 2009.

[80] A. Cardinali, F. Rotondo, F. Minervini et al., "Assessment of verbascoside absorption in human colonic tissues using the Ussing chamber model," *Food Research International*, vol. 54, pp. 132–138, 2013.

[81] E. M. Odiatou, A. L. Skaltsounis, and A. I. Constantinou, "Identification of the factors responsible for the *in vitro* pro-oxidant and cytotoxic activities of the olive polyphenols oleuropein and hydroxytyrosol," *Cancer Letters*, vol. 330, no. 1, pp. 113–121, 2013.

Hindawi Publishing Corporation
BioMed Research International
Volume 2014, Article ID 918209, 10 pages
http://dx.doi.org/10.1155/2014/918209

Research Article

Composition, In Vitro Antioxidant and Antimicrobial Activities of Essential Oil and Oleoresins Obtained from Black Cumin Seeds (*Nigella sativa* L.)

Sunita Singh,[1] S. S. Das,[1] G. Singh,[1] Carola Schuff,[2] Marina P. de Lampasona,[2] and César A. N. Catalán[2]

[1] *Chemistry Department, DDU Gorakhpur University, Gorakhpur, Uttar Pradesh 273009, India*
[2] *INQUINOA-CONICET, Instituto de Química Orgánica, Facultad de Bioquímica Química y Farmacia, Universidad Nacional de Tucumán, T4000INI San Miguel de Tucumán, Argentina*

Correspondence should be addressed to G. Singh; gsingh4us@yahoo.com

Received 6 April 2013; Accepted 24 October 2013; Published 6 February 2014

Academic Editor: Afaf K. El-Ansary

Gas chromatography-mass spectrometry (GC-MS) analysis revealed the major components in black cumin essential oils which were thymoquinone (37.6%) followed by p-cymene (31.2%), α-thujene (5.6%), thymohydroquinone (3.4%), and longifolene (2.0%), whereas the oleoresins extracted in different solvents contain linoleic acid as a major component. The antioxidant activity of essential oil and oleoresins was evaluated against linseed oil system at 200 ppm concentration by peroxide value, thiobarbituric acid value, ferric thiocyanate, ferrous ion chelating activity, and 1,1-diphenyl-2-picrylhydrazyl radical scavenging methods. The essential oil and ethyl acetate oleoresin were found to be better than synthetic antioxidants. The total phenol contents (gallic acid equivalents, mg GAE per g) in black cumin essential oil, ethyl acetate, ethanol, and n-hexane oleoresins were calculated as 11.47±0.05, 10.88±0.9, 9.68 ± 0.06, and 8.33 ± 0.01, respectively, by Folin-Ciocalteau method. The essential oil showed up to 90% zone inhibition against *Fusarium moniliforme* in inverted petri plate method. Using agar well diffusion method for evaluating antibacterial activity, the essential oil was found to be highly effective against Gram-positive bacteria.

1. Introduction

Preservation of food degradation, mainly by oxidation processes or by microorganism activity, during production, storage, and marketing is an important issue in the food industry. There is currently a large interest in substituting synthetic food preservatives and synthetic antioxidants for substance that can be marketed as natural. Synthetic antioxidants such as gallates, butylated hydroxytoluene (BHT), butylated hydroxyanisole (BHA), and tert-butyl hydroquinone (TBHQ) were the first preservatives designed for widespread industrial use. However, some physical properties of BHA and BHT, such as their high volatility and instability at elevated temperatures, strict legislation on the use of synthetic food additives, and consumer preferences, have shifted the attention of manufacturers from synthetic to natural antioxidant [1]. It is well known that most spices possess a wide range of biological and pharmacological activities.

Black cumin (*Nigella sativa* L.) belonging to family Ranunculaceae is a spice that has been used for decades for both culinary and medicinal purposes. It is also used as a natural remedy for asthma, hypertension, diabetes, inflammation, cough, bronchitis, headache, eczema, fever, dizziness, and influenza [2]. The seeds are known to be carminative, stimulant, and diuretic [3]. The essential oil from the seeds of this herbaceous plant has been found to contain high concentrations of thymoquinone and its related compounds such as thymol and dithymoquinone, which have been implicated in the prevention of inflammation [4], antioxidant activities [5], such as quenching reactive oxygen species, antimicrobial activity [6], and anticarcinogenic and antiulcer activity [2].

The present paper deals with the chemistry and antioxidative and antimicrobial behavior of essential oil and oleoresins (extracted in ethanol, ethyl acetate, and n-hexane) of black cumin seeds.

2. Materials and Methods

The seeds of black cumin were purchased from the local market of Gorakhpur, Uttar Pradesh, India. A voucher specimen was deposited at the herbarium of the Faculty of Science, DDU Gorakhpur University.

2.1. Reagents. Thiobarbituric acid (TBA), 1,1′-diphenyl-2-picrylhydrazyl radical (DPPH), and linoleic acid are of Acros (New Jersey, USA); butylated hydroxytoluene (BHT), butylated hydroxyanisole (BHA), and propyl gallate (PG) are of S D Fine Chemicals Ltd., Mumbai, India. Folin-Ciocalteu reagent and gallic acid were from Qualigens Chemicals Ltd., Mumbai, India, and Qualikems Chemicals Ltd., New Delhi, India, respectively. Tween 20 and ferrozine were from Merck Pvt. Ltd., Mumbai, India. Ampicillin was purchased from Ranbaxy Fine Chemicals (New Delhi), India. Crude linseed oil was obtained from local oil mill in Gorakhpur. All solvents used were of analytical grade.

2.2. Sample Extraction. Powdered seeds of black cumin (250 g) were subjected to hydrodistillation in Clevenger apparatus for 3 h according to the method recommended by European Pharmacopoeia, [7]. A volatile oil with light orange characteristic odour was obtained with yield of 0.9%. It was dried over anhydrous sodium sulphate and the sample was stored at 4°C before use.

Oleoresins were obtained by extracting 30 g of powdered spice with 300 mL of various solvents (ethanol, ethyl acetate, and n-hexane) for 3 h in Soxhlet extractor. Evaporation of the solvents at reduced pressure gave viscous extracts. The oleoresins were stored in freezer until further use.

2.3. Chemical Characterization

2.3.1. Gas Chromatography-Mass Spectrometry (GC-MS). Analysis of the volatile oils and oleoresins was run on a Hewlett Packard (6890) GC-Ms system coupled to a quadruple mass spectrometer (model HP 5973) with a capillary column of HP-5MS (5% phenyl methylsiloxane; length = 30 m, inner diameter = 0.25 mm, and film thickness = 0.25 μm). GC-MS interphase, ion source, and selective mass detector temperatures were maintained at 280°C, 230°C, and 150°C, respectively. Carrier gas used was helium with a flow rate of 1.0 mL min^{-1}. The oven temperature was programmed as follows.

For essential oil: at 60°C for 1 min then increased from 60 to 185°C at the rate of 1.5°C min^{-1} and held at the rate of 9°C min^{-1} and held at 275°C for 2 min.

For oleoresin: 60°C for zero min then increased from 60 to 300°C at the rate of 1.5°C min^{-1} and held at the rate of 5°C min^{-1} and held at 300°C for 10 min.

2.4. Identification of Components. Most of the components were identified on the basis of comparison of their retention indices and mass spectra with published data [6, 8, 9], and computer matching was done with the Wiley 275 and National Institute of Standards Technology libraries provided with the computer controlling GC-MS systems. The retention indices were calculated using a homologous series of n-alkanes C_8–C_{18} and C_8–C_{22} for essential oil and oleoresins, respectively, which are reported in Tables 1 and 2.

Table 1: Chemical composition of essential oil obtained from black cumin seeds analyzed by GC-MS.

Compounds	%MS	RI[#]	Identification[Φ]
α-Thujene	5.6	919	MS, RI, co-GC
α-Pinene	1.4	928	MS, RI, co-GC
Sabinene	0.8	967	MS, RI, co-GC
β-Pinene	1.7	973	MS, RI, co-GC
α-Phellandrene	0.1	1003	MS, RI
α-Terpinene	0.2	1012	MS, RI, co-GC
p-Cymene	31.4	1019	MS, RI, co-GC
Limonene	1.0	1024	MS, RI, co-GC
1,8-Cineole	0.1	1025	MS, RI, co-GC
γ-Terpinene	0.2	1050	MS, RI, co-GC
trans-Sabinene hydrate	0.1	1101	MS, RI
Unidentified B*	6.8	1113	–
Terpinen-4-ol	1.0	1172	MS, RI, co-GC
p-Cymen-8-ol	Trace	1179	MS, RI
α-Terpineol	Trace	1189	MS, RI, co-GC
Cuminal	Trace	1240	MS, RI
Carvone	Trace	1241	MS, RI
Thymoquinone	37.6	1248	MS, RI
trans-Sabinene hydrate acetate	0.1	1258	MS, RI
Bornyl acetate	0.2	1285	MS, RI
Thymol	0.2	1289	MS, RI
Carvacrol	1.4	1295	MS, RI
α-Longipinene	0.5	1353	MS, RI
Longifolene	2.0	1405	MS, RI
Thymohydroquinone	3.4	1559	MS, RI
10-epi-γ-Eudesmol	0.3	1625	MS, RI
β-Eudesmol	0.5	1652	MS, RI
α-Eudesmol	0.4	1655	MS, RI
Total		90.2%	

Trace < 0.05%; [#]the retention index was calculated using a homologous series of n-alkanes C8–C18; [Φ]Co-GC: coinjection with an authentic sample. Percentages were obtained from electronic integration Trace measurements using a selective mass detector.

3. Antioxidant Activity

The antioxidant activity is system dependent and according to the method adopted and lipid system used as substrate. Hence, different methods have been adopted in order to assess antioxidative potential of black cumin oil and its oleoresins are as follows.

3.1. Chelating Activity on Ferrous Ions. The chelating activity of the aqueous and ethanolic extract on ferrous ions (Fe^{2+}) was measured according to the method described by Decker and Welch [10]. Aliquots of 1 mL of different concentrations

Table 2: Chemical composition of oleoresins obtained from black cumin (*Nigella sativa* L.) seeds in different solvents analysed by GC-MS.

Compounds	M1	M2	M3	RI[#]	Identification[Φ]
α-Thujene	Trace	0.4	0.6	919	MS, RI, co-GC
p-Cymene	0.9	2.8	2.2	1019	MS, RI, co-GC
Unidentified A	0.5	0.5	0.4	1092	–
Thymoquinone	5.7	6.1	3.7	1248	MS, RI
Carvacrol	0.4	Trace	Trace	1295	MS, RI, co-GC
α-Longipinene	Trace	Trace	Trace	1353	MS, RI
Longifolene	0.5	0.6	0.3	1405	MS, RI
Thymohydroquinone	2.5	1.6	0.5	1559	MS, RI
Palmitic acid, ethyl ester	2.8	Trace	Trace	1979	MS, co-GC
Linoleic acid, methyl ester	0.6	0.5	0.5	–	MS, co-GC
Linoleic acid, ethyl ester	11.6	Trace	0.6	–	MS, co-GC
Oleic acid, ethyl ester	4.6	Trace	0.2	–	MS, co-GC
Oleic acid	0.3	Trace	0.2	–	MS, co-GC
Linoleic acid	33.0	43.9	27.7	–	MS,
Linoleic acid, butyl ester	0.9	5.7	16.0	–	MS
Oleic acid, butyl ester	1.2	4.5	7.3	–	MS
Glyceryl palmitate	3.7	1.6	2.3	–	MS
Glyceryl linoleate	27.7	21.9	23.1	–	MS
Sitosterol	Trace	1.3	Trace	–	MS, co-GC
Total	96.4%	90.9%	85.2%		

Trace < 0.05; [#]the retention index was calculated using a homologous series of n-alkanes C8–C20; [Φ]Co-GC: coinjection with an authentic sample.
Percentages were obtained from electronic integration measurements using selective mass detector.
M1: ethanol oleoresin; M2: ethyl acetate oleoresin; M3: n-hexane oleoresin.

of the samples were mixed with 3.7 mL of deionized water. The mixture was incubated with $FeCl_2$ (2 mM, 0.1 mL). After incubation the reaction was initiated by addition of ferrozine (5 mM and 0.2 mL) for 10 min at room temperature, and then the absorbance was measured at 562 nm in a spectrophotometer. A lower absorbance indicates a higher chelating power. The chelating activity of the extract on Fe^{2+} was compared with that of EDTA that was used as positive control. Chelating activity was calculated using the following formula:

$$\text{Chelating activity (\%)} = \left[1 - \left(\frac{\text{Absorbance of sample}}{\text{Absorbance of control}}\right)\right] \times 100. \quad (1)$$

3.2. Scavenging Effect on DPPH. The DPPH assay constitutes a quick and low cost method, which has frequently been used for the evaluation of the antioxidative potential of various natural products, [11]. Due to its odd electron, DPPH gives a strong absorption band at 517 nm (deep violet colour). In the presence of a free radical scavenger, this electron becomes paired, resulting in the absorption loss and consecutive stoichiometric decolorization with respect to the number of electron acquired. The absorbance change produced by this reaction is assessed to evaluate the antioxidant potential of the test sample. 5, 10, 15, and 20 μL of the sample were added to 5 mL of 0.004% methanol solution of DPPH. After a 30 min incubation period at room temperature, the absorbance was read against a blank at 515 nm. All determination was performed in triplicate and results were performed in triplicate and results are reported as scavenging effect (%) versus concentration in Figure 2.

3.3. Estimation of Total Phenolic Content (TPC). TPC were determined using the Folin-Ciocalteu reagent method described by Singleton and Rossi [12]. Gallic acid stock solution (1000 μg mL^{-1}) was prepared by dissolving 100 mg of gallic acid in 100 mL of ethanol. Various dilutions of standard gallic acid were prepared from this stock solution. Calibration curve (Figure 3) was plotted by mixing 1 mL aliquots of 10–100 μg mL^{-1} of gallic acid solutions with 5.0 mL of Folin-Ciocalteu reagent (diluted tenfold) and 4.0 mL of sodium carbonate solution (75 g L^{-1}). The absorbance was measured after 30 min at 20°C at 765 nm.

4. Evaluation of Antioxidant Activity for Linseed Oil System

For present investigation, crude linseed oil, having initial peroxide value 5.2 meq kg^{-1}, was taken to assess the antioxidant activity of black cumin oil and its oleoresins. This oil is most frequently used edible oil in central Europe and is rather unstable because of the presence of substantial amount of linoleic acid. The antioxidant activity of volatile oil and extract was examined by comparing the activity of known antioxidants such as PG, BHT, and BHA by the following peroxide value and thiobarbituric acid value methods.

4.1. Peroxide Value Method. For measuring the peroxide value (PV), a modified oven test was used [13]. The antioxidant activity of black cumin oil and its oleoresins in different solvents were compared with the synthetic antioxidants, such as PG, BHT, and BHA. For this purpose, calculated quantities of each (200 ppm) were dissolved to 30 g of linseed oil in an open mouthed beaker. The mixtures were thoroughly homogenized and placed in incubator at 80°C. The peroxide values (meq of oxygen kg^{-1}) were measured in every seven days and test was replicated for three times. A control sample was prepared under similar condition without any additive. The effects of oil and oleoresins in term of peroxidation at 90°C are shown in Figure 4.

4.2. Thiobarbituric Acid Value (TBA). TBA value of different samples was determined according to the method previously reported [13]. About 100 mg of oil sample was dissolved in 25 mL of 1-butanol. A 25 mL aliquot of the above solution was mixed thoroughly with 5.0 mL of TBA reagent (200 mg TBA in 100 mL of 1-butanol) and incubated at 95°C. After 2 h, the reaction mixture was cooled to room temperature under running water and absorbance was measured at 530 nm with Hitachi-U-2000 spectrophotometer (Tokyo, Japan). At the same time, a reagent blank (without TBA reagent) was also done. The thiobarbituric acid value (meq of malondialdehyde per g) was calculated as

$$\text{TBA value} = \frac{50 \times (A - B)}{M}, \quad (2)$$

where A is absorbance of the test sample, B is absorbance of the reagent blank, and M is mass of the sample.

4.3. Determination of Antioxidant Activity in Linoleic Acid System. Antioxidant activity of black cumin oil and its oleoresins was compared to synthetic standards according to the ferric thiocyanate method in linoleic acid emulsion [14]. The reaction medium contained black cumin oil and oleoresins at the concentration of 1 mg/100 mL of absolute ethanol (2 mL), an emulsion of 2.51% linoleic acid in ethanol (2 mL), 4 mL of 0.05 M-phosphate buffer (pH = 7.0), and 2 mL of distilled water. The solution (10 mL) was mixed and incubated at 40°C in the dark. The same solution, without any additives, was taken as control sample. At regular intervals during incubation, 0.1 mL aliquot of the mixture was diluted with 9.7 mL of 75% ethanol followed by the addition of 0.2 mL of 30% ammonium thiocyanate and 0.1 mL of 20 mM of $FeCl_2$ in 3.5% HCl; the absorbance of red colour was measured at 500 nm in Hitachi-U-2000 spectrophotometer (Tokyo, Japan). The control and standard were subjected to the same procedure except for the control, where there was no addition of sample and for the standard 1 mL of sample were replaced with 1 mg of PG, BHT, and BHA. These steps are repeated every 48 h until the control sample reached its maximum. Low absorbance value indicates the efficiency of the test samples to inhibit lipid oxidation. The results were reported as incubation time versus absorbance in Figure 6.

5. Antimicrobial Investigations

5.1. Antifungal Assay. The antifungal activity of the essential oil and extract against various pathogenic fungi, *Aspergillus lavus* (1884), *Aspergillus niger* (2479), *Fusarium moniliforme* (1893), *Fusarium graminearum* (2088), and *Penicillium viridicatum* (2007), were tested by the inverted petri plate [15] and poison food medium methods [16]. All the fungi cultures were procured from the Microbial Type Culture Collection (MTCC) and their reference numbers are given in the parentheses. The cultures were maintained in Czapek agar medium. Each test was replicated three times and fungi toxicity was measured in terms of percentage mycelial inhibition calculated with the following equation:

$$\text{mycelial inhibition (\%)} = \left[\frac{(d_c - d_t)}{d_c}\right] \times 100, \quad (3)$$

where d_c and d_t are the average diameters of the mycelial colony of the control and treated sets, respectively.

5.2. Antibacterial Assay. The essential oil and extract were individually tested against a panel of microorganisms using agar well diffusion method [17]. Three Gram-positive bacteria, *Staphylococcus aureus* (3103), *Bacillus cereus* (430), and *Bacillus subtilis* (1790), and two Gram negative bacteria, *Escherichia coli* (1672) and *Pseudomonas aeruginosa* (1942). All the bacterial strains were procured from the Microbial Type Culture Collection (MTCC), Institute of Microbial Technology (Chandigarh, India), and their reference numbers are given in parentheses. The bacterial cultures were grown on nutrient agar medium and stored at 4°C. In order to prepare a bacterial strain for test, initially one loopful of bacterial culture was transferred from slant to nutrient broth solution (10 mL) and was stored at 37°C for 24 h. The control plate without the addition of essential oil or extract containing DMSO was also maintained under the same conditions. After incubating for 24 h at 37°C, all plates were examined for any zones of growth inhibition and the diameters of these zones were measured in millimeters.

6. Statistical Analysis

For the essential oil or oleoresin, three samples were prepared for assays of every antioxidant and antimicrobial attribute. The data are presented as mean (standard deviation of three determinations (data are not shown). Statistical analyses were performed using a one-way analysis of variance [18]. A probability value of $P < 0.05$ was considered to be significant.

7. Results and Discussions

7.1. Phytochemistry. Careful and detailed interpretations of the experimental GC-MS data (EM fragmentation, retention indices) were carried out which permitted identification of a large number of components in essential oil and oleoresins (Tables 1 and 2). Table 1 shows identification of 33 components in black cumin oil, representing about 90.2% of the total amount. The major component in black cumin oil

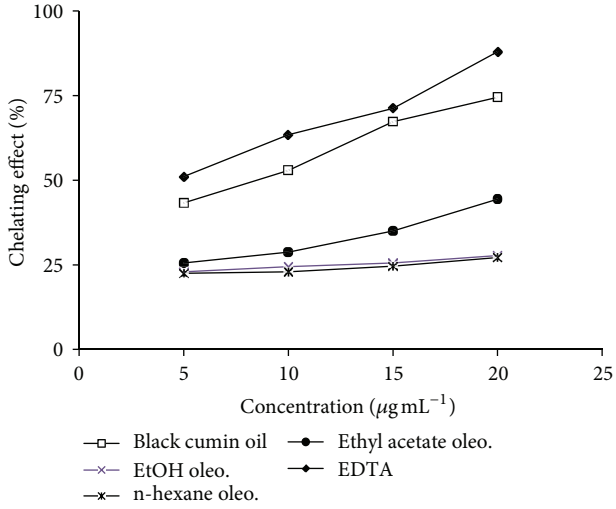

Figure 1: Chelating effect of black cumin oil and its different oleoresins.

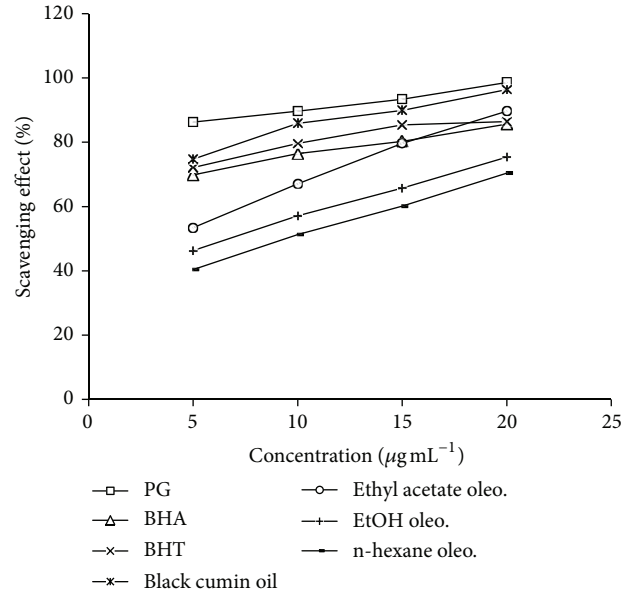

Figure 2: Scavenging effect (%) of black cumin oil and its oleoresins on DPPH radical.

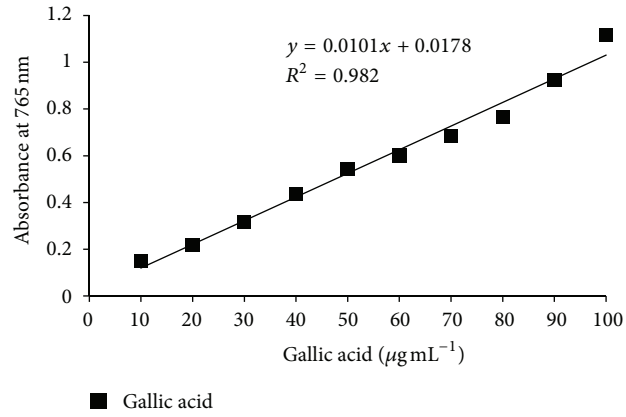

Figure 3: Calibration curve of gallic acid.

was thymoquinone (37.6%) followed by p-cymene (31.4%), α-thujene (5.6%), thymohydroquinone (3.4%), longifolene (2.0%), and carvacrol (1.4%). Burits and Bucar [8] characterized many components in black cumin essential oil such as thymoquinone (27.8–57.0%), p-cymene (7.1–15.5%), carvacrol (5.8–11.6%), trans-anethole (0.25–2.3%), 4-terpineol (2.0–6.6%), and 1.0–8.0% of longifolene. These results are slight different from the work reported by Hajhashemi et al. [19] who reported that p-cymene (37.3%) and thymoquinone (13.7%) were the major components of black cumin. Singh et al. [6] also reported p-cymene as the major component in the black cumin essential oil.

From Table 2, it is evident that, in ethanol oleoresin, 19 components constitute 96.4% of the total weight; in the ethyl acetate oleoresin, a total of 19 components making 90.9% of the whole mass and, in case of n-hexane oleoresin, 19 compounds constituting about 85.2% of the total weight were identified. The oleoresins were mainly comprised of unsaturated fatty acids and their different esters. The major components in all three oleoresins were linoleic acid (unsaturated fatty acid) followed by glyceryl linoleate, glyceryl palmitate, oleic acid, and other minor components. The presence of unsaturated fatty acids in oleoresins was well supported by the various reported work [20–26].

7.2. Antioxidant Investigations

7.2.1. Chelating Activity on Ferrous Ions. The ferrous ion (Fe^{2+}) chelating effect of black cumin oil and its different oleoresins is presented in Figure 1. The chelating activity of the extracts was concentration dependent. Black cumin oil exhibited higher chelating activity in comparison to the oleoresins but was not effective chelator as EDTA. Maximum chelating of metal ions at 200 μg mL^{-1} for black cumin oil and EDTA was found to be 74.56% and 87.90%, respectively, whereas the oleoresins were less effective in metal chelation and their metal chelating activity ranges from 22.1 to 44.5%.

7.2.2. Scavenging Effect on DPPH Radical. DPPH$^{\bullet}$ is a stable radical showing a maximum absorbance at 515 nm. In DPPH$^{\bullet}$ assay, the antioxidant was able to reduce the stable radical DPPH to the yellow-colored diphenylpicrylhydrazone. The method is based on the reduction of DPPH$^{\bullet}$ in alcoholic solution in the presence of a hydrogen-donating antioxidant due to formation of the nonradical form DPPH-H in the reaction. DPPH$^{\bullet}$ is usually used as a reagent to evaluate free radical and accepts an electron or hydrogen radical to become a stable diamagnetic molecule. The disappearance of the DPPH radical absorption at 515 nm by the action of antioxidants is taken as a measure of antioxidant activity. The scavenging effects of black cumin oil and oleoresins on DPPH radical linearly increased as concentration increased from 5 to 20 μg mL^{-1} (Figure 2). At 20 μg mL^{-1} the scavenging activity of black cumin oil and ethyl acetate oleoresin was 95.4% and 89.75%, respectively, comparatively higher than

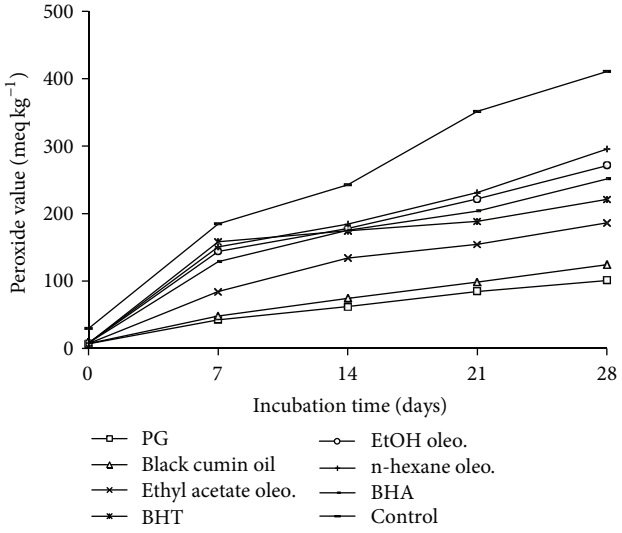

Figure 4: Inhibitory effect of black cumin oil and its oleoresins on the primary oxidation of linseed oil measured using peroxide value method.

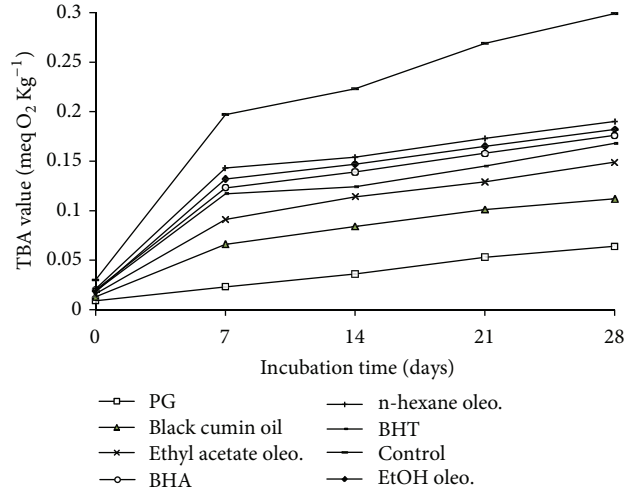

Figure 5: Inhibitory effect of black cumin oil and its oleoresins on the primary oxidation of linseed oil measured using TBA value method.

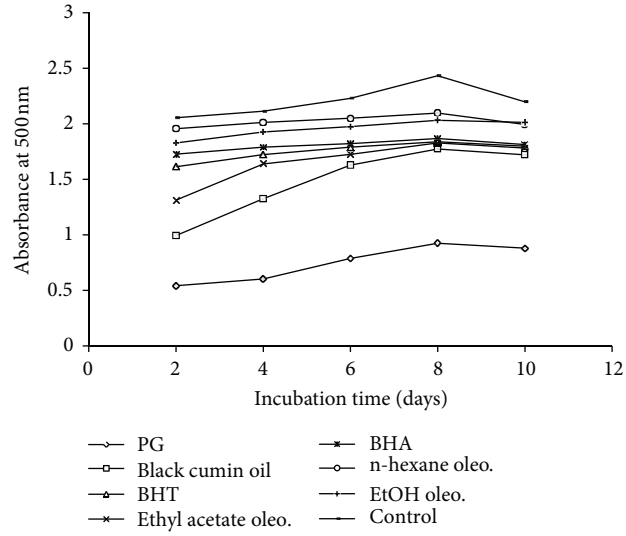

Figure 6: Inhibitory effect of black cumin oil and its oleoresins on the primary oxidation of linoleic acid system measured using ferric thiocyanate method.

BHT and BHA but lower than PG. However the scavenging activity of BHA, BHT, and PG was more effective at lower concentration and was 69.8%, 72.1%, and 86.3% at 5 μg mL^{-1} but as the concentration increases the differences in scavenging activity between BHA, BHT, and oleoresins (specially ethyl acetate) become less significant. Ethanol and n-hexane oleoresins showed moderate scavenging activity.

7.2.3. Estimation of TPC. The amount of total phenols was determined with Folin-Ciocalteu reagent. Gallic acid was used as standard compound. The absorbance for various dilutions of gallic acid with Folin-Ciocalteu reagent and sodium carbonate was obtained and found standard curve equation: $y = 0.0101x + 0.0178$, $R^2 = 0.982$ (Figure 3). The total phenol contents (gallic acid equivalents, mg GAE per g) in black cumin essential oil, ethyl acetate, ethanol and n-hexane oleoresins were calculated as 11.47 ± 0.05, 10.88 ± 0.9, 9.68 ± 0.06, and 8.33 ± 0.01, respectively. The value suggests that the black cumin oil and its oleoresins have lesser amount of total phenols [27]. The differences in the total phenolic content among the samples might be due to many differences, such as the environmental conditions, genetic background, or agricultural techniques applied.

7.3. Antioxidant Assays in Linseed Oil System. The changes of PV in linseed oil of all investigated samples are presented in Figure 4. The rate of oxidative reactions in linseed oil with additives was almost similar to that of the blank sample. The stability of the linseed oil samples to the formation of peroxides can be ranked in the following descending order:

PG > Black cumin oil > Ethyl acetate oleo. > BHT > BHA > EtOH oleo. > n-hexane oleo. > Control.

Simultaneously with the measurements of PV, changes in secondary product such as malondialdehyde, the compound used as an indicator of lipid peroxidation was measured by TBA values (Figure 5), were also determined after every seven days. Black cumin oil and its ethyl acetate oleoresin showed strong inhibition at 0.02% concentration as compared to BHT and BHA ($P < 0.05$) but lower than PG whereas the ethanol and n-hexane oleoresin showed moderate inhibition at 0.02% concentration as compared to the other additives. From the above results, it should be confirmed that formation of primary oxidation species, peroxides, was quite similar with the secondary oxidation products and the changes of both oxidation characteristics are in a good correlation.

7.4. Antioxidant Activity in Linoleic Acid System. The FTC method was used to measure the amount of peroxides at

the primary stage of linoleic acid peroxidation (Figure 6). Since the concentration of the peroxide decreases as the antioxidant activity increases, the intensity of the pigment will be reduced, leading to lower absorbance. Absorbance values of the control as well as black cumin oil and its oleoresins increase until day 10 and then decreased on day 12 due to the malondialdehyde formation from linoleic acid oxidation. There was a significant difference ($P < 0.05$) between the control and the tested essential oil and oleoresins. As can be seen in Figure 6, both black cumin oil and oleoresins showed good antioxidative property in the linoleic acid system and were significantly ($P < 0.05$) different from the control.

Antioxidant activities of essential oils and oleoresins may be related to the diverse compounds present in them including terpenes, sesquiterpenes, and phenolic acids, which act in various ways such as inhibition of peroxidation, scavenging the radicals, and chelating the metal ions. The main constituents of black cumin oil were thymoquinone (37.6%) and p-cymene (31.4%) with minor amounts of longifolene, carvacrol, and thymohydroquinone which were responsible for the antioxidant activity of black cumin oil [8, 9, 19, 28–31]. Furthermore, free radical scavenging effects of these components were studied on the reactions generating reactive oxygen species such as superoxide anion radical, hydroxyl radical using spectrophotometric methods [5]. The results obtained using different assays were well correlated with the previous work reported be many workers [5, 30] who found thymoquinone as a main constituent responsible for the activity. It has been suggested that phenolic content is correlated with the antioxidant activity [32]. It is considered that the antioxidant activity of phenolic compounds is due to their high redox potentials, which allow them to act as reducing agents, hydrogen donors. Thymoquinone was also present in small amount with higher percentage of unsaturated fatty acid, linoleic acid, in different oleoresins. Studies [33] have shown that these unsaturated fatty acids have anti-rather than pro-oxidant activity but still research has been going on for the exact role of unsaturated fatty acids against the oxidative stress.

7.5. Antimicrobial Investigations. Using inverted petri plate technique (Table 3), the volatile oil exhibited more than 90% zone inhibition for *F. moniliforme* and *P. viridicatum*. It was also found to be highly effective in controlling the growth of *Aspergillus* species and *F. graminearum* where (50%) and (65%) zone inhibition was observed, respectively. For other tested fungi, the essential oil exerted less activity. However using the same method, the oleoresins have revealed less activity except for *F. moniliforme*, in which only up to 40% mycelial zone inhibition was obtained. Moreover using food poison technique (Table 4), the volatile oil showed clear zone of growth inhibition against *F. graminearum* at 10 μL. The volatile oil showed strong antifungal activity against all tested *Aspergillus* species in the food poison method. Ethyl acetate and ethanol oleoresin showed up to 30% zone inhibition at 10 μL dose. The n-hexane oleoresin showed very feeble inhibition zone in both techniques. The lower antimicrobial efficacy of the oleoresins is due to their low volatility [34].

The antibacterial investigations were undertaken using agar well diffusion method (Table 4). Using this method, the black cumin oil has shown better activity than oleoresins and commercial bactericide, that is, ampicillin. The volatile oil was found to be highly effective against *B. subtilis, B. cereus, and S. aureus* and showed complete zone of inhibition at 3000 ppm concentration whereas in oleoresins more than 20 mm inhibition was obtained for Gram-positive bacteria. In addition, more than 20 and 25 mm zone inhibition was obtained for *P. aeruginosa* and *E. coli*. The results obtained using agar well diffusion method were well correlated with the earlier reported work [6, 30, 35] where black cumin seed oil has been shown to be effective against a wide spectrum of organisms, bacteria like *B. cereus, B. subtilis, S. aureus, S. epidermis, E. coli,* and *P. aeruginosa*.

The results obtained in antimicrobial investigations of black cumin oil and oleoresins were in good agreement with the previous reported work [36]. Thymoquinone, p-cymene (monoterpene), longifolene (sesquiterpene), and thymohydroquinone were responsible for strong antimicrobial activity of black cumin oil [29]. El Alfy et al. [35] isolated thymohydroquinone as antimicrobial compound from the volatile oil of *Nigella sativa* seeds. Oleoresins have high concentration of unsaturated fatty acids along with thymohydroquinone in small amount which is responsible for its moderate antimicrobial effects. Long chain fatty acids like linoleic acid and oleic acid were previously reported to possess antibacterial and antifungal activity [36–39]. *p*-Cymene is not an efficient antimicrobial compound when used alone, but it potentiate the activity of compounds like carvacrol [40]. The antimicrobial activity of essential oils can often be correlated to its content of phenolic constituents. The type of bacteria also has an influence on the effectiveness of the volatile oil and oleoresins. Gram-negative bacteria were generally less susceptible than Gram-positive bacteria [41]. The difference in the susceptibility of the bacteria arises as a result of differences in their cell membrane structure which is more complex in case of Gram-negative bacteria. The antimicrobial activity of a given essential oil may depend on only one or two of the major constituents that make up the oil. However, increasing amounts of evidence indicate that the inherent activity of essential oils may not only rely exclusively on the ratio in which the main active constituents are present, but also on interactions between these and minor constituents in the oils and oleoresins.

8. Conclusions

Seeds of black cumin seem to possess magical properties and have been worked out extensively. This study revealed that black cumin essential oil and its oleoresins constitute a good alternative source of essential fatty acids compared with common vegetable oil. The present results showed that essential oil and oleoresins of black cumin exhibited higher antioxidant activity than synthetic antioxidants. These findings could be used to prepare multipurpose products for pharmaceutical applications and its usage as dietary source of

Table 3: (a) Antifungal investigations of black cumin oil and its oleoresins (% zone inhibition[a]) using inverted petriplate method. (b) Antifungal investigations of black cumin oil and its oleoresins (% zone inhibition) using food poisoned method.

(a)

		Mycelial zone inhibition at different doses[a] of sample (%)				
Samples	Doses (μL)	AN	AF	FM	FG	PV
Black cumin oil	5	43.6 ± 0.30	45.7 ± 1.3	71.2 ± 0.50	39.7 ± 0.14	34.7 ± 0.6
	10	80.9 ± 0.36	70.3 ± 1.8	89.7 ± 0.20	65.7 ± 0.17	87.6 ± 0.7
EtOH oleoresin	5	5.7 ± 0.20	8.9 ± 0.20	17.8 ± 2.4	10.0 ± 0.20	9.9 ± 0.36
	10	11.2 ± 0.30	13.2 ± 0.30	41.9 ± 0.3	11.3 ± 0.14	13.7 ± 0.40
n-Hexane oleoresin	5	0.2 ± 0.44	4.3 ± 0.17	4.5 ± 1.2	2.4 ± 0.36	5.6 ± 0.54
	10	5.5 ± 0.46	7.6 ± 0.14	39.8 ± 0.1	9.1 ± 0.41	9.7 ± 0.6
Ethyl acetate oleoresin	5	19.8 ± 0.20	11.2 ± 0.7	20.1 ± 2.1	19.6 ± 1.1	18.1 ± 0.6
	10	25.2 ± 0.26	16.4 ± 3.6	49.2 ± 2.3	31.1 ± 1.7	20.9 ± 0.8

[a]Average of three replicates.
AN: *Aspergillus niger*, AF: *Aspergillus flavus*, FM: *Fusarium moniliforme*, FG: *Fusarium graminearum*, and PV: *Penicillium viridicatum*.
(−): no inhibition.

(b)

		Mycelial zone inhibition[a] at different doses of sample (%)				
Samples	Doses (ppm)	AN	AF	FM	FG	PV
Black cumin oil	5	65.9 ± 0.9	60.3 ± 0.1	42.2 ± 1.8	93.2 ± 1.2	50.8 ± 1.5
	10	81.2 ± 1.3	77.8 ± 0.2	61.7 ± 0.7	100 ± 0.8	55.4 ± 0.3
Ethanol oleoresin	5	25.2 ± 2.1	22.4 ± 1.7	–	31 ± 1.9	–
	10	30.3 ± 2.1	29.8 ± 1.4	10.7 ± 0.8	33.7 ± 1.4	–
n-Hexane oleoresin	5	16.7 ± 0.7	14.4 ± 0.6	–	17.9 ± 1.5	–
	10	21.4 ± 2.1	17.4 ± 0.1	–	19.9 ± 2.3	–
Ethyl acetate oleoresin	5	28.4 ± 1.4	23.7 ± 0.4	–	21.4 ± 1.4	–
	10	35.2 ± 1.1	28.4 ± 0.5	15.3 ± 1.2	25.9 ± 0.7	–

[a]Average of three replicates.
AN: *Aspergillus niger*, *AF*: *Aspergillus flavus*, FM: *Fusarium moniliforme*, FG: *Fusarium graminearum*, and PV: *Penicillium viridicatum*.
(−): no inhibition.

Table 4: Antibacterial activity of black cumin oil and its oleoresinsagainst a few bacterial species using agar well diffusion method.

		Diameter of inhibition zone (mm[a])				
Samples	Doses (ppm[b])	BS	BC	SA	EC	PA
Black cumin oil	1000	++	25.3 ± 1.4	++	–	18.9 ± 0.17
	3000	++	++	++	20.3 ± 0.14	27.9 ± 0.15
Ethanol oleoresin	1000	16.4 ± 0.81	–	15.6 ± 0.36	–	–
	3000	28.3 ± 0.20	–	25.9 ± 0.42	–	–
n-Hexane oleoresin	1000	11.5 ± 0.31	–	9.1 ± 1.1	–	–
	3000	20.9 ± 1.9	–	13.4 ± 2.6	–	–
Ethyl acetate oleoresin	1000	22.3 ± 0.8	–	17.7 ± 2.3	–	–
	3000	44.3 ± 0.7	–	40.9 ± 1.2	–	–
Ampicillin	1000	15.6 ± 0.32	–	9.1 ± 1.1	–	–
	3000	13.2 ± 0.2	–	13.4 ± 2.6	–	–

[a]Average of three replicates; ++ indicates complete inhibition and − indicates no inhibition.
[b]DMSO was used as solvent.
BS: *Bacillus subtilis*; SA: *Staphylococcus aureus*; BC: *Bacillus cereus*. EC: *Escherichia coli*; PA: *Pseudomonas aeruginosa*.

antioxidant should be considered largely for alleviating and ameliorating diseases.

Conflict of Interests

The authors declare that there is no conflict of interests regarding the publication of this paper.

Acknowledgments

The authors are grateful to the Head of Department of Chemistry, DDU Gorakhpur, University, Gorakhpur for providing laboratory facilities. The financial support from UGC to Sunita Singh (JRF) and Emeritus Fellow to Dr. Gurdip Singh is also acknowledged.

References

[1] G. Zengin, A. Aktumsek, G. O. Guler, Y. S. Cakmak, and E. Yildiztugay, "Antioxidant properties of methanolic extract and fatty acid composition of *Centaurea urvillei* DC. subsp. *hayekiana* Wagenitz," *Records of Natural Products*, vol. 5, no. 2, pp. 123–132, 2011.

[2] H. Lutterodt, M. Luther, M. Slavin et al., "Fatty acid profile, thymoquinone content, oxidative stability, and antioxidant properties of cold-pressed black cumin seed oils," *Food Science and Technology*, vol. 43, no. 9, pp. 1409–1413, 2010.

[3] S. Shah and K. S. Ray, "Study on antioxidant and antimicrobial properties of black cumin (*Nigella sativa* Linn)," *Journal of Food Science and Technology*, vol. 40, no. 1, pp. 70–73, 2003.

[4] I. Tekeoglu, A. Dogan, and L. Demiralp, "Effects of thymoquinone (volatile oil of black cumin) on rheumatoid arthritis in rat models," *Phytotherapy Research*, vol. 20, no. 10, pp. 869–871, 2006.

[5] I. Kruk, T. Michalska, K. Lichszteld, A. Kladna, and H. Y. Aboul-Enein, "The effect of thymol and its derivatives on reactions generating reactive oxygen species," *Chemosphere*, vol. 41, no. 7, pp. 1059–1064, 2000.

[6] G. Singh, P. Marimuthu, C. S. De Heluani, and C. Catalan, "Chemical constituents and antimicrobial and antioxidant potentials of essential oil and acetone extract of *Nigella sativa* seeds," *Journal of the Science of Food and Agriculture*, vol. 85, no. 13, pp. 2297–2306, 2005.

[7] S. A. Maisonneuve, *European Pharmacopoeia, Part 1*, Sainte-Ruffine, 1983.

[8] M. Burits and F. Bucar, "Antioxidant activity of Nigella sativaessential oil," *Phytotherapy Research*, vol. 14, pp. 323–328, 2000.

[9] N. Ilaiyaraja and F. Khanum, "*Nigella sativa* L: a review of therapeutic applications," *Journal of Herbal Medicine and Toxicology*, vol. 4, no. 2, pp. 1–8, 2010.

[10] E. A. Decker and B. Welch, "Role of ferritin as a lipid oxidation catalyst in muscle food," *Journal of Agricultural and Food Chemistry*, vol. 38, no. 3, pp. 674–677, 1990.

[11] W. Brand-Williams, M. E. Cuvelier, and C. Berset, "Use of a free radical method to evaluate antioxidant activity," *Food Science and Technology*, vol. 28, no. 1, pp. 25–30, 1995.

[12] V. L. Singleton and J. A. Rossi, "Colorimetry of total phenolics with phosphomolybdic-phosphotungstic as it reagents," *The American Journal of Enology and Viticulture*, vol. 16, pp. 144–158, 1965.

[13] K. D. Economou, V. Oreopoulou, and C. D. Thomopoulos, "Antioxidant activity of some plant extracts of the family labiatae," *Journal of the American Oil Chemists Society*, vol. 68, no. 2, pp. 109–113, 1991.

[14] G. Singh, S. Maurya, M. P. de Lampasona, and C. A. N. Catalan, "A comparison of chemical, antioxidant and antimicrobial studies of cinnamon leaf and bark volatile oils, oleoresins and their constituents," *Food and Chemical Toxicology*, vol. 45, no. 9, pp. 1650–1661, 2007.

[15] G. Singh, I. P. S. Kapoor, P. Singh, C. S. de Heluani, M. P. de Lampasona, and C. A. N. Catalan, "Chemistry, antioxidant and antimicrobial investigations on essential oil and oleoresins of Zingiber officinale," *Food and Chemical Toxicology*, vol. 46, no. 10, pp. 3295–3302, 2008.

[16] G. P. Rao and A. K. Shrivastava, "Toxicity of essential oils of higher plants against fungal pathogens of sugarcane," in *Current Trend in Sugarcane Pathology*, G. P. Rao, A. G. Gillasple, P. P. Upadhaya, A. Bergamin, V. P. Agnihotri, and C. T. Chen, Eds., pp. 347–365, International Books and Periodicals Supply Service, Delhi, India, 1994.

[17] K. Ramadas, G. Suresh, N. Janarthanan, and S. Masilamani, "Antifungal activity of 1,3-disubstituted symmetrical and unsymmetrical thioureas," *Pesticide Science*, vol. 52, no. 2, pp. 145–151, 1998.

[18] NCCLS (National Committee for Clinical Laboratory Standards), *Performance Standards for Antimicrobial Disc Susceptibility Test*, 6th edition, 1997.

[19] V. Hajhashemi, A. Ghannadi, and H. Jafarabadi, "Black cumin seed essential oil, as a potent analgesic and antiinflammatory drug," *Phytotherapy Research*, vol. 18, no. 3, pp. 195–199, 2004.

[20] P. J. Houghton, R. Zarka, B. De Las Heras, and J. R. S. Hoult, "Fixed oil of *Nigella sativa* and derived thymoquinone inhibit eicosanoid generation in leukocytes and membrane lipid peroxidation," *Planta Medica*, vol. 61, no. 1, pp. 33–36, 1995.

[21] M. T. Sultan, M. S. Butt, F. M. Anjum, A. Jamil, S. Akhtar, and M. Nasir, "Nutritional profile of indigenous cultivar of black cumin seeds and antioxidant potential of its fixed and essential oil," *Pakistan Journal of Botany*, vol. 41, no. 3, pp. 1321–1330, 2009.

[22] S. Cheikh-Rouhou, S. Besbes, G. Lognay, C. Blecker, C. Deroanne, and H. Attia, "Sterol composition of black cumin (*Nigella sativa* L.) and Aleppo pine (*Pinus halepensis* Mill.) seed oils," *Journal of Food Composition and Analysis*, vol. 21, no. 2, pp. 162–168, 2008.

[23] M. F. Ramadan, "Nutritional value, functional properties and nutraceutical applications of black cumin (*Nigella sativa* L.): an overview," *International Journal of Food Science and Technology*, vol. 42, no. 10, pp. 1208–1218, 2007.

[24] T. D. Parker, D. A. Adams, K. Zhou, M. Harris, and L. Yu, "Fatty acid composition and oxidative stability of cold-pressed edible seed oils," *Journal of Food Science*, vol. 68, no. 4, pp. 1240–1243, 2003.

[25] J. Parry, L. Su, M. Luther et al., "Fatty acid composition and antioxidant properties of cold-pressed marionberry, boysenberry, red raspberry, and blueberry seed oils," *Journal of American Oil Chemical Society*, vol. 83, pp. 847–854, 2006.

[26] J. Parry, L. Su, M. Luther et al., "Fatty acid composition and antioxidant properties of cold-pressed marionberry, boysenberry, red raspberry, and blueberry seed oils," *Journal of Agricultural and Food Chemistry*, vol. 53, no. 3, pp. 566–573, 2005.

[27] R. R. Sokal, *Introduction to Biostatistics*, W. H. Freeman, San Francisco, Calif, USA, 1973.

[28] H. Hosseinzadeh, S. Parvardeh, M. N. Asl, H. R. Sadeghnia, and T. Ziaee, "Effect of thymoquinone and *Nigella sativa* seeds oil on lipid peroxidation level during global cerebral ischemia-reperfusion injury in rat hippocampus," *Phytomedicine*, vol. 14, no. 9, pp. 621–627, 2007.

[29] S. Bourgou, A. Pichette, B. Marzouk, and J. Legault, "Bioactivities of black cumin essential oil and its main terpenes from Tunisia," *South African Journal of Botany*, vol. 76, no. 2, pp. 210–216, 2010.

[30] H. J. Harzallah, E. Noumi, K. Bekir et al., "Chemical composition, antibacterial and antifungal properties of Tunisian *Nigella sativa* fixed oil," *African Journal of Microbiology Research*, vol. 6, no. 22, pp. 4675–4679, 2012.

[31] V. S. Deepa and P. S. Kumar, "Preliminary phytochemical investigations and in vitro antioxidant activity in selected parts of *Andrographis* spp," *Journal of Pharmacological Research*, vol. 3, no. 9, pp. 2206–2210, 2010.

[32] M. Amensour, E. Sendra, A. Jamal, S. Bouhdid, J. A. Pérez-Alvarez, and J. Fernández-López, "Total phenolic content and antioxidant activity of myrtle (Myrtus communis) extracts," *Natural Product Communications*, vol. 4, no. 6, pp. 819–824, 2009.

[33] M. Di Nunzio, V. Valli, and A. Bordoni, "Pro- and anti-oxidant effects of polyunsaturated fatty acid supplementation in HepG2 cells," *Prostaglandins Leukotrienes and Essential Fatty Acids*, vol. 85, no. 3-4, pp. 121–127, 2011.

[34] G. Singh, S. Maurya, C. Catalan, and M. P. de Lampasona, "Studies on essential oils, part 42: chemical, antifungal, antioxidant and sprout suppressant studies on ginger essential oil and its oleoresin," *Flavour and Fragrance Journal*, vol. 20, no. 1, pp. 1–6, 2005.

[35] T. S. El Alfy, H. M. El Fatatry, and M. A. Toama, "Isolation and structure assignment of an antimicrobial principle from the volatile oil of *Nigella sativa* L. seeds," *Pharmazie*, vol. 30, no. 2, pp. 109–111, 1975.

[36] M. A. Khan, "Chemical composition and medicinal properties of *Nigella sativa* Linn," *Inflammopharmacology*, vol. 7, no. 1, pp. 15–35, 1999.

[37] L. J. McGaw, A. K. Jäger, and J. van Staden, "Isolation of antibacterial fatty acids from *Schotia brachypetala*," *Fitoterapia*, vol. 73, no. 5, pp. 431–433, 2002.

[38] A. R. McCutcheon, T. E. Roberts, E. Gibbons et al., "Antiviral screening of British Columbian medicinal plants," *Journal of Ethnopharmacology*, vol. 49, no. 2, pp. 101–110, 1995.

[39] S. Javed, A. A. Shahid, M. S. Haider et al., "Nutritional, phytochemical potential and pharmacological evaluation of *Nigella Sativa* (Kalonji) and *Trachyspermum Ammi* (Ajwain)," *Medicinal Plants Research*, vol. 6, no. 5, pp. 768–775, 2012.

[40] P. Rattanachaikunsopon and P. Phumkhachorn, "Assessment of factors influencing antimicrobial activity of carvacrol and cymene against *Vibrio cholerae* in food," *Journal of Bioscience and Bioengineering*, vol. 110, no. 5, pp. 614–619, 2010.

[41] M. Gilles, J. Zhao, M. An, and S. Agboola, "Chemical composition and antimicrobial properties of essential oils of three *Australian Eucalyptus* species," *Food Chemistry*, vol. 119, no. 2, pp. 731–737, 2010.

Hindawi Publishing Corporation
BioMed Research International
Volume 2014, Article ID 740105, 15 pages
http://dx.doi.org/10.1155/2014/740105

Research Article

The Renal Effects of Vanadate Exposure: Potential Biomarkers and Oxidative Stress as a Mechanism of Functional Renal Disorders—Preliminary Studies

Agnieszka Ścibior,[1,2] Dorota Gołębiowska,[1,2] Agnieszka Adamczyk,[1] Irmina Niedźwiecka,[1] and Emilia Fornal[3]

[1] *Laboratory of Physiology and Animal Biochemistry, Department of Zoology and Invertebrate Ecology, Institute of Environmental Protection, The John Paul II Catholic University of Lublin, 102 Kraśnicka Avenue, 20-718 Lublin, Poland*
[2] *Laboratory of Oxidative Stress, Center for Interdisciplinary Research, The John Paul II Catholic University of Lublin, 102 Kraśnicka Avenue, 20-718 Lublin, Poland*
[3] *Laboratory of Separation and Spectroscopic Method Applications, Center for Interdisciplinary Research, The John Paul II Catholic University of Lublin, 102 Kraśnicka Avenue, 20-718 Lublin, Poland*

Correspondence should be addressed to Agnieszka Ścibior; cellbiol@kul.lublin.pl

Received 30 April 2013; Revised 22 October 2013; Accepted 28 October 2013; Published 28 January 2014

Academic Editor: Maha Zaki Rizk

The alterations in the levels/activities of selected biomarkers for detecting kidney toxicity and in the levels of some oxidative stress (OS) markers and elements were studied in male rats to evaluate biochemically the degree of kidney damage, investigate the role of OS in the mechanism of functional renal disorders, reveal potential biomarkers of renal function, and assess the renal mineral changes in the conditions of a 12-week sodium metavanadate (SMV, 0.125 mg V/mL) exposure. The results showed that OS is involved in the mechanism underlying the development of SMV-induced functional renal disturbances. They also suggest that the urinary cystatin C ($CysC_u$) and kidney injury molecule-1 ($KIM\text{-}1_u$) could be the most appropriate to evaluate renal function at the conditions of SMV intoxication when the fluid intake, excreted urinary volume (EUV), body weight (BW), and the urinary creatinine excretion (Cre_u) decreased. The use of such tests as the urinary lactate dehydrogenase, alkaline phosphatase, γ-glutamyltranspeptidase, and N-acetyl-β-D-glucosaminidase (LDH_u, ALP_u, $GGTP_u$, and NAG_u) seems not to be valid given their reduced activities. The use of only traditional biomarkers of renal function in these conditions may, in turn, be insufficient because their alterations are greatly influenced by the changes in the fluid intake and/or BW.

1. Introduction

Vanadium (V) is a well-known powerful prooxidant. It may modify oxidative stress (OS) in the cells and be involved in oxidative injury mechanisms [1]. Its prooxidant action has been demonstrated in *in vivo* and *in vitro* conditions [2–7]. It has been shown that the free radical process-lipid peroxidation (LPO), which is a biochemical biomarker of cellular dysfunction and an index of cytotoxicity [8], is enhanced by V in the kidney [3, 8]. It has also been suggested that LPO may be predictive of renal dysfunction [8].

Kidney is particularly vulnerable to deleterious effects of V. The susceptibility of this organ to V may be a reflection of its accumulation in this tissue [8]. It has been reported that V may be present in tubular cells in a readily exchangeable form as well as in low and high molecular mass complexes, and it may be excreted free or bound to proteins after prolonged exposure [9, 10]. It has also been speculated that V may be involved in the pathogenesis of distal renal tubular acidosis (dRTA), renal stone disease, "uremic syndrome," and acquired cystic kidney disease [11–13]. A suggestion that prolonged intake of high-dose V supplements may cause serious kidney toxicity has been put forward as well [14, 15].

The occupational and environmental toxicological impact of V and the fact that kidneys are critical for its poisoning [16–19], the modest number of biomarkers of possible functional renal disturbances under vanadate exposure examined until now, and the insufficient information about the contribution of OS in the mechanism underlying the vanadate-induced functional kidney disorders prompted us to answer the following questions. (a) To what extent do the effects of 12-week sodium metavanadate ($NaVO_3$, SMV, 0.125 mg V/mL) exposure alter the levels/activities of some biomarkers of renal toxicity in rats? We intended to examine traditional biomarkers classified as not very specific or sensitive but routinely used in the diagnosis of kidney function and those that allow distinguishing, to some degree, structural and functional renal disorders and have a potential for determining the site of renal tubular damage [20–22]. (b) To what degree do the effects of SMV exposure change the homeostasis of some micro- and macroelements in the kidney? (c) Which of the biomarkers examined are the most sensitive in our experimental conditions? (d) What value/information do some biomarkers add to the existing data? (e) Is OS involved in the mechanism of the development of kidney function disorders during SMV intoxication? (f) Are there any significant relationships between the measured variables? Since the measurement of the activities of some enzymes in tissues and biological fluids may play a significant role in detection of tissue cellular injury and point to damage long before histological alterations, both cytosolic and lysosomal enzymes as well as those located on the brush-border membrane have been taken into consideration and illustrated in the present report.

2. Materials and Methods

2.1. Reagents. The kits for determination of the plasma concentrations of TP_p, U_p, UA_p, Mg_p, and Ca_p and the urinary levels of U_u, UA_u, and Cre_u were obtained from Emapol (Gdańsk, Poland), whereas the kits for determination of the plasma Cu_p and Zn_p levels were purchased from Sentinel Ch. kits (Milan, Italy). The reagents for determination of the levels/activities of the plasma (Cre_p, ALB_p, LDH_p, $GGTP_p$, and ALP_p), urinary (ALB_u, TP_u, LDH_u, $GGTP_u$, and ALP_u), and renal (LDH_k, $GGTP_k$, and ALP_k) biomarkers as well as the reagent for measurement of the levels of electrolytes in the plasma and urine ($Na_{p/u}$, $K_{p/u}$, and $Cl_{p/u}$) were acquired from Alpha Diagnostics (Warsaw, Poland). The kit for estimation of total antioxidant status in the kidney (TAS_k) was bought from Calbiochem-Novabiochem Corporation (San Diego, CA, USA), whereas the kits for determination of the urinary levels of NAG_u (E90069Ra), $CysC_u$ (E90896Ra), β_2M_u (E90260Ra), and KIM-1_u (E90785Ra) and of the plasma concentrations of $CysC_p$ (E90896Ra) and (β_2M_p E90260Ra) were derived from Uscn Life Science Inc. (Wuhan, China). $NaVO_3$, Triton X-100, and the caesium chloride lanthanum chloride buffer (CsClLaCl) were purchased from Sigma Chemical (St. Louis, USA). Nitric acid (HNO_3, 65% suprapure) and diethyl ether ($C_4H_{10}O$) were acquired from Merck (Darmstadt, Germany), whereas hydrogen peroxide (H_2O_2; 30% pure P.A.) and the physiological buffered saline (PBS) were purchased from POCH (Gliwice, Poland) and from the Serum and Vaccine Factory (Biomed, Lublin, Poland), respectively. Stocks of V, Mg, Zn, and Cu (Inorganic Ventures, Christiansburg, USA) and a stock of Ca (Spectracer, UK) atomic absorption standard solutions as well as a multielement standard solution for Na and K (Sigma-Aldrich) were used in the element analysis by the Atomic Absorption Spectrometry (AAS) method. Ultrapure water was received from an ultrapure water HLP Spring 5R system[1] (Hydrolab, Gdańsk, Poland). All the chemicals were of the highest quality available.

2.2. Animals and Experimental Design. The experiment was conducted according to the experimental protocol approved by the 1st Local Ethical Committee for Animal Studies in Lublin. Biological material used in this study originated from some of the outbred albino male Wistar rats used in the previous study [23]. The animals were kept in an animal room with controlled conventional conditions (one rat per stainless steel cage) and received, inter alia, deionised water (Group I, Control, 8 rats) or a water solution of $NaVO_3$ at a concentration of 0.125 mg V/mL (Group II, SMV, 8 rats) to drink in special bottles with the scale every day over a 12-week period. All the rats had *ad libitum* access to fresh deionised water, SMV solution, and a standard rodent diet (Labofeed B, Fodder and Concentrate Factory, Kcynia, Poland) in which the concentration of V had been assessed by Graphite Furnace AAS (GF-AAS) in our laboratory, and it was about 0.17 μg V/g. More details about the chow had been provided by us previously [23]. The intake of food, water, and SMV solution was monitored daily and body weight (BW) was obtained weekly. The water and SMV solution intake was expressed as mL/rat/24 h, whereas the food intake was expressed as g/rat/24 h. The daily V intake in the SMV-exposed rats was estimated based on the 24 h consumption of the drinking SMV solution and expressed as mg V/kg b. wt./24 h. During the whole experiment, the animals were observed in order to assess their general health. The doses of V presented in the study are within the broad dose range that was used for demonstrating the antidiabetic activity of V [19, 24] and for analysing its pharmacokinetic behaviour [25] on an animal model. The concentration of V in rats' urine determined in the present study may reflect exposure to this element occurring especially in persons occupationally exposed to this metal [26, 27].

Every second week in the course of the experiment and in the 11th week, 24-hour urine was collected from each rat placed individually in plastic metabolic cages not equipped with a cooling system (Tecniplast, Italy), which allowed separate collection of urine and faeces. During that time, each rat had access to food and water or the SMV solution. The urine samples from all the control and SMV-exposed rats were used immediately for determination of some biochemical parameters and for measurements of excreted urine volume (EUV) and urine pH. The volumes of excreted 24-hour urine were measured with a measuring cylinder, whereas urine pH and blood in the urine were tested on the H-100 urine analyser (DIRUI, China) using urinary dipsticks. Portions of the urine samples that were not used immediately were frozen

at −80°C in a deep-freezer HFU 486 Basic[1] (Thermo Fisher Scientific, Germany) and stored until further analyses.

All the rats were sectioned at the end of week 12. Whole blood was taken from the jugular vein into plastic tubes with heparin as an anticoagulant under anaesthesia with ketamine/xylazine cocktail (100 mg/mL and 20 mg/mL, resp., i.p.) and centrifuged (5 min, 1500 ×g, 4°C). Plasma portions were collected for routine analyses of clinical chemistry parameters and for other biological determinations. The kidneys and femurs (right and left) were immediately removed. The kidneys were washed in ice-cold physiological saline (0.9% NaCl) and weighted. The right femurs (after removal of the overlying tissue with stainless steel knives) were also washed in 0.9% NaCl, weighed, and stored frozen at −80°C until the time of bone digestion. Before digestion, all the collected right femurs were cut using a diamond-disk saw (Metkon Micracut 175)[1], cooled with ultrapure water to separate the proximal and distal femoral epiphysis (PFE and DFE) (a region of trabecular bone) from the femoral diaphysis (FD) (a region of cortical bone). Next, bone marrow was removed from all the FDs, which then were first soaked with ether (to remove fat content) and later in H_2O_2 (to remove remaining blood deposits). Afterwards, the cleaned FDs were washed in ice-cold PBS and then in ultrapure water. Next, they were dried at room temperature into constant mass. The cleaned and bone marrow-deprived FD samples (~0.355 g, mean) were used for digestion.

2.3. Decomposition of the Kidney, Urine, and FD. In order to determine Mg, Ca, V, Zn, Cu, Na, and K in the kidney and Mg, Ca, V, Zn, and Cu in the urine, 0.5 g of kidney and 1 mL of urine were wet-mineralized with 5 mL of 65% HNO_3 in 12 Teflon Fluor Modified (TFM) closed digestion vessels using a model Speedwave Four microwave digestion system[1] (Berghof, Germany) equipped with a temperature and pressure sensor in each vessel. In turn, ~0.355 g of FD was wet-mineralized in the same digestion system but in the presence of 5 mL of 65% HNO_3 and 1 mL of 30% H_2O_2 to determine V, Mg, and Ca. Before the measurements, all the decomposed samples of kidney, FD, and urine were transferred into 25 mL volumetric polypropylene flasks by washing the inner surface of the digestion vessels with ultrapure water three times and filled up to the mark with ultrapure water. Next, determinations of the selected elements were performed by the AAS method.

2.4. Determination of Some Renal Biomarkers. The concentrations of U_p, UA_p and TP_p in the plasma as well as U_u, UA_u, and Cre_u in 24-hour urine were determined colourimetrically by measuring the absorbance with a Thermo Spectronic BioMate5 UV-VIS spectrophotometer (UK). The concentrations of ALB_p, ALB_u, TP_u, and Cre_p and the activities of LDH_p, $GGTP_p$, ALP_p, LDH_u, $GGTP_u$, and ALP_u in the plasma and urine as well as the activities of LDH_k, $GGTP_k$, and ALP_k in the kidney were measured using an automatic biochemical analyser BS-120[1] (Mindray, China). The levels of $CysC_p$ and β_2M_p in the plasma and the levels of $CysC_u$, β_2M_u, $KIM\text{-}1_u$, and NAG_u in the urine were assessed by a traditional method using rat-specific commercial enzyme-linked immunosorbent assay (ELISA) kits and an ELISA microplate reader Synergy 2[1] equipped with an automated microplate strip washer ELx50[1] and a microplate shaker[1] (BIO-TEK Instruments Inc., USA). All the ELISA tests were performed according to the manufacturer's protocols. Before the measurements, thawed plasma and urine samples were mixed by inversion, centrifuged with cooling (1500 rpm for 10 min, 4°C, or 2000 rpm for 5 min, 4°C, resp.) using a centrifuge Heraeus Megafuge 11R[1] (Thermo Fisher Scientific, Germany), and immediately used for analysis. The optimal factors of dilution for some samples were chosen when necessary and the samples were diluted with ultrapure water or with PBS (pH 7.4 ± 0.2). In order to evaluate the glomerular filtration rate (GFR), calculation of creatinine clearance (CreC) was performed. The results for all the above-mentioned parameters are expressed as % of the control and presented in Figures 1(a), 2(a), 2(b), 3(a), 3(b), and 4(a).

2.5. Determination of Elements in Biological Fluids and Tissues

2.5.1. Spectrophotometric Determination of Ca, Mg, Zn, and Cu in the Plasma. The measurements of these elements were performed using a BioMate5 spectrophotometer with the direct colourimetric method according to the protocols of the kits, and their concentrations are presented in Figures 1(b) and 1(d).

2.5.2. Determination of Na, K, and Cl in the Plasma and Urine. The electrolytes mentioned were measured using an automatic EasyLyte analyser Na/K/Cl[1] (Medica). Their urinary excretion was first normalized against 24-hour diuresis and against 24-hour urinary Cre_u excretion, and their concentrations are presented in Figures 1(b), 1(c), 2(e), and 3(e).

2.5.3. Atomic Absorption Measurements of Mg, Ca, V, Zn, Cu, Na, and K in Digested Kidney Samples, Mg, Ca, V, Zn, and Cu in Digested Urine Samples, V, Mg, and Ca in Digested FD Samples, and V in Nondigested Plasma Samples. The elements were determined by Flame or Graphite Furnace AAS (F-AAS or GF-AAS, resp.) using a SpectrAA Z-2000 TANDEM atomic absorption spectrometer[1] (Hitachi, Japan) equipped with a Zeeman background corrector. A specific matrix modifier was used for V determination. In order to determine the V concentration in the plasma, the samples were diluted with 0.05% Triton X-100 and in ultrapure water when necessary. All the operating parameters of the instrument and the details of measurements of all the above-mentioned elements together with the values of the detection, quantification limits (LOD and LOQ, resp.), and the coefficient of variations (CV) are shown in Table 1.

The method of standard addition was performed in order to estimate the effect of interferences during Mg assessment. Mg, Ca, V, Zn, Cu, Na, and K were determined by application of a calibration curve using working standard solutions, which were obtained from a stock atomic absorption standard solutions containing 1000 μg Mg, Ca, V, Zn, Cu, Na, and

Table 1: Operating parameters of the atomic absorption spectrometer with details of measurement of the levels of elements in biological samples as well as the certified and determined values of elements for the selected Certified Reference Materials (CRMs).

Parameters	Elements						
	V	Cu	Mg	Ca	Zn	Na	K
Technique	GF-AAS	GF-AAS			F-AAS		
FT	—				Air-acetylene		
FF (L/min)	Argon with the flow rate of 200 (mL/min) in all the steps except the atomization stage when the flow rate was 30 (mL/min)				1.8		
GTT	PCGTs (PyroTube CHR)				—		
SV (μL)	20 (μL)				—		
SM	B-CIA				B-CIM		
LC (mA)	10	7.5	7.5	10	5.0	10.0	10.0
WL (nm)	318.4	324.8	285.2	422.7	213.9	589.0	766.5
SW (nm)	1.3	1.3	1.3	0.2	1.3	0.2	1.3
DL (LOD)	K: 0.11 (μg/L) U: 0.23 (μg/L) P: 0.23 (μg/L) FD: 0.47 (μg/L)	K: 0.28 (μg/L) U: 0.14 (μg/L) P: $\surd$	K: 1×10^{-5} (mg/L) U: 6×10^{-5} (mg/L) P: $\surd$ FD: 8×10^{-4} (mg/L)	K: 0.09 (mg/L) U: 0.36 (mg/L) P: $\surd$ FD: 0.13 (mg/L)	K: 1×10^{-3} (mg/L) U: 0.6 (μg/L) P: $\surd$	K: 3.1×10^{-3} (mg/L) U:** P:**	K: 5.5×10^{-3} (mg/L) U:** P:**
LOQ	K: 0.33 (μg/L) U: 0.69 (μg/L) P: 0.69 (μg/L) FD: 1.41 (μg/L)	K: 0.84 (μg/L) U: 0.42 (μg/L) P: $\surd$	K: 3×10^{-5} (mg/L) U: 1.8×10^{-4} (mg/L) P: $\surd$ FD: 2.4×10^{-3} (mg/L)	K: 0.27 (mg/L) U: 1.08 (mg/L) P: $\surd$ FD: 0.39 (mg/L)	K: 3×10^{-3} (mg/L) U: 1.8 (μg/L) P: $\surd$	K: 9.3×10^{-3} (mg/L) U:** P:**	K: 16.5×10^{-3} (mg/L) U:** P:**
CV (%)	0.2–2	0.5–2			0.5–1		

Table 1: Continued.

Elements	Bovine Liver 1577 c		Seronorm Trace Elements Urine 201205		Trace Elements in Natural Water 1640 a	
	Certified value	Determined value[§]	Certified value	Determined value[§]	Certified value	Determined value[§]
Mg	620 ± 42 (mg/kg)	657.4 ± 20.2 (mg/kg)	71.1 ± 2.5 (mg/L)	69.7 ± 2.3 (mg/L)	1.058 ± 0.0040 (mg/L)	1.059 ± 0.040 (mg/L)
Ca	131 ± 10 (mg/kg)	133.4 ± 15.2 (mg/kg)	111 ± 2 (mg/L)	111.9 ± 1.2 (mg/L)	5.615 ± 0.021 (mg/L)	5.649 ± 0.028 (mg/L)
V	8.17 ± 0.66 (μg/kg)	10.2 ± 1.6 (μg/kg)	25.2 ± 1.4 (μg/L)	22.43 ± 0.56 (μg/L)	12.99 ± 0.37 (μg/L)	12.33 ± 0.35 (μg/L)
Zn	181.1 ± 1.0 (mg/kg)	180.3 ± 8.7 (mg/kg)	1141 ± 79 (μg/L)	1100.6 ± 24.4 (μg/L)	55.64 ± 0.35 (μg/L)	55.50 ± 0.17 (μg/L)
Cu	275.2 ± 4.6 (mg/kg)	268.6 ± 4.7 (mg/kg)	78 ± 8 (μg/L)	92.4 ± 6.9 (μg/L)	85.75 ± 0.51 (μg/L)	85.45 ± 0.14 (μg/L)
Na	2.033 ± 0.064 (mg/kg)	1.969 ± 0.015 (mg/kg)	2307 ± 56 (mg/L)	2376 ± 45 (mg/L)	3.137 ± 0.031 (mg/L)	3.150 ± 0.025 (mg/L)
K	—	—	1903 ± 42 (mg/L)	1930 ± 40 (mg/L)	0.5799 ± 0.0023 (mg/L)	0.5818 ± 0.0209 (mg/L)

Elements	Bone Ash 1400	
	Certified value	Determined value[§]
Mg	6.84 ± 0.13 (mg/g)	6.774 ± 0.065 (mg/g)
Ca	381.8 ± 1.3 (mg/g)	384.8 ± 2.2 (mg/g)

FT: flame type; FF: fuel flow; GTT: graphite tube type; SV: sample volume; SM: signal mode; LC: lamp current; WL: wavelength; SW: slit width; PCGTs: pyrolytically coated graphite tubes; B-CIA: background-corrected integrated absorbance; B-CIM: background-corrected integral mode.

√,** Determined colourimetrically or by an EasyLyte analyser, respectively.

DL (LOD): detection limit.

LOQ: quantification limit.

CV: coefficient of variation.

K: kidney; U: urine; P: plasma; FD: femoral diaphysis.

[§]Mean ± SD, $n = 5$.

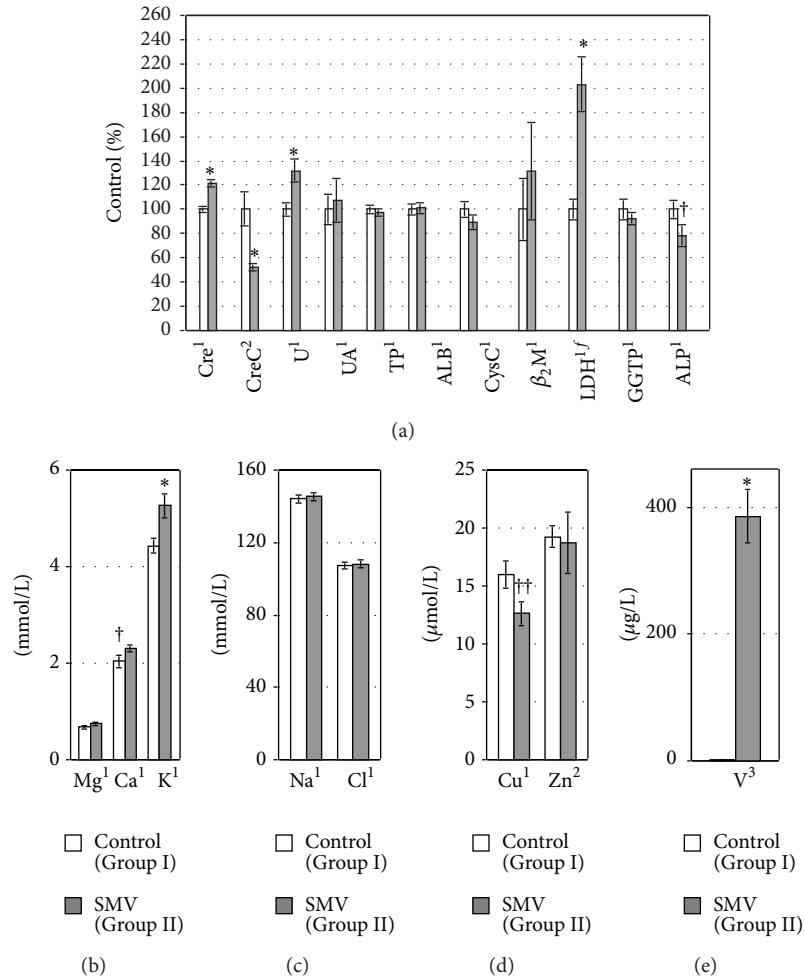

Figure 1: The levels/activities of some biomarkers of renal toxicity (a) and the concentrations of selected elements ((b)–(e)) in rat plasma. [1,2,3]Data were tested by Student's t-test, Welch's t-test, or Mann-Whitney's U test, respectively. *Significant differences, compared with the Control (Group I). [f]Logarithmically transformed data. [††,†]$P = 0.05$, $P = 0.08$, respectively, compared with the Control (Group I).

K/mL by dilution with 5% (v/v) HNO_3. The 10% CsClLaCl buffer was used to determine Ca. The analytical quality of the measurements was checked with the use of Certified Reference Materials (CRMs) such as Bovine Liver 1577 c (NIST), Seronorm Trace Elements Urine 201205 (SERO), Trace Elements in Natural Water 1640 a (NIST), and Bone Ash 1400 (NIST). The analysis of these CRMs confirmed the reliability of the proposed approach. The certified and determined values of all the elements examined in the above-mentioned CRMs are presented in Table 1. The plasma V level is presented in Figure 1(e). In turn, the urinary excretion of the above-mentioned elements investigated was also first normalized against 24-hour diuresis and against 24-hour urinary Cre_u excretion. This is illustrated in Figures 2(c), 2(d), 2(f), 3(c), 3(d), and 3(f). However, the renal V, Mg, Ca, Zn, Cu, Na, and K concentrations as well as the FD V, Mg, and Ca concentrations are presented in Figures 4(b)–4(e) and in Figures 5(a)–5(c).

2.6. Determination of Renal Lipid Peroxidation (LPO) and Total Antioxidant Status (TAS). All details concerning the methodology of determination of LPO and the preparation of kidney homogenates and supernatants for the renal MDA_k and TAS_k measurements had already been provided [2, 3]. The results of both the OS markers mentioned are expressed as % of control and illustrated in Figure 4(a).

2.7. Statistical Analysis. The statistical analysis of the data was performed with the Statistica and SPSS, versions 9.0 and 14.0 PL for Windows, respectively. The normal distribution of the data was tested by Shapiro-Wilk's normality test. Grubbs' test was performed to detect the presence of outliers from a normal distribution. The homogeneity of variances was verified employing Levene's test and sometimes additionally Hartley's Fmax, Cochran's C, and Bartlett's tests. Student's t-test and Welch's t-test were applied to compare the means of two independent groups when the data met the assumptions of ANOVA and when they had a normal distribution but the variances were not homogenous, respectively. In some cases, logarithmic transformation of the data was used to *make them more normal*. In turn, the nonparametric Mann-Whitney U

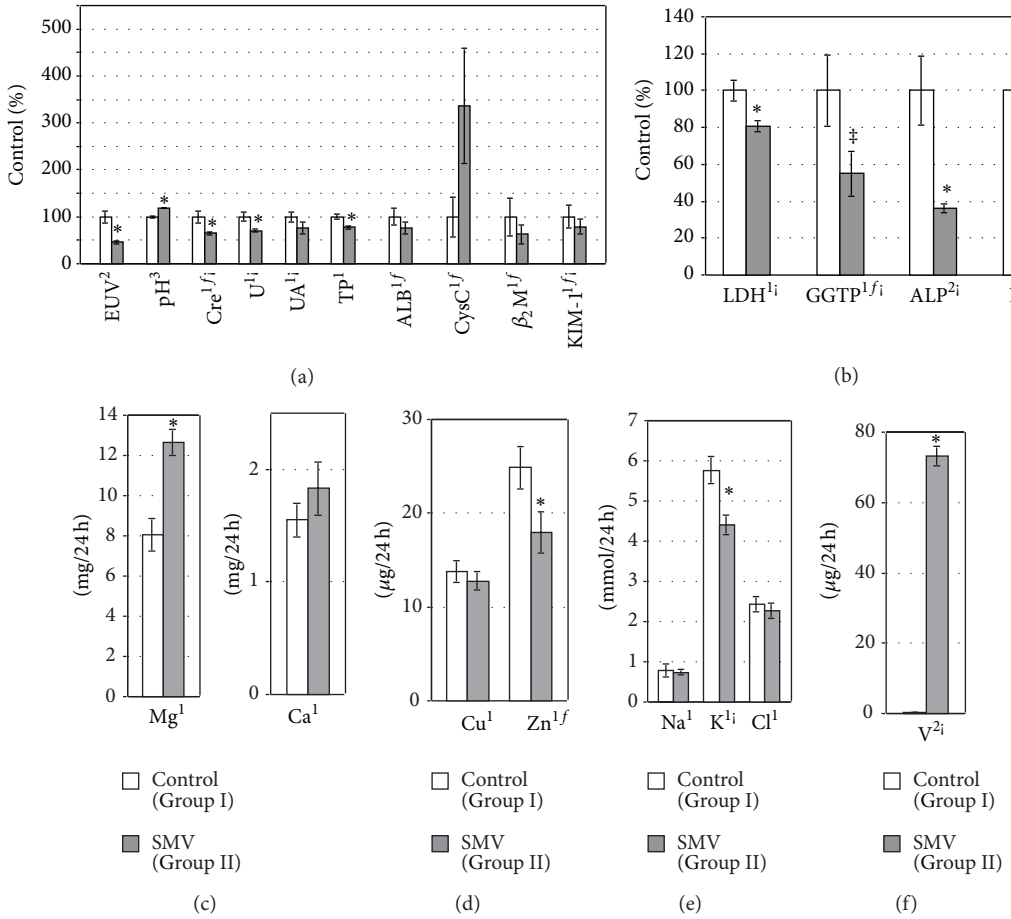

Figure 2: EUV, urine pH, and the urinary levels/activities of some biomarkers of renal toxicity ((a) and (b)) and the urinary levels of selected elements ((c)–(f)) normalized per 24-hour diuresis in the tested rats. [1,2,3]Data were tested by Student's t-test, Welch's t-test, or Mann-Whitney's U test, respectively. *Significant differences, compared with the Control (Group I). [f]Logarithmically transformed data. [i]Correlated with excreted urinary volume (EUV). [‡]$P = 0.06$, compared with the Control (Group I).

test was applied when the data did not meet the assumptions of ANOVA. The results were presented as mean ± the standard error of the mean (SEM). A P value less than 0.05 was taken as a criterion for a statistically significant difference. Pearson's correlation analyses were applied to assess the relationships between the measured variables. Correlations were considered statistically significant at $P < 0.05$.

3. Results

3.1. General Observation and Changes in Some Basic Parameters. In the animals exposed to SMV, no distinct differences in physical appearance and motor behaviour were observed during the 12-week experimental period, compared with the control. Some of the SMV-intoxicated rats had gastrointestinal disturbances probably caused by the consumption of the V dose. One-day diarrhoea was observed in four animals from this group in the first, second, third, or fourth week of the experiment. Only one rat from this group had three-day diarrhoea in the first week of the experiment. The fluid and food intake as well as BW (Table 2) and EUV (Figure 2(a)) in the SMV-exposed rats were lower, compared with the control animals. The dose of V consumed by the rats during the 12-week period reached the value of about 13 mg V/kg b. wt./24 h (Table 2).

3.2. Plasma, Urinary, and Renal Levels of the Examined Biomarkers and the Dipstick Urinalysis (Blood and pH). The concentrations of Cre_p and U_p in the SMV-exposed rats increased (Figure 1(a)), whereas CreC (Figure 1(a)) and the levels of urinary excretion of Cre_u (per 24 h) and U_u (per 24 h) decreased significantly (Figure 2(a)), in comparison with the control animals. In turn, the urinary level of U_u (per Cre_u/24 h) (Figure 3(a)) and the concentration of U_k in the kidney (Figure 4(a)) were unaltered. The levels of UA_p (Figure 1(a)) and UA_u (per 24 h and per Cre_u/24 h, Figures 2(a) and 3(a), resp.) also remained unchanged in response to the SMV exposure.

The levels of TP_p and ALB_p in the SMV-exposed rats did not alter significantly, compared with the control (Figure 1(a)), but the urinary excretion of TP_u (per 24 h)

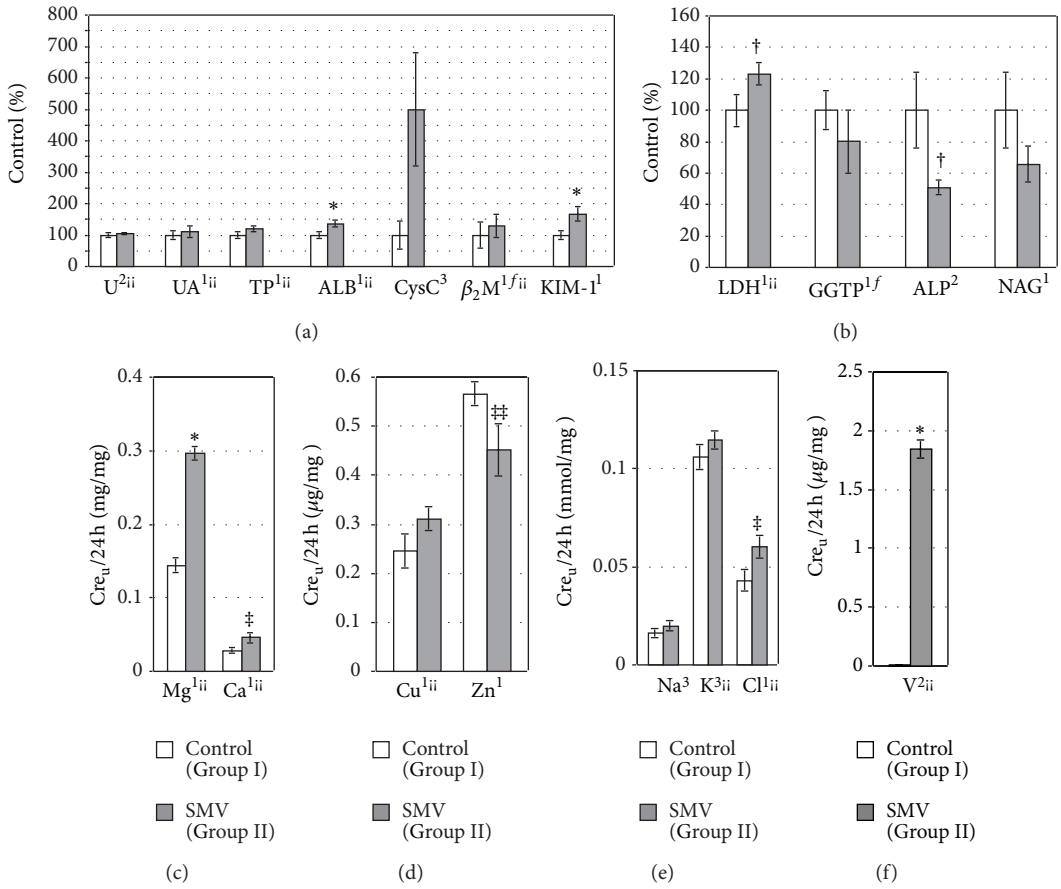

Figure 3: The urinary levels/activities of some biomarkers of renal toxicity ((a) and (b)) and the urinary levels of selected elements ((c)–(f)) normalized per 24-hour urinary Cre_u excretion in the tested rats. [1,2,3]Data were tested by Student's t-test, Welch's t-test, or Mann-Whitney's U test, respectively. [*]Significant differences, compared with the Control (Group I). [f]Logarithmically transformed data. [ii]Correlated with the urinary Cre_u excretion. [‡,‡‡,†] $P = 0.06$, $P = 0.07$, and $P = 0.08$, respectively, compared with the Control (Group I).

Table 2: Basic indices in the tested animal groups at week 12.

Parameters	Groups of animals		Percentage decrease (↓) compared with Group I, P value
	(I) Control	(II) SMV	
Fluid intake (mL/rat/24 h)[2]	58.53 ± 1.92	39.64 ± 0.73[*]	↓ 32 < 0.001
Food intake (g/rat/24 h)[1]	37.02 ± 0.86	28.73 ± 0.69[*]	↓ 22 < 0.001
Body weight (% of initial b. wt.)[1]	264.13 ± 23.59	190.46 ± 15.95[*]	↓ 28 < 0.05
V dose (mg V/kg b·wt./24 h)[#]	—	13.27 ± 0.33	

[1,2]Data were tested by Student's t-test or Welch's t-test, respectively.
[*]Significant differences ($P < 0.05$), compared with the Control (Group I).
[#]Consumed with drinking water.

and ALB_u (per 24 h) decreased and unchanged, respectively, (Figure 2(a)). On the contrary, the urinary levels of TP_u (per Cre_u/24 h) in the same group of rats were unaltered and ALB_u (per Cre_u/24 h) increased, in comparison with the control (Figure 3(a)). In turn, the renal concentration of TP_k and ALB_k did not change markedly (Figure 4(a)).

The concentrations of $CysC_p$ and β_2M_p remained unaltered between the groups (Figure 1(a)). However, the urinary excretion of $CysC_u$ (per 24 h, Figure 2(a), and per Cre_u/24 h, Figure 3(a)) increased markedly but the urinary β_2M_u level (per 24 h, Figure 2(a), and per Cre_u/24 h, Figure 3(a)) was unchanged. In turn, the urinary level of KIM-1_u (per 24 h, Figure 2(a), and per Cre_u/24 h, Figure 3(a)) in the SMV-intoxicated rats did not alter and increased, respectively, compared with the control.

The activity of LDH_p increased, ALP_p decreased, and $GGTP_p$ was unchanged in the rats after the SMV intoxication, in comparison with the control (Figure 1(a)). In turn, the

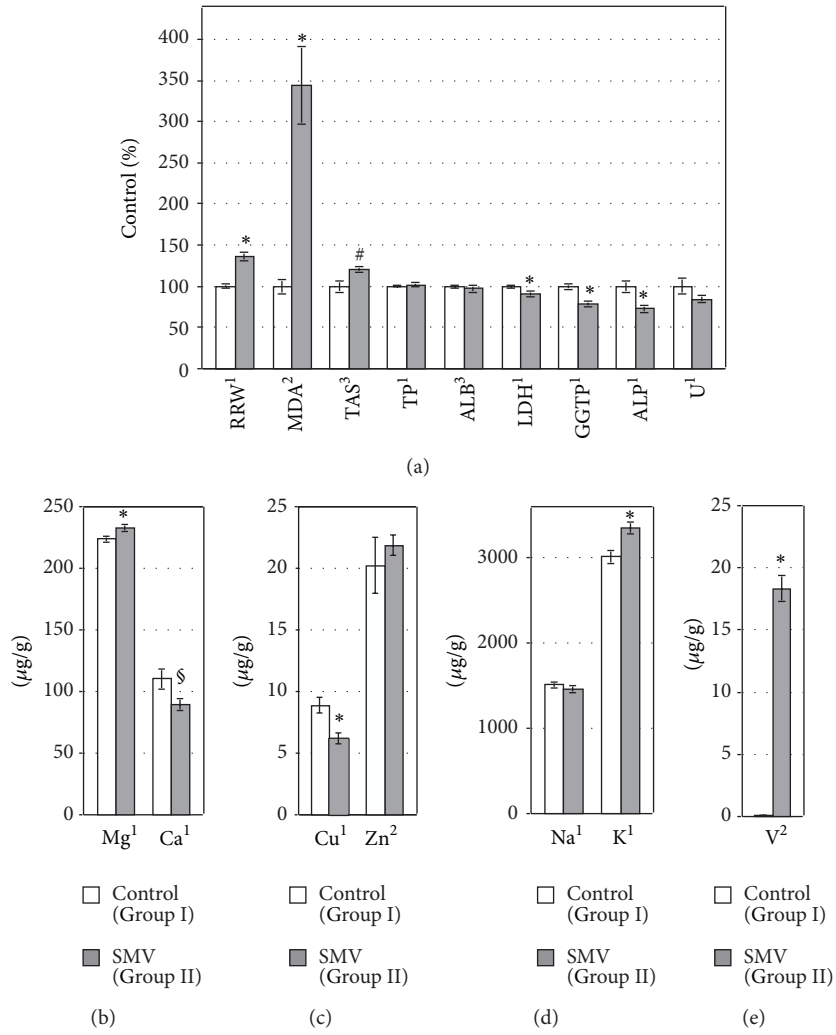

Figure 4: Renal relative weight (RRW), the levels/activities of some OS markers, proteins, and enzymes (a) in the kidney, and the concentrations of selected elements ((b)–(e)) in the same organ of the tested rats. [1,2,3]Data were tested by Student's t-test, Welch's t-test, or Mann-Whitney's U test, respectively. *Significant differences, compared with the Control (Group I). [#,§]$P = 0.09$, $P = 0.05$, respectively, compared with the Control (Group I).

urinary activities of LDH_u, $GGTP_u$, and ALP_u (per 24 h) as well as the urinary activities of $GGTP_u$ and ALP_u (per Cre_u/24 h) and NAG_u (per 24 h and per Cre_u/24 h) were lowered in the SMV-exposed rats, compared with the control (Figures 2(b) and 3(b)). However, the urinary activity of LDH_u (per Cre_u/24 h) only showed a visible trend toward an increase (Figure 3(b)). In turn, the renal activity of LDH_k, $GGTP_k$, and ALP_k in the SMV-intoxicated rats was lowered, in comparison with the control (Figure 4(a)).

Urine dipstick analysis did not reveal presence of blood in the urine of the SMV-intoxicated rats (data not shown). However, the urine pH in the same animals was markedly higher, compared with that in the control rats (Figure 2(a)).

3.3. Element Levels in the Plasma. The exposure to SMV led to a distinct elevation of the Ca_p and K_p concentrations (Figure 1(b)), produced a visible decrease in the plasma Cu_p level (Figure 1(d)), and increased the plasma V_p concentration (Figure 1(e)). However, no SMV intoxication-related effects on the concentrations of Mg_p, Na_p, Cl_p, and Zn_p (Figures 1(b), 1(c), and 1(d)) in the plasma were detected.

3.4. Excretion of Urinary Elements. In the SMV-intoxicated animals, Mg_u, Ca_u, and V_u were excreted in urine in higher amounts than those found in the control rats (Figures 2(c), 2(f), 3(c), and 3(f)). The urinary Cl_u excretion (per Cre_u/24 h) also tended to be higher, compared with the control (Figure 3(e)). In turn, the urinary excretion of Zn_u (per 24 h and per Cre_u/24 h) distinctly decreased in the SMV-exposed rats, in comparison with the control animals (Figures 2(d) and 3(d)), whereas the urinary K_u excretion (per 24 h, Figure 2(e), and per Cre_u/24 h, Figure 3(e)) dropped and did not change, respectively. However, the urinary levels of Cu_u and Na_u (per 24 h and per Cre_u/24 h), in the SMV-exposed rats, did not turn out to be significantly

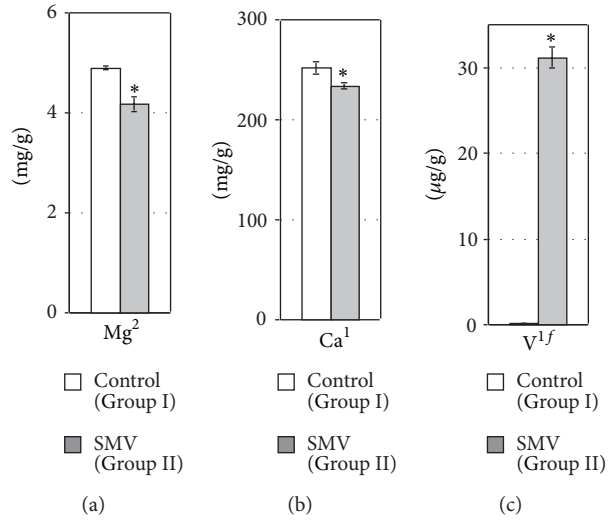

FIGURE 5: The concentration of Mg (a), Ca (b), and V (c) in the rat femoral diaphysis (FD). [1,2]Data were tested by Student's *t*-test or Welch's *t*-test, respectively. *Significant differences, compared with the Control (Group I).

altered, compared with the control animals (Figures 2(d), 2(e), 3(d), and 3(e)).

3.5. Concentrations of Elements in the Kidney and FD. The exposure to SMV elevated the concentrations of Mg_k, K_k (Figures 4(b) and 4(d)), and V_k (Figure 4(e)) and decreased the concentration of Cu_k (Figure 4(c)) in the kidney, compared with the control. A clear tendency toward decreased and increased concentrations of Ca_k and Zn_k, respectively (Figures 4(b) and 4(c)), was also observed in the SMV-intoxicated animals, in comparison with the control rats. However, the concentration of Na_k in the same organ of the SMV-exposed rats did not change markedly, compared with the control (Figure 4(d)). In turn, the concentrations of Mg_{FD} and Ca_{FD} in FD decreased (Figures 5(a) and 5(b)), whereas the concentration of V_{FD} in the same FD increased (Figure 5(c)) after the SMV intoxication, in comparison with the control.

3.6. Kidney Weight and Renal MDA and TAS Levels. The SMV-exposed rats had a significantly elevated relative renal weight (RRW) and the renal MDA_k level, compared with the control animals (Figure 4(a)). The renal TAS_k level in the same group of rats was also distinctly enhanced, in comparison with the control (Figure 4(a)).

3.7. Correlations between Some Measured Variables. Significant positive and negative correlations and trends toward them were revealed between many different parameters, among others, between the renal V_k concentration, the renal MDA_k, or TAS_k levels and some biomarkers and basic indices as well as between both OS markers (Table 3). They were also found between the fluid intake, BW, EUV, or the urinary Cre_u excretion and some investigated parameters (Table 3) as well as between the renal V_k concentration or the renal MDA_k level and the levels/concentrations of elements in the plasma, urine, kidney and FD (Table 4). The relationships between the urinary excretion of some elements and Cre_u or EUV were also indicated (Table 4).

4. Discussion

To our knowledge, the present report is the first to describe in a rat model the influence of the 12-week SMV exposure on the levels/activities of a wider panel of biomarkers of renal toxicity and on the concentrations of some elements in the kidney. It reveals a probable mechanism of the development of the SMV-induced functional renal disorders and proposes potential biomarkers of nephrotoxicity for specific conditions of SMV intoxication. It also illustrates for the first time many relationships between some explored indices. Because of different experimental conditions used, comparison of the results presented in the current report with literature data was difficult; therefore, the discussion section relies predominantly on our own results.

The increase in the kidney/body weight ratio observed by us in the present (Figure 4(a)) and previous study [28] in the SMV-intoxicated rats may indicate that V accumulated sufficiently in the kidney to manifest significant alterations in the size of this organ. Taking into account the fact that one of the main excretory routes for V within the body is the urinary system [29], V accumulation in the kidney may result in not only functional but also structural damage. Therefore, the estimation of the structural renal injury by histological examination in the rats after the 12-week SMV exposure is going to be performed in the nearest future. In this report, the degree of kidney damage has been evaluated only biochemically.

The decreased CreC together with the enhanced plasma Cre_p and U_p levels (Figure 1(a)), and the lowered urinary Cre_u and U_u excretion (Figure 2(a)) found in the SMV-exposed rats may indicate a problem with removal of Cre and U

Table 3: Correlation coefficients for compared variables.

Variables					
V_k		MDA_k		TAS_k	
Food-I	**−0.894**†	Food-I	**−0.817**†	Food-I	**−0.676**†
Fluid-I	**−0.905**†	Fluid-I	**−0.754**†	Fluid-I	**−0.707**†
RRW	**0.778**†	RRW	**0.531***	RRW	***0.406***^{f}
BW	**−0.601***	BW	**−0.672**†	BW	**−0.780**†
MDA_k	**0.889**†	TAS_k	**0.598***	LDH_k	***−0.472***^{a}
TAS_k	**0.590***	LDH_k	**−0.614***	ALP_k	***−0.492***†††
LDH_k	**−0.544***	ALP_k	**−0.757**†	$GGTP_k$	***−0.401***^{g}
ALP_k	**−0.669**†	$GGTP_k$	**−0.577***	EUV	***−0.412***^{f}
$GGTP_k$	**−0.759**†	U_k	***−0.445***^{c}	pH	**0.588***
EUV	**−0.716**†	ALB_k	**−0.549***	Cre_p	**0.624**†
pH	**0.917**†	EUV	**−0.613***	CreC	**−0.505***
Cre_u	**−0.630**†	pH	**0.761**†	$U_u{}'$	***−0.429***^{d}
U_p	***0.483*****	Cre_p	**0.757**†	$CysC_u{}'$	**0.601***
Cre_p	**0.818**†	CreC	**−0.606***	$\beta_2M_u{}'$	***−0.408***^{h}
CreC	**−0.652**†	TP_p	***−0.437***^{d}	$AlP_u{}'$	**−0.552***
ALP_p	***−0.448***^{c}	LDH_p	**0.539***	$NAG_u{}'$	***−0.448***^{c}
LDH_p	**0.757**†	Cre_u	**−0.572***		
$U_u{}'$	**−0.596***	$U_u{}'$	**−0.574***		
$TP_u{}'$	**−0.654**†	$TP_u{}'$	**−0.518***		
$CysC_u{}'$	***0.399***^{g}	$CysC_u{}'$	***0.496***^{f}		
$LDH_u{}'$	**−0.612***	$LDH_u{}'$	**−0.523***		
$AL\,P_u{}'$	**−0.656**†	$AL\,P_u{}'$	**−0.514***		
$GGTP_u{}'$	***−0.531***^{a}	$GGTP_u{}'$	***−0.425***^{i}		
$NAG_u{}'$	**−0.506***	$NAG_u{}'$	***−0.490***^{ff}		
Fluid-I		BW		EUV		Cre_u	
EUV	**0.759**†	Cre_p	**−0.773**†	Cre_u	**0.920**†	$U_u{}''$	**−0.561***
Cre_p	**−0.844**†	Cre_u	**0.595***	$U_u{}'$	**0.816**†	$UA_u{}''$	***−0.443***^{c}
Cre_u	**0.668**†	CreC	**0.762**†	$UA_u{}'$	**0.499***	$TP_u{}''$	**−0.786**†
CreC	**0.755**†	$U_u{}'$	**0.734**†	$LDH_u{}'$	**0.569***	$AL\,B_u{}''$	**−0.630**†
U_p	***−0.470***^{a}	$CysC_p$	***0.488***‡‡	$AL\,P_u{}'$	***0.424***^{e}	$\beta_2M_u{}''$	**−0.697**†
$U_u{}'$	**0.700**†	$CysC_u{}'$	***−0.482***^{a}	$GGTP_u{}'$	**0.643***	$LDH_u{}''$	**−0.776**†
				$NAG_u{}'$	**0.780**†		
				$KIM\text{-}1_u{}'$	***0.447***^{c}		

Data are presented as the correlation coefficients (r) and the levels of statistical significance (P).

^{p,u,k}Plasma, urine, and kidney (concentration), respectively.

Fluid-I, Food-I, RRW, BW, and EUV: fluid intake, food intake, renal relative weight, body weight, and excreted urinary volume, respectively.

$^{\dagger}P < 0.01$; $^{*}P < 0.05$; $^{f}P = 0.051$; $^{\dagger\dagger\dagger}P = 0.053$; $^{ff}P = 0.054$; $^{\ddagger\ddagger}P = 0.055$; $^{**}P = 0.058$; $^{a}P = 0.06$; $^{c}P = 0.08$; $^{d}P = 0.09$; $^{e}P = 0.10$; $^{f}P = 0.11$; $^{g}P = 0.12$; $^{h}P = 0.13$; $^{i}P = 0.14$.

$^{\prime,\prime\prime}$Expressed per 24 h and per Cre_u per 24 h, respectively.

The significant correlations and tendencies toward them are highlighted in normal and italic bold font, respectively.

from the body and implicate glomerular functional disorders reflected by decreased clearance of the above-mentioned compounds. However, the lowered basic parameters such as fluid intake (discussed by us more widely) [30] and BW found in the same group of animals (Table 2) and the significant correlations between them and Cre_u, Cre_p, CreC, U_u, and/or U_p (Table 3) do not allow us to exclude the possibility that dehydration and/or low BW affected the measured standard renal biomarkers. However, it is difficult to recognize to what extent they could influence the alterations in the biomarkers examined. The levels of Cre and U in the blood/urine are known to be affected not only by renal but also by some nonrenal factors [31–33]. On the other hand, the correlations between the renal V concentration (V_k) and Cre_u, Cre_p, CreC, U_u, and U_p (Table 3) confirm the involvement of V in the changes in the basic biomarkers explored. Moreover,

the correlations between V_k and both OS markers such as MDA_k and TAS_k as well as between MDA_k and Cre_u, Cre_p, CreC, and U_u (Table 3) also point to the involvement of the SMV-induced OS in their alterations observed. Additionally, the positive correlation between both OS markers allows us to definitively conclude that the changes in the renal TAS_k level (Table 3) are associated with the alterations in LPO in the kidney due to the SMV exposure.

The markedly elevated urinary excretion of $CysC_u$ (a tubular injury biomarker) [20, 32] demonstrated in the SMV-intoxicated rats (Figures 2(a) and 3(a)) without significant alterations in the plasma level of this protein ($CysC_p$) (Figure 1(a)) may point to decreased reabsorption of CysC by injured tubules. Moreover, the positive correlation of $CysC_u$ with TAS_k as well as the clear trends toward the positive correlations of $CysC_u$ with V_k and MDA_k (Table 3) can suggest involvement of the renal V prooxidative action in the proximal tubular dysfunction (PTD), which consequently led to the urinary CysC wasting. It has been reported that when the renal proximal tubule remains intact CysC is completely taken up by the proximal tubular cells (PTC) [32], but in the case of tubular disease and the proximal convoluted tubule (PCT) injury the concentration of this protein in the urine is significantly elevated [34, 35]. In addition, the markedly enhanced urinary KIM-1_u excretion (Figure 3(a)) found in the same group of rats may also point to damage to PTC due to the SMV exposure. KIM-1 is expressed at very high levels in proximal tubule epithelial cells after toxic injury and it is present in urine when the injury of PTC occurs [20].

In turn, the lowered urinary activities of LDH_u, ALP_u, $GGTP_u$, and NAG_u, demonstrated in the SMV-exposed rats (Figure 2(b)), allow us to suggest that the use of these tests for monitoring kidney injury during the SMV intoxication may not be valid, as the activity of these enzymes in the urine usually rises due to release from damaged cells. The lowered urinary ALP_u and GGT_u excretion and the simultaneous increase in the urinary LDH_u and NAG_u excretion were demonstrated by De la Torre et al. [36] in adult rats after vanadate intoxication. The discrepancies between our results concerning the urinary excretion of LDH and NAG and the results obtained by the above-mentioned investigators draw attention to the dependence of the renal effects on the conditions of vanadate exposure. In turn, the significant negative correlations found between the renal V_k concentration and the renal LDH_k, ALP_k, and $GGTP_k$ activities (Table 3) may indicate a direct V impact. The direct inhibitory effect of both vanadate and vanadyl on the ALP activity was described by Cortizo et al. [37]. However, the marked increase in the plasma LDH activity (LDH_p) demonstrated in the SMV-exposed rats (Figure 1(a)) requires further analyses. The measurement of the LDH isoenzyme might be the next important point in a more precise explanation of the significant increase in the activity of this enzyme in the plasma because the total plasma LDH is a highly sensitive test but, simultaneously, it is nonspecific. At the present stage of our study, we may only confirm the involvement of V and the SMV-induced OS in the changes in the activity of LDH in the blood, as evidenced by the significant positive correlations of LDH_p with V_k and MDA_k (Table 3).

Table 4: Correlation coefficients for measured variables.

	Variables	
	V_k	MDA_k
V_p	**0.872**†	**0.710**†
Cu_p	**−0.520***	***−0.445***^{b}
K_p	**0.621***	—
V_u'	**0.977**†	**0.795**†
Mg_u'	**0.798**†	**0.678**†
Zn_u'	**−0.555***	**−0.618***
K_u'	**−0.600***	**−0.535***
Cu_k	**−0.687**†	**−0.628**†
Mg_k	**0.527***	—
K_k	**0.599***	—
V_k	—	**0.889**†
Ca_k	***−0.486***$^{\#}$	***−0.479***^{a}
Mg_{FD}	**−0.767**†	**−0.725**†
Ca_{FD}	***−0.492***$^{\partial}$	***−0.334***^{c}
	V_{FD}	
Mg_{FD}	**−0.768***	
Ca_{FD}	**−0.547***	
	EUV	
V_u'	**−0.722**†	
K_u'	**0.856**†	
	Cre_u	
V_u''	**−0.600***	
Mg_u''	**−0.602***	
Ca_u''	**−0.633**†	
Cu_u''	**−0.688**†	
K_u''	**−0.540***	
Cl_u''	**−0.735**†	

Data are presented as the correlation coefficients (r) and the levels of statistical significance (P).

^{p,u,FD,k}Plasma, urine, femoral diaphysis, and kidney (concentration), respectively.

EUV: excreted urinary volume.

$^{\dagger}P < 0.01$; $^{*}P < 0.05$; $^{\partial}P = 0.053$; $^{\#}P = 0.056$; $^{a}P = 0.061$; $^{b}P = 0.08$; $^{c}P = 0.20$.

$^{\prime,\prime\prime}$Expressed per 24 h and per Cre_u per 24 h.

The significant correlations and tendencies toward them are highlighted in normal and italic bold font, respectively.

Additionally, the strong positive correlations of the urinary pH with V_k and with both OS markers (Table 3) and the correlation between the renal V_k and K_k concentration and between the renal V_k concentration and the plasma K_p level (Table 4) also suggest involvement of OS in the mechanism of the rise in urine pH under the conditions of the SMV exposure (Figure 2(a)). They also confirm the dependence between the accumulation of V in the kidney and disorders in K homeostasis (Figures 1(b) and 4(d)). All these results suggest further measurements to elucidate the mechanism(s) of the changes observed in our experimental conditions.

The urinary Mg wasting (Figures 2(c) and 3(c)) and its elevated and diminished concentration in the kidney and FD, respectively (Figures 4(b) and 5(a)), as well as the clearly enhanced plasma and urinary Ca level (Figures 1(b) and

2(c)) and its lowered FD concentration (Figure 5(b)) point to disorders in the homeostasis of both macroelements during the SMV exposure. These changes may be partly explained by the influence of SMV on the bone tissue which is the main site of V uptake and deposition and in which the level of this element has been found to be significantly higher (Figure 5(c)). The presence of V in the bone might lead to mobilization of Mg and Ca from this tissue and cause the alterations observed. The negative correlations between the FD V, Mg, and Ca concentrations (Table 4) confirm the connection between the bone V accumulation and the bone Mg and Ca imbalance. Moreover, the negative correlation of V_k and MDA_k with the Mg_{FD} concentration and the clear trend toward this correlation between V_k and MDA_k with Ca_{FD} concentration (Table 4) also allow us to conclude that disturbances in bone Mg and Ca homeostasis observed in the rats at the SMV-exposure are associated both with the rise in the renal V accumulation and with the SMV-induced OS in the kidney. The changes in the levels of the other elements in biological fluids and in the kidney were also modified in correlation with the renal V_k concentration and/or with the SMV-intensified LPO in the kidney (Table 4).

Studies on the mechanisms of V action have shown that, as a transition metal, it may generate reactive oxygen species (ROS) and/or free radicals (FRs) and stimulate LPO or indirectly modify OS in cells, by releasing FR-generating metals from tissues, modifying enzymatic and antioxidant defence, or interacting with mitochondria [1, 38–40]. The literature data [1, 41] have revealed that OS may be involved in the mechanisms of the toxic action of vanadate. The correlations or clear trends toward them between the basic indices explored, some biomarkers of renal toxicity, or elements and the renal MDA_k and/or TAS_k levels (Table 3) suggest that in our experimental conditions the mechanism of the deleterious action of vanadate (as SMV) was associated with generation of OS in the kidney, as evidenced by the SMV-induced increase in both OS markers in this organ.

Finally, the lowered urinary excretion of Cre_u, U_u, UA_u, KIM-1_u, LDH_u, $GGTP_u$, ALP_u, NAG_u, and K_u, when normalized per 24 h (Figure 2), and the unaltered or enhanced levels/activities of U_u, UA_u, TP_u, ALB_u, β_2M_u, LDH_u, NAG_u, and some elements in the urine, when normalized per Cre_u/24 h (Figure 3), might be in part a consequence of the reduced EUV or the lowered urinary Cre_u excretion (Figure 2(a)), respectively, as indicated by the correlations of EUV or Cre_u with the above-mentioned indices (Tables 3 and 4).

5. Conclusions

The results of this preliminary study demonstrated that the exposure to SMV led to alterations in the levels/activities of some examined biomarkers of nephrotoxicity and caused renal mineral imbalance. They also pointed to a contribution of SMV-induced OS in the mechanism underlying the changes. Moreover, our findings revealed that the use of standard biomarkers of renal toxicity, such as Cre and U, and calculation of CreC for evaluation of kidney function at the SMV-induced fall in the fluid intake and BW may have a weak diagnostic value, since CreC and the plasma and urinary levels of Cre and U are greatly influenced by both the indices mentioned. In addition, the results simultaneously showed that the use of other classical enzymatic tests such as LDH_u, ALP_u, $GGTP_u$, and NAG_u might not be valid either, due to their reduced urinary activities. Our results suggest that, from among the biomarkers tested, $CysC_u$ and KIM-1_u might be the most appropriate in monitoring kidney function at the SMV exposure. The elevated urinary levels of both compounds may point to the proximal tubular dysfunction. Finally, for the first time our results also revealed many significant relationships between the parameters explored.

Endnotes

1. They were bought as part of the Project entitled "Building of the Center for Interdisciplinary Research" realized within the frame of the Operating Programme "Development of Eastern Poland" 2007–2013, Priority I: Modern Economy, Action I.3. The Advancement of Innovation, cofinanced by the European Regional Development Fund.

Conflict of Interests

The authors declare that there is no conflict of interests regarding the publication of this paper.

Acknowledgments

The authors would like to thank very much the former Vice-Rector of John Paul II Catholic University of Lublin Rev. Professor Stanisław Zięba and Dr. Emilia Fornal from Laboratory of Separation and Spectroscopic Method Applications, Center for Interdisciplinary Research, the John Paul II Catholic University of Lublin for providing partial financial support of the studies. They would also like to thank very much Dr. Jakub Nowak from the Laboratory of Composite and Biomimetic Materials, Center for Interdisciplinary Research, the John Paul II Catholic University of Lublin for providing them with a diamond-disc saw for cutting the bones and Anna Gromba M.S. and Wojciech Gierad M.S. for their help in cutting the rat bones.

References

[1] J. Z. Byczkowski and A. P. Kulkarni, "Oxidative stress and prooxidant biological effects of vanadium," in *Vanadium in the Environment Part II: Health Effects*, J. O. Nriagu, Ed., pp. 235–264, John Wiley and Sons, New York, NY, USA, 1998.

[2] A. Ścibior, H. Zaporowska, and I. Niedźwiecka, "Lipid peroxidation in the liver of rats treated with V and/or Mg in drinking water," *Journal of Applied Toxicology*, vol. 29, no. 7, pp. 619–628, 2009.

[3] A. Ścibior, H. Zaporowska, and I. Niedźwiecka, "Lipid peroxidation in the kidney of rats treated with V and/or Mg in drinking water," *Journal of Applied Toxicology*, vol. 30, no. 5, pp. 487–496, 2010.

[4] A. Ścibior, D. Gołębiowska, and I. Niedźwiecka, "Magnesium can protect against vanadium-induced lipid peroxidation in the hepatic tissue," *Oxidaive Medicine and Cellular Longevity*, vol. 2013, Article ID 802734, 11 pages, 2013.

[5] J. Donaldson and F. LaBella, "Prooxidant properties of vanadate *in vitro* on catecholamines and on lipid peroxidation by mouse and rat tissues," *Journal of Toxicology and Environmental Health*, vol. 12, no. 1, pp. 119–126, 1983.

[6] M. H. Oster, J. M. Llobet, J. L. Domingo, J. B. German, and C. L. Keen, "Vanadium treatment of diabetic Sprague-Dawley rats results in tissue vanadium accumulation and pro-oxidant effects," *Toxicology*, vol. 83, no. 1–3, pp. 115–130, 1993.

[7] S. S. Soares, H. Martins, R. O. Duarte et al., "Vanadium distribution, lipid peroxidation and oxidative stress markers upon decavanadate *in vivo* administration," *Journal of Inorganic Biochemistry*, vol. 101, no. 1, pp. 80–88, 2007.

[8] J. Donaldson, R. Hemming, and F. LaBella, "Vanadium exposure enhances lipid peroxidation in the kidney of rats and mice," *Canadian Journal of Physiology and Pharmacology*, vol. 63, no. 3, pp. 196–199, 1985.

[9] M. Carmignani, A. R. Volpe, E. Sabbioni, M. Felaco, and P. Boscolo, "Vanadium and the cardiovascular system: regulatory effects and toxicity," in *Vanadium in the Environment Part II: Health Effects*, J. O. Nriagu, Ed., vol. 31, pp. 181–219, John Wiley and Sons, New York, NY, USA, 1998.

[10] K. De Cremer, M. Van Hulle, C. Chéry et al., "Fractionation of vanadium complexes in serum, packed cells and tissues of Wistar rats by means of gel filtration and anion-exchange chromatography," *Journal of Biological Inorganic Chemistry*, vol. 7, no. 7-8, pp. 884–890, 2002.

[11] V. Sitprija, K. Tungsanga, P. Tosukhowong et al., "Metabolic problems in northeastern Thailand: possible role of vanadium," *Mineral and Electrolyte Metabolism*, vol. 19, no. 1, pp. 51–56, 1993.

[12] E. Dafnis and S. Sabatini, "Biochemistry and pathophysiology of vanadium," *Nephron*, vol. 67, no. 2, pp. 133–143, 1994.

[13] P. Tosukhowong, K. Tungsanga, S. Eiam-Ong, and V. Sitprija, "Environmental distal renal tubular acidosis in Thailand: an enigma," *American Journal of Kidney Diseases*, vol. 33, no. 6, pp. 1180–1186, 1999.

[14] A. S. Tracey, G. R. Willsky, and E. S. Takeuchi, *Vanadium—Chemistry, Biochemistry, Pharmacology and Practical Applications*, Taylor and Francis, Boca Raton, Fla, USA, 2007.

[15] S. M. Talbott and K. Hughes, *The Health Professional's Guide to Dietary Supplements*, Lippincott Williams and Wilkins, 2007.

[16] V. Sitprija and S. Eiam-Ong, "Vanadium and metabolic problems," in *Vanadium in the Environment Part II: Health Effects*, J. O. Nriagu, Ed., pp. 91–120, John Wiley and Sons, New York, NY, USA, 1998.

[17] Y. Teng, S. Ni, C. Zhang, J. Wang, X. Lin, and Y. Huang, "Environmental geochemistry and ecological risk of vanadium pollution in Panzhihua mining and smelting area, Sichuan, China," *Chinese Journal of Geochemistry*, vol. 25, no. 4, pp. 379–385, 2006.

[18] Expert group on vitamins and minerals, Review of vanadium. EVM/00/04.REVISEDAUG, 2002.

[19] K. H. Thompson, M. Battell, and J. H. McNeill, "Toxicology of vanadium in mammals," in *Vanadium in the Environment Part II: Health Effects*, J. O. Nriagu, Ed., pp. 21–38, John Wiley and Sons, New York, NY, USA, 1998.

[20] R. G. Fassett, S. K. Venuthurupalli, G. C. Gobe, J. S. Coombes, M. A. Cooper, and W. E. Hoy, "Biomarkers in chronic kidney disease: a review," *Kidney International*, vol. 80, no. 8, pp. 806–821, 2011.

[21] G. D'Amico and C. Bazzi, "Urinary protein and enzyme excretion as markers of tubular damage," *Current Opinion in Nephrology and Hypertension*, vol. 12, no. 6, pp. 639–643, 2003.

[22] V. S. Vaidya, V. Ramirez, T. Ichimura, N. A. Bobadilla, and J. V. Bonventre, "Urinary kidney injury molecule-1: a sensitive quantitative biomarker for early detection of kidney tubular injury," *American Journal of Physiology—Renal Physiology*, vol. 290, no. 2, pp. F517–F529, 2006.

[23] A. Ścibior, A. Adamczyk, D. Gołebiowska, and I. Niedźwiecka, "Effect of 12-week vanadate and magnesium co-administration on chosen haematological parameters as well as on some indices of iron and copper metabolism and biomarkers of oxidative stress in rats," *Environmental Toxicology and Pharmacology*, vol. 34, no. 2, pp. 235–252, 2012.

[24] J. L. Domingo, M. Gomez, D. J. Sanchez, J. M. Llobet, and C. L. Keen, "Toxicology of vanadium compounds in diabetic rats: the action of chelating agents on vanadium accumulation," *Molecular and Cellular Biochemistry*, vol. 153, no. 1-2, pp. 233–240, 1995.

[25] J. Azay, J. Brès, M. Krosniak et al., "Vanadium pharmacokinetics and oral bioavailability upon single-dose administration of vanadyl sulfate to rats," *Fundamental and Clinical Pharmacology*, vol. 15, no. 5, pp. 313–324, 2001.

[26] World Health Organization, *Vanadium Pentoxide and Other Inorganic Vanadium Compounds*, WHO, Geneva, Switzerland, 2001.

[27] International Agency for Research on Cancer Monographs on the evaluation of carcinogenic risks to humans, *Cobalt in Hard Metals and Cobalt Sulfate, Gallium Arsenide, Indium Phosphide and Vanadium Pentoxide*, vol. 86, Lyon, France, 2006.

[28] A. Ścibior and H. Zaporowska, "Effects of vanadium(V) and/or chromium(III) on L-ascorbic acid and glutathione as well as iron, zinc, and copper levels in rat liver and kidney," *Journal of Toxicology and Environmental Health A*, vol. 70, no. 8, pp. 696–704, 2007.

[29] D. A. Barrio and S. B. Etcheverry, "Vanadium and bone development: putative signaling pathways," *Canadian Journal of Physiology and Pharmacology*, vol. 84, no. 7, pp. 677–686, 2006.

[30] A. Ścibior, H. Zaporowska, A. Wolińska, and J. Ostrowski, "Antioxidant enzyme activity and lipid peroxidation in the blood of rats co-treated with vanadium (V^{+5}) and chromium (Cr^{+3})," *Cell Biology and Toxicology*, vol. 26, no. 6, pp. 509–526, 2010.

[31] A. C. Baxmann, M. S. Ahmed, N. C. Marques et al., "Influence of muscle mass and physical activity on serum and urinary creatinine and serum cystatin C," *Clinical Journal of the American Society of Nephrology*, vol. 3, no. 2, pp. 348–354, 2008.

[32] P. D. Sarkar, G. Rajeshwari, and T. M. Shivaprakash, "Cystatin C—A novel marker of glomerular filtration: a review," *Indian Journal of Clinical Biochemistry*, vol. 20, no. 1, pp. 139–144, 2005.

[33] G. H. Tesch, "Review: serum and urine biomarkers of kidney disease: a pathophysiological perspective," *Nephrology*, vol. 15, no. 6, pp. 609–616, 2010.

[34] M. Warwas and A. Piwowar, "Moczowa cystatyna C jako biomarker uszkodzenia kanalików nerkowych," *Postępy Higieny i Medycyny Doświadczalnej*, vol. 65, pp. 562–568, 2011.

[35] J. Westhuyzen, "Cystatin C: a promising marker and predictor of impaired renal function," *Annals of Clinical and Laboratory Science*, vol. 36, no. 4, pp. 387–394, 2006.

[36] A. De La Torre, S. Granero, E. Mayayo, J. Corbella, and J. L. Domingo, "Effect of age on vanadium nephrotoxicity in rats," *Toxicology Letters*, vol. 105, no. 1, pp. 75–82, 1999.

[37] A. M. Cortizo, V. C. Salice, and S. B. Etcheverry, "Vanadium compounds: their action on alkaline phosphatase activity," *Biological Trace Element Research*, vol. 41, no. 3, pp. 331–339, 1994.

[38] A. M. Evangelou, "Vanadium in cancer treatment," *Critical Reviews in Oncology/Hematology*, vol. 42, no. 3, pp. 249–265, 2002.

[39] A. Ścibior and H. Zaporowska, "Effects of combined vanadate and magnesium treatment on erythrocyte antioxidant defence system in rats," *Environmental Toxicology and Pharmacology*, vol. 30, no. 2, pp. 153–161, 2010.

[40] X.-G. Yang, X.-D. Yang, L. Yuan, K. Wang, and D. C. Crans, "The permeability and cytotoxicity of insulin-mimetic vanadium compounds," *Pharmaceutical Research*, vol. 21, no. 6, pp. 1026–1033, 2004.

[41] J. Liu, H. Cui, X. Liu et al., "Dietary high vanadium causes oxidative damage-induced renal and hepatic toxicity in broilers," *Biological Trace Element Research*, vol. 145, no. 2, pp. 189–200, 2012.

Hindawi Publishing Corporation
BioMed Research International
Volume 2014, Article ID 761264, 19 pages
http://dx.doi.org/10.1155/2014/761264

Review Article

Oxidative Stress, Prooxidants, and Antioxidants: The Interplay

Anu Rahal,[1] Amit Kumar,[2] Vivek Singh,[3] Brijesh Yadav,[4] Ruchi Tiwari,[2] Sandip Chakraborty,[5] and Kuldeep Dhama[6]

[1] *Department of Veterinary Pharmacology and Toxicology, Uttar Pradesh Pandit, Deen Dayal Upadhayay Pashu Chikitsa Vigyan Vishwa Vidyalaya Evam Go-Anusandhan Sansthan (DUVASU), Mathura 281001, India*
[2] *Department of Veterinary Microbiology and Immunology, Uttar Pradesh Pandit, Deen Dayal Upadhayay Pashu Chikitsa Vigyan Vishwa Vidyalaya Evam Go-Anusandhan Sansthan (DUVASU), Mathura 281001, India*
[3] *Department of Animal Husbandry, Kuchaman, Rajasthan 341508, India*
[4] *Department of Veterinary Physiology, Uttar Pradesh Pandit, Deen Dayal Upadhayay Pashu Chikitsa Vigyan Vishwa Vidyalaya Evam Go-Anusandhan Sansthan (DUVASU), Mathura 281001, India*
[5] *Animal Resources Development Department, Pt. Nehru Complex, Agartala 799006, India*
[6] *Division of Pathology, Indian Veterinary Research Institute, Izatnagar, Bareilly 243122, India*

Correspondence should be addressed to Amit Kumar; balyan74@gmail.com

Received 19 May 2013; Revised 3 November 2013; Accepted 6 November 2013; Published 23 January 2014

Academic Editor: Afaf K. El-Ansary

Oxidative stress is a normal phenomenon in the body. Under normal conditions, the physiologically important intracellular levels of reactive oxygen species (ROS) are maintained at low levels by various enzyme systems participating in the *in vivo* redox homeostasis. Therefore, oxidative stress can also be viewed as an imbalance between the prooxidants and antioxidants in the body. For the last two decades, oxidative stress has been one of the most burning topics among the biological researchers all over the world. Several reasons can be assigned to justify its importance: knowledge about reactive oxygen and nitrogen species production and metabolism; identification of biomarkers for oxidative damage; evidence relating manifestation of chronic and some acute health problems to oxidative stress; identification of various dietary antioxidants present in plant foods as bioactive molecules; and so on. This review discusses the importance of oxidative stress in the body growth and development as well as proteomic and genomic evidences of its relationship with disease development, incidence of malignancies and autoimmune disorders, increased susceptibility to bacterial, viral, and parasitic diseases, and an interplay with prooxidants and antioxidants for maintaining a sound health, which would be helpful in enhancing the knowledge of any biochemist, pathophysiologist, or medical personnel regarding this important issue.

1. Introduction

Man and animals are exposed to a large number of biological and environmental factors like alterations in feed and husbandry practices, climatic variables, transportation, regrouping, the therapeutic and prophylactic activities, various stressors, and so forth. The ability of the man and animal to fight against these factors is important for maintenance of their health and productivity. Today, the entire world is witnessing an upsurge in chronic health complications like cardiovascular disease, hypertension, diabetes mellitus, different forms of cancer, and other maladies. Medical surveys suggest that diet may serve as a potential tool for the control of these chronic diseases [1, 2]. Regular chewing of tobacco along with inadequate diet is the most prominent finding to mortality due to lung cancer in USA [3]. Diets rich in fruit and vegetables have been reported to exert a protective effect against a variety of diseases, particularly the cardiovascular disease and cancer [4–10]. The primary nutrients thought to provide protection afforded by fruit and vegetables are the antioxidants [11, 12]. In an analysis, Potter [13] reviewed 200 epidemiological studies, the majority of which showed a protective effect of increased fruit and vegetable intake and concluded that the high content of polyphenolic antioxidants in fruits and vegetables is probably the main factor responsible for the beneficial effects. This awareness has led to a tremendous increase in the proportion of fruits and vegetables rich in antioxidant molecules on the dining table in the last two

decades, but still the risk of chronic health problems refuses to decline, rather it upsurged with an enhanced vigour, giving rise to a very important question—why? If the health associated problems are due to oxidative stress and the dietary constituents are potent antioxidants, then the question of problem arrival should not be there. What happens when these antioxidants reach the body tissues of interest or are there other factors still to be unrevealed?

2. Stress

The term "stress" has been used in physics since unknown time as it appears in the definition of Hooke's law of 1658, but its first use in the biological science dates back to Sir Hans Selye's letter to the Editor of Nature in 1936. At that time, it was not accepted, but later on, after the famous address of Hans Selye at the prestigious College of France, it received approval among scientific community, but defining stress again troubled Selye over several years. Today, stress can be defined as a process of altered biochemical homeostasis produced by psychological, physiological, or environmental stressors [14]. Any stimulus, no matter whether social, physiological, or physical, that is perceived by the body as challenging, threatening, or demanding can be labeled as a stressor. The presence of a stressor leads to the activation of neurohormonal regulatory mechanisms of the body, through which it maintains the homeostasis [14]. The overall physiological impact of these factors and the adaptation ability of the body determine the variations in growth, development, productivity, and health status of the animals [15–17]. These alterations can be viewed as a consequence of general adaptation syndrome as postulated by Hans Selye [18] and usually return to their normal status once the stimulus has disappeared from the scene. Strong and sustained exposure to stress [16, 19, 20] may result in higher energy negative balance and may ultimately result in reduction in adaptation mechanisms, increase in the susceptibility to infection by pathogens, decline in productivity, and finally a huge economical loss [16, 19, 21].

Many of us puzzle between distress, stress, and oxidative stress. Distress differs from stress, which is a physiological reaction that can lead to an adaptive response [22]. Distress is comparatively difficult to define and generally refers to a state in which an animal cannot escape from or adapt to the external or internal stressors or conditions it experiences resulting in negative effects upon its well-being [22]. Stress leads to adaptation but distress does not. Stress is a commonly used term for oxidative stress. Any alteration in homeostasis leads to an increased production of these free radicals, much above the detoxifying capability of the local tissues [23]. These excessive free radicals then interact with other molecules within cells and cause oxidative damage to proteins, membranes, and genes. In this process they often create more free radicals, sparking off a chain of destruction. Oxidative damage has been implicated in the cause of many diseases such as cardiovascular diseases, neuronal degeneration, and cancer and has an impact on the body's aging process too. An altered response to the therapeutic agents has also been observed [12]. External factors such as pollution, sunlight, and smoking also trigger the production of free radicals.

Most importantly, stress is one of the basic etiologies of disease [24]. It can have several origins like environmental extremes for example, cold, heat, hypoxia, physical exercise or malnutrition (Figure 1).

On the basis of duration and onset, stress might be acute and chronic stress. The stress due to exposure of cold or heat is generally of acute type and is released with the removal of cause. Similarly, stress due to physical exercises or complete immobilization [25] is also acute in nature. The nutritional and environmental stresses, where the causes persist for a longer period of time, are chronic stress.

2.1. Cold Stress. Cold stress is evident whenever the temperature falls below 18°C and the body experiences severe cold related illness and permanent tissue damage. An acute cold stress (−20°C for 4 hours) in rats causes profound reduction in contraction amplitude with an increase in heart rate in the isolated heart preparations [26]. The decrease in amplitudes is associated with inadequate ATP formation. While changing perfusion of poststress isolated heart, myocardial rigidity further slows down and this seemed to be associated with activated glycolysis. There are no signs of cardiomyocytic lesion after cold stress. Reduced coronary flow is the only abnormal effect of acute cold stress under these conditions. High cardiac resistance to the damaging effect of cold is likely to be related to increased processes of glycolysis and glycogenolysis in the cardiomyocytes. The activity of succinate dehydrogenase also gets elevated indicating the influence of cold stress on the Krebs cycle [27]. Coronary blood flow is also reduced and later on results in an altered basophils activity in the myocardium [28].

2.2. Physical Exercise and Stress. Health benefits of regular physical exercise are undebatable. Both resting and contracting skeletal muscles produce reactive oxygen and nitrogen species (ROS, RNS). Low physiological levels of ROS are generated in the muscles to maintain the normal tone and contractility, but excessive generation of ROS promotes contractile dysfunction resulting in muscle weakness and fatigue [29]. This is perhaps the reason why intense and prolonged exercise results in oxidative damage to both proteins and lipids in the contracting muscle fibers [30].

Regular exercise induces changes in both enzymatic and nonenzymatic antioxidants in the skeletal muscle. Furthermore, oxidants can modulate a number of cell signaling pathways and regulate the expression of multiple genes in eukaryotic cells. This oxidant-mediated change in gene expression involves changes at transcriptional, mRNA stability, and signal transduction levels. The magnitude of exercise-mediated changes in superoxide dismutase (SOD) activity of skeletal muscle increases as a function of the intensity and duration of exercise [31, 32]. Mild physical activity increases nuclear factor-*kappa* B (NF-κB) activity in the muscle of rats as well as the gene expression for manganese superoxide dismutase (MnSOD) and endothelial nitric oxide synthase (eNOS) [33].

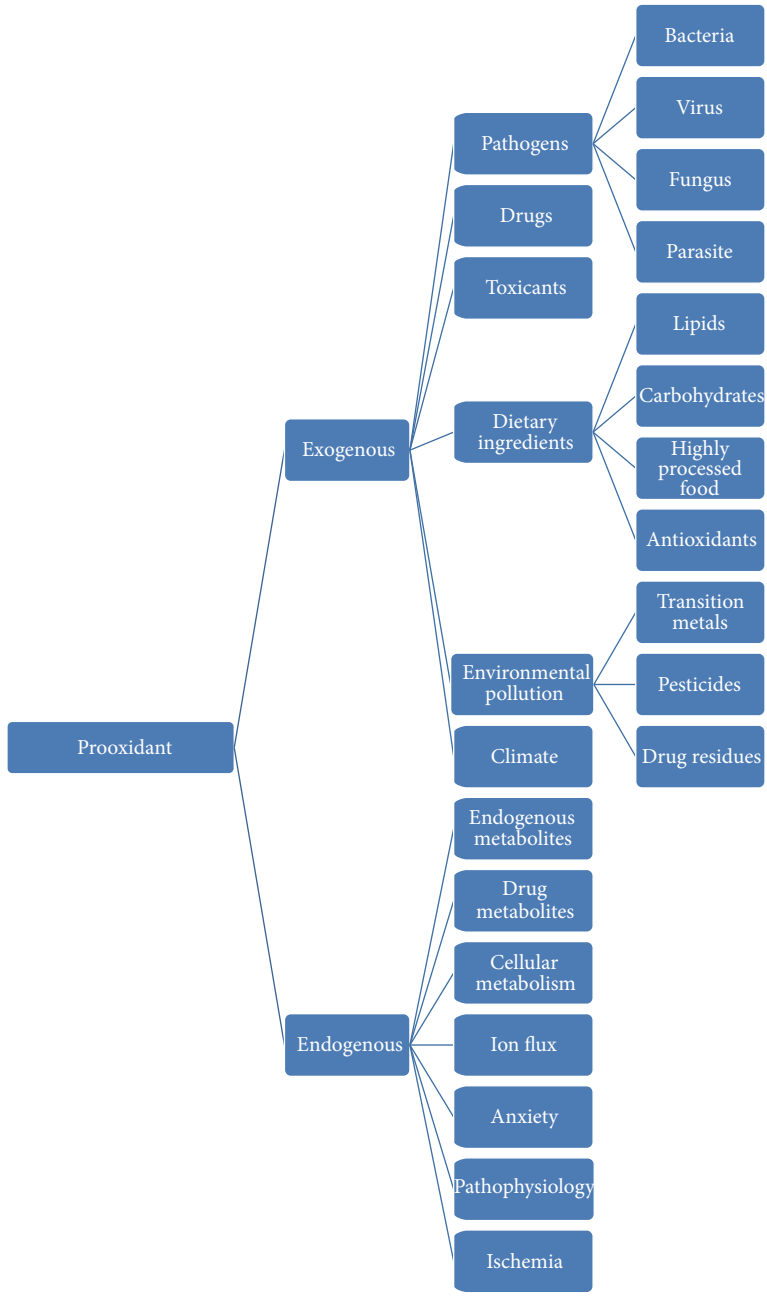

Figure 1: General classification of prooxidants.

2.3. Chronic Stress. Chronic stress significantly alters limbic neuroarchitecture and function and potentiates oxidative stress [25] and emotionality in rats [34]. Chronic restraining of laboratory animals has been found to increase aggression, potentiate anxiety, and enhance fear conditioning [34]. Chronic immobilization induces anxiety behavior and dendritic hypertrophy in the basolateral amygdala, which persist beyond a recovery period. Restraint of rats causes increased mucin release, as measured by [3H] glucosamine incorporation and goblet cell depletion, prostaglandin E2 (PGE2) secretion, and mast cell activation in colonic explants [35]. Upregulation of the neurotensin precursor mRNA in the paraventricular nucleus of the hypothalamus after immobilization has also been reported [36]. Neurotensin stimulates mucin secretion from human colonic goblet cell line by a receptor mediated mechanism [37].

2.4. Nutritional Stress. Nutrition is one of the most significant external etiologies for oxidative stress including its characteristics, type and quality, ratio of the various nutrients, dietary balance with regard to protein, carbohydrates, fats, macro- and trace elements, and so forth. Feed exercises a considerable influence over the physiological condition and thus the homeostasis of the animal body [16, 19, 38–42].

Feeding of endogenous or exogenous antioxidants can sensitively regulate glycolysis and the Warburg effect in hepatoma cells [43]. Fasting induces an increase in total leukocytes counts, eosinophils, and metamyelocytes in the blood profile, accompanied by a decrease in the basophils and monocytes, a typical "stress leukogram" produced in the animal body due to the increased endogenous production of cortisol from the adrenal glands during oxidative stress [16, 19, 38–42]. The leukocytosis with neutrophilia associated with fasting may be a consequence of an inflammatory reaction, caused by the direct action of ammonia on the rumen wall [38, 44]. The monocytopenia may be a result of adaptation and defense mechanism undergoing in the body and leads to higher susceptibility to pathogens [21, 45].

Nutritional stress causes adrenal gland hyperfunction and, thus, an increased release of catecholamines in the blood, with a simultaneous inhibition of the production of insulin in the pancreas [20, 38, 46–48]. The process of glycogenolysis is observed in the first 24 hours of fasting [20, 39, 46–49]. Thereafter, gluconeogenesis from amino acid precursors and lipolysis from glycerol, as well as from lactate through the Cori cycle, maintain a regular supply of glucose. Lactate gets transformed into pyruvate and participates in the gluconeogenesis along with the deaminated amino acids. The increased production of catecholamines (epinephrine and dopamine) owing to fasting results in peripheral vasoconstriction and redistribution in blood which is expressed as erythrocytosis, leukocytosis, and neutrophilia [47].

2.5. Hypoxic Stress. Hypoxia is known to stimulate mitochondria to release ROS (mROS). Under hypoxic conditions, mitochondria participate in a ROS burst generated at complex III of the electron transport chain [50]. Hypoxia and reoxygenation result in reversible derangement of ATPase and architecture of mitochondrial membrane. Cardiac hemodynamic parameters, which decline immediately under hypoxic conditions, recover during reoxygenation [51], but the biochemical and histopathological studies provide a complicated pattern [52]. High CAT (carboxyatractyloside) sensitivity of the ATPase is observed at 5 min of hypoxia. The initial phase in hypoxic perfusion (<15 min) exhibits a steep increase of ADP contents and ATPase activities and a drastic fall of ATP/ADP ratios in mitochondria, as well as in tissues. Furthermore, the number of ATPase particles visible at the inner aspect of mitochondrial membrane decreases. During the second phase of hypoxic perfusion (from 30 min onwards), the count of ATPase particles visible at the inner mitochondrial membrane further decreases. ATPase activities fluctuate, retaining close contact with the membrane during hypoxia. The mitochondrial ultrastructural damage becomes more evident. High-energy phosphates reserves of myocardium could help myocardial cells to maintain their structural integrity [52]. ATP/ADP ratios attain values of almost 1. During reoxygenation (after 30 min of hypoxia), the levels of mitochondrial adenine nucleotides, oxidative phosphorylation rate, and respiratory control index increase within 20 min and then slightly decline again. The ATP/ADP ratio is diminished in the course of reoxygenation. ATPase activity also decreases within 20 min of reoxygenation and the ADP/O ratio reaches control values. The ATPase activity gains its highest sensitivity towards catalase at 10 min of reoxygenation attaining a value similar to that of 5 min of hypoxic perfusion.

3. Stress and Well-Being

Each cell in the human body maintains a condition of homeostasis between the oxidant and antioxidant species [53]. Up to 1–3% of the pulmonary intake of oxygen by humans is converted into ROS [54]. Under conditions of normal metabolism, the continuous formation of ROS and other free radicals is important for normal physiological functions like generation of ATP, various catabolic and anabolic processes and the accompanying cellular redox cycles. However, excessive generation of free radicals can occur due to endogenous biological or exogenous environmental factors, such as chemical exposure, pollution, or radiation.

There are ROS subgroups: free radicals such as superoxide radicals ($O_2^{\bullet -}$) and nonradical ROS such as hydrogen peroxide (H_2O_2) [55]. The primary free radicals generated in cells are superoxide ($O_2^{\bullet}$) and nitric oxide (NO). Superoxide is generated through either incomplete reduction of oxygen in electron transport systems or as a specific product of enzymatic systems, while NO is generated by a series of specific enzymes (the nitric oxide synthases). Both superoxide and NO are reactive and can readily react to form a series of other ROS and RNS.

Generally, mitochondria are the most important source of cellular ROS where continuous production of ROS takes place [55]. This is the result of the electron transport chain located in the mitochondrial membrane, which is essential for the energy production inside the cell [56, 57]. Additionally, some cytochrome 450 enzymes are also known to produce ROS [58].

4. Biochemical Basis of Stress

Several endogenous cells and cellular components participate in initiation and propagation of ROS (Table 1) [59–63].

All these factors play a crucial role in maintenance of cellular homeostasis. A stressor works by initiating any of these mechanisms. Oxidative stress occurs when the homeostatic processes fail and free radical generation is much beyond the capacity of the body's defenses, thus promoting cellular injury and tissue damage. This damage may involve DNA and protein content of the cells with lipid peroxidation of cellular membranes, calcium influx, and mitochondrial swelling and lysis [60, 63, 64]. ROS are also appreciated as signaling molecules to regulate a wide variety of physiology. It was first proposed in the 1990s when hydrogen peroxide was shown to be required for cytokine, insulin, growth factor, activator protein-1 (AP-1), and NF-κB signaling [65, 66]. The role of hydrogen peroxide in promoting phosphatase inactivation by cysteine oxidation provided a likely biochemical mechanism by which ROS can impinge on signaling pathways [67]. The role of ROS in signaling of cytochrome c mediated apoptosis is also well established [68]. ROS can cause reversible

Table 1: Endogenous mediators of oxidative stress.

Leakage of free radicals	Membrane-bound enzymes	NADPH oxidase
	Electron transport systems	Mixed function oxidases
Activation of oxygen	Soluble cell constituents	Transition metals, thiol containing proteins, quinine derivatives, epinephrine, metalloproteins, hemeproteins, and flavoproteins
	Xenobiotic metabolizing enzymes	Cyt P_{450}-dependent monooxygenases, Cyt b_5, and NADPH-dependent cytochrome reductases
ROS generation/propagation	Soluble cytosolic enzymes	Xanthine oxidase, superoxide dismutase, catalase
	Phagocytic cells	Neutrophils, macrophages, and monocytes involved in inflammation, respiratory burst, and removal of toxic molecules
	Local ischemia	Damaged blood supply due to injury or surgery

posttranslational protein modifications to regulate signaling pathways. A typical example of the beneficial physiological role of free radicals is a molecule of nitric oxide (NO). NO is formed from arginine by the action of NO-synthase (NOS) [69]. NO is produced by constitutive NOS during vasodilating processes (eNOS) or during transmission of nerve impulses (nNOS). In the presence of stressors, NO is produced by catalytic action of inducible NOS (iNOS) and is at higher concentrations [70–72]. NO can cause damage to proteins, lipids, and DNA either directly or after reaction with superoxide, leading to the formation of the very reactive peroxynitrite anion (nitroperoxide) ONOO– [73–75].

Lipid peroxidation of polyunsaturated lipids is one of the most preferred markers for oxidative stress. The product of lipid peroxidation, malondialdehyde, is easily detected in blood/plasma and has been used as a measure of oxidative stress. In addition, the unsaturated aldehydes produced from these reactions have been implicated in modification of cellular proteins and other constituents [76]. The peroxidized lipid can produce peroxy radicals and singlet oxygen.

5. Physiological Role of Stress

Stress has a significant ecological and evolutionary role and may help in understanding the functional interactions among life history traits [77–79]. Stress leads to a number of physiological changes in the body including altered locomotor activity and general exploratory behavior. The physiological role of ROS is associated with almost all of the body processes, for example, with reproductive processes [80]. Since under physiological conditions a certain level of free radicals and reactive metabolites is required, complete suppression of FR formation would not be beneficial [81]. One further beneficial example of ROS seen at low/moderate concentrations is the induction of a mitogenic response.

Stress leads to activation of hypothalamic-pituitary-adrenal axis. The increased endogenous catecholamine release has been observed in cold environmental conditions. The activity of succinate dehydrogenase also gets elevated indicating the influence of ROS as evident in cold environmental conditions [27]. Coronary blood flow is reduced and an altered basophils activity in the myocardium is also observed [28].

Free radicals play an irreplaceable role in phagocytosis as one of the significant microbicidal systems [82], or in several biochemical reactions, for example, hydroxylating, carboxylating, or peroxidating reactions, or in the reduction of ribonucleotides [83]. At present, free radicals and their metabolites are assumed to have important biomodulating activities and a regulatory ability in signal transduction process during transduction of intercellular information [83].

Among the reactive oxygen species, H_2O_2 best fulfills the requirements of being a second messenger [84]. Its enzymatic production and degradation, along with its functional requirement for thiol oxidation, facilitate the specificity for time and place that are required in signaling. Both the thermodynamic and kinetic considerations support that among different possible oxidation states of cysteine, formation of sulfenic acid derivatives or disulfides can be applicable as thiol redox switches in signaling. H_2O_2 readily diffuses across biological membranes, and so it is well-suited as a diffusible messenger [85, 86].

In the presence of transition metals such as iron or copper, H_2O_2 can give rise to the indiscriminately reactive and toxic hydroxyl radical ($HO^{\bullet}$) by Fenton chemistry. Increasing evidence indicates that H_2O_2 is a particularly an intriguing candidate as an intracellular and intercellular signaling molecule because it is neutral and membrane permeable [84, 87].

Specifically, H_2O_2 can oxidize thiol (–SH) of cysteine residues and form sulphenic acid (–SOH), which can get glutathionylated (–SSG), form a disulfide bond (–SS–) with adjacent thiols, or form a sulfenyl amide (–SN–) with amides [88]. Each of these modifications modifies the activity of the target protein and thus its function in a signaling pathway. Phosphatases appear to be susceptible to regulation by ROS in this manner, as they possess a reactive cysteine moiety in their catalytic domain that can be reversibly oxidized, which inhibits their dephosphorylation activity [67]. Specific examples of phosphatases known to be regulated in this manner are PTP1b, PTEN, and MAPK phosphatases [89].

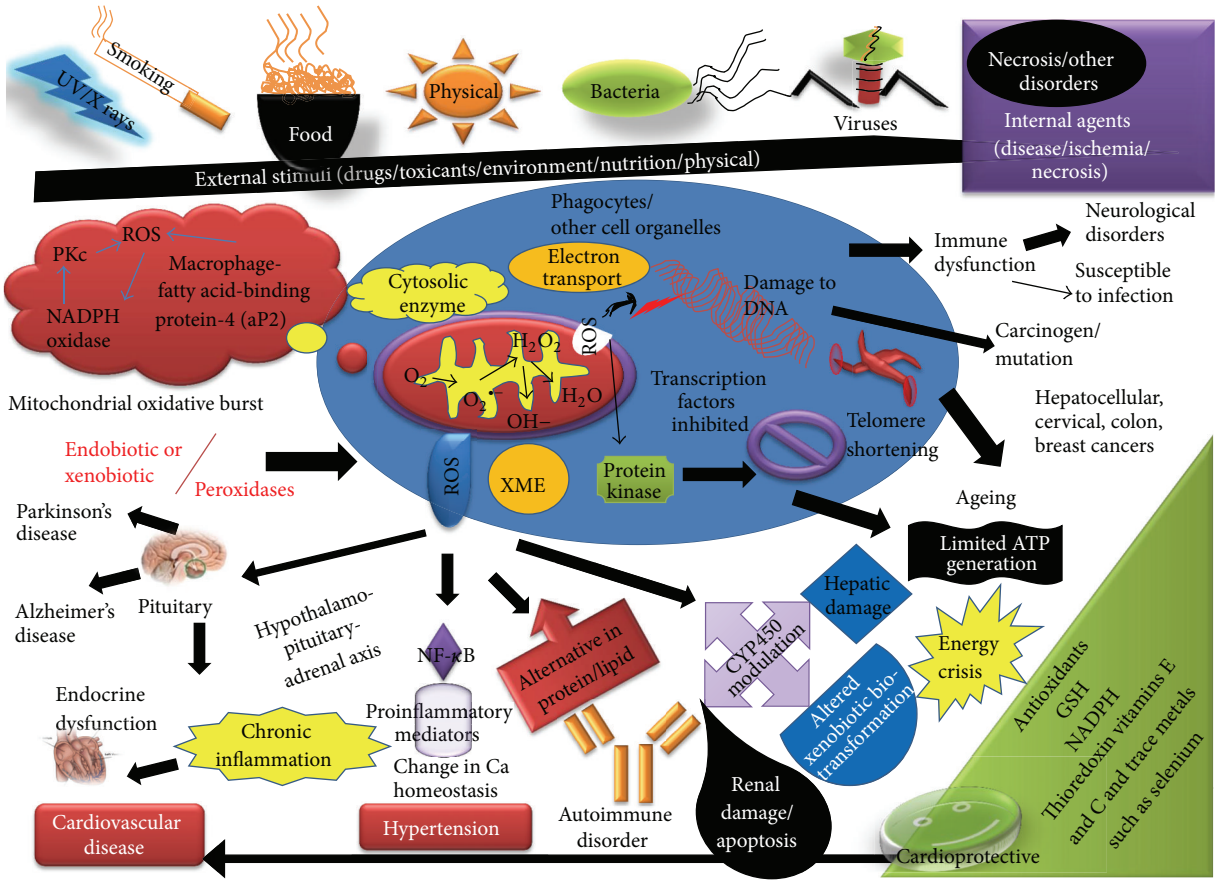

Figure 2: Oxidative stress and disease development.

Any emotional stress leads to a decrease in sympathetic outflow as well as energy production of the tissues [27].

6. Oxidative Stress

The harmful effect of free ROS and RNS radicals causing potential biological damage is termed oxidative stress and nitrosative stress, respectively [90–92]. This is evident in biological systems when there is either an excessive production of ROS/RNS and/or a deficiency of enzymatic and nonenzymatic antioxidants. The redox stress/oxidative stress is a complex process. Its impact on the organism depends on the type of oxidant, on the site and intensity of its production, on the composition and activities of various antioxidants, and on the ability of repair systems [93].

The term "ROS" includes all unstable metabolites of molecular oxygen (O_2) that have higher reactivity than O_2 like superoxide radical ($O_2^{\bullet}$) and hydroxyl radical ($HO^{\bullet}$) and nonradical molecules like hydrogen peroxide (H_2O_2). These ROS are generated as byproduct of normal aerobic metabolism, but their level increases under stress which proves to be a basic health hazard. Mitochondrion is the major cell organelle responsible for ROS production [50, 57]. It generates ATP through a series of oxidative phosphorylation processes. During this process, one- or two-electron reductions instead of four electron reductions of O_2 can occur, leading to the formation of $O_2^{\bullet}$ or H_2O_2, and these species can be converted to other ROS. Other sources of ROS may be reactions involving peroxisomal oxidases [94], cytochrome *P*-450 enzymes [95], NAD (P)H oxidases [96], or xanthine oxidase [97].

7. Oxidative Stress and Diseases

Today the world is experiencing a rise in age related chronic health diseases like cardiovascular disorders, cancer, and so forth and their associated negative health impacts and mortality/casualty [98–101]. Some metabolic diseases like diabetes are also associated with an enhanced level of lipoperoxidation (Figure 2).

The central nervous system (CNS) is extremely sensitive to free radical damage because of a relatively small total antioxidant capacity. The ROS produced in the tissues can inflict direct damage to macromolecules, such as lipids, nucleic acids, and proteins [102]. The polyunsaturated fatty acids are one of the favored oxidation targets for ROS. Oxygen-free radicals, particularly superoxide anion radical ($O_2^{\bullet -}$), hydroxyl radical ($OH^{\bullet -}$), and alkylperoxyl radical ($^{\bullet}OOCR$), are potent initiators of lipid peroxidation, the role of which is well established in the pathogenesis of a wide range of diseases. Once lipid peroxidation is initiated, a propagation of chain reactions will take place until termination

products are produced. Therefore, end products of lipid peroxidation, such as malondialdehyde (MDA), 4-hydroxy-2-nonenol (4-HNE), and F2-isoprostanes, are accumulated in biological systems. DNA bases are also very susceptible to ROS oxidation, and the predominant detectable oxidation product of DNA bases *in vivo* is 8-hydroxy-2-deoxyguanosine. Oxidation of DNA bases can cause mutations and deletions in both nuclear and mitochondrial DNA. Mitochondrial DNA is especially prone to oxidative damage due to its proximity to a primary source of ROS and its deficient repair capacity compared with nuclear DNA. These oxidative modifications lead to functional changes in various types of proteins (enzymatic and structural), which can have substantial physiological impact. Similarly, redox modulation of transcription factors produces an increase or decrease in their specific DNA binding activities, thus modifying the gene expression.

Among different markers of oxidative stress, malondialdehyde (MDA) and the natural antioxidants, metalloenzymes Cu, Zn-superoxide dismutase (Cu, Zn-SOD), and selenium dependent glutathione peroxidase (GSHPx), are currently considered to be the most important markers [103–106]. Malondialdehyde (MDA) is a three-carbon compound formed from peroxidized polyunsaturated fatty acids, mainly arachidonic acid. It is one of the end products of membrane lipid peroxidation. Since MDA levels are increased in various diseases with excess of oxygen free radicals, many relationships with free radical damage were observed.

Cu, Zn-SOD is an intracellular enzyme present in all oxygen-metabolizing cells, which dismutates the extremely toxic superoxide radical into potentially less toxic hydrogen peroxide. Cu, Zn-SOD is widespread in nature, but being a metalloenzyme, its activity depends upon the free copper and zinc reserves in the tissues. GSHPx, an intracellular enzyme, belongs to several proteins in mammalian cells that can metabolize hydrogen peroxide and lipid hydroperoxides.

8. Oxidative Stress and Altered Immune Function

The relationship between oxidative stress and immune function of the body is well established. The immune defense mechanism uses the lethal effects of oxidants in a beneficial manner with ROS and RNS playing a pivotal role in the killing of pathogens. The skilled phagocytic cells (macrophages, eosinophils, heterophils), as well as B and T lymphocytes, contain an enzyme, the nicotinamide adenine dinucleotide phosphate (NADPH) oxidase [107, 108], which is responsible for the production of ROS following an immune challenge. At the onset of an immune response, phagocytes increase their oxygen uptake as much as 10–20 folds (respiratory burst). The $O^{\bullet -}$ generated by this enzyme serves as the starting material for the production of a suite of reactive species. Direct evidence also certifies production of other powerful prooxidants, such as hydrogen peroxide (H_2O_2), hypochlorous acid (HOCl), peroxynitrite (ONOO–), and, possibly, hydroxyl ($OH^{\bullet}$) and ozone (O_3) by these cells. Although the use of these highly reactive endogenous metabolites in the cytotoxic response of phagocytes also injures the host tissues, the nonspecificity of these oxidants is an advantage since they take care of all the antigenic components of the pathogenic cell [109].

Several studies have demonstrated the interdependency of oxidative stress, immune system, and inflammation. Increased expression of NO has been documented in dengue and in monocyte cultures infected with different types of viral infections. Increased production of NO has also been accompanied with enhancement in oxidative markers like lipid peroxidation and an altered enzymatic and nonenzymatic antioxidative response in dengue infected monocyte cultures [110]. More specifically, the oxygen stress related to immune system dysfunction seems to have a key role in senescence, in agreement with the oxidation/inflammation theory of aging. Moreover, it has been revealed that reduced NADPH oxidase is present in the pollen grains and can lead to induction of airway associated oxidative stress. Such oxidative insult is responsible for developing allergic inflammation in sensitized animals. There is triggering of production of interleukin (IL)-8 along with proinflammatory cytokines, namely, tumor necrosis factor (TNF)-alpha and IL-6. There is initiation of dendritic cell (DC) maturation that causes significant upregulation of the expression of cluster of differentiation (CD)-80, 86 and 83 with a slight overexpression of CD-40 in the membrane. So altogether, innate immunity locally may be alleviated due to oxidative stress induced by exposure to pollen. This in turn helps in participation to initiate adaptive immune response to pollen antigens [111].

The immune status directly interplays with disease production process. The role of physical and psychological stressors contributes to incidences and severity of various viral and bacterial infections. Both innate as well as acquired immune responses are affected by the altered IFN-γ secretion, expression of CD14, production of the acute-phase proteins, and induction of TNF-α. Fatal viral diseases produce severe oxidative stress (OS) leading to rigorous cellular damage. However, initiation, progress, and reduction of damages are governed by the redox balance of oxidation and antioxidation. The major pathway of pathogenesis for cell damage is via lipid peroxidation particularly in microsomes, mitochondria, and endoplasmic reticulum due to OS and free radicals [112, 113]. All the factors responsible for the oxidative stress directly or indirectly participate in immune system defense mechanism. Any alteration leading to immunosuppression can trigger the disease production (Table 2).

9. Oxidative Stress and Incidence of Autoimmune Diseases

Oxidative stress can induce production of free radicals that can modify proteins. Alterations in self-antigens (i.e., modified proteins) can instigate the process of autoimmune diseases [114, 115]. Under oxidative stress, cells may produce an excess of ROS/RNS which react with and modify lipids and proteins in the cell [116]. The end products of these reactions may be stable molecules such as 3-chlorothyrosine and 3-nitrotyrosine that may not only block natural biotransformations of the tyrosine like phosphorylation but also change the antigenic profile of the protein. The oxidative

Table 2: Deadly diseases that have got positive correlation to oxidative stress.

Sl. number	Disease	Organs involved	Etiology	References
(1)	Macular degeneration	Eyes	Reactive oxygen intermediates (ROI)	[206]
(2)	Diabetes	Multi-organ	Superoxide dismutase, catalase, glutathione reductase, glutathione peroxidase	[207]
(3)	Chronic fatigue	Multiorgan	C-reactive protein	[208]
(4)	Atherosclerosis	Blood vessels	Reduced NADPH oxidase system	[209]
(5)	Autoimmune disorders (systemic lupus erythematosus)	Immune system	R_o ribonucleoprotein	[118]
(6)	Neurodegenerative diseases (Alzheimer's and Parkinson's disease)	Brain	Reactive oxygen species (ROS)	[210]
(7)	Asthma	Lungs	ROS particularly H_2O_2	[211]
(8)	Rheumatoid and osteoarthritis	Joints	Radical oxygen species	[212]
(9)	Nephritis	Kidney	Glutathione transferase kappa (GSTK 1-1)	[213]
(10)	Melanoma	Skin	Pathophysiological processes including DNA damage and lipid peroxidation (LPO)	[214]
(11)	Myocardial infarction	Heart	Reactive oxygen species (ROS)	[215]

modification of the proteins not only changes the antigenic profile of latter but also enhances the antigenicity as well [117]. There exist several examples of autoimmune diseases resulting from oxidative modifications of self-proteins, namely, systemic lupus erythematosus (60 kD Ro ribonucleoprotein) [118], diabetes mellitus (high molecular weight complexes of glutamic acid decarboxylase) [119], and diffuse scleroderma (oxidation of beta-2-glycoprotein) [120, 121].

Moreover, oxidative stress poses an additional threat to the target tissues as in the case of insulin-producing beta cells in the islet of Langerhans [122]. To add to this, autoimmune diseases often occur only in a single tissue irrespective of the fact that other tissues also contain the same antigen but perhaps lack the level of oxidative stress required to initiate the process. This pathological autoreactivity targeted towards redox-modified self-antigens and diagnostic assays designed to measure its cross-reactivity to normal self-antigens further complicate the detection of autoimmune diseases [123]. In the development of autoimmune disease pathogenesis, there is possibly role of psychological stress along with major hormones that are related to stress. It is thereby presumed that the neuroendocrine hormones triggered by stress lead to dysregulation of the immune system ultimately resulting in autoimmune diseases by alteration and amplification of production of cytokine [124].

10. Oxidative Stress and Altered Susceptibility to Bacterial, Viral, and Parasitic Infections

All pathogens, irrespective of their classification, bacterial, viral, or parasitic, with impaired antioxidant defenses show increased susceptibility to phagocytic killing in the host tissues, indicating a microbicidal role of ROS [80]. Vice versa to this, different studies have proven that individuals deficient in antioxidative mechanism are more susceptible to severe bacterial and fungal infections as in case of HIV infections [125]. Reactive species are important in killing pathogens but as a negative side effect can also injure the host tissues (immunopathology). This is particularly apparent during chronic inflammation, which may cause extensive tissue damage with a subsequent burst in oxidative stress [126]. The production of free radicals involves macrophages and neutrophils to combat the invading microbes. The whole of the process is performed in host cells during the activation of phagocytes or the effect of bacteria, virus, parasites, and their cell products reactivity with specific receptors. The multicomponent flavoprotein NADPH oxidase plays vital role in inflammatory processes by catalyzing the production of superoxide anion radical O_2^- and excessive production of reactive oxygen species (ROS) leads to cellular damage. These cellular damages in general lead to altering immune response to microbes and ultimately altered susceptibility to bacterial, viral, and parasitic infections [127].

11. Oxidative Stress and Increase in Levels of Incidence and Prevalence of Various Malignancies

Carcinogenesis can be defined as a progressive erosion of interactions between multiple activating and deactivating biological activities (both immune and nonimmune) of host tissue resulting in progressive loss of integrity of susceptible tissues. The primitive steps in development of cancer, mutation, and ageing are the result of oxidative damage to the DNA in a cell. A list of oxidized DNA products has been identified currently which can lead to mutation and cancer. Major change noticed due to ROS caused DNA damage is the break in the DNA strand, due to the alterations in the purine or pyrimidine ring [56, 66]. Alongside with ROS other redox metals also play a critical role in development of ageing,

mutation, and tumour [128]. In regular cellular mechanism, free radicals scavenger vitamin E, C and glutathione along with enzymes like catalase, peroxidases, and superoxide dismutase control the mechanism of DNA repair. These damages are either in the form of single strand breaks (SSBs), double strand breaks (DSBs), or oxidatively generated clustered DNA lesions (OCDLs). Irregular repair or absence of repair of damaged DNA due to OS might lead to mutagenesis and genetic transformation along with alteration in apoptotic pathway [129].

Oxidative stress produced due to unresolved and persistent inflammation can be a major factor involved in the change of the dynamics of immune responses. These alterations can create an immunological chaos that could lead to loss of architectural integrity of cells and tissues ultimately leading to chronic conditions or cancers [130]. Oxidative stress is reported to be the cause of induction of allergies, autoimmune or neurodegenerative diseases along with altered cell growth, chronic infections leading to neoplasia, metastatic cancer, and angiogenesis [131]. Damage to the cellular components such as proteins, genes, and vasculature is behind such alterations. Moreover, further accumulation of confluent, useless, and complex cells causes additional oxidative stress and maintains continuous activation of immune system and unanswered inflammation [132]. Tissue necrosis and cellular growth are stimulated by coexpression of inflammatory mediators due to oxidative stress-induced altered activity of the cells of the immune system. Such changes of tissue function are mainly responsible for autoimmune, neurodegenerative, and cancerous conditions [133, 134]. Various factors produced due to oxidative stress along with excessively produced wound healing and apoptotic factors, namely, TNF, proteases, ROSs, and kinases, actively participate in tumor growth and proliferation. These factors are also required for the membrane degradation, invasion of neighboring tissues, and migration of tumor cells through vasculature and lymphatic channels for metastasis [135–137]. The incidences of thyroid cancers have increased in the last decades worldwide which is most likely due to exposure of human population in mass to radiation causing increased free radical generation [138].

12. Oxidative Stress and Aging

Aging is an inherent mechanism existing in all living cells. There is a decline in organ functions progressively along with the age-related disease development. The two most important theories related to ageing are free radical and mitochondrial theories, and these have passed through the test of time. There is claim by such theories that a vicious cycle is generated within mitochondria wherein reactive oxygen species (ROS) is produced in increased amount thereby augmenting the damage potential [139]. Oxidative stress is present at genetic, molecular, cellular, tissue, and system levels of all living beings and is usually manifested as a progressive accumulation of diverse deleterious changes in cells and tissues with advancing age that increase the risk of disease and death [140]. Recent studies have shown that with age, ROS levels show accumulation in major organ systems such as liver, heart, brain, and skeletal muscle [141–145] either due to their increased production or reduced detoxification. Thus, aging may be referred to as a progressive decline in biological function of the tissues with respect to time as well as a decrease in the adaptability to different kinds of stress or briefly an overall increase in susceptibility to diseases [146]. Oxidative stress theory is presently the most accepted explanation for the aging which holds that increases in ROS lead to functional alterations, pathological conditions and other clinically observable signs of aging, and finally death [147]. No matter whether mitochondrial DNA damage is involved or electron transport chain damage is responsible for aging, modulation of cellular signal response to stress or activation of redox-sensitive transcriptional factors by age-related oxidative stress causes the upregulation of proinflammatory gene expression, finally leading to an increase in the ROS levels [146].

13. Genomic Evidences of the Stress-Disease Development Interrelationship

Persistent oxidative stress due to altered inflammation acts as precancerous state of host cells leading to the initiation of genetic mutations, genetic errors, epigenetic abnormalities, wrongly coded genome, and impaired regulation of gene expression [148]. Events like methylation of nucleic acid, binding of DNA proteins, formation and binding of histone proteins, function of repair, and enzyme mediated modifications are sensitive to free radicals formed during oxidative stress [149]. These events involved in epigenetic modification and telomere-telomerase pathways can induce mutations of suppressor genes [150]. The suppression of genes alters somatic maintenance and repair leading to altered proliferative control of gene expression, polymorphism, and contact inhibition regulation and telomere shortening [151]. The activation or progressive transformation of cancer cells is also augmented by inactivated or mutated suppressor gene pathways. Moreover, abnormal DNA methylation of CpG and various enzymatic pathways influence inflammation and carcinogenesis [152]. The theory of modus operandi for pathogenesis of vitiligo, a multifactorial polygenic disorder, also moves around autoimmune, cytotoxic, oxidant-antioxidant, and neural mechanisms [153].

Lipid originated atherosclerosis also involves endoplasmic reticulum (ER) stress in macrophages. ER stress mitigation with a chemical chaperone leads to massive protection against macrophage associated lipotoxic death. This causes prevention of expression of macrophage-fatty acid-binding protein-4 (aP2). There is also an increase in the phospholipid (rich in monounsaturated fatty acid as well as bioactive lipids) production due to absence of lipid chaperones. There is also further impact of aP2 on metabolism of lipid in the macrophages. The stress response in ER is also mediated by key lipogenic enzymes upregulation in the liver [154]. Similarly, OS due to alcohol toxicity triggers the release of certain cytokines to activate collagen gene expression in liver stellate cells leading to progression of liver fibrosis [155].

Table 3: Different classes of prooxidants and their common mechanism for development of oxidative stress.

Sl. number	Class	Examples	Mechanism
(1)	Drugs	Common over-the-counter drug like analgesic (paracetamol) or anticancerous drug (methotrexate)	ROS generation leading to alterations in macromolecules which finally can fatally damage the tissues mainly liver and kidney
(2)	Transition metals	Magnesium, iron, copper, zinc, and so forth	These metals induce Fenton reaction and Haber-Weiss reaction leading to generation of excessive ROS. Chronic magnesium is a classic prooxidant disease. The other can be hemochromatosis due to high iron levels or Wilson disease due to copper
(3)	Pesticide	BHC, DDT, and so forth	Stimulation of free radical production, induction of lipid peroxidation, alterations in antioxidant enzymes and the glutathione redox system
(4)	Physical exercise	Running, weight lifting	Relaxationcontraction of muscle involves production of ROS. Rigorous exercise leads to excessive ROS
(5)	Mental anxiety	Tension, apprehension	Imbalance in the redox system plays a role in neuroinflammation and neurodegeneration, mitochondrial dysfunction, altered neuronal signaling, and inhibition of neurogenesis
(6)	Pathophysiology	Local ischemia	Gives rise to increased ROS generation
(7)	Environmental factor	Extreme weather (heat, cold, thunderstorm)	During adaptation, mitochondrial membrane fluidity decreases which may disrupt the transfer of electrons, thereby increasing the production of ROS
(8)	Antioxidants	Ascorbic acid, vitamin E, polyphenols	Act as prooxidant under certain circumstances, for example, heavy metals

14. Proteomic Evidences of the Stress-Disease Development Interrelationship

Oxidative damages mediated by free radicals lead to protein modification and ultimately cellular damages and disease pathogenesis. There lies equilibrium between the antioxidants level and cellular prooxidants under normal conditions of physiology. But when there is occurrence of environmental factors or stressors, there exists an imbalance in the homeostasis which is in favour of prooxidants. This results in the oxidative stress phenomenon [156]. An antioxidant deficiency can also result in oxidative stress leading to generation of reactive oxygen or nitrogen species in excess [157]. The 20S proteosome often removes the proteins that are damaged oxidatively. The proteosome systemic defects result in increased levels of proteins that are oxidatively modified along with development of neurotoxicity [158–162]. For instance, oxidation of nucleic acid and protein along with peroxidation of lipid is highest and most severe in the hippocampus of the brain, which is involved in the processing of memory along with cognitive function [158, 159]. Such study is strongly suggestive of the fact that a primary event in the Alzheimer's disease development is an oxidative stress [163]. These alterations and modifications in proteomes elicit antibodies formation in diseases like rheumatoid arthritis (RA), diabetes mellitus (DM), and systemic lupus erythematosus [164].

15. Assessment of Oxidative Stress

The concentration of different reductant-oxidant markers is considered an important parameter for assessing the prooxidant status in the body tissues [83]. Several indicators of *in vivo* redox status are available, including the ratios of GSH to GSSG, NADPH to $NAPD^{-}$, and NADH to NAD^{-}, as well as the balance between reduced and oxidized thioredoxin. Out of these redox pairs, the GSH-to-GSSG ratio is thought to be one of most abundant redox buffer systems in mammalian species [93]. A decrease in this ratio indicates a relative shift from a reduced to an oxidized form of GSH, suggesting the presence of oxidative stress at the cellular or tissue level. In aging, an age-related shift from a redox balance to an oxidative profile is observed which results in a reduced ability to buffer ROS that are generated in both "normal" conditions and at times of challenge [23, 83, 93, 147]. Thus, a progressive shift in cellular redox status could potentially be one of the primary molecular mechanisms contributing to the aging process and accompanying functional declines.

16. Prooxidants

Prooxidant refers to any endobiotic or xenobiotic that induces oxidative stress either by generation of ROS or by inhibiting antioxidant systems. It can include all reactive, free radical containing molecules in cells or tissues. Prooxidants may be classified into several categories (Table 3).

Some of the popular and well known antioxidant flavonoids have been reported to act as prooxidant also when a transition metal is available [165]. These have been found to be mutagenic *in vitro* [102, 166–168]. The antioxidant activities and the copper-initiated prooxidant activities of these flavonoids depend on their structures. The OH substitution is necessary for the antioxidant activity of a flavonoid [169]. Flavone and flavanone, which have no OH substitutions and which provide the basic chemical structures for the flavonoids, show neither antioxidant activities nor copper-initiated prooxidant activities. The copper initiated prooxidant activity of a flavonoid also depends on the number of free OH substitutions on its structure [170]. The more the OH substitutions, the stronger the prooxidant activity. *O*-Methylation and probably also other *O*-modifications of the flavonoid OH substitutions inactivate both the antioxidant and the prooxidant activities of the flavonoids.

The antioxidant activity of quercetin has been found to be better than its monoglucosides in a test system wherein lipid peroxidation was facilitated by aqueous oxygen radicals [171]. Luteolin has also proved to be a significantly stronger antioxidant than its two glycosides [172].

Flavonoids generally occur in foods as *O*-glycosides with sugars bound at the C3 position. Methylation or glycosidic modification of the OH substitutions leads to inactivation of transition metal-initiated prooxidant activity of a flavonoid.

The protection provided by fruits and vegetables against diseases, including cancer and cardiovascular diseases, has been attributed to the various antioxidants, including flavonoids, contained in these foods. Flavonoids, such as quercetin and kaempferol, induce nuclear DNA damage and lipid peroxidation in the presence of transition metals. The *in vivo* copper-initiated prooxidant actions of flavonoids and other antioxidants including ascorbic acid and α-tocopherol are generally not considered significant, as copper ion will be largely sequestered in the tissues, except in case of metal toxicity. The prevention of iron-induced lipid peroxidation in hepatocytes by some flavonoids including quercetin is well known [49, 173].

17. Antioxidants

To counteract the harmful effects taking place in the cell, system has evolved itself with some strategies like prevention of damage, repair mechanism to alleviate the oxidative damages, physical protection mechanism against damage, and the final most important is the antioxidant defense mechanisms. Based on the oxidative stress related free radical theory, the antioxidants are the first line of choice to take care of the stress. Endogenous antioxidant defenses include a network of compartmentalized antioxidant enzymic and nonenzymic molecules that are usually distributed within the cytoplasm and various cell organelles. In eukaryotic organisms, several ubiquitous primary antioxidant enzymes, such as SOD, catalase, and several peroxidases catalyze a complex cascade of reactions to convert ROS to more stable molecules, such as water and O_2. Besides the primary antioxidant enzymes, a large number of secondary enzymes act in close association with small molecular-weight antioxidants to form redox cycles that provide necessary cofactors for primary antioxidant enzyme functions. Small molecular-weight nonenzymic antioxidants (e.g., GSH, NADPH, thioredoxin, vitamins E and C, and trace metals, such as selenium) also function as direct scavengers of ROS. These enzymatic and nonenzymatic antioxidant systems are necessary for sustaining life by maintaining a delicate intracellular redox balance and minimizing undesirable cellular damage caused by ROS [83]. Endogenous and exogenous antioxidants include some high molecular weight (SOD, GPx, Catalse, albumin, transferring, metallothionein) and some low molecular weight substances (uric acid, ascorbic acid, lipoic acid, glutathione, ubiquinol, tocopherol/vitamin E, flavonoids).

Natural food-derived components have received great attention in the last two decades, and several biological activities showing promising anti-inflammatory, antioxidant, and anti-apoptotic-modulatory potential have been identified [17, 174, 175]. Flavonoids comprise a large heterogeneous group of benzopyran derivatives present in fruits, vegetables, and herbs. They are secondary plant metabolites and more than 4000 molecular species have been described. Flavonoids exert a positive health effect in cancer and neurodegenerative disorders, owing to their free radical-scavenging activities [169]. One of the most abundant natural flavonoids present in a large number of fruits and vegetables is quercetin (3,5,7,3′,4′, pentahydroxyflavone) which prevents oxidative injury and cell death by scavenging free radicals, donating hydrogen compound, quenching singlet oxygen, and preventing lipid peroxidation or chelating metal ions [176]. Red wines also have a high content of phenolic substances including catechin and resveratrol [177], which are responsible for the antioxidant action, anti-inflammatory, antiatherogenic property, oestrogenic growth-promoting effect, and immunomodulation. Recently, the potential of resveratrol as an antiaging agent in treating age-related human diseases has also been proven.

18. Interplay of Antioxidative and Prooxidative Role of Antioxidants

Ascorbic acid has both antioxidant and prooxidant effects, depending upon the dose [178]. Low electron potential and resonance stability of ascorbate and the ascorbyl radical have enabled ascorbic acid to enjoy the privilege as an antioxidant [179, 180]. In ascorbic acid alone treated rats, ascorbic acid has been found to act as a CYP inhibitor. Similar activity has also been observed for other antioxidants-quercetin [181] and chitosan oligosaccahrides [182], which may act as potential CYP inhibitors. Specifically, Phase I genes of xenobiotic biotransformation, namely, CYP1A1, CYP2E1, and CYP2C29, have been previously reported to be downregulated in female rats in the presence of a well known antioxidant, resveratrol [183]. The antioxidant and prooxidant role of ascorbic acid in low (30 and 100 mg/kg body weight) and high doses (1000 mg/kg body weight), respectively, has also been reported in case of ischemia induced oxidative stress [178]. The *in vivo* prooxidant/antioxidant activity of betacarotene and lycopene has also been found to depend on their interaction with biological membranes and the other

co-antioxidant molecules like vitamin C or E [184]. At higher oxygen tension, carotenoids tend to lose their effectiveness as antioxidants. In a turn around to this, the prooxidant effect of low levels of tocopherol is evident at low oxygen tension [185].

Moreover, α-lipoic acid exerts a protective effect on the kidney of diabetic rats but a prooxidant effect in nondiabetic animals [186]. The prooxidant effects have been attributed to dehydroxylipoic acid (DHLA), the reduced metabolite of α-lipoic acid owing to its ability to reduce iron, initiate reactive sulfur-containing radicals, and thus damage proteins such as alpha 1-antiproteinase and creatine kinase playing a role in renal homeostasis [186]. An increase in α-lipoic acid and DHLA-induced mitochondrial and submitochondrial O_2^- production in rat liver [187] and NADPH-induced O_2^- and expression of p47phox in the nondiabetic kidney has also been observed [186].

Withaferins, the pharmacological molecules of *Withania somnifera* L. Dunal (commonly known as Ashwagandha), have been used safely for thousands of years in Ayurvedic medicine practice for the treatment of various disorders [188–191]. In the last 5–10 years, numerous reports revealed the proapoptotic effects of withaferins [192–198]. Withaferins can also initiate apoptosis and prevent metastasis of breast carcinomas under the influence of interleukin-6-induced activation and transcription [176] and prove to be of tremendous clinical benefit to human patients. In accordance to these reports, recently withaferin-induced apoptosis has been found to be mediated by ROS production due to inhibition of mitochondrial respiration [199].

Use of ginseng and *Eleutherococcus senticosus* is thought to increase the body's capacity to tolerate external stresses, leading to increased physical or mental performance [200]. Although an extensive literature documenting adaptogenic effects in laboratory animal systems exists, results from human clinical studies are conflicting and variable [200–202]. However, there is evidence that extracts of ginseng and *Eleutherococcus* sp. can have an immunostimulatory effect in humans, and this may contribute to the adaptogen or tonic effects of these plants [200, 203]. From laboratory studies, it has been suggested that the pharmacological target sites for these compounds involve the hypothalamus-pituitary-adrenal axis due to the observed effects upon serum levels of adrenocorticotropic hormone and corticosterone [202]. However, it should also be noted that the overall effects of the ginsenosides can be quite complex due to their potential for multiple actions even within a single tissue [201].

The flavonoids present in ginkgo extracts exist primarily as glycosylated derivatives of kaempferol and quercetin [203–205]. These flavonoid glycosides have been shown to be extremely effective free radical scavengers [201, 202, 205]. It is believed that the collective action of these components leads to a reduction in damage and improved functioning of the blood vessels [200, 202].

Depending on the type and level of ROS and RNS, duration of exposure, antioxidant status of tissues, exposure to free radicals and their metabolites leads to different responses—increased proliferation, interrupted cell cycle, apoptosis, or necrosis [165]. A typical example is a hydrophilic antioxidant, ascorbic acid (vitamin C). Ascorbic acid reacts with free radicals to produce semidehydro- or dehydroascorbic acids (DHA). DHA is then regenerated by antioxidant enzymes present in the organism (semidehydroascorbic acid reductase and dehydroascorbic acid reductase) back to the functional ascorbate. In the presence of ions of transition metals, ascorbic acid reduces them and it gets oxidized to DHA. Hydrogen peroxide formed in the reaction further reacts with reduced metal ions leading to generation of hydroxyl radical through Fenton type reaction. Iron ions practically never occur in the free form in the tissues; therefore, the occurrence of Fenton type reaction *in vivo* is not likely.

Recently, toxicity of ascorbic acid has also been attributed to its autooxidation. Ascorbic acid can be oxidized in the extracellular environment in the presence of metal ions to dehydroascorbic acid, which is transported into the cell through the glucose transporter (GLUT). Here it is reduced back to ascorbate. This movement of electrons changes the redox state of the cell influencing gene expression.

19. Conclusions

Oxidative stress is nothing but the imbalance between oxidants and antioxidants in favor of the oxidants which are formed as a normal product of aerobic metabolism but during pathophysiological conditions can be produced at an elevated rate. Both enzymatic and nonenzymatic strategies are involved in antioxidant defense, and antioxidant efficacy of any molecule depends on the cooxidant. Well proven free radical scavengers can be prooxidant unless linked to a radical sink. Moreover, as the free radicals share a physiological as well as pathological role in the body, the same antioxidant molecule just due to its free radical scavenging activity may act as disease promoter, by neutralizing the physiologically desired ROS molecules, and as disease alleviator by removing the excessive levels of ROS species. The importance of several vitamins like vitamin A and tocopherols as well as carotenes, oxycarotenoids, and ubiquinols in their lipid phase has been understood in recent years. Low molecular mass antioxidant molecules that include nuclear as well as mitochondrial matrices, extracellular fluids, and so forth have been studied vividly to understand how they accelerate the body defense significantly. Protection from the influence of oxidants being an important issue has become the centre of attraction of the scientists and various research groups in recent years to understand the mechanism of action of various antioxidants present in herbs as well as fruits and vegetables that can act as antiaging agents as well. There has been ever increasing knowledge in the role of oxygen derived prooxidants and antioxidants that play crucial role in both normal metabolism and several clinical disease states. Advances in the field of biochemistry including enzymology have led to the use of various enzymes as well as endogenous and exogenous antioxidants having low molecular weight that can inhibit the harmful effect of oxidants. Still much research works are needed to understand the antioxidant status of any organ that is susceptible to oxidative stress induced damage particularly the involvement of genetic codes and gene protein interaction. Understanding of genetic alterations and molecular

mechanism is certainly helping out to reveal the interaction of free radicals and their role in proteomics, genomics and disease development process. Moreover, the prooxidant or antioxidant behavior of the universally accepted antioxidant molecules is now duly expressed in term of dependence upon the actual molecular conditions prevailing in the tissues.

Nevertheless, other environmental factors like oxygen tension, concentration of transition metals along with their redox status will also be a deciding factor. Thus, it can be concluded that a thorough knowledge of biochemistry and general chemistry will help the researchers to explore more the interplay between oxidative stress, prooxidants, and antioxidants.

Conflict of Interests

The authors declare that there is no conflict of interests regarding the publication of this paper.

References

[1] A. Kumar, A. Rahal, S. K. Diwedi, and M. K. Gupta, "Bacterial prevalence and antibiotic resistance profile from bovine mastitis in Mathura, India," *Egyptian Journal of Dairy Sciences*, vol. 38, no. 1, pp. 31–34, 2010.

[2] A. Kumar, A. Rahal, and A. K. Verma, "*In-Vitro* antibacterial activity of hot aqueous extract (HAE) of *Ocimum sanctum* (Tulsi) leaves," *Indian Journal of Veterinary Medicine*, vol. 36, no. 2, pp. 75–76, 2011.

[3] J. M. McGinnis and W. H. Foege, "Actual causes of death in the United States," *Journal of the American Medical Association*, vol. 270, no. 18, pp. 2207–2212, 1993.

[4] Mahima, A. Rahal, R. Deb et al., "Immunomodulatory and therapeutic potentials of herbal, traditional/indeginous and ethnoveterinary medicines," *Pakistan Journal of Biological Sciences*, vol. 15, no. 16, pp. 754–774, 2012.

[5] A. H. Ahmad, A. Rahal, and A. Tripathi, "Optimising drug potential of plants," in *Proceedings of the 6th Annual Conference of the Recent Trends in Development of Herbal Drugs: Challenges and Opportunities (ISVPT '06)*, pp. 23–25, Bihar, India, 2006.

[6] A. H. Ahmad, A. Rahal, and N. Siddiqui, "Bioprospecting of medicinal plants," in *Proceedings of the National Conference on Increasing Production and Productivity of Medicinal and Aromatic Plants Through Traditional Practices*, Department of Plant Pathology, College of Agriculture, GBPUA&T, Uttrakhand, India, September 2008.

[7] M. W. Gillman, L. A. Cupples, D. Gagnon et al., "Protective effect of fruits and vegetables on development of stroke in men," *Journal of the American Medical Association*, vol. 273, no. 14, pp. 1113–1117, 1995.

[8] K. J. Joshipura, A. Ascherio, J. E. Manson et al., "Fruit and vegetable intake in relation to risk of ischemic stroke," *Journal of the American Medical Association*, vol. 282, no. 13, pp. 1233–1239, 1999.

[9] B. D. Cox, M. J. Whichelow, and A. T. Prevost, "Seasonal consumption of salad vegetables and fresh fruit in relation to the development of cardiovascular disease and cancer," *Public Health Nutrition*, vol. 3, no. 1, pp. 19–29, 2000.

[10] E. Strandhagen, P.-O. Hansson, I. Bosaeus, B. Isaksson, and H. Eriksson, "High fruit intake may reduce mortality among middle-aged and elderly men. The study of men born in 1913," *European Journal of Clinical Nutrition*, vol. 54, no. 4, pp. 337–341, 2000.

[11] M. A. Eastwood, "Interaction of dietary antioxidants *in vivo*: how fruit and vegetables prevent disease?" *QJM*, vol. 92, no. 9, pp. 527–530, 1999.

[12] A. Rahal, A. H. Ahmad, A. Kumar et al., "Clinical drug interactions: a holistic view," *Pakistan Journal of Biological Sciences*, vol. 16, no. 16, pp. 751–758, 2013.

[13] J. D. Potter, "Cancer prevention: epidemiology and experiment," *Cancer Letters*, vol. 114, no. 1-2, pp. 7–9, 1997.

[14] N. T. Dimitrios, K. C. Geogrios, and I. X. H. Dmitrios, "Neurohormonal hypothesis in heart failure," *Hellenic Journal of Cardiology*, vol. 44, no. 3, pp. 195–205, 2003.

[15] K. Lundgren, K. Kalev, G. A. O. Chuansi, and H. Ingvar, "Effects of heat stress on working populations when facing climate change," *Industrial Health*, vol. 51, pp. 3–15, 2013.

[16] M. D. Kock, D. A. Jessup, R. K. Clark, and C. E. Franti, "Effects of capture on biological parameters in free-ranging bighorn sheep (*Ovis canadensis*): evaluation of drop-net, drive-net, chemical immobilization and the net-gun," *Journal of Wildlife Diseases*, vol. 23, no. 4, pp. 641–651, 1987.

[17] J. R. S. Hoult, M. A. Moroney, and M. Paya, "Actions of flavonoids and coumarins on lipoxygenase and cyclooxygenase," *Methods in Enzymology*, vol. 234, pp. 443–454, 1994.

[18] M. Y. Akhalaya, A. G. Platonov, and A. A. Baizhumanov, "Short-term cold exposure improves antioxidant status and general resistance of animals," *Bulletin of Experimental Biology and Medicine*, vol. 141, no. 1, pp. 26–29, 2006.

[19] M. D. Kock, R. K. Clark, C. E. Franti, D. A. Jessup, and J. D. Wehausen, "Effects of capture on biological parameters in free-ranging bighorn sheep (*Ovis canadensis*): evaluation of normal, stressed and mortality outcomes and documentation of postcapture survival," *Journal of Wildlife Diseases*, vol. 23, no. 4, pp. 652–662, 1987.

[20] R. Ziegler, "Changes in lipid and carbohydrate metabolism during starvation in adult *Manduca sexta*," *Journal of Comparative Physiology B*, vol. 161, no. 2, pp. 125–131, 1991.

[21] N. Golikov, *Adaptation in Farm Animals*, Agropromizdat, Sofia, Bulgaria, 1985.

[22] C. Pekow, "Defining, measuring, and interpreting stress in laboratory animals," *Contemporary Topics in Laboratory Animal Science*, vol. 44, no. 2, pp. 41–45, 2005.

[23] D. Trachootham, W. Lu, M. A. Ogasawara, N. R. Valle, and P. Huang, "Redox regulation of cell survival," *Antioxidants and Redox Signaling*, vol. 10, no. 8, pp. 1343–1374, 2008.

[24] S. Dhanalakshmi, R. Srikumar, S. Manikandan, N. J. Parthasarathy, and R. S. Devi, "Antioxidant property of triphala on cold stress induced oxidative stress in experimental rats," *Journal of Health Science*, vol. 52, no. 6, pp. 843–847, 2006.

[25] A. Rahal, V. Singh, D. Mehra, S. Rajesh, and A. H. Ahmad, "Prophylactic efficacy of *Podophyllum hexandrum* in alleviation of immobilization stress induced oxidative damage in rats," *Journal of Natural Products*, vol. 2, pp. 110–115, 2009.

[26] I. Lishmanov, T. V. Lasukova, S. A. Afanas'ev, L. N. Maslov, N. M. Krotenko, and N. V. Naryzhnaia, "Effect of cold stress on the contractile activity, carbohydrate and energy metabolism in the isolated rat heart," *Patologicheskaia Fiziologiia i èksperimental'naia Terapiia*, no. 1, pp. 28–31, 1997.

[27] V. N. Gurin, V. I. Lapsha, and L. G. Streletskaia, "Changes in the catecholamine level and energy metabolism of the myocardium in rats during cold and emotional stress," *Fiziologicheskii zhurnal SSSR imeni I. M. Sechenova*, vol. 75, no. 4, pp. 542–547, 1989.

[28] S. A. Afanas'ev, B. I. Kondrat'ev, E. D. Alekseeva, and I. B. Lishmanov, "Effect of the acute exposure to cold on the heart muscle," *Rossiiskii Fiziologicheskii Zhurnal imeni I.M. Sechenova*, vol. 83, no. 4, pp. 98–102, 1997.

[29] S. K. Powers and M. J. Jackson, "Exercise-induced oxidative stress: cellular mechanisms and impact on muscle force production," *Physiological Reviews*, vol. 88, no. 4, pp. 1243–1276, 2008.

[30] J. Vina, C. Borras, M. Gomez-Cabrera, and W. C. Orr, "Part of the series: from dietary antioxidants to regulators in cellular signalling and gene expression. Role of reactive oxygen species and (phyto)oestrogens in the modulation of adaptive response to stress," *Free Radical Research*, vol. 40, no. 2, pp. 111–119, 2006.

[31] S. K. Powers, D. Criswell, J. Lawler et al., "Influence of exercise and fiber type on antioxidant enzyme activity in rat skeletal muscle," *American Journal of Physiology*, vol. 266, no. 2, pp. R375–R380, 1994.

[32] S. K. Powers, D. Criswell, J. Lawler et al., "Regional training-induced alterations in diaphragmatic oxidative and antioxidant enzymes," *Respiration Physiology*, vol. 95, no. 2, pp. 227–237, 1994.

[33] M. C. Gomez-Cabrera, E. Domenech, and J. Viña, "Moderate exercise is an antioxidant: upregulation of antioxidant genes by training," *Free Radical Biology and Medicine*, vol. 44, no. 2, pp. 126–131, 2008.

[34] G. E. Wood, E. H. Norris, E. Waters, J. T. Stoldt, and B. S. McEwen, "Chronic immobilization stress alters aspects of emotionality and associative learning in the rat," *Behavioral Neuroscience*, vol. 122, no. 2, pp. 282–292, 2008.

[35] I. Castagliuolo, J. T. LaMont, B. Qiu et al., "Acute stress causes mucin release from rat colon: role of corticotropin releasing factor and mast cells," *American Journal of Physiology*, vol. 271, no. 5, pp. G884–G892, 1996.

[36] S. Ceccatelli, M. Eriksson, and T. Hokfelt, "Distribution and coexistence of corticotropin-releasing factor-, neurotensin-, enkephalin-, cholecystokinin-, galanin- and vasoactive intestinal polypeptide/peptide histidine isoleucine-like peptides in the parvocellular part of the paraventricular nucleus," *Neuroendocrinology*, vol. 49, no. 3, pp. 309–323, 1989.

[37] C. Augeron, T. Voisin, J. J. Maoret, B. Berthon, M. Laburthe, and C. L. Laboisse, "Neurotensin and neuromedin N stimulate mucin output from human goblet cells (Cl.16E) via neurotensin receptors," *American Journal of Physiology*, vol. 262, no. 3, pp. G470–G476, 1992.

[38] N. Sandner, M. Stangassinger, and D. Giesecke, "The effect of glucocorticoid on the glucose metabolism of pigmy goats. 1. Selected metabolites of energy metabolism," *Zentralblatt fur Veterinarmedizin A*, vol. 37, no. 1, pp. 35–44, 1990.

[39] J. Duhault, F. Lacour, J. Espinal, and Y. Rolland, "Effect of activation of the serotoninergic system during prolonged starvation on subsequent caloric intake and macronutrient selection in the Zucker rat," *Appetite*, vol. 20, no. 2, pp. 135–144, 1993.

[40] T. Ohama, N. Matsuki, H. Saito et al., "Effect of starving and refeeding on lipid metabolism in suncus," *Journal of Biochemistry*, vol. 115, no. 2, pp. 190–193, 1994.

[41] I. C. Munch, "Influences of time intervals between meals and total food intake on resting metabolic rate in rats," *Acta Physiologica Scandinavica*, vol. 153, no. 3, pp. 243–247, 1995.

[42] H. C. Chung, S. H. Sung, J. S. Kim, Y. C. Kim, and S. G. Kim, "Lack of cytochrome P450 2E1 (CYP2E1) induction in the rat liver by starvation without coprophagy," *Drug Metabolism and Disposition*, vol. 29, no. 3, pp. 213–216, 2001.

[43] D. Shi, F. Xie, C. Zhai, J. S. Stern, Y. Liu, and S. Liu, "The role of cellular oxidative stress in regulating glycolysis energy metabolism in hepatoma cells," *Molecular Cancer*, vol. 8, p. 32, 2009.

[44] E. L. Potter and B. A. Dehority, "Effects of changes in feed level, starvation, and level of feed after starvation upon the concentration of rumen protozoa in the ovine," *Applied Microbiology*, vol. 26, no. 5, pp. 692–698, 1973.

[45] G. V. Burxer, "Stress in farm animals," *Veterinaria*, vol. 8, pp. 92–94, 1974.

[46] H. Peng and M. J. Coon, "Regulation of rabbit cytochrome P450 2E1 expression in HepG2 cells by insulin and thyroid hormone," *Molecular Pharmacology*, vol. 54, no. 4, pp. 740–747, 1998.

[47] Y. Yamazoe, N. Murayama, M. Shimada, K. Yamauchi, and R. Kato, "Cytochrome P450 in livers of diabetic rats: regulation by growth hormone and insulin," *Archives of Biochemistry and Biophysics*, vol. 268, no. 2, pp. 567–575, 1989.

[48] M. H. Son, K. W. Kang, E. J. Kim et al., "Role of glucose utilization in the restoration of hypophysectomy-induced hepatic cytochrome P450 2E1 by growth hormone in rats," *Chemico-Biological Interactions*, vol. 127, no. 1, pp. 13–28, 2000.

[49] U. Sinsch, R. Seine, and N. Sherif, "Seasonal changes in the tolerance of osmotic stress in natterjack toads (*Bufo calamita*)," *Comparative Biochemistry and Physiology*, vol. 101, no. 2, pp. 353–360, 1992.

[50] Y. Liu, G. Fiskum, and D. Schubert, "Generation of reactive oxygen species by the mitochondrial electron transport chain," *Journal of Neurochemistry*, vol. 80, no. 5, pp. 780–787, 2002.

[51] H. J. Freisleben, H. Kriege, C. Clarke, F. Beyersdorf, and G. Zimmer, "Hemodynamic and mitochondrial parameters during hypoxia and reoxygenation in working rat hearts," *Arzneimittel-Forschung*, vol. 41, no. 1, pp. 81–88, 1991.

[52] D. Feuvray, F. James, and J. De Leiris, "Protective effect of endogenous catecholamine depletion against hypoxic and reoxygenation damage in isolated rat heart: an ultrastructural study," *Journal de Physiologie*, vol. 76, no. 7, pp. 717–722, 1980.

[53] G. Poli, G. Leonarduzzi, F. Biasi, and E. Chiarpotto, "Oxidative stress and cell signalling," *Current Medicinal Chemistry*, vol. 11, no. 9, pp. 1163–1182, 2004.

[54] R. S. Sohal, "Role of oxidative stress and protein oxidation in the aging process," *Free Radical Biology and Medicine*, vol. 33, no. 1, pp. 37–44, 2002.

[55] A. D. Ahmed, C. Hye-Yeon, K. Jung-Hyun, and C. Ssang-Goo, "Role of oxidative stress in stem, cancer, and cancer stem cells," *Cancers*, vol. 2, no. 2, pp. 859–884, 2010.

[56] M. Valko, C. J. Rhodes, J. Moncol, M. Izakovic, and M. Mazur, "Free radicals, metals and antioxidants in oxidative stress-induced cancer," *Chemico-Biological Interactions*, vol. 160, no. 1, pp. 1–40, 2006.

[57] M. Inoue, E. F. Sato, M. Nishikawa et al., "Mitochondrial generation of reactive oxygen species and its role in aerobic life," *Current Medicinal Chemistry*, vol. 10, no. 23, pp. 2495–2505, 2003.

[58] D. V. Parke and A. Sapota, "Chemical toxicity and reactive oxygen species," *International Journal of Occupational Medicine and Environmental Health*, vol. 9, no. 4, pp. 331–340, 1996.

[59] H. P. Misra and I. Fridovich, "The role of superoxide anion in the autoxidation of epinephrine and a simple assay for superoxide dismutase," *Journal of Biological Chemistry*, vol. 247, no. 10, pp. 3170–3175, 1972.

[60] D. J. Reed, "Toxicity of oxygen," in *Molecular and Cellular Mechanisms of Toxicity*, F. De Matteis and L. L. Smith, Eds., pp. 35–68, CRC Press, Boca Raton, Fla, USA, 1995.

[61] B. P. Yu, "Cellular defenses against damage from reactive oxygen species," *Physiological Reviews*, vol. 74, no. 1, pp. 139–162, 1994.

[62] I. Stoian, A. Oros, and E. Moldoveanu, "Apoptosis and free radicals," *Biochemical and Molecular Medicine*, vol. 59, no. 2, pp. 93–97, 1996.

[63] M. Younes, "Free radicals and reactive oxygen species, in toxicology, 'By H. Marguardt, Mechanisms of antioxidant and pro-oxidant effects of lipoic acid in the diabetic and nondiabetic kidney," *Kidney International*, vol. 67, no. 4, pp. 1371–1380, 1999.

[64] D. B. Marks, A. D. Marks, and C. M. Smith, "Oxygen metabolism and toxicityin," in *Basic Medical Biochemistry: A Clinical Approach*, pp. 327–340, Williams and Wilkins, Baltimore, Md, USA, 1996.

[65] P. P. Tak and G. S. Firestein, "NF-κB: a key role in inflammatory diseases," *Journal of Clinical Investigation*, vol. 107, no. 1, pp. 7–11, 2001.

[66] T. Aw Tak, "Molecular and cellular responses to oxidative stress and changes in oxidation-reduction imbalance in the intestine," *American Journal of Clinical Nutrition*, vol. 70, no. 4, pp. 557–565, 1999.

[67] S. G. Rhee, Y. S. Bae, S. R. Lee, and J. Kwon, "Hydrogen peroxide: a key messenger that modulates protein phosphorylation through cysteine oxidation," *Science STKE*, vol. 10, no. 53, p. 1, 2000.

[68] X. Liu, C. N. Kim, J. Yang, R. Jemmerson, and X. Wang, "Induction of apoptotic program in cell-free extracts: requirement for dATP and cytochrome c," *Cell*, vol. 86, no. 1, pp. 147–157, 1996.

[69] W. A. Pryor, K. N. Houk, C. S. Foote et al., "Free radical biology and medicine: it's a gas, man!," *American Journal of Physiology*, vol. 291, no. 3, pp. R491–R511, 2006.

[70] R. Olszanecki, A. Gębska, V. I. Kozlovski, and R. J. Gryglewski, "Flavonoids and nitric oxide synthase," *Journal of Physiology and Pharmacology*, vol. 53, no. 4, pp. 571–584, 2002.

[71] A. Pavanato, M. J. Tuñón, S. Sánchez-Campos, C. A. Marroni, S. Llesuy, and J. González-Gallego, "Effects of quercetin on liver damage in rats with carbon tetrachloride-induced cirrhosis," *Digestive Diseases and Sciences*, vol. 48, no. 4, pp. 824–829, 2003.

[72] M. Miyamoto, K. Hashimoto, K. Minagawa et al., "Effect of poly-herbal formula on NO production by LPS-stimulated mouse macrophage-like cells," *Anticancer Research A*, vol. 22, no. 6, pp. 3293–3301, 2002.

[73] O. Akyol, S. Zoroglu, F. Armutcu, S. Sahin, and A. Gurel, "Nitric oxide as a physiopathological factor in neuropsychiatric disorders," *In Vivo*, vol. 18, no. 3, pp. 377–390, 2004.

[74] B. Halliwell and M. Whiteman, "Measuring reactive species and oxidative damage *in vivo* and in cell culture: how should you do it and what do the results mean?" *British Journal of Pharmacology*, vol. 142, no. 2, pp. 231–255, 2004.

[75] A. B. Knott and E. Bossy-Wetzel, "Nitric oxide in health and disease of the nervous system," *Antioxidants and Redox Signaling*, vol. 11, no. 3, pp. 541–553, 2009.

[76] L. J. Marnett, "Oxyradicals and DNA damage," *Carcinogenesis*, vol. 21, no. 3, pp. 361–370, 2000.

[77] T. von Schantz, S. Bensch, M. Grahn, D. Hasselquist, and H. Wittzell, "Good genes, oxidative stress and condition-dependent sexual signals," *Proceedings of the Royal Society B*, vol. 266, no. 1414, pp. 1–12, 1999.

[78] D. Costantini, "Oxidative stress in ecology and evolution: lessons from avian studies," *Ecology Letters*, vol. 11, no. 11, pp. 1238–1251, 2008.

[79] P. Monaghan, N. B. Metcalfe, and R. Torres, "Oxidative stress as a mediator of life history trade-offs: mechanisms, measurements and interpretation," *Ecology Letters*, vol. 12, no. 1, pp. 75–92, 2009.

[80] B. Halliwell and J. M. C. Gutteridge, *Free Radicals in Biology and Medicine*, Oxford University Press, Oxford, UK, 3rd edition, 2007.

[81] Z. Ďuračková, Ľ. Bergendi, and J. Čársky, Eds., *Free Radicals and Antioxidants in Medicine (II)*, SAP, Bratislava, Slovakia, 1999.

[82] A. H. Klimp, E. G. E. De Vries, G. L. Scherphof, and T. Daemen, "A potential role of macrophage activation in the treatment of cancer," *Critical Reviews in Oncology and Hematology*, vol. 44, no. 2, pp. 143–161, 2002.

[83] Z. Ďuračková, "Some current insights into oxidative stress," *Physiological Research*, vol. 59, no. 4, pp. 459–469, 2010.

[84] H. Forman, M. Maiorino, and F. Ursini, "Signaling functions of reactive oxygen species," *Biochemistry*, vol. 49, no. 5, pp. 835–842, 2010.

[85] G. P. Bienert, A. L. B. Møller, K. A. Kristiansen et al., "Specific aquaporins facilitate the diffusion of hydrogen peroxide across membranes," *Journal of Biological Chemistry*, vol. 282, no. 2, pp. 1183–1192, 2007.

[86] N. Makino, K. Sasaki, K. Hashida, and Y. Sakakura, "A metabolic model describing the H_2O_2 elimination by mammalian cells including H_2O_2 permeation through cytoplasmic and peroxisomal membranes: comparison with experimental data," *Biochimica et Biophysica Acta*, vol. 1673, no. 3, pp. 149–159, 2004.

[87] R. Nisticò, S. Piccirilli, M. L. Cucchiaroni et al., "Neuroprotective effect of hydrogen peroxide on an *in vitro* model of brain ischaemia," *British Journal of Pharmacology*, vol. 153, no. 5, pp. 1022–1029, 2008.

[88] T. Finkel, "Oxygen radicals and signaling," *Current Opinion in Cell Biology*, vol. 10, no. 2, pp. 248–253, 1998.

[89] N. K. Tonks, "Redox redux: revisiting PTPs and the control of cell signaling," *Cell*, vol. 121, no. 5, pp. 667–670, 2005.

[90] P. Kovacic and J. D. Jacintho, "Mechanisms of carcinogenesis: focus on oxidative stress and electron transfer," *Current Medicinal Chemistry*, vol. 8, no. 7, pp. 773–796, 2001.

[91] L. A. Ridnour, J. S. Isenberg, M. G. Espey, D. D. Thomas, D. D. Roberts, and D. A. Wink, "Nitric oxide regulates angiogenesis through a functional switch involving thrombospondin-1," *Proceedings of the National Academy of Sciences of the United States of America*, vol. 102, no. 37, pp. 13147–13152, 2005.

[92] M. Valko, H. Morris, M. Mazúr, P. Rapta, and R. F. Bilton, "Oxygen free radical generating mechanisms in the colon: do the semiquinones of vitamin K play a role in the aetiology of colon cancer?" *Biochimica et Biophysica Acta*, vol. 1527, no. 3, pp. 161–166, 2001.

[93] Z. Ďuračková, "Oxidants, antioxidants and redox stress," in *The Activity of Natural Compounds in Diseases Prevention and Therapy*, Z. Ďuračková and S. Knasmüller, Eds., pp. 11–59, SAP, Bratislava, Slovakia, 2007.

[94] M. Dvorakova, B. Höhler, R. Vollerthun, T. Fischbach, and W. Kummer, "Macrophages: a major source of cytochrome b558 in the rat carotid body," *Brain Research*, vol. 852, no. 2, pp. 349–354, 2000.

[95] M. Geiszt, A. Kapus, K. Német, L. Farkas, and E. Ligeti, "Regulation of capacitative Ca^{2+} influx in human neutrophil granulocytes. Alterations in chronic granulomatous disease," *Journal of Biological Chemistry*, vol. 272, no. 42, pp. 26471–26478, 1997.

[96] G. Cheng, Z. Cao, X. Xu, E. G. V. Meir, and J. D. Lambeth, "Homologs of gp91phox: cloning and tissue expression of Nox3, Nox4, and Nox5," *Gene*, vol. 269, no. 1-2, pp. 131–140, 2001.

[97] G. Dorsam, M. M. Taher, K. C. Valerie, N. B. Kuemmerle, J. C. Chan, and R. C. Franson, "Diphenyleneiodium chloride blocks inflammatory cytokine-induced up-regulation of group IIA phospholipase A(2) in rat mesangial cells," *Journal of Pharmacology and Experimental Therapeutics*, vol. 292, no. 1, pp. 271–279, 2000.

[98] J. Racek, V. Treska, V. Krizan, V. Holecek, and Z. Jerabek, "The significance of free radicals in operations of acute ischaemia of the limbs," *Zeitschrift für klinische Chemie und klinische Biochemie*, vol. 3, pp. 103–105, 1995.

[99] I. Pechan, K. Danova, I. Olejarova, L. Halcak, V. Rendekova, and J. Fabian, "Oxidative stress and antioxidant defense systems in patients after heart transplantation," *Wiener Klinische Wochenschrift*, vol. 115, no. 17-18, pp. 648–651, 2003.

[100] S. W. Ballinger, "Mitochondrial dysfunction in cardiovascular disease," *Free Radical Biology and Medicine*, vol. 38, no. 10, pp. 1278–1295, 2005.

[101] A. Rahman, F. Fazal, J. Greensill, K. Ainley, J. H. Parish, and S. M. Hadi, "Strand scission in DNA induced by dietary flavonoids: role of Cu(I) and oxygen free radicals and biological consequences of scission," *Molecular and Cellular Biochemistry*, vol. 111, no. 1-2, pp. 3–9, 1992.

[102] A. Cherubini, C. Ruggiero, M. C. Polidori, and P. Mecocci, "Potential markers of oxidative stress in stroke," *Free Radical Biology and Medicine*, vol. 39, no. 7, pp. 841–852, 2005.

[103] K. P. Singh, A. H. Ahmad, S. K. Hore, V. Singh, M. Lohani, and A. Rahal, "Effect of *Emblica officinalis* on antioxidative and haematological parameters following mercury induced toxicity," in *Proceedings of the 6th Annual conference of ISVPT*, Patna, India, November 2006.

[104] V. Singh, A. Rahal, K. P. Singh, and A. H. Ahmad, "Effect of ethanolic extract of *Withania somnifera* roots on antioxidant defence in mercury induced toxicity in HepG2 cell line," *Online Journal of Pharmacology and Pharmacokinetics*, vol. 5, pp. 65–72, 2009.

[105] V. Singh, A. Rahal, K. P. Singh, and A. H. Ahmad, "Evaluation of prophylactic potential of *Withania somnifera* roots extract on mercury-induced oxidative damage in various rat tissues," *Journal of Veterinary Pharmacology and Toxicology*, vol. 9, no. 1-2, pp. 64–67, 2010.

[106] K. P. Singh, A. H. Ahmad, V. Singh, K. Pant, and A. Rahal, "Effect of *Emblica officinalis* fruit in combating mercury-induced hepatic oxidative stress in rats," *Indian Journal of Animal Sciences*, vol. 81, no. 3, pp. 260–262, 2011.

[107] M. B. Hampton, A. J. Kettle, and C. C. Winterbourn, "Inside the neutrophil phagosome: oxidants, myeloperoxidase, and bacterial killing," *Blood*, vol. 92, no. 9, pp. 3007–3017, 1998.

[108] B. M. Babior, "NADPH oxidase: an update," *Blood*, vol. 93, no. 5, pp. 1464–1476, 1999.

[109] C. A. Rice-Evans and V. Gopinathan, "Oxygen toxicity, free radicals and antioxidants in human disease: biochemical implications in atherosclerosis and the problems of premature neonates," *Essays in Biochemistry*, vol. 29, pp. 39–63, 1995.

[110] N. Valero, J. Mosquera, G. Añez, A. Levy, R. Marcucci, and D. M. Melchor, "Differential oxidative stress Induced by dengue virus in monocytes from human neonates, adult and elderly individuals," *PLoS ONE*, vol. 8, no. 9, Article ID e73221, 2013.

[111] A. Csillag, I. Boldogh, K. Pazmandi et al., "Pollen-induced oxidative stress influences both innate and adaptive immune responses via altering dendritic cell functions," *Journal of Immunology*, vol. 184, no. 5, pp. 2377–2385, 2010.

[112] W. E. Stehbens, "Oxidative stress in viral hepatitis and AIDS," *Experimental and Molecular Pathology*, vol. 77, no. 2, pp. 121–132, 2004.

[113] P. D. Hodgson, P. Aich, J. Stookey et al., "Stress significantly increases mortality following a secondary bacterial respiratory infection," *Veterinary Research*, vol. 43, p. 21, 2012.

[114] E. E. Gordon, "Altered oligosaccharides as the initiating autoantigen in rheumatoid arthritis," *Medical Hypotheses*, vol. 10, no. 4, pp. 347–352, 1983.

[115] M. Abu-Shakra and Y. Shoenfeld, "Parasitic infection and autoimmunity," *Autoimmunity*, vol. 9, no. 4, pp. 337–344, 1991.

[116] I. Dalle-Donne, A. Scaloni, D. Giustarini et al., "Proteins as biomarkers of oxidattiv/e/nitrosative stress in diseases: the contribution of redox proteomics," *Mass Spectrometry Reviews*, vol. 24, no. 1, pp. 55–99, 2005.

[117] M. E. Allison and D. T. Fearon, "Enhanced immunogenicity of aldehyde bearing antigens: a possible link between innate and adaptive immunity," *European Journal of Immunology*, vol. 10, pp. 2881–2887, 2000.

[118] R. H. Scofield, B. T. Kurien, S. Ganick et al., "Modification of lupus-associated 60-kDa Ro protein with the lipid oxidation product 4-hydroxy-2-nonenal increases antigenicity and facilitates epitope spreading," *Free Radical Biology and Medicine*, vol. 38, no. 6, pp. 719–728, 2005.

[119] S. M. Trigwell, P. M. Radford, S. R. Page et al., "Islet glutamic acid decarboxylase modified by reactive oxygen species is recognized by antibodies from patients with type 1 diabetes mellitus," *Clinical and Experimental Immunology*, vol. 126, no. 2, pp. 242–249, 2001.

[120] L. Casciola-Rosen, F. Wigley, and A. Rosen, "Scleroderma autoantigens are uniquely fragmented by metal-catalyzed oxidation reactions: implications for pathogenesis," *Journal of Experimental Medicine*, vol. 185, no. 1, pp. 71–79, 1997.

[121] B. Buttari, E. Profumo, V. Mattei et al., "Oxidized β2-glycoprotein I induces human dendritic cell maturation and promotes a T helper type 1 response," *Blood*, vol. 106, no. 12, pp. 3880–3887, 2005.

[122] S. E. Gandy, M. G. Buse, and R. K. Crouch, "Protective role of superoxide dismutase against diabetogenic drugs," *Journal of Clinical Investigation*, vol. 70, no. 3, pp. 650–658, 1982.

[123] I. C. Gerling, "Oxidative Stress, altered-Self and autoimmunity," *The Open Autoimmunity Journal*, vol. 1, pp. 33–36, 2009.

[124] L. Stojanovich, "Stress and autoimmunity," *Autoimmunity Reviews*, vol. 9, no. 5, pp. A271–A276, 2010.

[125] C. Nathan and M. U. Shiloh, "Reactive oxygen and nitrogen intermediates in the relationship between mammalian hosts and microbial pathogens," *Proceedings of the National Academy of Sciences of the United States of America*, vol. 97, no. 16, pp. 8841–8848, 2000.

[126] G. Sorci and B. Faivre, "Inflammation and oxidative stress in vertebrate host-parasite systems," *Philosophical Transactions of the Royal Society B*, vol. 364, no. 1513, pp. 71–83, 2009.

[127] M. A. Puertollano, E. Puertollano, G. Á. de Cienfuegos, and M. A. de Pablo, "Dietary antioxidants: immunity and host defense," *Current Topics in Medicinal Chemistry*, vol. 11, no. 14, pp. 1752–1766, 2011.

[128] S. S. Leonard, G. K. Harris, and X. Shi, "Metal-induced oxidative stress and signal transduction," *Free Radical Biology and Medicine*, vol. 37, no. 12, pp. 1921–1942, 2004.

[129] T. B. Kryston, A. B. Georgiev, P. Pissis, and A. G. Georgakilas, "Role of oxidative stress and DNA damage in human carcinogenesis," *Mutation Research*, vol. 711, no. 1-2, pp. 193–201, 2011.

[130] M. Khatami, "Unresolved inflammation: "Immune tsunami" or erosion of integrity in immune-privileged and immune-responsive tissues and acute and chronic inflammatory diseases or cancer," *Expert Opinion on Biological Therapy*, vol. 11, no. 11, pp. 1419–1432, 2011.

[131] K. O'Brien, D. C. Fitzgerald, K. Naiken, K. R. Alugupalli, A. M. Rostami, and B. Gran, "Role of the innate immune system in autoimmune inflammatory demyelination," *Current Medicinal Chemistry*, vol. 15, no. 11, pp. 1105–1115, 2008.

[132] R. Schneider, A. N. Mohebiany, I. Ifergan et al., "B cell-derived IL-15 enhances CD8 T cell cytotoxicity and is increased in multiple sclerosis patients," *Journal of Immunology*, vol. 187, no. 8, pp. 4119–4128, 2011.

[133] A. J. Muller, M. D. Sharma, P. R. Chandler et al., "Chronic inflammation that facilitates tumor progression creates local immune suppression by inducing indoleamine 2,3 dioxygenase," *Proceedings of the National Academy of Sciences of the United States of America*, vol. 105, no. 44, pp. 17073–17078, 2008.

[134] K. Zhang, "Integration of ER stress, oxidative stress and the inflammatory response in health and disease," *International Journal of Clinical and Experimental Medicine*, vol. 3, no. 1, pp. 33–40, 2010.

[135] A. R. Davalos, J. Coppe, J. Campisi, and P. Desprez, "Senescent cells as a source of inflammatory factors for tumor progression," *Cancer and Metastasis Reviews*, vol. 29, no. 2, pp. 273–283, 2010.

[136] F. Innocenti, N. J. Cox, and M. E. Dolan, "The use of genomic information to optimize cancer chemotherapy," *Seminars in Oncology*, vol. 38, no. 2, pp. 186–195, 2011.

[137] B. Vire, A. David, and A. Wiestner, "TOSO, the Fcμ receptor, is highly expressed on chronic lymphocytic leukemia B cells, internalizes upon IgM binding, shuttles to the lysosome, and is downregulated in response to TLR activation," *Journal of Immunology*, vol. 187, no. 8, pp. 4040–4050, 2011.

[138] G. Pellegriti, F. Frasca, C. Regalbuto, S. Squatrito, and R. Vigneri, "Worldwide increasing incidence of thyroid cancer: update on epidemiology and risk factors," *Journal of Cancer Epidemiology*, vol. 2013, Article ID 965212, 10 pages, 2013.

[139] A. D. Romano, G. Serviddio, A. De Matthaeis, F. Bellanti, and G. Vendemiale, "Oxidative stress and aging," *Journal of Nephrology*, vol. 23, supplement 15, pp. S29–S36, 2010.

[140] D. Harman, "Aging: overview," *Annals of the New York Academy of Sciences*, vol. 928, pp. 1–21, 2001.

[141] J. Bejma and L. L. Ji, "Aging and acute exercise enhance free radical generation in rat skeletal muscle," *Journal of Applied Physiology*, vol. 87, no. 1, pp. 465–470, 1999.

[142] B. Bejma, R. Ramires, and J. Ji, "Free radical generation and oxidative stress with ageing and exercise: differential effects in the myocardium and liver," *Acta Physiologica Scandinavica*, vol. 169, no. 4, pp. 343–351, 2000.

[143] A. S. Driver, P. R. S. Kodavanti, and W. R. Mundy, "Age-related changes in reactive oxygen species production in rat brain homogenates," *Neurotoxicology and Teratology*, vol. 22, no. 2, pp. 175–181, 2000.

[144] F. Gomi, H. Utsumi, A. Hamada, and M. Matsuo, "Aging retards spin clearance from mouse brain and food restriction prevents its age-dependent retardation," *Life Sciences*, vol. 52, no. 25, pp. 2027–2033, 1993.

[145] H. J. Zhang, L. Xu, V. J. Drake, L. Xie, L. W. Oberley, and K. C. Kregel, "Heat-induced liver injury in old rats is associated with exaggerated oxidative stress and altered transcription factor activation," *FASEB Journal*, vol. 17, no. 15, pp. 2293–2295, 2003.

[146] K. C. Kregel and H. J. Zhang, "An integrated view of oxidative stress in aging: basic mechanisms, functional effects, and pathological considerations," *American Journal of Physiology*, vol. 292, no. 1, pp. R18–R36, 2007.

[147] T. M. Hagen, "Oxidative stress, redox imbalance, and the aging process," *Antioxidants and Redox Signaling*, vol. 5, no. 5, pp. 503–506, 2003.

[148] N. Babbar and E. W. Gerner, "Targeting polyamines and inflammation for cancer prevention," *Recent Results in Cancer Research*, vol. 188, pp. 49–64, 2011.

[149] D. S. Shames, J. D. Minna, and A. F. Gazdar, "DNA methylation in health, disease, and cancer," *Current Molecular Medicine*, vol. 7, no. 1, pp. 85–102, 2007.

[150] G. Aubert and P. M. Lansdorp, "Telomeres and aging," *Physiological Reviews*, vol. 88, no. 2, pp. 557–579, 2008.

[151] J. M. Zingg, A. Azzi, and M. Meydani, "Genetic polymorphisms as determinants for disease-preventive effects of vitamin E," *Nutrition Reviews*, vol. 66, no. 7, pp. 406–414, 2008.

[152] M. Khatami, "Inflammation, aging, and cancer: tumoricidal versus tumorigenesis of immunity," *Cell Biochemistry and Biophysics*, vol. 55, no. 2, pp. 55–79, 2009.

[153] N. C. Laddha, M. Dwivedi, M. S. Mansuri et al., "Vitiligo: interplay between oxidative stress and immune system," *Experimental Dermatology*, vol. 22, no. 4, pp. 245–250, 2013.

[154] E. Erbay, V. R. Babaev, J. R. Mayers et al., "Reducing endoplasmic reticulum stress through a macrophage lipid chaperone alleviates atherosclerosis," *Natural Medicine*, vol. 15, pp. 1383–1391, 2009.

[155] E. Albano, "Oxidative mechanisms in the pathogenesis of alcoholic liver disease," *Molecular Aspects of Medicine*, vol. 29, no. 1-2, pp. 9–16, 2008.

[156] B. Halliwell, "Oxidative stress and neurodegeneration: where are we now?" *Journal of Neurochemistry*, vol. 97, no. 6, pp. 1634–1658, 2006.

[157] L. A. Brown, F. L. Harris, and D. P. Jones, "Ascorbate deficiency and oxidative stress in the alveolar type II cell," *American Journal of Physiology*, vol. 273, no. 4, pp. L782–L788, 1997.

[158] W. R. Markesbery, "Oxidative stress hypothesis in Alzheimer's disease," *Free Radical Biology and Medicine*, vol. 23, no. 1, pp. 134–147, 1997.

[159] D. A. Butterfield and J. Kanski, "Brain protein oxidation in age-related neurodegenerative disorders that are associated with aggregated proteins," *Mechanisms of Ageing and Development*, vol. 122, no. 9, pp. 945–962, 2001.

[160] D. A. Butterfield and C. M. Lauderback, "Lipid peroxidation and protein oxidation in Alzheimer's disease brain: potential causes and consequences involving amyloid β-peptide-associated free radical oxidative stress," *Free Radical Biology and Medicine*, vol. 32, no. 11, pp. 1050–1060, 2002.

[161] B. I. Giasson, H. Ischiropoulos, V. M.-Y. Lee, and J. Q. Trojanowski, "The relationship between oxidative/nitrative stress and pathological inclusions in Alzheimer's and Parkinson's diseases," *Free Radical Biology and Medicine*, vol. 32, no. 12, pp. 1264–1275, 2002.

[162] X. Zhu, M. A. Smith, G. Perry, and G. Aliev, "Mitochondrial failures in Alzheimer's disease," *American Journal of Alzheimer's Disease and other Dementias*, vol. 19, no. 6, pp. 345–352, 2004.

[163] I. Dalle-Donne, R. Rossi, R. Colombo, D. Giustarini, and A. Milzani, "Biomarkers of oxidative damage in human disease," *Clinical Chemistry*, vol. 52, no. 4, pp. 601–623, 2006.

[164] B. T. Kurien, K. Hensley, M. Bachmann, and R. H. Scofield, "Oxidatively modified autoantigens in autoimmune diseases," *Free Radical Biology and Medicine*, vol. 41, no. 4, pp. 549–556, 2006.

[165] B. Halliwell, "Are polyphenols antioxidants or pro-oxidants? What do we learn from cell culture and *in vivo* studies?" *Archives of Biochemistry and Biophysics*, vol. 476, no. 2, pp. 107–112, 2008.

[166] S. C. Sahu and G. C. Gray, "Interactions of flavonoids, trace metals, and oxygen: nuclear DNA damage and lipid peroxidation induced by myricetin," *Cancer Letters*, vol. 70, no. 1-2, pp. 73–79, 1993.

[167] S. C. Sahu and G. C. Gray, "Kaempferol-induced nuclear DNA damage and lipid peroxidation," *Cancer Letters*, vol. 85, no. 2, pp. 159–164, 1994.

[168] M. S. Ahmad, F. Fazal, A. Rahman, S. M. Hadi, and J. H. Parish, "Activities of flavonoids for the cleavage of DNA in the presence of Cu(II): correlation with generation of active oxygen species," *Carcinogenesis*, vol. 13, no. 4, pp. 605–608, 1992.

[169] C. A. Rice-Evans, N. J. Miller, P. G. Bolwell, P. M. Bramley, and J. B. Pridham, "The relative antioxidant activities of plant-derived polyphenolic flavonoids," *Free Radical Research*, vol. 22, no. 4, pp. 375–383, 1995.

[170] G. Guohua, S. Emin, and L. Ronald, "Antioxidant and prooxidant behavior of flavonoids: structure-activity relationships," *Free Radical Biology and Medicine*, vol. 22, no. 5, pp. 749–760, 1997.

[171] K. Ioku, T. Tsushida, Y. Takei, N. Nakatani, and J. Terao, "Antioxidative activity of quercetin and quercetin monoglucosides in solution and phospholipid bilayers," *Biochimica et Biophysica Acta*, vol. 1234, no. 1, pp. 99–104, 1995.

[172] G. O. Igile, W. Oleszek, M. Jurzysta, S. Burda, M. Fafunso, and A. A. Fasanmade, "Flavonoids from *Vernonia amygdalina* and their antioxidant activities," *Journal of Agricultural and Food Chemistry*, vol. 42, no. 11, pp. 2445–2448, 1994.

[173] G. Weiss, G. Werner-Felmayer, E. R. Werner, K. Grünewald, H. Wachter, and M. W. Hentze, "Iron regulates nitric oxide synthase activity by controlling nuclear transcription," *Journal of Experimental Medicine*, vol. 180, no. 3, pp. 969–976, 1994.

[174] M. J. Laughton, P. J. Evans, M. A. Moroney, J. R. S. Hoult, and B. Halliwell, "Inhibition of mammalian 5-lipoxygenase and cyclo-oxygenase by flavonoids and phenolic dietary additives. Relationship to antioxidant activity and to iron ion-reducing ability," *Biochemical Pharmacology*, vol. 42, no. 9, pp. 1673–1681, 1991.

[175] A. P. Lin, W. J. Tsai, C. Y. Fan, and M. J. Lee, "*Vandellia cordifolia* regulated cell proliferation and cytokines production in human mononuclear cells," *American Journal of Chinese Medicine*, vol. 28, no. 3-4, pp. 313–323, 2000.

[176] J. Lee, E. R. Hahm, and S. V. Singh, "Withaferin A inhibits activation of signal transducer and activator of transcription 3 in human breast cancer cells," *Carcinogenesis*, vol. 31, no. 11, pp. 1991–1998, 2010.

[177] C. A. Lastra and I. Villegas, "Resveratrol as an antioxidant and pro-oxidant agent: mechanisms and clinical implications," *Biochemical Society Transactions*, vol. 35, no. 5, pp. 1156–1160, 2007.

[178] M. Y. Seo and S. M. Lee, "Protective effect of low dose of ascorbic acid on hepatobiliary function in hepatic ischemia/reperfusion in rats," *Journal of Hepatology*, vol. 36, no. 1, pp. 72–77, 2002.

[179] G. R. Buettner and B. A. Jurkiewicz, "Catalytic metals, ascorbate and free radicals: combinations to avoid," *Radiation Research*, vol. 145, no. 5, pp. 532–541, 1996.

[180] G. R. Buettner, "The pecking order of free radicals and antioxidants: lipid peroxidation, α-tocopherol, and ascorbate," *Archives of Biochemistry and Biophysics*, vol. 300, no. 2, pp. 535–543, 1993.

[181] F.-F. Zhang, Y.-F. Zheng, H.-J. Zhu, X.-Y. Shen, and X.-Q. Zhu, "Effects of kaempferol and quercetin on cytochrome 450 activities in primarily cultured rat hepatocytes," *Zhejiang Da Xue Xue Bao Yi Xue Ban*, vol. 35, no. 1, pp. 18–22, 2006.

[182] H.-T. Yao, M.-N. Luo, L.-B. Hung et al., "Effects of chitosan oligosaccharides on drug-metabolizing enzymes in rat liver and kidneys," *Food and Chemical Toxicology*, vol. 50, no. 5, pp. 1171–1177, 2012.

[183] V. Hebbar, G. Shen, R. Hu et al., "Toxicogenomics of resveratrol in rat liver," *Life Sciences*, vol. 76, no. 20, pp. 2299–2314, 2005.

[184] A. J. Young and G. M. Lowe, "Antioxidant and prooxidant properties of carotenoids," *Archives of Biochemistry and Biophysics*, vol. 385, no. 1, pp. 20–27, 2001.

[185] A. Kontush, B. Finckh, B. Karten, A. Kohlschütter, and U. Beisiegel, "Antioxidant and prooxidant activity of α-tocopherol in human plasma and low density lipoprotein," *Journal of Lipid Research*, vol. 37, no. 7, pp. 1436–1448, 1996.

[186] B. C. Scott, O. I. Aruoma, P. J. Evansi et al., "Lipoic and dihydrolipoic acids as antioxidants. A critical evaluation," *Free Radical Research*, vol. 20, no. 2, pp. 119–133, 1994.

[187] H. Moini, L. Packer, and N. L. Saris, "Antioxidant and prooxidant activities of α-lipoic acid and dihydrolipoic acid," *Toxicology and Applied Pharmacology*, vol. 182, no. 1, pp. 84–90, 2002.

[188] M. Rasool and P. Varalakshmi, "Immunomodulatory role of *Withania somnifera* root powder on experimental induced inflammation: an *in vivo* and *in vitro* study," *Vascular Pharmacology*, vol. 44, no. 6, pp. 406–410, 2006.

[189] M. Ahmad, S. Saleem, A. S. Ahmad et al., "Neuroprotective effects of *Withania somnifera* on 6-hydroxydopamine induced Parkinsonism in rats," *Human and Experimental Toxicology*, vol. 24, no. 3, pp. 137–147, 2005.

[190] M. Owais, K. S. Sharad, A. Shehbaz, and M. Saleemuddin, "Antibacterial efficacy of *Withania somnifera* (ashwagandha) an indigenous medicinal plant against experimental murine salmonellosis," *Phytomedicine*, vol. 12, no. 3, pp. 229–235, 2005.

[191] S. K. Gupta, I. Mohanty, K. K. Talwar et al., "Cardioprotection from ischemia and reperfusion injury by *Withania somnifera*: a hemodynamic, biochemical and histopathological assessment," *Molecular and Cellular Biochemistry*, vol. 260, no. 1, pp. 39–47, 2004.

[192] S. Srinivasan, R. S. Ranga, R. Burikhanov, S. Han, and D. Chendil, "Par-4-dependent apoptosis by the dietary compound withaferin A in prostate cancer cells," *Cancer Research*, vol. 67, no. 1, pp. 246–253, 2007.

[193] F. Malik, A. Kumar, S. Bhushan et al., "Reactive oxygen species generation and mitochondrial dysfunction in the apoptotic cell death of human myeloid leukemia HL-60 cells by a dietary compound withaferin A with concomitant protection by N-acetyl cysteine," *Apoptosis*, vol. 12, no. 11, pp. 2115–2133, 2007.

[194] S. D. Stan, E. Hahm, R. Warin, and S. V. Singh, "Withaferin A causes FOXO3a- and Bim-dependent apoptosis and inhibits growth of human breast cancer cells *in vivo*," *Cancer Research*, vol. 68, no. 18, pp. 7661–7669, 2008.

[195] S. D. Stan, Y. Zeng, and S. V. Singh, "Ayurvedic medicine constituent withaferin a causes G2 and M phase cell cycle arrest

in human breast cancer cells," *Nutrition and Cancer*, vol. 60, no. 1, pp. 51–60, 2008.

[196] J. H. Oh, T. Lee, S. H. Kim et al., "Induction of apoptosis by withaferin A in human leukemia U937 cells through down-regulation of Akt phosphorylation," *Apoptosis*, vol. 13, no. 12, pp. 1494–1504, 2008.

[197] C. Mandal, A. Dutta, A. Mallick et al., "Withaferin A induces apoptosis by activating p38 mitogen-activated protein kinase signaling cascade in leukemic cells of lymphoid and myeloid origin through mitochondrial death cascade," *Apoptosis*, vol. 13, no. 12, pp. 1450–1464, 2008.

[198] Y. Yu, A. Hamza, T. Zhang et al., "Withaferin A targets heat shock protein 90 in pancreatic cancer cells," *Biochemical Pharmacology*, vol. 79, no. 4, pp. 542–551, 2010.

[199] E. R. Hahm, M. B. Moura, E. E. Kelley, B. van Houten, S. Shiva, and S. V. Singh, "Withaferin a-induced apoptosis in human breast cancer cells is mediated by reactive oxygen species," *PLoS ONE*, vol. 6, no. 8, Article ID e23354, 2011.

[200] V. Schulz, R. Hänsel, and V. Tyler, *Rational Phytotherapy: A Physician's Guide to Herbal Medicine*, Springer, Berlin, Germany, 1998.

[201] A. S. Attele, J. A. Wu, and C. Yuan, "Ginseng pharmacology: multiple constituents and multiple actions," *Biochemical Pharmacology*, vol. 58, no. 11, pp. 1685–1693, 1999.

[202] K. C. Huang, *Pharmacology of Chinese Herbs*, CRC Press, Boca Raton, Fla, USA, 1999.

[203] M. Blumenthal, A. Goldberg, and J. Brinckmann, "Herbal medicine: expanded commission E monographs," *Integrative Medicine Communications*, vol. 133, no. 6, p. 487, 2000.

[204] J. Bruneton, *Pharmacognosy, Phytochemistry, Medicinal Plants*, Lavisior, Paris, France, 1995.

[205] P. M. Dewick, *Medicinal Natural Products*, John Wiley & Sons, West Sussex, UK, 1997.

[206] S. Beatty, H. Koh, M. Phil, D. Henson, and M. Boulton, "The role of oxidative stress in the pathogenesis of age-related macular degeneration," *Survey of Ophthalmology*, vol. 45, no. 2, pp. 115–134, 2000.

[207] A. C. Maritim, R. A. Sanders, and J. B. Watkins III, "Diabetes, oxidative stress, and antioxidants: a review," *Journal of Biochemical and Molecular Toxicology*, vol. 17, no. 1, pp. 24–38, 2003.

[208] S. Fulle, T. Pietrangelo, R. Mancinelli, R. Saggini, and G. Fanò, "Specific correlations between muscle oxidative stress and chronic fatigue syndrome: a working hypothesis," *Journal of Muscle Research and Cell Motility*, vol. 28, no. 6, pp. 355–362, 2007.

[209] U. Singh and I. Jialal, "Oxidative stress and atherosclerosis," *Pathophysiology*, vol. 13, no. 3, pp. 129–142, 2006.

[210] B. Uttara, A. V. Singh, P. Zamboni, and R. T. Mahajan, "Oxidative stress and neurodegenerative diseases: a review of upstream and downstream antioxidant therapeutic options," *Current Neuropharmacology*, vol. 7, no. 1, pp. 65–74, 2009.

[211] Y. S. Cho and H. Moon, "The role of oxidative stress in the pathogenesis of asthma," *Allergy, Asthma and Immunology Research*, vol. 2, no. 3, pp. 183–187, 2010.

[212] A. C. Blackburn, M. Coggan, A. J. Shield et al., "Glutathione transferase kappa deficiency causes glomerular nephropathy without overt oxidative stress," *Laboratory Investigation*, vol. 91, no. 11, pp. 1572–1583, 2011.

[213] C. Ziskoven, M. Jäger, C. Zilkens, W. Bloch, K. Brixius, and R. Krauspe, "Oxidative stress in secondary osteoarthritis: from cartilage destruction to clinical presentation?" *Orthopedic Reviews*, vol. 2, no. 2, p. e23, 2010.

[214] C. S. Sander, F. Hamm, P. Elsner, and J. J. Thiele, "Oxidative stress in malignant melanoma and non-melanoma skin cancer," *British Journal of Dermatology*, vol. 148, no. 5, pp. 913–922, 2003.

[215] C. D. Filippo, S. Cuzzocrea, F. Rossi, R. Marfella, and M. D'Amico, "Oxidative stress as the leading cause of acute myocardial infarction in diabetics," *Cardiovascular Drug Reviews*, vol. 24, no. 2, pp. 77–87, 2006.

Hindawi Publishing Corporation
BioMed Research International
Volume 2014, Article ID 895049, 5 pages
http://dx.doi.org/10.1155/2014/895049

Research Article

Protective Effect of Alpha-Tocopherol Isomer from Vitamin E against the H_2O_2 Induced Toxicity on Dental Pulp Cells

Fernanda da Silveira Vargas,[1] Diana Gabriela Soares,[1] Ana Paula Dias Ribeiro,[2] Josimeri Hebling,[3] and Carlos Alberto De Souza Costa[4]

[1] *Oral Rehabilitation Program, Department of Dental Materials and Prosthodontics, University Estadual Paulista, UNESP, Araraquara School of Dentistry, Humaitá Street 1680, 14801-903 Araraquara, SP, Brazil*
[2] *Department of Operative Dentistry, Brasilia University, School of Dentistry, Darcy Ribeiro Center, 70910-900 Brasília, DF, Brazil*
[3] *Department of Orthodontics and Pediatric Dentistry, University Estadual Paulista, UNESP, Araraquara School of Dentistry, Humaitá Street 1680, 14801-903 Araraquara, SP, Brazil*
[4] *Department of Physiology and Pathology, University Estadual Paulista, UNESP, Araraquara School of Dentistry, Humaitá Street 1680, 14801-903 Araraquara, SP, Brazil*

Correspondence should be addressed to Carlos Alberto De Souza Costa; casouzac@foar.unesp.br

Received 30 April 2013; Accepted 28 October 2013; Published 21 January 2014

Academic Editor: Maha Zaki Rizk

The aim of this study was to evaluate the protective effects of different concentrations of vitamin E alpha-tocopherol (α-T) isomer against the toxicity of hydrogen peroxide (H_2O_2) on dental pulp cells. The cells (MDPC-23) were seeded in 96-well plates for 72 hours, followed by treatment with 1, 3, 5, or 10 mM α-T for 60 minutes. They were then exposed or not to H_2O_2 for 30 minutes. In positive and negative control groups, the cells were exposed to culture medium with or without H_2O_2 (0.018%), respectively. Cell viability was evaluated by MTT assay (Kruskal-Wallis and Mann-Whitney tests; $\alpha = 5\%$). Significant reduction of cell viability (58.5%) was observed in positive control compared with the negative control. Cells pretreated with α-T at 1, 3, 5, and 10 mM concentrations and exposed to H_2O_2 had their viability decreased by 43%, 32%, 25%, and 27.5%, respectively. These values were significantly lower than those observed in the positive control, thereby showing a protective effect of α-T against the H_2O_2 toxicity. Overall, the vitamin E α-T isomer protected the immortalized MDPC-23 pulp cells against the toxic effects of H_2O_2. The most effective cell protection was provided by 5 and 10 mM concentrations of α-T.

1. Introduction

Hydrogen peroxide (H_2O_2) is a thermally instable chemical agent with high oxidative power, which dissociates into free radicals and other reactive oxygen species (ROS), such as hydroxyl radicals (OH^-), singlet oxygen (O^{2-}), and superoxide anion (O_2^-) [1]. This molecule has been widely used in dentistry to treat discolored teeth, because of its capability to oxidize the complex organic molecules of the dental structure that respond for the darker coloration of the teeth [2]. However, these highly oxidative molecules can diffuse through mineralized tooth structures, such as enamel and dentin, to reach the subjacent pulp tissue, a specialized connective tissue responsible for maintaining the tooth viability [3, 4]. The contact of the pulp cells with ROS results in oxidative stress generation, mainly because of the imbalance between the amount of ROS and endogenous antioxidants [1]. This oxidative stress damages the cell membrane and causes cell viability reduction, extracellular matrix degradation, inflammatory tissue reaction, and even pulpal necrosis [3–5].

The treatment of dental pulp cells with antioxidants has been proposed in order to prevent the oxidative damage from components leached by dental materials and bleaching gels, which are capable of diffusing across mineralized tissues of teeth [6, 7]. Vitamin E (VE) has a recognized anti-inflammatory and antioxidant activity in different cell

lineages, such as fibroblast, osteoblasts, and neurons [8]. This kind of vitamin is composed of a blend of tocopherols and tocotrienols; however, the antioxidant action of VE is mediated by the alpha-tocopherol (α-T) isomer [9]. The α-T is capable of stabilizing cell membrane against reactive oxygen species (ROS) produced during normal cellular metabolic activities, preventing the chain propagation from the oxidative stress [10]. The protective activity of this molecule against the oxidative damage related to different conditions, as atherosclerosis, diabetes, Alzheimer, and Parkinson diseases, has been widely described [8]. In view of this, it was hypothesized that the VE antioxidant property may also protect pulp cells against the oxidative toxic effects caused by components leached by dental bleaching gels. Therefore, the aim of this study was to evaluate the protective effects of different concentrations of VE α-T isomer against the toxicity of H_2O_2 applied on the immortalized odontoblast-like MDPC-23 cell line.

2. Materials and Methods

The H_2O_2 concentration capable of reducing the cell viability by approximately 50% (IC-50) was determined. For such purpose, solutions containing decreasing H_2O_2 concentrations were prepared (0.035%, 0.018%, 0.009%, and 0.045%) in serum-free DMEM (Dulbecco's Modified Eagle's Medium; Sigma Aldrich Corp., St. Louis, MO, USA). Then, odontoblast-like MDPC-23 cells were seeded in DMEM supplemented with 10% fetal bovine serum (FBS; Gibco Co., Grand Island, NY, USA) and antibiotics (IU/mL penicillin, 100 μg/mL streptomycin, and 2 mmol/L glutamine; Gibco Co.), in 96-well plates (1×10^4 cells/well) (Costar Corp., Cambridge, MA, USA) during 72 h at 37°C and 5% CO_2. After that, the DMEM was aspirated and 100 μL of the H_2O_2 solutions were applied on the cells during 30 minutes. Cell viability was evaluated by the cytochemical demonstration of the succinic dehydrogenase (SDH) enzyme using the methyl tetrazolium (MTT) assay (Gibco Co.) [3, 4]. The absorbance values of the groups (570 nm) were transformed into percentages of cell viability, considering the negative control group (DMEM) as having 100% of cell viability. The 0.018% H_2O_2 concentration resulted in 59% of cell viability reduction and was selected to evaluate the α-T protective effect against H_2O_2 aggression.

In order to evaluate the protective effect of α-T against H_2O_2 toxicity, four decreasing concentrations of this molecule (1, 3, 5, and 10 mM) were prepared by diluting a stock α-T solution (Sigma Chemical Co.) in DMEM with 5% dimethyl sulfoxide (DMSO). In this way, experimental groups were formed according to the treatment of the MDPC-23 cells with different α-T concentrations followed by exposition or not of the cells to a 0.018% H_2O_2 solution for 30 minutes. To evaluate α-T toxicity (α-T+ H_2O_2−), the α-T solutions were applied on cultured cells for 60 minutes; to evaluate α-T protective effect against H_2O_2 aggression, the solutions were applied for 60 minutes and then aspirated, followed by H_2O_2 application for 30 minutes (α-T+ H_2O_2+). In negative control group, DMEM containing 5% DMSO was applied (α-T− H_2O_2−) on the MDPC-23 cells. In positive control group, 0.018% H_2O_2 was applied on the cultured cells for 30 minutes. After treatments, the MTT assay was performed and percentages of cell viability for each experimental group were determined. Data were subjected Kruskal-Wallis complemented by the Mann-Whitney test. The significance level was set at 5% and the following null hypotheses were established: (1) H_2O_2 does not cause toxic effects to odontoblast-like cells; (2) α-T cannot eliminate or at least reduce the oxidative effects of H_2O_2. Three independent experiments were performed at different times to demonstrate the reproducibility of data, and, in each appointment, a total of six replicates ($n = 6$) were used for each group.

Table 1: Results of the viability of the MDPC-23 cells exposed to different hydrogen peroxide (H_2O_2) concentrations for determination of the IC-50.

H_2O_2 concentration	Cell viability (%)
0	100
0.035%	5
0.018%	41
0.009%	77
0.0045%	72

Table 2: Control and experimental groups ($n = 6$) formed according to the treatment of the MDPC-23 cells with different alpha-tocopherol (α-T) concentrations followed by exposure or not to hydrogen peroxide (H_2O_2).

Groups	Treatment
G1	(α-T− H_2O_2−)
G2	(α-T− H_2O_2+)
G3	(1 mM+ H_2O_2−)
G4	(3 mM+ H_2O_2−)
G5	(5 mM+ H_2O_2−)
G6	(10 mM+ H_2O_2−)
G7	(1 mM+ H_2O_2+)
G8	(3 mM+ H_2O_2+)
G9	(5 mM+ H_2O_2+)
G10	(10 mM+ H_2O_2+)

3. Results

Table 1 shows the results for the H_2O_2 IC-50. The experimental groups used to assess the protective role of α-T against cell toxicity mediated by H_2O_2 are summarized in Table 2. Cell viability data obtained after cell treatment with α-T followed or not by exposure to H_2O_2 are shown in Table 3. Considering the negative control group (G1) as having 100% of cell viability, there was a 58.5% decrease in the positive control group (G2) that was lower than that observed in the experimental groups ($P < 0.05$). The cell viability reduction in groups G3, G4, G5, and G6, in which the MDPC-23 cells were treated with different concentrations of α-T, was 6%, 13%, 10%, and 14%, respectively. Despite being considered discrete, the cell viability reduction for G4, G5, and G6 was

Table 3: Percentage of viability of MDPC-23 cells treated with different alpha-tocopherol concentrations followed by exposure or not to hydrogen peroxide.

H_2O_2	Alpha-tocopherol concentrations				
	0	1 mM	3 mM	5 mM	10 mM
0%	100.5 (97–104)^{a,A,G1}	94 (87–100)^{ab,A,G3}	87 (86–91)^{bc,A,G4}	90 (79–92)^{bc,AB,G5}	86 (77–88)^{c,AB,G6}
0.018%	41.5 (36–43.5)^{a,B,G2}	57 (52–60)^{b,B,G7}	68 (64–73)^{bc,B,G8}	75 (67–84)^{c,A,G9}	72.5 (69–78)^{c,A,G10}

Lowercase letters permit comparisons within rows while uppercase letters permit comparisons within columns. Groups identified with the same letters do not differ significantly (Mann-Whitney test, $P > 0.05$).

significant when compared with the negative control group (G1, $P < 0.05$). In groups G7, G8, G9, and G10, in which the cultured cells were pretreated with α-T before being exposed to H_2O_2, the cell viability reduction was 43%, 32%, 25%, and 27.5%, respectively. The protective effect against H_2O_2 cytotoxicity observed in G7, G8, G9, and G10 was significantly higher when compared to the positive control group (G2) regardless of the α-T concentration ($P < 0.05$). G8, G9, and G10 presented the highest values of cell viability recovery, with no significant difference among them ($P > 0.05$) (Table 3, rows). G9 and G10, which did not show significant difference when the cells were treated or not with H_2O_2 ($P > 0.05$) (Table 3, columns), presented the best results for cell viability recovery.

Based on the fact that H_2O_2 caused toxic effects to the cultured odontoblast-like cells and that α-T reduced the oxidative effects of this unstable chemical agent to the immortalized pulp cell line, both null hypotheses presented in this study were rejected.

4. Discussion

In spite of being very popular in dental offices, vital tooth bleaching has been associated with postoperative sensitivity and pulpal damage [3–5]. In view of this, different therapies have been suggested to minimize these adverse effects, including pretreatment with antioxidant agents to reduce the oxidative stress generated by bleaching gel components to the pulp cells [7]. In the present study, the biological activity of VE α-T isomer against the toxic effects of H_2O_2 to MDPC-23 cells was evaluated. This specific kind of pulp cell, which presents odontoblast phenotype, was used in this study because in mammalian teeth odontoblasts are organized in a monolayer to underlie the dentinal tissue. Therefore, odontoblasts are the first pulp cells to be reached by components of dental products capable of diffusing through enamel and dentin [11]. In addition, for over a decade, this immortalized pulp cell line has widely been used to evaluate the cytotoxicity of different dental products and their isolated chemical components [3, 4, 7].

It was shown that all concentrations of α-T assessed in the present study presented cell-protective effect. The MDPC-23 cells pretreated with α-T for 60 minutes and exposed to the H_2O_2 showed higher viability compared with the group exposed only to H_2O_2 (G2, positive control). This protective effect of α-T against oxidizing agents was reported in previous investigations [9, 10]. A recent study demonstrated that the combination of vitamins E and C protected brain cells against the toxic effects induced by diazinon, a widely used pesticide in agriculture that causes brain oxidative stress [12]. Another *in vivo* study found that VE plus selenium acted as a potent antioxidant agent, reducing the oxidative stress in pregnant rats and preventing the development of gestational diabetes mellitus [13]. It is known that VE is composed of a mixture of tocopherols and tocotrienols [8], which can be distinguished from each other by the lateral chain unsaturation. It has been described that α-T is the compound responsible for great part of the VE antioxidant action [14]. According to previous studies, α-T is the predominant component of biomembranes, being effective in electron donation due to the orthoposition of its methyl group, compared with the other VE isomers [15]. Therefore, α-T can prevent oxidative stress propagation and stabilize the cell membrane, thus preventing the disruption of the amphipathic balance of this cell structure [14]. Antioxidants such as α-T can stop free radicals by donating one of their electrons to the free radical. However, α-T does not become a new free radical because it remains stable before and after donating the electron, which characterizes its antioxidant action [14]. It has also been shown that VE can prevent diseases such as atherosclerosis as well as cardiovascular and inflammatory disorders [16]. Some researchers have reported that VE is directly involved in the maintenance of the balance of oxidative reactions generated during the inflammation [17–20]. The authors showed that this kind of vitamin can block nitric oxide synthase (iNOS), COX-2 expression, and the NF-κB signaling pathway in cultured monocytes stimulated by *E. coli* LPS. Additionally, VE was capable of inhibiting the synthesis of PGE2 and inflammatory cytokines, such as TNF-a, IL-4, and IL-8. Therefore, one can consider that VE has a broad therapeutic potential. The present investigation revealed that cells exposed only to H_2O_2 (G2) presented a 58.5% reduction in cell viability. The toxic effect of H_2O_2 was also reported in previous studies in which the authors evaluated the trans-enamel and trans-dentinal cytotoxicity of high concentrations of H_2O_2 on odontoblast-like cells [3, 4]. On the other hand, the treatment of MDPC-23 cells with different concentrations of α-T prior to their exposition to H_2O_2 increased the cell viability by 16–33.5%.

Despite the important protective effect, α-T alone caused a slight cell viability reduction in those groups in which the cells were not exposed to H_2O_2 (G3 to G6). It was shown that 1 mM α-T concentration was statistically similar to the control (G1). On the other hand, 3, 5, and 10 mM α-T concentrations were significantly different from G1. These data suggest that an increase of the α-T concentration

available to the cells might cause a prooxidant action of this VE isomer, resulting in reduction in the viability of the treated cells. Some studies have demonstrated the prooxidant action of α-T at high concentrations or in the presence of heavy metals or peroxides [21–23]. These findings could explain the results observed in those groups in which the MDPC-23 cells were exposed only to α-T (G3 to G6). However, while a slight prooxidant action of α-T was observed (6–14% cell viability reduction), this molecule was capable of minimizing the oxidant effect caused by H_2O_2 on cultured MDPC-23 cells (G7 to G10). The most relevant protective effects were obtained with 5 mM (G9) and 10 mM (G10) α-T concentrations, in which 33.5 and 31% of cell viability recovery were observed, respectively. Since no significant difference was found between G9 and G10, it may be suggested that the best α-T concentration for pretreatment of odontoblast-like cells would be 5 mM. This is not only because of the protective effect of this molecule against the H_2O_2 cell damage but also due to its slight toxicity (G5–10% cell viability reduction).

Overall, this *in vitro* study demonstrated the potential of α-T as an antioxidant agent because this VE isomer was capable of protecting pulp cells against the harmful effects of H_2O_2, which is the main active component of tooth bleaching gels. Although the present laboratory-based results cannot be directly extrapolated to clinical situation, the original data obtained under the tested experimental conditions are promising.

5. Conclusion

It can be concluded that previous exposition of odontoblast-like MDPC-23 pulp cells to VE α-T isomer protects this cell line against the toxic effects generated by hydrogen peroxide *in vitro*. These data can drive further *in vivo* studies with the purpose of establishing specific therapies capable of preventing or at least minimizing the pulpal damage caused by tooth bleaching techniques widely used in dentistry. This may avoid the postbleaching tooth sensitivity, making this esthetic clinical procedure safer and more comfortable to the patients.

Conflict of Interests

The authors have no conflict of interests.

Acknowledgments

The authors acknowledge the partial support by the Conselho Nacional de Desenvolvimento Científico e Tecnológico-CNPq (Grant no. 301291/2010-1), Fundação Amparo à Pesquisa do Estado de São Paulo-FAPESP (Grant nos. 2011/15366-5 and 2011/12938-8) and FUNDUNESP (Grant no. 0024/021/13-PROPe-CDC).

References

[1] V. Cecarini, J. Gee, E. Fioretti et al., "Protein oxidation and cellular homeostasis: emphasis on metabolism," *Biochimica et Biophysica Acta*, vol. 1773, no. 2, pp. 93–104, 2007.

[2] M. A. M. Sulieman, "An overview of tooth-bleaching techniques: chemistry, safety and efficacy," *Periodontology 2000*, vol. 48, no. 1, pp. 148–169, 2008.

[3] F. Z. Trindade, A. P. D. Ribeiro, N. T. Sacono et al., "Trans-enamel and trans-dentinal cytotoxic effects of a 35% H_2O_2 bleaching gel on cultured odontoblast cell lines after consecutive applications," *International Endodontic Journal*, vol. 42, no. 6, pp. 516–524, 2009.

[4] D. G. Soares, A. P. Ribeiro, F. da Silveira Vargas, J. Hebling, and C. A. de Souza Costa, "Efficacy and cytotoxicity of a bleaching gel after short application times on dental enamel," *Clinical Oral Investigations*, vol. 17, no. 8, pp. 1901–1909, 2013.

[5] C. A. de Souza Costa, H. Riehl, J. F. Kina, N. T. Sacono, and J. Hebling, "Human pulp responses to in-office tooth bleaching," *Oral Surgery, Oral Medicine, Oral Pathology, Oral Radiology and Endodontology*, vol. 109, no. 4, pp. e59–e64, 2010.

[6] E. S. Majd, M. Goldberg, and L. Stanislawski, "In vitro effects of ascorbate and Trolox on the biocompatibility of dental restorative materials," *Biomaterials*, vol. 24, no. 1, pp. 3–9, 2003.

[7] A. F. Lima, F. C. R. Lessa, M. N. Gasparoto Mancini, J. Hebling, C. A. de Souza Costa, and G. M. Marchi, "Transdentinal protective role of sodium ascorbate against the cytopathic effects of H_2O_2 released from bleaching agents," *Oral Surgery, Oral Medicine, Oral Pathology, Oral Radiology and Endodontology*, vol. 109, no. 4, pp. e70–e76, 2010.

[8] B. B. Aggarwal, C. Sundaram, S. Prasad, and R. Kannappan, "Tocotrienols, the vitamin E of the 21st century: its potential against cancer and other chronic diseases," *Biochemical Pharmacology*, vol. 80, no. 11, pp. 1613–1631, 2010.

[9] N. Lu, W. Chen, and Y. Peng, "Effects of glutathione, Trolox and desferrioxamine on hemoglobin-induced protein oxidative damage: anti-oxidant or pro-oxidant?" *European Journal of Pharmacology*, vol. 659, no. 2-3, pp. 95–101, 2011.

[10] J. Upadhyay and K. Misra, "Towards the interaction mechanism of tocopherols and tocotrienols (vitamin E) with selected metabolizing enzymes," *Bioinformation*, vol. 3, no. 8, pp. 326–331, 2009.

[11] M. Goldberg and A. J. Smith, "Cells and extracellular matrices of dentin and pulp: a biological basis for repair and tissue engineering," *Critical Review of Oral Biologics and Medicine*, vol. 15, no. 1, pp. 13–12, 2004.

[12] N. Yilmaz, M. Yilmaz, and I. Altuntas, "Diazinon-induced brain toxicity and protection by vitamins e plus C," *Toxicology and Industrial Health*, vol. 28, no. 1, pp. 51–57, 2012.

[13] M. Guney, E. Erdemoglu, and T. Mungan, "Selenium-vitamin E combination and melatonin modulates diabetes-induced blood oxidative damage and fetal outcomes in pregnant rats," *Biological Trace Element Research*, vol. 143, no. 2, pp. 1091–1102, 2011.

[14] X. Wang and P. J. Quinn, "Vitamin E and its function in membranes," *Progress in Lipid Research*, vol. 38, no. 4, pp. 309–336, 1999.

[15] R. S. Parker, "Dietary and biochemical aspects of vitamin E," *Advances in Food and Nutrition Research*, vol. 33, pp. 157–232, 1989.

[16] E. Niki, "Do free radicals play causal role in atherosclerosis? Low density lipoprotein oxidation and vitamin E revisited," *Journal of Clinical Biochemistry and Nutrition*, vol. 48, no. 1, pp. 3–7, 2011.

[17] E. S. Wintergerst, S. Maggini, and D. H. Hornig, "Contribution of selected vitamins and trace elements to immune function," *Annals of Nutrition and Metabolism*, vol. 51, no. 4, pp. 301–323, 2007.

[18] E. Reiter, Q. Jiang, and S. Christen, "Anti-inflammatory properties of α- and γ-tocopherol," *Molecular Aspects of Medicine*, vol. 28, no. 5-6, pp. 668–691, 2007.

[19] Q. Jiang, X. Yin, M. A. Lil, M. L. Danielson, H. Freiser, and J. Huang, "Long-chain carboxychromanols, metabolites of vitamin E, are potent inhibitors of cyclooxygenases," *Proceedings of the National Academy of Sciences of the United States of America*, vol. 105, no. 51, pp. 20464–20469, 2008.

[20] D. Wu and S. N. Meydani, "Age-associated changes in immune and inflammatory responses: impact of vitamin E intervention," *Journal of Leukocyte Biology*, vol. 84, no. 4, pp. 900–914, 2008.

[21] V. W. Bowry, K. U. Ingold, and R. Stocker, "Vitamin E in human low-density lipoprotein. When and how this antioxidant becomes a pro-oxidant," *Biochemical Journal*, vol. 288, no. 2, pp. 341–344, 1992.

[22] M. Tokuda and M. Takeuchi, "Effects of excess doses of α-tocopherol on the lipids and function of rainbow trout liver," *Journal of Nutritional Science and Vitaminology*, vol. 41, no. 1, pp. 25–32, 1995.

[23] P. Pearson, S. A. Lewis, J. Britton, I. S. Young, and A. Fogarty, "The pro-oxidant activity of high-dose vitamin E supplements in vivo," *BioDrugs*, vol. 20, no. 5, pp. 271–273, 2006.

Hindawi Publishing Corporation
BioMed Research International
Volume 2014, Article ID 581256, 9 pages
http://dx.doi.org/10.1155/2014/581256

Review Article

Nigral Iron Elevation Is an Invariable Feature of Parkinson's Disease and Is a Sufficient Cause of Neurodegeneration

Scott Ayton and Peng Lei

The Florey Institute of Neuroscience and Mental Health, University of Melbourne, Kenneth Myer Building at Genetics Lane on Royal Parade, Parkville, VIC 3010, Australia

Correspondence should be addressed to Scott Ayton; scott.ayton@unimelb.edu.au and Peng Lei; peng.lei@florey.edu.au

Received 30 April 2013; Accepted 28 October 2013; Published 16 January 2014

Academic Editor: Maha Zaki Rizk

Parkinson's disease (PD) is a neurodegenerative disorder characterized by motor deficits accompanying degeneration of substantia nigra pars compactor (SNc) neurons. Although familial forms of the disease exist, the cause of sporadic PD is unknown. Symptomatic treatments are available for PD, but there are no disease modifying therapies. While the neurodegenerative processes in PD may be multifactorial, this paper will review the evidence that prooxidant iron elevation in the SNc is an invariable feature of sporadic and familial PD forms, participates in the disease mechanism, and presents as a tractable target for a disease modifying therapy.

1. Introduction

The substantia nigra pars compactor (SNc) degenerates in Parkinson's disease (PD), which precipitates motor disabilities such as tremor and bradykinesia that characterize the disease. Symptomatic therapy, such as Levodopa, restores dopamine levels but is ineffectual in altering the progression of the disease. While multiple brain regions are decorated by Lewy bodies (the defining pathological feature of PD) [1], it is unknown why the SNc is selectively vulnerable to neurodegeneration. Prooxidant iron accumulation in this nucleus is one possible reason. The SNc is particularly rich in iron [2], which increases with age [3]. PD is complicated by exaggerated iron retention in this nucleus, which was a historically early finding [4], and has since been repeatedly observed using various quantifiable techniques (Table 1). It is proposed that this high basal iron content, with the vulnerability to accumulate iron with age and in disease, makes this region susceptible to PD neurodegeneration. However, a limitation of postmortem tissue analysis is that, most likely, the tissues analyzed were obtained from end-stage patients, and from this evidence alone it is not possible to claim if iron is pathogenic in the disease or if it is an epiphenomenon.

2. Iron Accumulation in Parkinson's Disease: Cause or Effect?

Is iron elevation contributing to neuronal death in Parkinson's disease, or is it simply a feature of dying neurons? To address this important question, this paper will review three separate lines of evidence: (1) *in vivo* iron-imaging technology, (2) rare genetic disorders of iron metabolism, and (3) animal models.

2.1. In Vivo Iron-Imaging Technology. The iron hypothesis of Parkinson's disease has been revitalized by the ability to visualize and quantify iron elevation in the SNc of living patients, first by a technique called transcranial sonography (TCS) then later by T_2^*-weighted MRI. TCS has been employed for a number of years to quantify the echogenicity of the SN in PD patients. Echogenicity refers to the ability of a substance to return the sound wave back to the receiver. Tissue laden with iron has greater echogenicity allowing iron elevation in PD to be visualized with this technique [5–11]. TCS is a promising diagnostic tool for PD with positive predictive value of 85.7% and a negative predictive value of 82.9% [10]. TCS has been suggested as the earliest predictive test for PD (with the exception of genetic testing in rare

Table 1: Reports of quantifiable iron in PD SN.

Iron measurement technique	Fe in PD SN (% control)	Reference
ICP-MS	135	[116]
SP	176	[117]
SP	177	[118]
AAS	107	[119]
ICP-MS	133	[120]
ICP-MS	130	[121]
X-Ray Microprobe analysis	340	[122]
SP	150	[123]
Laser microprobe analysis	145	[124]
ICPMS	156	[125]
Colorimetry	82	[126]
X-Ray absorption fine structure	201	[127]
Electron probe X-Ray microanalysis coupled with cathodoluminescence spectroscopy	200	[128]
AAS	144	[96]
X-Ray fluorescence	155	[129]
ICP-MS	140	[110]
AAS	139	[26]
Average	159.5	

ICPMS: inductively coupled plasma mass spectrometry; SP: spectrophotometry; AAS: atomic absorption spectrometry.

familial cases) [12]. Increased echogenicity in otherwise healthy individuals has been associated with reduced [18F]-dopa uptake in the striatum [13] and minor motor abnormalities in older patients [14] possibly suggesting early, presymptomatic degeneration. Tellingly, nonsymptomatic individuals with increased echogenicity have 17 times the risk of acquiring PD after 3 years when compared to individuals with a normal echogenetic profile [15]. The early elevation of iron identified using *in vivo* imaging techniques could position this phenomenon upstream of neurodegeneration in the PD mechanism.

Increased iron in the SN has also been determined by quantifying relaxation times of T_2- and T_2^*-weighted MRI, which strongly correlates with tissue iron levels [16]. Iron elevation by MRI has been correlated with disease severity [17, 18] and duration [19]. In a 3-year-followup study, iron measured by T_2^* MRI was shown to progressively increase in PD subjects but not controls [20]. It also has been implicated in diagnosis of PD with reported sensitivity of 100% and specificity of 80% in a small cohort [21].

Iron elevation is also a common feature of familial PD. PD-associated Park genes encoding proteins, alpha synuclein, leucine-rich repeat kinase 2 (LRRK2), PTEN-induced putative kinase 1 (PINK1), Parkin, and DJ-1, are associated with iron accumulation in the SN as measured by TCS, demonstrating that iron elevation is an invariable feature of multiple PD modalities (Table 2).

Imaging technology has allowed visualization of iron elevation as (a) a risk factor for PD, (b) an early event in the progression of the disease, (c) a feature that correlates with disease severity and duration, and (d) a feature of all causes of PD (measured so far). But imaging technology has not afforded us direct evidence to conclude if iron elevation is epiphenomenal or part of the disease process.

2.2. Rare Genetic Disorders of Brain Iron Metabolism Often Present as PD. Evidence placing iron as a mediating factor of PD neurodegeneration is drawn from rare genetic disorders that are known to interfere with the iron-handling pathway. The following examples demonstrate that a primary elevation in nigral iron is a sufficient cause of Parkinsonian neurodegeneration; thus iron elevation evidenced in familial and sporadic cases of PD has the clear potential to contribute to the degenerative process.

2.2.1. Aceruloplasminemia. Ceruloplasmin is multicopper oxidase that converts ferrous to ferric iron and is required for the export of iron from cells [22]. Aceruloplasminemia is a rare genetic disorder of ceruloplasmin dysfunction that results in an iron retention within various tissues [23, 24] that can be recapitulated in ceruloplasmin knockout mice [25–27]. Dozens of ceruloplasmin mutations have been identified and some induce Parkinsonism in affected individuals [28]. In particular, three missense mutations in ceruloplasmin-I63T, D554E, and R793H, have been shown to exhibit reduced ferroxidase activity in the plasma of patients [29], increased nigral iron content, and a Parkinsonian presentation in affected individuals [30].

2.2.2. Neurodegeneration with Brain Iron Accumulation Type 1. Neurodegeneration with brain iron accumulation type 1 (NBIA1) is caused by a mutation in pantothenate kinase 2 (PANK2). PANK2 catalyses the initial step in coenzyme A synthesis and mutations have reduced catalytic activity [31] and basal ganglia iron accumulation [32]. Patients with this mutation often present with Parkinsonism [33]. Brains of affected patients contain the Parkinson's Lewy body pathology [34–36], possibly suggesting that iron accumulation is upstream of alpha synuclein deposition in idiopathic PD.

2.2.3. Neuroferritinopathy. Neuroferritinopathy, also called neurodegeneration with brain iron accumulation type 2, is a rare autosomal dominant neurodegenerative disease caused by one of seven known mutations to the ferritin light chain protein [37–43]. The mutation causes increased iron and ferritin deposition in the brain but not other organs. Iron elevation in the brain results in various extrapyramidal motor symptoms including dystonia, chorea, parkinsonism, and tremor.

2.3. Animal Models. A variety of animal models have demonstrated that iron elevation is sufficient to cause neurodegeneration in the nigra. Direct injection of iron into the midbrain region of rats causes SN neuronal loss [44]. A number of studies employing an iron feeding protocol to neonatal mice have shown Parkinsonism and nigral degeneration in these mice when they reach adulthood [45–47]. These studies take

Table 2: Iron elevation (TCS) in the genetics of PD.

Locus	Gene	Mutation	Comments	Iron elevation	Reference
PARK1/4	Alpha synuclein	3 point mutations, duplication, triplication	Onset age 40–50 Rapid progression, frequent dementia. Lewy bodies present	Yes	[130]
PARK2	Parkin	>100 mutations	Age of onset 17–24 years Parkinsonism Other motor symptoms but no dementia. Lewy bodies present	Yes	[130, 131]
PARK6	PINK1	>20 mutations	Onset age 30–50 Clinical features resemble Parkin mutations. Lewy bodies present	Yes	[130, 132]
PARK7	DJ-1	3 point mutations	Onset age 20–40 Clinical features resemble Parkin mutations. Unknown if Lewy bodies are present	Yes	[130]
PARK8	LRRK2	6 point mutations	Age of onset 50s Resembles idiopathic PD. Lewy bodies present	Yes	[130, 133]
PARK9	ATP13A2	1 mutation	Age of onset 10–30 years Parkinsonism, supranuclear gaze paresis, pyramidal signs, and dementia. Unknown if Lewy bodies are present	??	
PARK14	PLA2G6	2 mutations	Age of onset 20–40 Parkinsonism Dementia, psychosis, dystonia, and hyperreflexia. Unknown if Lewy bodies are present	??	
PARK15	FBXO7	3 mutations	Age of onset 7–22 Parkinsonism, hyperreflexia, and spasticity. Unknown if Lewy bodies are present	??	

Iron accumulation [130–133] and Lewy bodies [134].

advantage of the immature blood brain barrier which allows elevated systemic iron to permeate the brain. Neonatal iron fed mice are also more susceptible to 1-methyl-4-phenyl-1,2,3,6-tetrahydropyridine (MPTP) intoxication [48].

Toxin models of PD, MPTP, and 6-hydroxydopamine (6-OHDA) also recapitulate iron elevation within the SN [49, 50]. The changes in iron within the SN cells are complex and poorly understood. Within the first 2–4 days after treatment of MPTP, there is an increase in chelatable iron within the mitochondria [51], preceding total iron elevation, 1-2 weeks after administration. Iron chelator drugs are effective in attenuating the damage caused by these Parkinsonian toxins [52, 53] demonstrating that iron is a mediator of neurodegeneration in toxin models of PD and that iron chelation is an attractive therapeutic option for PD.

3. The Consequences of Iron Elevation: Implications for the Disease Mechanism

3.1. Oxidative Stress. Iron elevation can cause oxidative stress-mediated cell death. Within biological systems iron can react with oxygen to catalyze the formation of the toxic hydroxyl radical via the Fenton reaction. This reaction is dependent on the ability of iron to alter its valence state between ferrous (Fe^{2+}) and ferric (Fe^{3+}) species [54]. Inappropriate iron retention in PD could promote oxidative stress within this tissue. Post mortem PD-affected brains display increased lipid peroxidation [55], oxidative damage to DNA [56], and lowered levels of the reduced form of glutathione [57], which all reflect oxidative stress.

3.2. Alpha Synuclein Deposition. Alpha synuclein is often considered the Parkinson's protein owning to extensive links to the disease. Three genetic mutations of alpha synuclein, A53T [58], A30P [59], and E46K [60], along with gene duplication [61] or triplication [62] have been associated with inheritable forms of PD. Aggregated alpha synuclein is also the major component of Lewy bodies, the pathological hallmark for PD [63]. Alpha synuclein deposition could be contributed to by iron exposure. Alpha synuclein binds to iron [64–66], which accelerates its aggregation into fibrils [67, 68]. Alpha synuclein has also been shown to directly generate hydrogen peroxide when it aggregates and, in the presence of iron, produce toxic hydroxyl radicals [69]. In cultured neurons, iron has been shown to cause aggregation of alpha synuclein [70–73]. Collectively these findings demonstrate that iron can theoretically impact the aggregation of alpha synuclein. Iron is also found enriched in Lewy bodies [74], providing *in vivo* evidence that iron elevation could induce Lewy body deposition in PD.

4. Mechanisms of Iron Accumulation in PD

Understanding how iron accumulates in PD may provide opportunities to target this process pharmacologically. There is only a weak association between environmental iron exposure and development of PD [75, 76], suggesting that endogenous factors or metabolic dysregulation is the genesis for elevated iron in PD. Peripheral iron status, modified by diet or various genetic disorders (e.g., hemochromatosis), is rarely reflected by concomitant changes to iron in the brain. While peripheral iron has access to the brain [77] and iron consumed in the diet is distributed to the brain in comparable levels to other organs [78], the brain retains mostly stable throughout life [79–81]. The brain is able to control iron levels in a narrow range by recruiting various protein machinery. While many reviews discuss the iron regulatory pathways of the brain [82, 83], this paper will discuss the evidence that fatigue to these machinery results in iron accumulation in PD.

Various iron associated proteins have been investigated for their potential to contribute to iron accumulation in PD. The earliest such study surveyed the iron storage protein ferritin in post mortem PD brains, demonstrating a decrease in this protein compared to controls [84]. Increased iron with a concomitant decrease in ferritin within the SN could suggest an increase in the labile iron pool, making iron more available for toxic interactions. Ferritin elevation, therefore, might be neuroprotective in the disease. This was demonstrated in the MPTP model, where ferritin overexpressing mice were protected against the toxin [52].

While changes in ferritin could relate to cellular buffering capacity of iron, this does not easily explain why iron accumulates in PD. Iron elevation in PD could be contributed to by increased cellular iron uptake via transferrin receptor 1 (TfR1). However, the levels of this protein were shown not to be altered in PD (when loss of neurons was accounted for) [85], nor in the 6-OHDA model [86], arguing against a role for this protein in iron accumulation of PD. Within the periphery, the transferrin receptor is inhibited by the hemochromatosis protein as a normal component of the iron homeostatic mechanism. However, loss of function genetic mutations in the hemochromatosis protein causes pathological iron retention in peripheral tissues in hereditary hemochromatosis. The iron overload associated with hemochromatosis in peripheral tissue is also not convincingly linked to PD. The C282Y mutation in hemochromatosis protein was initially shown to increase the risk of PD and Parkinsonism [87] and this was supported by a later study [88]. However further investigations have failed to find an association with C282Y mutation and PD [89–91], although one study found two single nucleotide polymorphisms (K92N and I217T) in a single PD patient and not in controls [89]. It remains unclear what role hemochromatosis protein plays in either genetic or idiopathic PD; further it is not known if individuals with hereditary hemochromatosis have brain iron accumulation. It is likely that the peripheral hemochromatosis hormone plays a minor role in brain iron homeostasis; indeed staining for the hemochromatosis protein in brain reveals only scattered staining for the protein, localized to parts of cortex, cerebellum, and brain endothelium [92].

Another iron importing protein, transferrin receptor 2 (TfR2) was found to be increased in the rotenone model of PD [93]. It is proposed in the paper by Mastroberardino et al. [93] that TfR2 signals for iron to be deposited in the mitochondria leading to iron accumulation and oxidative damage within the SN. The function consequence of this process is unclear and TfR2 has yet to be explored in human PD tissue.

Both TfR1 and TfR2 receive iron from the transferrin protein. The complex then undergoes endocytosis where iron is transported across the endosome by the divalent metal ion transporter (DMT1). An isoform of DMT1 with an iron responsive element (DMT1 + IRE) was shown to be increased in cultured cells exposed to 6-OHDA [94] and early after MPTP intoxication in mice [95], which was later replicated [96]. Salazar et al. [96] additionally used mice with a loss of function mutation of DMT1 and showed that this was protective against MPTP induced iron elevation and toxicity. Importantly, Salazar et al. [96] also showed that DMT1+IRE was elevated in the SN of PD patients, which implicates overexpression of this protein in iron accumulation in PD.

Iron elevation in PD could also be contributed by failure of iron export. Ferroportin is the only known iron exporting channel in mammals [97]. Ferroportin requires cooperation with a ferroxidase that converts intracellular ferrous iron (Fe^{2+}) to ferric iron (Fe^{3+}) so that extracellular ferric-binding transferrin protein can remove iron from ferroportin [98]. Ceruloplasmin is the best characterized ferroxidase protein and has been investigated as a possible contributor to iron elevation in PD. Decreased ceruloplasmin ferroxidase activity has been observed in PD cerebrospinal fluid (CSF) [99–101] and serum [102–107], while low serum ceruloplasmin activity is correlated with earlier age of PD onset [103, 105, 106]. Loss of peripheral ceruloplasmin function could therefore impact brain iron levels, and indeed peripheral and brain-derived pools of ceruloplasmin are in exchange [26]. The level of ceruloplasmin in the PD SN is unaltered in the disease [108], but its activity is selectively reduced in the SNc [26]. This is important since loss of ceruloplasmin function, as in aceruloplasminemia, often causes Parkinsonism in affected individuals [28].

Iron export could also be impacted by the tau protein. Tau protein is famously linked with Alzheimer's disease and frontotemporal dementia, but tau protein has been implicated in PD from genetic, pathological, and biochemical perspectives [109]. Tau levels are reduced in the substantia nigra in PD, which obtunds amyloid precursor protein (APP) mediated iron export [110]. APP binds to ferroportin to facilitate iron export [111], and loss of tau prevents APP trafficking to the neuronal surface to perform this function [110]. Tau knockout mice develop iron-mediated Parkinsonism [110], highlighting the neurotoxic potential for a disturbance to this pathway.

5. Conclusions and Therapeutic Implications

So is iron elevation the cause of PD? Quite simply the answer has to be no, since there has to be some other process that causes iron to elevate in the first place. The same could be said of any other factor implicated in PD. If alpha synuclein is the cause of Parkinson's disease, what causes the protein

to aggregate? Understanding the cause of PD may indeed be impossible to define. Even if this was understood, the factor(s) inducing the degenerative process in PD may not be propagating disease progression by the time the patient initially presents with symptoms. The degenerative processes in PD are likely to involve multiple pathways; the goal of our field should be to identify components of the disease mechanism that can be targeted pharmacologically. Iron is one such component. Iron is elevated invariably in the SNc of PD-effected brains, early in the disease processes, and brain iron overload is sufficient to cause Parkinsonism in rare genetic cases or brain iron overload, or in various animal models of PD.

Iron is also a tractable target for pharmacotherapy. Numerous iron chelators are currently in use for peripheral disorders of iron overload [112]. Iron chelator, Deferiprone, was recently shown to benefit PD patients in a phase II clinical trial (PMID: 24251381) [113]. This is the first drug to show a disease-modifying effect for PD, which highlights the potential for targeting iron for PD pharmacotherapy, and strongly implicates iron in the disease mechanism. A limitation of the iron chelators presently in the market is that they were developed to treat peripheral disorders of iron metabolism [114]. Iron chelators that have greater access to the brain through BBB are currently in development [52, 53, 110, 115].

There is also opportunity to target cellular mechanisms that cause iron to be elevated in PD. Preventing elevation of DMT1, or restoring the loss of tau or ceruloplasmin, might be additional ways to target the iron lesion. While strategies that prevent the rise in iron or remove excess iron in the disease might not be silver bullets that halt neurodegeneration altogether, the evidence outlined in this review suggests that these approaches might slow the degenerative process and therefore are attractive options for the first disease-modifying therapy for PD.

Conflict of Interests

The authors declare that there is no conflict of interests regarding the publication of this paper.

Acknowledgments

This paper is supported by funds from the Australian National Health and Medical Research Council (NHMRC), the Alzheimer's Australia Dementia Research Foundation, and the Operational Infrastructure Support Victorian State Government.

References

[1] H. Braak, U. Rüb, W. P. Gai, and K. Del Tredici, "Idiopathic Parkinson's disease: possible routes by which vulnerable neuronal types may be subject to neuroinvasion by an unknown pathogen," *Journal of Neural Transmission*, vol. 110, no. 5, pp. 517–536, 2003.

[2] M. E. Götz, K. Double, M. Gerlach, M. B. H. Youdim, and P. Riederer, "The relevance of iron in the pathogenesis of Parkinson's disease," *Annals of the New York Academy of Sciences*, vol. 1012, pp. 193–208, 2004.

[3] L. Zecca, M. Gallorini, V. Schünemann et al., "Iron, neuromelanin and ferritin content in the substantia nigra of normal subjects at different ages: consequences for iron storage and neurodegenerative processes," *Journal of Neurochemistry*, vol. 76, no. 6, pp. 1766–1773, 2001.

[4] J. Lhermitte, W. M. Kraus, and D. McAlpine, "On the occurrence of abnormal deposits of iron in the brain in parkinsonism with special reference to its localisation," *Journal of Neurology, Neurosurgery & Psychiatry*, vol. 195, pp. s1–s5, 1924.

[5] D. Berg, C. Grote, W.-D. Rausch et al., "Iron accumulation in the substantia nigra in rats visualized by ultrasound," *Ultrasound in Medicine and Biology*, vol. 25, no. 6, pp. 901–904, 1999.

[6] D. Berg, W. Roggendorf, U. Schröder et al., "Echogenicity of the substantia nigra: association with increased iron content and marker for susceptibility to nigrostriatal injury," *Archives of Neurology*, vol. 59, no. 6, pp. 999–1005, 2002.

[7] L. Zecca, D. Berg, T. Arzberger et al., "In vivo detection of iron and neuromelanin by transcranial sonography: a new approach for early detection of substantia nigra damage," *Movement Disorders*, vol. 20, no. 10, pp. 1278–1285, 2005.

[8] D. Berg, "In vivo detection of iron and neuromelanin by transcranial sonography—a new approach for early detection of substantia nigra damage," *Journal of Neural Transmission*, vol. 113, no. 6, pp. 775–780, 2006.

[9] D. Berg, H. Hochstrasser, K. J. Schweitzer, and O. Riess, "Disturbance of iron metabolism in Parkinson's disease—ultrasonography as a biomarker," *Neurotoxicity Research*, vol. 9, no. 1, pp. 1–13, 2006.

[10] J. Prestel, K. J. Schweitzer, A. Hofer, T. Gasser, and D. Berg, "Predictive value of transcranial sonography in the diagnosis of Parkinson's disease," *Movement Disorders*, vol. 21, no. 10, pp. 1763–1765, 2006.

[11] G. Becker, J. Seufert, U. Bogdahn, H. Reichmann, and K. Reiners, "Degeneration of substantia nigra in chronic Parkinson's disease visualized by transcranial color-coded real-time sonography," *Neurology*, vol. 45, no. 1, pp. 182–184, 1995.

[12] D. Berg, "Transcranial ultrasound as a risk marker for Parkinson's disease," *Movement Disorders*, vol. 24, supplement 2, pp. S677–S683, 2009.

[13] S. Behnke, U. Schroeder, U. Dillmann et al., "Hyperechogenicity of the substantia nigra in healthy controls is related to MRI changes and to neuronal loss as determined by F-Dopa PET," *NeuroImage*, vol. 47, no. 4, pp. 1237–1243, 2009.

[14] D. Berg, C. Siefker, P. Ruprecht-Dörfler, and G. Becker, "Relationship of substantia nigra echogenicity and motor function in elderly subjects," *Neurology*, vol. 56, no. 1, pp. 13–17, 2001.

[15] D. Berg, K. Seppi, S. Behnke et al., "Enlarged substantia Nigra hyperechogenicity and risk for Parkinson disease: a 37-month 3-center study of 1847 older persons," *Archives of Neurology*, vol. 68, no. 7, pp. 932–937, 2011.

[16] N. Gelman, J. M. Gorell, P. B. Barker et al., "MR imaging of human brain at 3.0 T: preliminary report on transverse relaxation rates and relation to estimated iron content," *Radiology*, vol. 210, no. 3, pp. 759–767, 1999.

[17] G. Gorell, "Increased iron-related MRI contrast in the substantia nigra in Parkinson's disease," *Neurology*, vol. 45, no. 7, pp. 1138–1143, 1995.

[18] H. T. Atasoy, O. Nuyan, T. Tunc, M. Yorubulut, A. E. Unal, and L. E. Inan, "T2-weighted MRI in Parkinson's disease; substantia nigra pars compacta hypointensity correlates with the clinical scores," *Neurology India*, vol. 52, no. 3, pp. 332–337, 2004.

[19] P. Ryvlin, E. Broussolle, H. Piollet, F. Viallet, Y. Khalfallah, and G. Chazot, "Magnetic resonance imaging evidence of decreased putamenal iron content in idiopathic Parkinson's disease," *Archives of Neurology*, vol. 52, no. 6, pp. 583–588, 1995.

[20] M. Ulla, J. Marie Bonny, L. Ouchchane et al., "Is r2* a new MRI biomarker for the progression of Parkinson's disease? A longitudinal follow-up," *PloS ONE*, vol. 8, Article ID e57904, 2013.

[21] R. A. Menke, J. Scholz, K. L. Miller et al., "MRI characteristics of the substantia nigra in Parkinson's disease: a combined quantitative T1 and DTI study," *NeuroImage*, vol. 47, no. 2, pp. 435–441, 2009.

[22] S. Osaki, D. A. Johnson, and E. Frieden, "The possible significance of the ferrous oxidase activity of ceruloplasmin in normal human serum," *The Journal of Biological Chemistry*, vol. 241, no. 12, pp. 2746–2751, 1966.

[23] H. Miyajima, Y. Nishimura, and K. Mizoguchi, "Familial apoceruloplasmin deficiency associated with blepharospasm and retinal degeneration," *Neurology*, vol. 37, no. 5, pp. 761–767, 1987.

[24] K. Yoshida, K. Furihata, S. Takeda et al., "A mutation in the ceruloplasmin gene is associated with systemic hemosiderosis in humans," *Nature Genetics*, vol. 9, no. 3, pp. 267–272, 1995.

[25] B. N. Patel, R. J. Dunn, S. Y. Jeong, Q. Zhu, J.-P. Julien, and S. David, "Ceruloplasmin regulates iron levels in the CNS and prevents free radical injury," *Journal of Neuroscience*, vol. 22, no. 15, pp. 6578–6586, 2002.

[26] S. Ayton, P. Lei, J. A. Duce et al., "Ceruloplasmin dysfunction and therapeutic potential for parkinson disease," *Annals of Neurology*, vol. 73, article 554, 2013.

[27] Z. L. Harris, A. P. Durley, T. K. Man, and J. D. Gitlin, "Targeted gene disruption reveals an essential role for ceruloplasmin in cellular iron efflux," *Proceedings of the National Academy of Sciences of the United States of America*, vol. 96, no. 19, pp. 10812–10817, 1999.

[28] A. McNeill, M. Pandolfo, J. Kuhn, H. Shang, and H. Miyajima, "The neurological presentation of ceruloplasmin gene mutations," *European Neurology*, vol. 60, no. 4, pp. 200–205, 2008.

[29] H. Hochstrasser, J. Tomiuk, U. Walter et al., "Functional relevance of ceruloplasmin mutations in Parkinson's disease," *The FASEB Journal*, vol. 19, article 1851, 2005.

[30] H. Hochstrasser, P. Bauer, U. Walter et al., "Ceruloplasmin gene variations and substantia nigra hyperechogenicity in Parkinson disease," *Neurology*, vol. 63, no. 10, pp. 1912–1917, 2004.

[31] P. T. Kotzbauer, A. C. Truax, J. Q. Trojanowski, and V. M.-Y. Lee, "Altered neuronal mitochondrial coenzyme A synthesis in neurodegeneration with brain iron accumulation caused by abnormal processing, stability, and catalytic activity of mutant pantothenate kinase 2," *Journal of Neuroscience*, vol. 25, no. 3, pp. 689–698, 2005.

[32] K. F. Swaiman, "Hallervorden-Spatz syndrome and brain iron metabolism," *Archives of Neurology*, vol. 48, no. 12, pp. 1285–1293, 1991.

[33] R. Alberca, E. Rafel, I. Chinchon, J. Vadillo, and A. Navarro, "Late onset Parkinsonian syndrome in Hallervorden-Spatz disease," *Journal of Neurology Neurosurgery and Psychiatry*, vol. 50, no. 12, pp. 1665–1668, 1987.

[34] S. Arawaka, Y. Saito, S. Murayama, and H. Mori, "Lewy body in neurodegeneration with brain iron accumulation type 1 is immunoreactive for α-synuclein," *Neurology*, vol. 51, no. 3, pp. 887–889, 1998.

[35] G. K. Tofaris, T. Revesz, T. S. Jacques, S. Papacostas, and J. Chataway, "Adult-onset neurodegeneration with brain iron accumulation and cortical α-synuclein and tau pathology: a distinct clinicopathological entity," *Archives of Neurology*, vol. 64, no. 2, pp. 280–282, 2007.

[36] J. E. Galvin, B. Giasson, H. I. Hurtig, V. M.-Y. Lee, and J. Q. Trojanowski, "Neurodegeneration with brain iron accumulation, type 1 is characterized by α-, β-, and γ-synuclein neuropathology," *The American Journal of Pathology*, vol. 157, no. 2, pp. 361–368, 2000.

[37] A. R. J. Curtis, C. Fey, C. M. Morris et al., "Mutation in the gene encoding ferritin light polypeptide causes dominant adult-onset basal ganglia disease," *Nature Genetics*, vol. 28, no. 4, pp. 350–354, 2001.

[38] R. Vidal, B. Ghetti, M. Takao et al., "Intracellular ferritin accumulation in neural and extraneural tissue characterizes a neurodegenerative disease associated with a mutation in the ferritin light polypeptide gene," *Journal of Neuropathology and Experimental Neurology*, vol. 63, no. 4, pp. 363–380, 2004.

[39] M. Mancuso, G. Davidzon, R. M. Kurlan et al., "Hereditary ferritinopathy: a novel mutation, its cellular pathology, and pathogenetic insights," *Journal of Neuropathology and Experimental Neurology*, vol. 64, no. 4, pp. 280–294, 2005.

[40] P. Maciel, V. T. Cruz, M. Constante et al., "Neuroferritinopathy: missense mutation in FTL causing early-onset bilateral pallidal involvement," *Neurology*, vol. 65, no. 4, pp. 603–605, 2005.

[41] E. Ohta, T. Nagasaka, K. Shindo et al., "Neuroferritinopathy in a Japanese family with a duplication in the ferritin light chain gene," *Neurology*, vol. 70, no. 16, pp. 1493–1494, 2008.

[42] D. Devos, P. J. Tchofo, I. Vuillaume et al., "Clinical features and natural history of neuroferritinopathy caused by the 458dupA FTL mutation," *Brain*, vol. 132, no. 6, article e109, 2009.

[43] A. Kunota, A. Hida, Y. Ichikawa et al., "A novel ferritin light chain gene mutation in a Japanese family with neuroferritinopathy: description of clinical features and implications for genotype-phenotype correlations," *Movement Disorders*, vol. 24, no. 3, pp. 441–445, 2009.

[44] D. Ben-Shachar and M. B. H. Youdim, "Intranigral iron injection induces behavioral and biochemical "Parkinsonism" in rats," *Journal of Neurochemistry*, vol. 57, no. 6, pp. 2133–2135, 1991.

[45] F. Dal-Pizzol, F. Klamt, J. Frota M.L.C. et al., "Neonatal iron exposure induces oxidative stress in adult Wistar rat," *Developmental Brain Research*, vol. 130, no. 1, pp. 109–114, 2001.

[46] P. Budni, M. N. M. De Lima, M. Polydoro, J. C. F. Moreira, N. Schroder, and F. Dal-Pizzol, "Antioxidant effects of selegiline in oxidative stress induced by iron neonatal treatment in rats," *Neurochemical Research*, vol. 32, no. 6, pp. 965–972, 2007.

[47] D. Kaur, J. Peng, S. J. Chinta et al., "Increased murine neonatal iron intake results in Parkinson-like neurodegeneration with age," *Neurobiology of Aging*, vol. 28, no. 6, pp. 907–913, 2007.

[48] J. Lan and D. H. Jiang, "Desferrioxamine and vitamin E protect against iron and MPTP-induced neurodegeneration in mice," *Journal of Neural Transmission*, vol. 104, no. 4-5, pp. 469–481, 1997.

[49] J. A. Temlett, J. P. Landsberg, F. Watt, and G. W. Grime, "Increased iron in the substantia nigra compacta of the MPTP-lesioned hemiparkinsonian African Green monkey: evidence

from proton microprobe elemental microanalysis," *Journal of Neurochemistry*, vol. 62, no. 1, pp. 134–146, 1994.

[50] H. Jiang, W.-F. Chen, and J.-X. Xie, "Relationship between dopamine and iron contents in the brain of Parkinsonian rats," *Acta Physiologica Sinica*, vol. 53, no. 5, pp. 334–338, 2001.

[51] L.-P. Liang and M. Patel, "Iron-sulfur enzyme mediated mitochondrial superoxide toxicity in experimental Parkinson's disease," *Journal of Neurochemistry*, vol. 90, no. 5, pp. 1076–1084, 2004.

[52] D. Kaur, F. Yantiri, S. Rajagopalan et al., "Genetic or pharmacological iron chelation prevents MPTP-induced neurotoxicity in vivo: a novel therapy for Parkinson's disease," *Neuron*, vol. 37, no. 6, pp. 899–909, 2003.

[53] D. B. Shachar, N. Kahana, V. Kampel, A. Warshawsky, and M. B. H. Youdim, "Neuroprotection by a novel brain permeable iron chelator, VK-28, against 6-hydroxydopamine lession in rats," *Neuropharmacology*, vol. 46, no. 2, pp. 254–263, 2004.

[54] K. J. Barnham, C. L. Masters, and A. I. Bush, "Neurodegenerative diseases and oxidatives stress," *Nature Reviews Drug Discovery*, vol. 3, no. 3, pp. 205–214, 2004.

[55] D. T. Dexter, C. J. Carter, F. R. Wells et al., "Basal lipid peroxidation in substantia nigra is increased in Parkinson's disease," *Journal of Neurochemistry*, vol. 52, no. 2, pp. 381–389, 1989.

[56] Z. I. Alam, A. Jenner, S. E. Daniel et al., "Oxidative DNA damage in the Parkinsonian brain: an apparent selective increase in 8-hydroxyguanine levels in substantia nigra," *Journal of Neurochemistry*, vol. 69, no. 3, pp. 1196–1203, 1997.

[57] J. Sian, D. T. Dexter, A. J. Lees et al., "Alterations in glutathione levels in Parkinson's disease and other neurodegenerative disorders affecting basal ganglia," *Annals of Neurology*, vol. 36, no. 3, pp. 348–355, 1994.

[58] M. H. Polymeropoulos, C. Lavedan, E. Leroy et al., "Mutation in the α-synuclein gene identified in families with Parkinson's disease," *Science*, vol. 276, no. 5321, pp. 2045–2047, 1997.

[59] R. Krüger, W. Kuhn, T. Müller et al., "Ala30Pro mutation in the gene encoding α-synuclein in Parkinson's disease," *Nature Genetics*, vol. 18, no. 2, pp. 106–108, 1998.

[60] J. J. Zarranz, J. Alegre, J. C. Gómez-Esteban et al., "The new mutation, E46K, of α-synuclein causes parkinson and lewy body dementia," *Annals of Neurology*, vol. 55, no. 2, pp. 164–173, 2004.

[61] M.-C. Chartier-Harlin, J. Kachergus, C. Roumier et al., "α-synuclein locus duplication as a cause of familial Parkinson's disease," *The Lancet*, vol. 364, no. 9440, pp. 1167–1169, 2004.

[62] D. W. Miller, S. M. Hague, J. Clarimon et al., "α-synuclein in blood and brain from familial Parkinson disease with SNCA locus triplication," *Neurology*, vol. 62, no. 10, pp. 1835–1838, 2004.

[63] M. G. Spillantini, M. L. Schmidt, V. M.-Y. Lee, J. Q. Trojanowski, R. Jakes, and M. Goedert, "α-synuclein in Lewy bodies," *Nature*, vol. 388, no. 6645, pp. 839–840, 1997.

[64] B. Bharathi, S. S. Indi, and K. S. J. Rao, "Copper- and iron-induced differential fibril formation in α-synuclein: TEM study," *Neuroscience Letters*, vol. 424, no. 2, pp. 78–82, 2007.

[65] B. Bharathi and K. S. J. Rao, "Thermodynamics imprinting reveals differential binding of metals to α-synuclein: relevance to parkinson's disease," *Biochemical and Biophysical Research Communications*, vol. 359, no. 1, pp. 115–120, 2007.

[66] Y. Peng, C. Wang, H. H. Xu, Y.-N. Liu, and F. Zhou, "Binding of α-synuclein with Fe(III) and with Fe(II) and biological implications of the resultant complexes," *Journal of Inorganic Biochemistry*, vol. 104, no. 4, pp. 365–370, 2010.

[67] S. R. Paik, H.-J. Shin, and J.-H. Lee, "Metal-catalyzed oxidation of α-synuclein in the presence of copper(II) and hydrogen peroxide," *Archives of Biochemistry and Biophysics*, vol. 378, no. 2, pp. 269–277, 2000.

[68] N. Golts, H. Snyder, M. Frasier, C. Theisler, P. Choi, and B. Wolozin, "Magnesium inhibits spontaneous and iron-induced aggregation of α-synuclein," *The Journal of Biological Chemistry*, vol. 277, no. 18, pp. 16116–16123, 2002.

[69] S. Turnbull, B. J. Tabner, O. M. A. El-Agnaf, S. Moore, Y. Davies, and D. Allsop, "α-synuclein implicated in Parkinson's disease catalyses the formation of hydrogen peroxide in vitro," *Free Radical Biology and Medicine*, vol. 30, no. 10, pp. 1163–1170, 2001.

[70] Q. He, N. Song, H. Xu, R. Wang, J. Xie, and H. Jiang, "Alpha-synuclein aggregation is involved in the toxicity induced by ferric iron to SK-N-SH neuroblastoma cells," *Journal of Neural Transmission*, vol. 118, no. 3, pp. 397–406, 2011.

[71] W.-J. Li, H. Jiang, N. Song, and J.-X. Xie, "Dose- and time-dependent α-synuclein aggregation induced by ferric iron in SK-N-SH cells," *Neuroscience Bulletin*, vol. 26, no. 3, pp. 205–210, 2010.

[72] N. Ostrerova-Golts, L. Petrucelli, J. Hardy, J. M. Lee, M. Farer, and B. Wolozin, "The A53T α-synuclein mutation increases iron-dependent aggregation and toxicity," *Journal of Neuroscience*, vol. 20, no. 16, pp. 6048–6054, 2000.

[73] W. Li, H. Jiang, N. Song, and J. Xie, "Oxidative stress partially contributes to iron-induced alpha-synuclein aggregation in SK-N-SH cells," *Neurotoxicity Research*, vol. 19, no. 3, pp. 435–442, 2011.

[74] R. J. Castellani, S. L. Siedlak, G. Perry, and M. A. Smith, "Sequestration of iron by Lewy bodies in Parkinson's disease," *Acta Neuropathologica*, vol. 100, no. 2, pp. 111–114, 2000.

[75] J. Zayed, S. Ducic, G. Campanella et al., "Environmental factors in the etiology of Parkinson's disease," *Canadian Journal of Neurological Sciences*, vol. 17, no. 3, pp. 286–291, 1990.

[76] G. Logroscino, K. Marder, J. Graziano et al., "Dietary iron, animal fats, and risk of Parkinson's disease," *Movement Disorders*, vol. 13, supplement 1, pp. 13–16, 1998.

[77] E. H. Morgan and T. Moos, "Mechanism and developmental changes in iron transport across the blood-brain barrier," *Developmental Neuroscience*, vol. 24, no. 2-3, pp. 106–113, 2002.

[78] J. H. Chen, S. Shahnavas, N. Singh, W. Y. Ong, and T. Walczyk, "Stable iron isotope tracing reveals significant brain iron uptake in adult rats," *Metallomics*, vol. 5, article 167, 2013.

[79] P. R. Dallman, M. A. Siimes, and E. C. Manies, "Brain iron: persistent deficiency following short term iron deprivation in the young rat," *British Journal of Haematology*, vol. 31, no. 2, pp. 209–215, 1975.

[80] P. R. Dallman and R. A. Spirito, "Brain iron in the rat: extremely slow turnover in normal rats may explain long lasting effects of early iron deficiency," *Journal of Nutrition*, vol. 107, no. 6, pp. 1075–1081, 1977.

[81] D. Ben-Shachar, R. Ashkenazi, and M. B. H. Youdim, "Long-term consequence of early iron-deficiency on dopaminergic neurotransmission in rats," *International Journal of Developmental Neuroscience*, vol. 4, no. 1, pp. 81–88, 1986.

[82] S. Ayton, P. Lei, and A. I. Bush, "Metallostasis in Alzheimer's disease," *Free Radical Biolology and Medicine*, vol. 62, pp. 76–89, 2013.

[83] D. Hare, S. Ayton, A. Bush, and P. Lei, "A delicate balance: iron metabolism and diseases of the brain," *Frontiers in Aging Neuroscience*, vol. 5, 34, 2013.

[84] D. T. Dexter, A. Carayon, M. Vidailhet et al., "Decreased ferritin levels in brain in Parkinson's disease," *Journal of Neurochemistry*, vol. 55, no. 1, pp. 16–20, 1990.

[85] B. A. Faucheux, J.-J. Hauw, Y. Agid, and E. C. Hirsch, "The density of [125I]-transferrin binding sites on perikarya of melanized neurons of the substantia nigra is decreased in Parkinson's disease," *Brain Research*, vol. 749, no. 1, pp. 170–174, 1997.

[86] Y. He, T. Lee, and S. K. Leong, "Time course of dopaminergic cell death and changes in iron, ferritin and transferrin levels in the rat substantia nigra after 6-hydroxydopamine (6-OHDA) lesioning," *Free Radical Research*, vol. 31, no. 2, pp. 103–112, 1999.

[87] M. C. J. Dekker, P. C. Giesbergen, O. T. Njajou et al., "Mutations in the hemochromatosis gene (HFE), Parkinson's disease and parkinsonism," *Neuroscience Letters*, vol. 348, no. 2, pp. 117–119, 2003.

[88] R. J. Guerreiro, J. M. Bras, I. Santana et al., "Association of HFE common mutations with Parkinson's disease, Alzheimer's disease and mild cognitive impairment in a Portuguese cohort," *BMC Neurology*, vol. 6, article 24, 2006.

[89] N. Akbas, H. Hochstrasser, J. Deplazes et al., "Screening for mutations of the HFE gene in Parkinson's disease patients with hyperechogenicity of the substantia nigra," *Neuroscience Letters*, vol. 407, no. 1, pp. 16–19, 2006.

[90] G. Biasiotto, S. Goldwurm, D. Finazzi et al., "HFE gene mutations in a population of Italian Parkinson's disease patients," *Parkinsonism and Related Disorders*, vol. 14, no. 5, pp. 426–430, 2008.

[91] A. H. Aamodt, L. J. Stovner, K. Thorstensen, S. Lydersen, L. R. White, and J. O. Aasly, "Prevalence of haemochromatosis gene mutations in Parkinson's disease," *Journal of Neurology, Neurosurgery and Psychiatry*, vol. 78, no. 3, pp. 315–317, 2007.

[92] J. M. Bastin, M. Jones, C. A. O'Callaghan, L. Schimanski, D. Y. Mason, and A. R. M. Townsend, "Kupffer cell staining by an HFE-specific monoclonal antibody: implications for hereditary haemochromatosis," *British Journal of Haematology*, vol. 103, no. 4, pp. 931–941, 1998.

[93] P. G. Mastroberardino, E. K. Hoffman, M. P. Horowitz et al., "A novel transferrin/TfR2-mediated mitochondrial iron transport system is disrupted in Parkinson's disease," *Neurobiology of Disease*, vol. 34, no. 3, pp. 417–431, 2009.

[94] N. Song, H. Jiang, J. Wang, and J.-X. Xie, "Divalent metal transporter 1 up-regulation is involved in the 6-hydroxydopamine-induced ferrous iron influx," *Journal of Neuroscience Research*, vol. 85, no. 14, pp. 3118–3126, 2007.

[95] H. Jiang, Z.-M. Qian, and J.-X. Xie, "Increased DMT1 expression and iron content in MPTP-treated C57BL/6 mice," *Acta Physiologica Sinica*, vol. 55, no. 5, pp. 571–576, 2003.

[96] J. Salazar, N. Mena, S. Hunot et al., "Divalent metal transporter 1 (DMT1) contributes to neurodegeneration in animal models of Parkinson's disease," *Proceedings of the National Academy of Sciences of the United States of America*, vol. 105, no. 47, pp. 18578–18583, 2008.

[97] A. Donovan, C. A. Lima, J. L. Pinkus et al., "The iron exporter ferroportin/Slc40a1 is essential for iron homeostasis," *Cell Metabolism*, vol. 1, no. 3, pp. 191–200, 2005.

[98] N. E. Hellman and J. D. Gitlin, "Ceruloplasmin metabolism and function," *Annual Review of Nutrition*, vol. 22, pp. 439–458, 2002.

[99] M.-C. Boll, M. Alcaraz-Zubeldia, S. Montes, and C. Rios, "Free copper, ferroxidase and SOD1 activities, lipid peroxidation and NOx content in the CSF. A different marker profile in four neurodegenerative diseases," *Neurochemical Research*, vol. 33, no. 9, pp. 1717–1723, 2008.

[100] M.-C. Boll, J. Sotelo, E. Otero, M. Alcaraz-Zubeldia, and C. Rios, "Reduced ferroxidase activity in the cerebrospinal fluid from patients with Parkinson's disease," *Neuroscience Letters*, vol. 265, no. 3, pp. 155–158, 1999.

[101] S. Olivieri, A. Conti, S. Iannaccone et al., "Ceruloplasmin oxidation, a feature of parkinson's disease CSF, inhibits ferroxidase activity and promotes cellular iron retention," *Journal of Neuroscience*, vol. 31, no. 50, pp. 18568–18577, 2011.

[102] R. Martínez-Hernández, S. Montes, J. Higuera-Calleja et al., "Plasma ceruloplasmin ferroxidase activity correlates with the nigral sonographic area in Parkinson's disease patients: a pilot study," *Neurochemical Research*, vol. 36, no. 11, pp. 2111–2115, 2011.

[103] K. J. Bharucha, J. K. Friedman, A. S. Vincent, and E. D. Ross, "Lower serum ceruloplasmin levels correlate with younger age of onset in Parkinson's disease," *Journal of Neurology*, vol. 255, no. 12, pp. 1957–1962, 2008.

[104] G. Tórsdóttir, J. Kristinsson, S. Sveinbjörnsdóttir, J. Snaedal, and T. Jóhannesson, "Copper, ceruloplasmin, superoxide dismutase and iron parameters in Parkinson's disease," *Pharmacology and Toxicology*, vol. 85, no. 5, pp. 239–243, 1999.

[105] L. Jin, J. Wang, L. Zhao et al., "Decreased serum ceruloplasmin levels characteristically aggravate nigral iron deposition in Parkinson's disease," *Brain*, vol. 134, no. 1, pp. 50–58, 2011.

[106] L. Jin, J. Wang, H. Jin et al., "Nigral iron deposition occurs across motor phenotypes of Parkinson's disease," *European Journal of Neurology*, vol. 19, no. 7, pp. 969–976, 2012.

[107] G. Tórsdóttir, S. Sveinbjörnsdóttir, J. Kristinsson, J. Snaedal, and T. Jóhannesson, "Ceruloplasmin and superoxide dismutase (SOD1) in Parkinson's disease: a follow-up study," *Journal of the Neurological Sciences*, vol. 241, no. 1-2, pp. 53–58, 2006.

[108] D. A. Loeffler, P. A. LeWitt, P. L. Juneau et al., "Increased regional brain concentrations of ceruloplasmin in neurodegenerative disorders," *Brain Research*, vol. 738, no. 2, pp. 265–274, 1996.

[109] P. Lei, S. Ayton, D. I. Finkelstein, P. A. Adlard, C. L. Masters, and A. I. Bush, "Tau protein: relevance to Parkinson's disease," *International Journal of Biochemistry and Cell Biology*, vol. 42, no. 11, pp. 1775–1778, 2010.

[110] P. Lei, S. Ayton, D. I. Finkelstein et al., "Tau deficiency induces parkinsonism with dementia by impairing APP-mediated iron export," *Nature Medicine*, vol. 18, no. 2, pp. 291–295, 2012.

[111] J. A. Duce, A. Tsatsanis, M. A. Cater et al., "Iron-export ferroxidase activity of β-amyloid precursor protein is inhibited by zinc in Alzheimer's disease," *Cell*, vol. 142, no. 6, pp. 857–867, 2010.

[112] D. S. Kalinowski and D. R. Richardson, "The evolution of iron chelators for the treatment of iron overload disease and cancer," *Pharmacological Reviews*, vol. 57, no. 4, pp. 547–583, 2005.

[113] D. Devos, C. Moreau, J. C. Devedjian et al., "Targeting chelatable iron as a therapeutic modality in Parkinson's disease," *Antioxidants and Redox Signaling*.

[114] M. D. Habgood, Z. D. Liu, L. S. Dehkordi, H. H. Khodr, J. Abbott, and R. C. Hider, "Investigation into the correlation between the structure of hydroxypyridinones and blood-brain barrier permeability," *Biochemical Pharmacology*, vol. 57, no. 11, pp. 1305–1310, 1999.

[115] S. Gal, H. Zheng, M. Fridkin, and M. B. H. Youdim, "Restoration of nigrostriatal dopamine neurons in post-MPTP treatment by the novel multifunctional brain-permeable iron chelator-monoamine oxidase inhibitor drug, M30," *Neurotoxicity Research*, vol. 17, no. 1, pp. 15–27, 2010.

[116] D. T. Dexter, F. R. Wells, F. Agid et al., "Increased nigral iron content in postmortem Parkinsonian brain," *The Lancet*, vol. 2, no. 8569, pp. 1219–1220, 1987.

[117] E. Sofic, P. Riederer, H. Heinsen et al., "Increased iron (III) and total iron content in post mortem substantia nigra of parkinsonian brain," *Journal of Neural Transmission*, vol. 74, no. 3, pp. 199–205, 1988.

[118] P. Riederer, E. Sofic, W.-D. Rausch et al., "Transition metals, ferritin, glutathione, and ascorbic acid in parkinsonian brains," *Journal of Neurochemistry*, vol. 52, no. 2, pp. 515–520, 1989.

[119] R. J. Uitti, A. H. Rajput, B. Rozdilsky, M. Bickis, T. Wollin, and W. K. Yuen, "Regional metal concentrations in Parkinson's disease, other chronic neurological diseases, and control brains," *Canadian Journal of Neurological Sciences*, vol. 16, no. 3, pp. 310–314, 1989.

[120] D. T. Dexter, F. R. Wells, A. J. Lees et al., "Increased nigral iron content and alterations in other metal ions occurring in brain in Parkinson's disease," *Journal of Neurochemistry*, vol. 52, no. 6, pp. 1830–1836, 1989.

[121] D. T. Dexter, A. Carayon, F. Javoy-Agid et al., "Alterations in the levels of iron, ferritin and other trace metals in Parkinson's disease and other neurodegenerative diseases affecting the basal ganglia," *Brain*, vol. 114, no. 4, pp. 1953–1975, 1991.

[122] E. C. Hirsch, J.-P. Brandel, P. Galle, F. Javoy-Agid, and Y. Agid, "Iron and aluminum increase in the substantia nigra of patients with Parkinson's disease: an X-ray microanalysis," *Journal of Neurochemistry*, vol. 56, no. 2, pp. 446–451, 1991.

[123] E. Sofic, W. Paulus, K. Jellinger, P. Riederer, and M. B. H. Youdim, "Selective increase of iron in substantia nigra zona compacta of Parkinsonian brains," *Journal of Neurochemistry*, vol. 56, no. 3, pp. 978–982, 1991.

[124] P. F. Good, C. W. Olanow, and D. P. Perl, "Neuromelanin-containing neurons of the substantia nigra accumulate iron and aluminum in Parkinson's disease: a LAMMA study," *Brain Research*, vol. 593, no. 2, pp. 343–346, 1992.

[125] V. M. Mann, J. M. Cooper, S. E. Daniel et al., "Complex I, iron, and ferritin in Parkinson's disease substantia nigra," *Annals of Neurology*, vol. 36, no. 6, pp. 876–881, 1994.

[126] D. A. Loeffler, J. R. Connor, P. L. Juneau et al., "Transferrin and iron in normal, Alzheimer's disease, and Parkinson's disease brain regions," *Journal of Neurochemistry*, vol. 65, no. 2, pp. 710–716, 1995.

[127] P. D. Griffiths, B. R. Dobson, G. R. Jones, and D. T. Clarke, "Iron in the basal ganglia in Parkinson's disease. An in vitro study using extended X-ray absorption fine structure and cryo-electron microscopy," *Brain*, vol. 122, no. 4, pp. 667–673, 1999.

[128] A. E. Oakley, J. F. Collingwood, J. Dobson et al., "Individual dopaminergic neurons show raised iron levels in Parkinson disease," *Neurology*, vol. 68, no. 21, pp. 1820–1825, 2007.

[129] B. F. G. Popescu, M. J. George, U. Bergmann et al., "Mapping metals in Parkinson's and normal brain using rapid-scanning x-ray fluorescence," *Physics in Medicine and Biology*, vol. 54, no. 3, pp. 651–663, 2009.

[130] K. J. Schweitzer, T. Brüssel, P. Leitner et al., "Transcranial ultrasound in different monogenetic subtypes of Parkinson's disease," *Journal of Neurology*, vol. 254, no. 5, pp. 613–616, 2007.

[131] J. M. Hagenah, I. R. König, B. Becker et al., "Substantia nigra hyperechogenicity correlates with clinical status and number of Parkin mutated alleles," *Journal of Neurology*, vol. 254, no. 10, pp. 1407–1413, 2007.

[132] J. M. Hagenah, B. Becker, N. Brüggemann et al., "Transcranial sonography findings in a large family with homozygous and heterozygous PINK1 mutations," *Journal of Neurology, Neurosurgery and Psychiatry*, vol. 79, no. 9, pp. 1071–1074, 2008.

[133] N. Brüggemann, J. Hagenah, K. Stanley et al., "Substantia nigra hyperechogenicity with LRRK2 G2019S mutations," *Movement Disorders*, vol. 26, no. 5, pp. 885–888, 2011.

[134] J. M. Shulman, P. L. De Jager, and M. B. Feany, "Parkinson's disease: genetics and pathogenesis," *Annual Review of Pathology*, vol. 6, pp. 193–222, 2011.

Hindawi Publishing Corporation
BioMed Research International
Volume 2014, Article ID 706302, 6 pages
http://dx.doi.org/10.1155/2014/706302

Review Article

Some *In Vitro/In Vivo* Chemically-Induced Experimental Models of Liver Oxidative Stress in Rats

Rumyana Simeonova, Magdalena Kondeva-Burdina, Vessela Vitcheva, and Mitka Mitcheva

Laboratory of Drug Metabolism and Drug Toxicity, Department of Pharmacology, Pharmacotherapy and Toxicology, Faculty of Pharmacy, Medical University 2 Dunav Street, 1000 Sofia, Bulgaria

Correspondence should be addressed to Rumyana Simeonova; rsimeonova@yahoo.com

Received 27 April 2013; Accepted 24 October 2013; Published 16 January 2014

Academic Editor: Afaf K. El-Ansary

Oxidative stress is critically involved in a variety of diseases. Reactive oxygen species (ROS) are highly toxic molecules that are generated during the body's metabolic reactions and can react with and damage some cellular molecules such as lipids, proteins, or DNA. Liver is an important target of the oxidative stress because of its exposure to various prooxidant toxic compounds as well as of its metabolic function and ability to transform some xenobiotics to reactive toxic metabolites (as ROS). To investigate the processes of liver injuries and especially liver oxidative damages there are many experimental models, some of which we discuss further.

1. Introduction

Oxidative stress is an imbalance between the production and scavenging of reactive oxygen and nitrogen species (ROS and RNS) and free radicals that can induce lipid peroxidation, DNA fragmentation, and protein oxidation [1]. These damages result in the loss of membrane integrity, structural and functional changes in proteins, and gene mutations [2]. Normally, the affected cells are trying to neutralise reactive molecules by deploying their antioxidative defense that include reduced glutathione (GSH), alpha-tocopherol, ascorbic acid, antioxidant enzymes catalase (CAT), superoxide dismutase (SOD), glutathione peroxidase (GPx), glutathione reductase (GR), and glutathione-S-transferase (GST).

Oxidative stress is critically involved in a variety of diseases. ROS are highly dangerous molecules that are generated during the body's metabolic reactions and can react with and damage some cellular molecules such as lipids, proteins, or DNA.

Liver plays a pivotal role in the regulation of various physiological processes in the body such as carbohydrate metabolism and storage, fat metabolism, bile acid synthesis, and so forth besides being the most important organ involved in the detoxification of various drugs as well as xenobiotics in our body [3].

It is highly susceptible to damage by xenobiotics owing to its continuous exposure to these toxicants via the portal blood circulation [4]. Various chemicals, like carbon tetrachloride (CCl_4), tert-butyl hydroperoxide (t-BHP), alcohol, paracetamol, galactosamine (GalN), and others, can cause potential damage to the liver cells leading to progressive dysfunction. Most of the hepatotoxic chemicals cause damage to the hepatocytes by inducing lipid peroxidation [5, 6]. Thus, the disorders associated with liver are numerous and varied.

One of the most important liver toxicity mechanisms might be a consequence of cell damage by ROS and RNS. Kupffer cells release reactive oxygen species (ROS), cytokines, and chemokines, which induce neutrophil extravasation and activation. Also the liver expresses many cytochrome P450 isoforms, including ethanol-induced CYP2E1. CYP2E1 generates ROS, activates many toxicologically important substrates, and may be the central pathway by which some substances cause oxidative stress (ethanol, carbon tetrachloride, etc.) [7].

In this review we summarize some commonly used toxic models employed in the study of hepatotoxicity and hepatoprotection. A number of models of hepatic disorders support the notion that ROS have a causal role in liver injuries. Experimental liver injuries are induced by specific

toxic compounds, because the formation of ROS is stimulated by a number of xenobiotics.

2. Carbon Tetrachloride (CCl_4)

Carbon tetrachloride (CCl_4) is the most widely used model to develop oxidative stress and liver toxicity in rats. Hepatic injury through carbon tetrachloride induced lipid peroxidation is well known and has been extensively used in the experimental models to understand the cellular mechanisms behind oxidative damage and further to evaluate the therapeutic potential of drugs and dietary antioxidants [8].

CCl_4 is activated by cytochrome CYP2E1, CYP2B1, or CYP2B2, and possibly CYP3A, to form the trichloromethyl radical, $CCl3^*$ [9]. This radical can bind to cellular molecules (nucleic acid, protein, lipid), impairing crucial cellular processes such as lipid metabolism, with the potential outcome of fatty degeneration (steatosis) [10]. This radical can also react with oxygen to form the trichloromethylperoxy radical CCl_3OO^*, a highly reactive species. CCl_3OO^* initiates the chain reaction of lipid peroxidation, which attacks and destroys polyunsaturated fatty acids [9]. Among the degradation products of fatty acids are reactive aldehydes, malondialdehyde (MDA), and 4-hydroxynonenal, which bind easily to functional groups of proteins and inhibit important enzyme activities. Disturbed cellular processes are most likely due to increased levels of these thiobarbituric acid reactive species (TBARS) [11], lactate dehydrogenase (LDH) leakage as a result of membrane breakdown and concomitant increase in membrane permeability [12], loss of cell protection, witnessed by GSH depletion and as a result of all these changes—cell death.

In our laboratory we use some *in vitro* and *in vivo* hepatotoxicity models based on CCl_4-induced liver damage in Wistar rats and in spontaneously hypertensive rats (SHR). *In vitro* experiments are carried out in primary isolated rat hepatocytes [13] or liver microsomes [14]. Cell incubation with CCl_4 (86 μmol L^{-1}) leads to a significant decrease in cell viability, increased LDH leakage, decreased levels of cellular GSH, and elevation in MDA quantity. Enzyme-induced LPO is started with 20 mM CCl_4 in the presence of 1 mM NADPH [14]. For *in vivo* experiments Wistar rats are challenged with a single dose (2 mL/kg) of 20% of CCl_4 in olive oil [15]. These *in vitro/in vivo* CCl_4-induced liver injury models are useful for investigations on hepatoprotective and antioxidant properties of some plant-derived biologically active compounds [13–17].

We found that ROS, produced by CCl_4, decrease the activities not only of antioxidant enzymes such as catalase (CAT), superoxide dismutase (SOD), glutathione peroxidase (GPx), glutathione reductase (GR), and glutathione-S-transferase (GST) [18], but also the activities of some drug metabolizing enzymes such as CYP2E1 and CYP3A, involved in their production [15].

3. Tert-Butyl Hydroperoxide (t-BHP)

The cellular system of energy supply localized in mitochondria is another target of many hepatotoxic substances causing oxidative stress and is one of the most important mechanisms through which hepatotoxic factors induced apoptotic and necrotic processes [19].

Tert-butyl hydroperoxide caused necrosis through inducing mitochondrial reactive oxygen formation [20]. As a prooxidant, t-BHP was widely used and many effects on cell metabolism have been described, for example, changes in calcium homeostasis [21], increase of lipid peroxidation, or decrease of mitochondrial membrane potential [22, 23]. Two mechanisms for t-BHP action were proposed: depletion of cellular stores of GSH and oxidation of functionally important SH groups on mitochondrial enzymes [24] and/or changes of mitochondrial membrane integrity induced by peroxidation of membrane lipids [22, 23]. The metabolism of t-BHP to free radicals undergoes through several steps. In microsomal suspension, in the absence of NADPH, it has been shown to undergo one-electron oxidation to a peroxyl radical (1), whereas in the presence of NADPH it has been shown to undergo one-electron reduction to an alkoxyl radical (2). In isolated mitochondria and intact cells, the t-BHP has been shown to undergo β-scission to the methyl radical (3). All these radicals cause lipid peroxidation process [25, 26]:

$$(CH_3)_3COOH \longrightarrow (CH_3)_3COO^{\bullet} + e^{-} + H^{+} \quad (1)$$

$$(CH_3)_3COOH + e^{-} \longrightarrow (CH_3)_3CO^{\bullet} + OH^{-} \quad (2)$$

$$(CH_3)_3CO^{\bullet} \longrightarrow (CH_3)_2CO + {}^{\bullet}CH_3 \quad (3)$$

Experiments on isolated hepatocytes are thus a useful model system for evaluation of the toxic effect of various prooxidants which act directly on mitochondrial enzymes. In our experiments using freshly isolated rat hepatocytes we found that t-BHP (75 μmol L^{-1}) decreases cell viability [27, 28]. It causes leakage of lactate dehydrogenase (LDH) and formation of malondialdehyde in hepatocytes. Furthermore, t-BHP causes the depletion of cellular GSH levels. These data correlate with the results obtained by many authors [23–25].

Enhanced formation of ROS has been suggested to play a role in some liver disease processes, including alcohol-induced liver injury [29–31], paracetamol-induced liver failure [32, 33], and many others. Many other drugs as isoniazide, amiodarone, and valproic acid as well as widely used and abused substances as nicotine and cocaine damage liver cells by producing toxic ROS. Because of their widespread consumption, they are also used as experimental models of liver injuries.

4. Ethanol

Acute and chronic ethanol treatments increase the production of ROS, lower cellular antioxidant levels, and enhance oxidative stress in many tissues, especially the liver. Ethanol-induced oxidative stress plays a major role in the mechanisms by which ethanol produces liver injury [34].

The liver expresses many cytochrome P450 isoforms, including ethanol-induced CYP2E1. CYP2E1 generates ROS, activates many toxicologically important substrates, and may

be the central pathway by which ethanol causes oxidative stress [7].

CYP2E1 metabolizes and activates many toxicologically important substrates, including ethanol, carbon tetrachloride, acetaminophen, and N-nitrosodimethylamine, to more toxic products [35, 36]. Induction of CYP2E1 by ethanol is a central pathway by which ethanol generates oxidative stress. In our intragastric model of ethanol feeding (3 g/kg, 14 days) of spontaneously hypertensive rats (SHR) a prominent induction of CYP2E1 occurs along with significant alcohol liver injury [37]. Lipid peroxidation also occurs, and ethanol-induced liver pathology correlates with CYP2E1 levels and elevated lipid peroxidation [38]. Chronic ethanol consumption is associated with reduced liver GSH and alpha-tocopherol level and with reduced superoxide dismutase (SOD), catalase (CAT) and glutathione peroxidase (GPx) activity [39]. Our results, concerning normotensive rats (Wistar-Kyoto), are in accordance with these data, whereas alcohol intake in SHR increases significantly SOD and CAT activities by approximately 50% [37]. We suggested that the differences in antioxidant status and the effect of ethanol between the strains might be due to the oxidative stress state in the hypertensive pathological model. Additionally we found that multiple ethanol treatment resulted in less pronounced effect on the assessed parameters (MDA, GSH, nNOS) in the female SHR, compared to male SHR [38]. These results might be due to a protective effect of estrogens on the oxidative stress and to a stimulation of the antioxidant defense systems, in liver.

5. Paracetamol

Paracetamol (PCM) is primarily metabolized by sulfation and glucuronidation, but with an increasing dose rate; these pathways become saturated and a greater proportion of the drug is available for oxidation by the microsomal cytochrome P-450 system [40]. N-Acetyl-P-benzoquinone Imine (NAPQI) is the product of this pathway which is thought to be responsible for the subsequent hepatic damage [41]. N-acetyl-P-benzoquinone imine (NAPQI) is a highly reactive electrophile and is detoxified in liver by either reduction to the parent compound, acetaminophen, or conjugation at the metaposition with glutathione, in which both reactions consume GSH [42].

Glutathione (GSH) plays an important role in protecting cells from electrophilic compounds and free radicals such as reactive oxygen species generated during cellular metabolism. Reduced glutathione can act as a reductant, reducing hydrogen peroxide and lipid hydroperoxides directly to H_2O, a reaction catalyzed by GSH-Px [43]. Depletion of intracellular GSH, under conditions of continuous intracellular oxidative stress, leads to oxidation and damage of lipids, proteins, and DNA by the reactive oxygen species [44, 45].

The importance of glutathione in PCM toxicity is further emphasized by the large body of evidence which indicates that interventions which increase GSH content can dramatically reduce PCM and NAPQI-induced hepatic injury [46, 47]. Our previous studies have shown that GSH content in animal livers decreases after PCM overdose (2 g/kg, i.p. single dose) [15] and have proved that biologically active compounds derived from plants are useful for treatment of PCM-induced liver disorders, because of a stimulation of GSH synthesis.

Oxidative stress is also considered to be involved in the induction of hepatotoxicity by PCM. Oxidation of PCM by CYPs may generate ROS. Hydrogen peroxide and superoxide are produced during metabolic activation of PCM in the mixed function oxidase system [47].

6. Nicotine

During smoking, nicotine is rapidly absorbed into the circulatory system where more than 80% is metabolized in the liver [48]. Liver is an important organ and is responsible for biotransformation of drugs and other toxins to remove them from the body. Nicotine from heavy smoking increases the risk of developing some dangerous liver disorders by one of the main mechanisms being the oxidative stress. Increased production of free radicals or decreased function of the defense system play an important role in nicotine toxicity [49]. Also maternal nicotine exposure induces oxidative stress and causes histopathological changes in the lung and liver of lactating offspring [50]. Nicotine induces oxidative stress both *in vivo* and *in vitro* that causes a peroxidant/antioxidant imbalance in blood cells, blood plasma, and other tissues [51]. Some authors [50, 52] reported that nicotine induces oxidative stress and depleted antioxidant defense mechanisms through reduction of glutathione peroxidase in liver, lung, and kidney. Oxidative stress generates free radicals that attack the membrane lipids resulting in the formation of malondialdehyde (MDA), which causes peroxidative tissue damage [53]. Animal's studies have shown significantly higher liver and serum levels of MDA, conjugated dienes, hydroperoxides, and free fatty acids in rats intoxicated by nicotine [54, 55].

Nicotine is not recognized as a common experimental model for liver injuries, but because of its well-established prooxidant mechanisms of hepatotoxicity, and widespread consumption is used from many authors [51, 53, 55, 56] for investigations of antioxidant and protective properties of natural compounds.

In our previous experiments [57, 58] enhanced level of tissue lipid peroxides in nicotine treated rats (1 mg/kg i.p; 6,5 mg/kg p.o.) has been shown to be accompanied by a significant decrease in the levels of GSH, glutathione peroxidase (GPx), superoxide dismutase (SOD), and catalase (CAT) and increased glutathione reductase (GR) activity in Wistar rat liver.

7. D-Galactosamine (GAL)

D-Galactosamine is a well-known experimental hepatotoxin usually used to produce acute toxicity in rat liver. Galactosamine metabolism depletes the uridine pool of hepatocytes, thus inducing transcriptional arrest and causing an increase in sensitization to cytokines such as TNF-α and an

increase in oxidative stress and GSH depletion, which lead to mitochondrial dysfunction and cell death [59]. Both oxidative and nitrosative stress play a key role in the pathogenesis of GAL-induced hepatic injury [60].

Usually rats are injected (i.p.) with GAL (400 mg/kg b.w.) as a single dose [61].

8. Cocaine

Cocaine is a psychoactive drug that has been recognized as one of the most significant examples of drug abuse. Its misuse can induce severe toxic effects, including neurotoxicity, cardiotoxicity, and hepatotoxicity. One of the main mechanisms discussed for cocaine-induced liver injury is promotion of lipid peroxidation by ROS which are produced during cocaine bioactivation to norcocaine through N-demethylation by cytochrome P 450 and flavin adenine dinucleotide containing monooxygenases [62].

A large body of evidence in both human and experimental models suggests that impairment of the antioxidant defense system by cocaine and its metabolites plays a role in the pathogenesis of cocaine hepatotoxicity [62–64]. In particular, glutathione seems to play an important protective role against cocaine-induced hepatic injury. For example, the acute administration of cocaine to rats [65] and multiple treatments of mice [63] have been shown to deplete the cellular reduced glutathione, to decrease the activity of superoxide dismutase (SOD), catalase (CAT), and glutathione peroxidase (GPx) and to increase glutathione reductase (GR) activity. The GSH depletion, induced by cocaine administration, observed in these and other studies [62, 66] might be explained by increased utilization of GSH for detoxification of ROS and lipid peroxidation products. The critical role of ROS and oxidative stress in the pathogenesis of cocaine-induced liver damage was demonstrated by the observed ameliorating effects of bioactive compounds with an antioxidant activity, administered several days before cocaine treatment [65, 67]. The bioactive compounds were found to decrease cocaine toxicity both by increasing GSH levels and antioxidant enzyme activities.

Conflict of Interests

The authors declare that there is no conflict of interests regarding the publication of this paper.

References

[1] C. Nencini, G. Giorgi, and L. Micheli, "Protective effect of silymarin on oxidative stress in rat brain," *Phytomedicine*, vol. 14, no. 2-3, pp. 129–135, 2007.

[2] B. V. Reddy, J. S. Sundari, E. Balamurugan, and V. P. Menon, "Prevention of nicotine and streptozotocin treatment induced circulatory oxidative stress by bis-1,7-(2-hydroxyphenyl)-hepta-1,6-diene-3,5-dione in diabetic rats," *Molecular and Cellular Biochemistry*, vol. 331, no. 1-2, pp. 127–133, 2009.

[3] S. K. Sharma, S. M. Arogya, D. H. Bhaskarmurthy, A. Agarwal, and C. C. Velusami, "Hepatoprotective activity of the *Phyllanthus* species on tert-butyl hydroperoxide (t-BH)-induced cytotoxicity in HepG2 cells," *Pharmacognosy Magazine*, vol. 7, no. 27, pp. 229–233, 2011.

[4] V. M. Piñeiro-Carrero and E. O. Piñeiro, "Liver," *Pediatrics*, vol. 113, no. 4, pp. 1097–1106, 2004.

[5] A. Subramoniam and P. Pushpangadan, "Development of phytomedicines for liver diseases," *Indian Journal of Pharmacology*, vol. 31, no. 3, pp. 166–175, 1999.

[6] M. Joyeux, A. Rolland, J. Fleurentin, F. Mortier, and P. Dorfman, "Tert-butyl hydroperoxide-induced injury in isolated rat hepatocytes: a model for studying anti-hepatotoxic crude drugs," *Planta Medica*, vol. 56, no. 2, pp. 171–174, 1990.

[7] H. Jaeschke, G. J. Gores, A. I. Cederbaum, J. A. Hinson, D. Pessayre, and J. J. Lemasters, "Mechanisms of hepatotoxicity," *Toxicological Sciences*, vol. 65, no. 2, pp. 166–176, 2002.

[8] S. Basu, "Carbon tetrachloride-induced lipid peroxidation: eicosanoid formation and their regulation by antioxidant nutrients," *Toxicology*, vol. 189, no. 1-2, pp. 113–127, 2003.

[9] L. W. D. Weber, M. Boll, and A. Stampfl, "Hepatotoxicity and mechanism of action of haloalkanes: carbon tetrachloride as a toxicological model," *Critical Reviews in Toxicology*, vol. 33, no. 2, pp. 105–136, 2003.

[10] Y. Masuda, "Learning toxicology from carbon tetrachloride-induced hepatotoxicity," *Yakugaku Zasshi*, vol. 126, no. 10, pp. 885–889, 2006.

[11] M. Bhadauria, S. K. Nirala, and S. Shukla, "Propolis protects CYP 2E1 enzymatic activity and oxidative stress induced by carbon tetrachloride," *Molecular and Cellular Biochemistry*, vol. 302, no. 1-2, pp. 215–224, 2007.

[12] S. Sahreen, M. R. Khan, and R. A. Khan, "Hepatoprotective effects of methanol extract of *Carissa opaca* leaves on CCl_4-induced damage in rat," *BMC Complementary and Alternative Medicine*, vol. 11, article 48, 2011.

[13] M. Kondeva, M. Mitcheva, and S. Nikolov, "Effect of the Diosgenin in fresh isolated rat hepatocytes treated with carbon tetrachloride," *European Journal of Drug Metabolism and Pharmacokinetics*, vol. 28, no. 1, pp. 1–3, 2003.

[14] R. L. Simeonova, V. B. Vitcheva, M. S. Kondeva-Burdina, I. N. Krasteva, S. D. Nikolov, and M. K. Mitcheva, "Effect of purified saponin mixture from *Astragalus corniculatus* on enzyme- and non-enzyme-induced lipid peroxidation in liver microsomes from spontaneously hypertensive rats and normotensive rats," *Phytomedicine*, vol. 17, no. 5, pp. 346–349, 2010.

[15] V. Vitcheva, R. Simeonova, I. Krasteva, S. Nikolov, and M. Mitcheva, "Protective effects of a purified saponin mixture from*Astragalus corniculatus Bieb., in vivo*hepatotoxicity models," *Phytotherapy Research*, vol. 27, no. 5, pp. 731–736, 2013.

[16] S. A. Ali, M. Z. Rizk, N. A. Ibrahim, M. S. Abdallah, H. M. Sharara, and M. M. Moustafa, "Protective role of *Juniperus phoenicea* and *Cupressus sempervirens* against CCl_4," *World Journal Gastrointestinal Pharmacology and Therapeutics*, vol. 1, no. 6, pp. 123–131, 2010.

[17] F. Sun, E. Hamagawa, C. Tsutsui, Y. Ono, Y. Ogiri, and S. Kojo, "Evaluation of oxidative stress during apoptosis and necrosis caused by carbon tetrachloride in rat liver," *Biochimica et Biophysica Acta*, vol. 1535, no. 2, pp. 186–191, 2001.

[18] R. Simeonova, I. Krasteva, M. Kondeva-Burdina, and N. Benbassat, "Effects of extract from *Astragalus Glycyphylloides* on Carbon tetrachloride-induced hepatotoxicity in Wistar rats," *International Journal of Pharma and Bio Sciences*, vol. 4, no. 3, pp. 179–186, 2013.

[19] G. Kroemer, B. Dallaporta, and M. Resche-Rigon, "The mitochondrial death/life regulator in apoptosis and necrosis," *Annual Review of Physiology*, vol. 60, pp. 619–642, 1998.

[20] Z. Drahota, P. Křiváková, Z. Červinková et al., "Tert-butyl hydroperoxide selectively inhibits mitochondrial respiratory-chain enzymes in isolated rat hepatocytes," *Physiology Research*, vol. 54, pp. 67–72, 2005.

[21] P. Nicotera, D. McConkey, S.-A. Svensson, G. Bellomo, and S. Orrenius, "Correlation between cytosolic Ca^{2+} concentration and cytotoxicity in hepatocytes exposed to oxidative stress," *Toxicology*, vol. 52, no. 1-2, pp. 55–63, 1988.

[22] R. Rubin and J. L. Farber, "Mechanisms of the killing of cultured hepatocytes by hydrogen peroxide," *Archives of Biochemistry and Biophysics*, vol. 228, no. 2, pp. 450–459, 1984.

[23] E. Kmoníčková, Z. Drahota, L. Kameníková, Z. Červinková, K. Mašek, and H. Farghali, "Modulatory effect of cyclosporin A on tert-butyl hydroperoxide-induced oxidative damage in hepatocytes," *Immunopharmacology Immunotoxicology*, vol. 23, pp. 43–54, 2001.

[24] N. Masaki, M. E. Kyle, A. Serroni, and J. L. Farber, "Mitochondrial damage as a mechanism of cell injury in the killing of cultured hepatocytes by tert-butyl hydroperoxide," *Archives of Biochemistry and Biophysics*, vol. 270, no. 2, pp. 672–680, 1989.

[25] K. Ollinger and U. T. Brunk, "Cellular injury induced by oxidative stress is mediated through lysosomal damage," *Free Radical Biology and Medicine*, vol. 19, no. 5, pp. 565–574, 1995.

[26] V. O'Donnell and M. J. Burkitt, "Mitochondrial metabolism of a hydroperoxide to free radicals in human endothelial cells: an electron spin resonance spin-trapping investigation," *Biochemical Journal*, vol. 304, no. 3, pp. 707–713, 1994.

[27] M. Mitcheva, M. Kondeva-Burdina, V. Vitcheva, I. Krasteva, and S. Nikolov, "Effect of purified saponin mixture from *Astragalus corniculatus* on toxicity models in isolated rat hepatocytes," *Pharmaceutical Biology*, vol. 46, no. 12, pp. 866–870, 2008.

[28] M. Mitcheva, M. Kondeva-Burdina, I. Krasteva, and S. Nikolov, "Protective effect of purified saponin mixture from *Astragalus corniculatus* on toxicity models *in vitro*," in *Medical Management of Chemical and Biological Casualties*, S. Tonev, K. Kanev, and C. Dishovsky, Eds., pp. 239–251, Publishing house IRITA, Sofia, Bulgaria, 2009.

[29] M. Adachi and H. Ishii, "Role of mitochondria in alcoholic liver injury," *Free Radical Biology and Medicine*, vol. 32, no. 6, pp. 487–491, 2002.

[30] G. E. Arteel, "Oxidants and antioxidants in alcohol-induced liver disease," *Gastroenterology*, vol. 124, no. 3, pp. 778–790, 2003.

[31] A. Dey and A. I. Cederbaum, "Alcohol and oxidative liver injury," *Hepatology*, vol. 43, no. 2, pp. S63–S74, 2006.

[32] H. Jaeschke and M. L. Bajt, "Intracellular signaling mechanisms of acetaminophen-induced liver cell death," *Toxicological Sciences*, vol. 89, no. 1, pp. 31–41, 2006.

[33] H. Jaeschke, T. R. Knight, and M. L. Bajt, "The role of oxidant stress and reactive nitrogen species in acetaminophen hepatotoxicity," *Toxicology Letters*, vol. 144, no. 3, pp. 279–288, 2003.

[34] A. I. Cederbaum, Y. Lu, and D. Wu, "Role of oxidative stress in alcohol-induced liver injury," *Archives of Toxicology*, vol. 83, no. 6, pp. 519–548, 2009.

[35] F. P. Guengerich, D.-H. Kim, and M. Iwasaki, "Role of human cytochrome P-450 IIE1 in the oxidation of many low molecular weight cancer suspects," *Chemical Research in Toxicology*, vol. 4, no. 2, pp. 168–179, 1991.

[36] D. R. Koop, "Oxidative and reductive metabolism by cytochrome P450 2E1," *The FASEB Journal*, vol. 6, no. 2, pp. 724–730, 1992.

[37] R. Simeonova, V. Vitcheva, and M. Mitcheva, "Effect of multiple treatments with alcohol on some liver antioxidant biochemical parameters in spontaneously hypertensive rats (SHRs) versus normotensive rats (NTRs)," *Toxicology Letters*, vol. 189, 2009.

[38] R. Simeonova, V. Vitcheva, and M. Mitcheva, "Effect of ethanol on some hepatic and brain parameters in male and female spontaneously hypertensive rats (SHRs)," *Toxicology Letters*, vol. 196, 2010.

[39] T. Radosavljević, D. Mladenović, and D. Vucević, "The role of oxidative stress in alcoholic liver injury," *Medicinski Pregled*, vol. 62, no. 11-12, pp. 547–553, 2009.

[40] P. J. Amar and E. R. Schiff, "Acetaminophen safety and hepatotoxicity: where do we go from here?" *Expert Opinion on Drug Safety*, vol. 6, no. 4, pp. 341–355, 2007.

[41] L. M. Aleksunes, S. N. Campion, M. J. Goedken, and J. E. Manautou, "Acquired resistance to acetaminophen hepatotoxicity is associated with induction of multidrug resistance-associated protein 4 (Mrp4) in proliferating hepatocytes," *Toxicological Sciences*, vol. 104, no. 2, pp. 261–273, 2008.

[42] S. U. Ruepp, R. P. Tonge, J. Shaw, N. Wallis, and F. Pognan, "Genomics and proteomics analysis of acetaminophen toxicity in mouse liver," *Toxicological Sciences*, vol. 65, no. 1, pp. 135–150, 2002.

[43] M. Anoush, M. A. Eghbal, F. Fathiazad, H. Hamzeiy, and N. S. Kouzehkonani, "The protective effects of garlic extract against acetaminophen-induced oxidative stress and Glutathione depletion," *Pakistan Journal of Biological Sciences*, vol. 12, no. 10, pp. 765–771, 2009.

[44] N. Kaplowitz, "Mechanisms of liver cell injury," *Journal of Hepatology*, vol. 32, no. 1, pp. 39–47, 2000.

[45] J. Nordberg and E. S. J. Arnér, "Reactive oxygen species, antioxidants, and the mammalian thioredoxin system," *Free Radical Biology and Medicine*, vol. 31, no. 11, pp. 1287–1312, 2001.

[46] J. R. Mitchell, D. J. Jollow, and W. Z. Potter, "Acetaminophen induced hepatic necrosis. IV. Protective role of glutathione," *Journal of Pharmacology and Experimental Therapeutics*, vol. 187, no. 1, pp. 211–217, 1973.

[47] T. Amimoto, T. Matsura, S.-Y. Koyama, T. Nakanishi, K. Yamada, and G. Kajiyama, "Acetaminophen-induced hepatic injury in mice: the role of lipid peroxidation and effects of pretreatment with coenzyme Q10 and α- tocopherol," *Free Radical Biology and Medicine*, vol. 19, no. 2, pp. 169–176, 1995.

[48] A.-R. El-Zayadi, "Heavy smoking and liver," *World Journal of Gastroenterology*, vol. 12, no. 38, pp. 6098–6101, 2006.

[49] K. Chattopadhyay and B. D. Chattopadyay, "Effect of Nicotine on lipid profile, peroxidation & antioxidant enzymes in female rats with restricted dietary protein," *Indian Journal of Medical Research*, vol. 127, no. 6, pp. 571–576, 2008.

[50] B. H. Ozukutat, K. U. Ozkan, C. F. Ibrahim, E. Guldur, M. S. Kilinc, and F. Inan, "Effects of maternal nicotine exposure during on breast-fed rat pups," *Biology in Neonats*, vol. 88, no. 2, pp. 113–117, 2005.

[51] H. Suleyman, K. Gumustekin, S. Taysi et al., "Beneficial effects of *Hippophae rhamnoides* L. on nicotine induced oxidative stress in rat blood compared with vitamin E," *Biological and Pharmaceutical Bulletin*, vol. 25, no. 9, pp. 1133–1136, 2002.

[52] G. H. El-Sokkary, S. Cuzzocrea, and R. J. Reiter, "Effect of chronic nicotine administration on the rat lung and liver: beneficial role of melatonin," *Toxicology*, vol. 239, no. 1-2, pp. 60–67, 2007.

[53] K. N. Srinivasan and K. V. Pugalendi, "Effect of excessive intake of thermally oxidized sesame oil on lipids, lipid peroxidation and antioxidants' status in rats," *Indian Journal of Experimental Biology*, vol. 38, no. 8, pp. 777–780, 2000.

[54] L. Ashakumary and P. L. Vijayammal, "Additive effect of alcohol and nicotine on lipid peroxidation and antioxidant defence mechanism in rats," *Journal of Applied Toxicology*, vol. 16, pp. 305–308, 1996.

[55] J. Zhang, S. Jiang, and R. R. Watson, "Antioxidant supplementation prevents oxidation and inflammatory responses induced by sidestream cigarette smoke in old mice," *Environmental Health Perspectives*, vol. 109, no. 10, pp. 1007–1009, 2001.

[56] A. M. Gawish, A. M. Issa, N. S. Bassily, and S. M. Manaa, "Role of green tea on nicotine toxicity on liver and lung of mice: histological and morphometrical studies," *African Journal of Biotechnology*, vol. 11, no. 8, pp. 2013–2025, 2012.

[57] R. Simeonova, V. Vitcheva, G. Gorneva, and M. Mitcheva, "Effects of myosmine on antioxidative defence in rat liver," *Arhiv za Higijenu Rada i Toksikologiju*, vol. 63, no. 1, pp. 7–14, 2012.

[58] M. Micheva, M. Kondeva-Burdina, and V. Vicheva, "Study on hepatotoxicity of cytisine (Tabex) compared with nicotine in freshly isolated rat hepatocytes," *Pharmacia*, vol. 56, no. 1–4, pp. 27–32, 2009.

[59] N. Alva, D. Cruz, S. Sanchez, J. Ma Valentin, and T. C. Bermudez, "Nitric oxide as a mediator of fructose 1, 6-bisphosphate protection in galactosamine-induced hepatotoxicity in rats," *Nitric Oxide*, vol. 28, pp. 17–23, 2013.

[60] J. Das, J. Ghosh, A. Roy, and P. C. Sil, "Mangiferin exerts hepatoprotective activity against D-galactosamine induced acute toxicity and oxidative/nitrosative stress via Nrf2-NFκB pathways," *Toxicology and Applied Pharmacology*, vol. 260, no. 1, pp. 35–47, 2012.

[61] G. Pushpavalli, C. Veeramani, and K. V. Pugalendi, "Effect of Piper betle on plasma antioxidant status and lipid profile against D-galactosamine-induced hepatitis in rats," *Redox Report*, vol. 14, no. 1, pp. 7–12, 2009.

[62] R. Labib, R. Turkall, and M. S. Abdel-Rahman, "Oral cocaine produces dose-related hepatotoxicity in male mice," *Toxicology Letters*, vol. 125, no. 1–3, pp. 29–37, 2001.

[63] R. Labib, R. Turkall, and M. S. Abdel-Rahman, "Inhibition of cocaine oxidative metabolism attenuates endotoxin potentiation of cocaine mediated hepatotoxicity," *Toxicology*, vol. 179, no. 1-2, pp. 9–19, 2002.

[64] P. Kovacic, "Role of oxidative metabolites of cocaine in toxicity and addiction: oxidative stress and electron transfer," *Medical Hypotheses*, vol. 64, no. 2, pp. 350–356, 2005.

[65] V. Vitcheva, R. Simeonova, I. Krasteva, M. Yotova, S. Nikolov, and M. Mitcheva, "Hepatoprotective effects of saponarin, isolated from *Gypsophila trichotoma* wend. on cocaine-induced oxidative stress in rats," *Redox Report*, vol. 16, no. 2, pp. 56–61, 2011.

[66] T. Visalli, R. Turkall, and M. S. Abdel-Rahman, "Cocaine hepatotoxicity and its potentiation by lipopolysaccharide: treatment and gender effects," *International Journal of Toxicology*, vol. 23, no. 3, pp. 163–170, 2004.

[67] Q.-Y. Cai, H.-B. Chen, S.-Q. Cai et al., "Effect of roots of Ficus hirta on cocaine-induced hepatotoxicity and active components," *Zhongguo Zhongyao Zazhi*, vol. 32, no. 12, pp. 1190–1193, 2007.

Hindawi Publishing Corporation
BioMed Research International
Volume 2013, Article ID 740573, 8 pages
http://dx.doi.org/10.1155/2013/740573

Review Article

Prooxidant Mechanisms in Iron Overload Cardiomyopathy

Ching-Feng Cheng[1,2] and Wei-Shiung Lian[1,2]

[1] *Department of Medical Research, Tzu Chi General Hospital and Department of Pediatrics, Tzu Chi University, Hualien, Taiwan*
[2] *Institute of Biomedical Sciences, Academia Sinica, Taipei, Taiwan*

Correspondence should be addressed to Ching-Feng Cheng; chengcf@mail.tcu.edu.tw

Received 5 June 2013; Accepted 28 October 2013

Academic Editor: Maha Zaki Rizk

Iron overload cardiomyopathy (IOC), defined as the presence of systolic or diastolic cardiac dysfunction secondary to increased deposition of iron, is emerging as an important cause of heart failure due to the increased incidence of this disorder seen in thalassemic patients and in patients of primary hemochromatosis. At present, although palliative treatment by regular iron chelation was recommended; whereas IOC is still the major cause for mortality in patient with chronic heart failure induced by iron-overloading. Because iron is a prooxidant and the associated mechanism seen in iron-overload heart is still unclear; therefore, we intend to delineate the multiple signaling pathways involved in IOC. These pathways may include organelles such as calcium channels, mitochondria; paracrine effects from both macrophages and fibroblast, and novel mediators such as thromboxane A2 and adiponectin; with increased oxidative stress and inflammation found commonly in these signaling pathways. With further understanding on these complex and inter-related molecular mechanisms, we can propose potential therapeutic strategies to ameliorate the cardiac toxicity induced by iron-overloading.

1. An Introduction to Iron Overload Cardiomyopathy

Heart failure due to iron overload can develop either as a result from repeated blood transfusions seen in thalassemias or hereditary hemochromatosis. The most important clinical conditions leading to iron overload cardiomyopathy (IOC) is thalassemia major, in which heart failure remains the major cause of death (60%), greatly exceeding deaths from infection (13%) and liver disease (6%) [1]. In patients of thalassemias and hemoglobinopathies, aggressive transfusion therapy and iron chelation have been palliatively applied to them before the 80's in order to improved their quality of life and decreased the morbidity and mortality rates associated with these diseases [2]. The only curative treatment for these diseases, bone marrow transplantation (BMT) was first successfully used to treat a thalassemic patient in 1982 [3]. Since then, more than 1000 patients have been treated with BMT around the world [4] and the outcome of these transplants from centers in Europe, North America, and Asia was around 80% of patients who survive long term and of these nearly 90% are cured of their diseases [5]. The risks of BMT using HLA-identical sibling donor could be predicted in advance according to the presence or absence of only three criteria: hepatomegaly, evidence of portal fibrosis, and inadequate iron chelation with existence of hemochromatosis. The latter could result in IOC and hepatic damages. Even for thalassemic patients, who have successfully undergone BMT and acquired normal hematologic status, the most important long-term consequences for those patients would be the complications associated with their moderate-severe iron overload [6].

IOC, defined as the presence of systolic or diastolic cardiac dysfunction secondary to increased deposition of iron, is emerging as an important cause of heart failure due to increased incidence of this disorder seen in thalassemic patients and in patients of primary hemochromatosis [7, 8]. Clinical iron-overload leads to a classical cardiomyopathy of restrictive physiology with severe diastolic dysfunction, but preserved systolic function in the early stages of the disorder that correspond with lower concentration of iron were reported by researchers in National Taiwan University

Hospital [9]. Moreover, in the later stages with high levels of iron, heart failure progress quickly with severe systolic dysfunction, and ventricular dilation in these patients. Death ensues promptly in the later stages due to heart failure and/or severe arrhythmia [7, 10]. Although the exact mechanism of iron-induced heart failure remains to be elucidated, excess iron-catalyzed free radical generation and cytotoxic aldehyde production are believed to play a role in damaging the myocardium and altering cardiac function [11]. Due to the complication of chronic transfusion and ineffectiveness to reverse the course of iron overloading even in post-BMT patients of thalassemia major and/or hereditary hemochromatosis, iron overload heart diseases are commonly seen among these patients. At present, only palliative treatment by regular desferrioxamine administration was recommended to these patients whereas its effect is setback by both high cost and poor patient compliance in the long term period; or its limited therapeutic effect on severe iron-overload condition.

During iron overload, transferrin, the carrier of iron in the circulation, which is normally 30% saturation, becomes fully saturated, and the toxic nontransferrin bound iron species appear in the circulation [12]. Uptakes of the latter in hepatocytes, cardiac myocytes, and endocrine gland cells lead to tissue iron overload [13]. The pathophysiology of IOC is clearly mediated by reactive oxidative stress whereby the cytoplasmic iron pool become available for fenton-type reactions, leading to the conversion of Fe^{2+} into Fe^{3+} generates free radicals including the highly reactive hydroxyl radicals, in which leading to increased peroxidation and damage into lipids, proteins, and nucleic acids, triggering cellular damage and depletion of antioxidants [14]. Although the production of hydroxyl radical and lipid peroxidation are important in initiation of IOC [15], it is likely that no single signaling pathway can account for its complex pathophysiology.

2. Iron Enters Cardiomyocytes through Calcium Channel in IOC

In iron overload conditions, nontransferrin-bound iron (NTBI) enters the cardiomyocytes through L-type Ca^{2+} channels (LTCC) and divalent metal transporter and leads to iron-overload cardiomyopathy [16–18]. The Fe^{2+} induced slowing of Ca^{2+} current inactivation results in a increase in the time integral of the Ca^{2+} current and the net Ca^{2+} influx, which may possibly contribute to the impaired diastolic function observed during the early stages of iron overload [19, 20]. With higher concentration of Fe^{2+} associated with diseased progression, Ca^{2+} influx became decreased as competing with ferrous ion, contributing to systolic dysfunction that is characteristic of more advanced IOC. Cardiac excitation-contraction coupling are highly sensitive to changes in cellular redox state leading to reduced systolic and elevated diastolic function characteristic of IOC. Using a patch clamp technique, it has been shown that the iron current competes with the calcium current, and is inhibited by a calcium channel blocker [17, 21]. Other in vivo studies, using chronic iron overload mice models, demonstrated the inhibitory effect of LTCC blockers on cardiac iron uptake, showing decreased tissue iron content [14, 18], preserve cardiac function, and improved survival. Recent studies from Kumfu et al., showed that the use of efonidipine, a proposed specific T type Ca channel (TTCC) blockers, can lower mortality, prevented myocardial iron deposition and oxidative stress with improved cardiac function in their iron overloaded thalassemic murine model [22]. The work of Kumfu et al. actually finds that LTCC blockers were as effective as putative TTCC blockers, and more important, the TTCC blockers they used is nonspecific and blocks LTCC with a potency that is very similar to TTCC. Although TTCC are specifically confined to the SA and AV nodes in the normal healthy hearts, TTCC expression and currents are re-expressed in the ventricular myocytes under pathological conditions. However, the administration of verapamil, an LTCC blocker, likely resulted in negative inotropic effects and hypotension, which may explain the lack of a mortality benefits in iron-overload mice. Therefore, future studies are needed to provide more definitive evidence for a role of the TTCC in iron-overloaded cardiomyopathy. These findings from Kumfu et al. indicated that, unlike ferrous ion, ferric ion (Fe^{3+}) uptake in cultured thalassemic cardiomyocytes is not mediated by LTCC, DMT1, or TTCC, suggesting that another alternative pathway could play a major role in thalassemic heart cells [23]. As LTCC is located in Ca^{2+}-release channel/ryanodine receptor complexes in cardiomyocytes and ryanodine receptor (RYR2) are very sensitive to oxidation; therefore, Fe^{2+} entry via calcium channels is expected to have direct effect on RYR2 function and Ca^{2+} homeostasis [24, 25]. In addition, a recent paper by Rose et al. demonstrated that chronic iron loading could selectively reduce Ca(V)1.3-mediated LTCC leading to bradycardia, slowing of electrical conduction, and atrial fibrillation in patients with IOC [26].

3. Reactive Oxidative Stress and Mitochondria Pathway in IOC

In iron overloaded cardiac cells, free (redox active) iron that catalyzed the formation of highly toxic reactive oxidative species (ROS) can damage intracellular lipid, proteins, and DNA [27]. These iron driven oxidation events required that the metal interacts with cellular reducing and oxidizing equivalents such as superoxide and hydrogen peroxide, in which mitochondrial electron transport chain is a major source for supplying these pools of electrons. Therefore, mitochondrial dysfunction is likely to occur in IOC [28]. Recent studies from Gao et al. reported that increased iron exposure to cardiac myocyte cell lines could result in progressive loss of mitochondrial DNA, with decreased mRNA and protein activity for complexes I, III, and IV and mitochondrial respiration. Their followed-up in vivo study using iron dextran injection mice models showed similar results with 60–70% loss of mRNA encoded by mitochondrial DNA, yet with no change in mRNA abundance for nuclear-encoded respiratory subunits [29]. Cochrane et al. reported that oxidant-induced damage to naked DNA and intracellular DNA is greatly enhanced by iron [30, 31]. In the absence of

transition metals such as iron and copper, DNA is quite unreactive with oxidants such as H_2O_2 whereas, in the presence of iron, oxidative DNA scission occurs readily [32, 33]. Compared to nuclear DNA, mitochondrial DNA is more sensitive to oxidant damage [34, 35]. The reason may include that mitochondria can generates ROS and mtDNA lacks histones to protect DNA from oxidant damage. In addition, repair to mtDNA is less effective as compared to nuclear DNA. The authors suggested that chronic iron overload leads to cumulativeiron-mediated damage to mtDNA and impaired synthesis of mitochondrial respiratory chain subunits. The resulting respiratory dysfunction may partly explain the slow progression of IOC.

The mechanism of iron acquisition by mitochondria of cardiac cells was further elucidated by Shvartsman et al. [36]. They used online fluorescence monitoring on iron for tracing the mobility of the metal from medium to cell cytosol and mitochondria in rat primary cardiomyocytes [37]. The results indicate that mitochondria rapidly taken up iron supplied to the cells as NTBI form and that the cytosolic iron traffic to the mitochondrial organelles could not be abolished by iron chelators. Under iron overload condition, it is apparently that mitochondria has limited ability to relieve themselves from labile iron accumulation, thus result in oxidative stress and ensuring damages to these critical organelles.

4. Reactive Oxidative Stress Associated Inflammation and Fibrosis in IOC

Excess iron injures cells primarily by catalyzing the production of ROS in excess of the capacity of cellular antioxidant systems. These ROS cause lipid peroxidation, oxidation of amino acids with consequent protein-protein fragmentation, and DNA damage. Therefore, the effect of chelation therapy can remove excessive iron from body and also scavenge and tightly bind labile iron to prevent the generation of ROS [38, 39]. In our prior studies, we intend to use G-CSF to treat chronic heart failure induced by IOC in the hypothesis that G-CSF can mobilize endogenous stem cells in which has been reported to offer beneficial effect to acute myocardial infarction. Although our data showed that G-CSF can mobilize autologous stem cells in the IOC mice, on the contrary, G-CSF supplement worsened the IOC induced cardiac dysfunction through aggravating iron induced oxidative stress, and cardiac inflammatory profiles with systemic leukocytosis [40]. The cardiac pathology of the G-CSF added IOC heart demonstrated ventricular fibrosis with macrophages infiltration. In addition, immune-histochemical analysis revealed increased tissue factor expression and colocalization with macrophage markers CD13 [40].

Our results showing that G-CSF can promote inflammatory profiles in IOC that leads to cardiac dysfunction, are in contrast to previous reports showing G-CSF therapy to be beneficial in acute myocardial infarction [41–44] and chronic cardiomyopathy induced by doxorubicin toxicity [45]. One explanation for these disparate results could be that chronic iron loading increases oxidative stress [46]. Although G-CSF recruits hematogenic stem cells, a simultaneous induction of macrophage and tissue factor gathering "gears up" the pro-inflammatory state and drives the inflammation-fibrosis circuit. Similar study that G-CSF exacerbates cardiac fibrosis after rat myocardial infarction with increasing circulating WBCs, neutrophils, and monocytes were also reported [47, 48]. In addition to IOC, heart remodeling and failure is persistent even with optimal chelation therapy in some of the β-thalassemic patients. Such clinical observation may let us raise questions on whether thalassemic cardiac dysfunction can occur in the absence of transfusion related iron-overload and myocardial iron deposition. In vivo evidence was provided by a recent study by Stoyanova et al. [49]. They used $Hbb^{d3th/d3th}$ gene deleted mouse, a mouse model closely reproduced human β-thalassemia major or intermedia disease, and echocardiography to follow their cardiac function longitudinally for 6 months without blood transfusion [50, 51]. These mice first demonstrated anemia associated compensated hypertrophy, then, developed age-dependent deterioration of left ventricular contractility and dysfunction that led toward decompensated heart failure. The histopathology revealed cardiac remodeling with increased interstitial fibrosis, but virtual absence of myocardial iron deposits. This study suggested that another paracrine and cardiomyocyte independent mechanism may be involved in cardiac fibrosis seen in the thalassemic hearts.

5. Macrophage and Arachidonic Acid Associated Paracrine Pathway in IOC

Recent studies further demonstrated that iron overload could enhance arachidonic acid release and eicosanoids production in cultured cardiomyocytes, and suggested a causal connection between these signals electromechanical abnormalities in iron-overload cardiomyopathy [52]. Nevertheless, limit information is available regarding the downstream signaling alterations. Because expression of both PGI2 and TXA_2 can be found in heart tissue, and PGI2 and its analogue have been reported to exert beneficial effect is cardiac ischemic injury [53]; therefore, we hypothesize that TXA_2 may be the major eicosanoids that mediates the iron overload induced cardiomyopathy.

Using iron-overload mouse model, along with TXAS gene deleted mouse, recent study from Lin et al. set out to elucidate the role of TXA_2 in cardiac iron-overload cardiomyopathy [54]. This study first demonstrated that iron loading can induce TXAS and its product TXB2 expression in mouse heart. Second, they found that the development of iron-induced cardiac fibrosis required TXAS product TXB_2, which is inflammation dependent. Their data showed that attenuation of iron deposition was found in the TXAS KO hearts, suggesting that TXAS is involved in the iron deposition itself in the heart. Because iron appears to be accumulated mainly in nonmyocytes macrophage cells located in the interstitial space, in which also has TXAS expression [55]. Therefore, we suggested that activated macrophages that taken up iron have increase TXAS expression, thus activated the TP receptor in cardiomyocytes in a paracrine TXA_2-TP signaling manner. This study also demonstrates that a lack

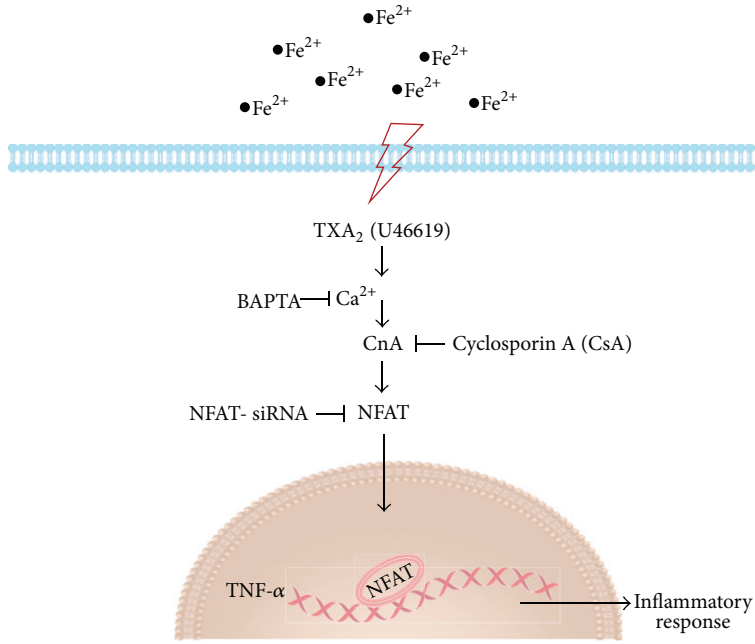

Figure 1: TXA_2 mediates iron overload cardiomyopathy through TNF-α associated calcineurin-NFAT signaling pathway. The schematic diagram depicted that iron loading can activate TXA_2 and induces TNF-α production in which can be inhibited by NFAT-SiRNA, calcineurin inhibitor (CsA), or calcium chelator (BAPTA). Addition of TXA_2 agonist, U46619, can facilitate nuclear translocation of NFAT, thus increase proinflammatory marker TNF-α expression. These findings demonstrate a novel molecular mechanism of TXA_2 in mediating iron overdosed cardiomyopathy and the involvement of calcineurin-NFAT signaling cascades in cardiac chronic inflammation.

of TXAS can attenuate cardiac fibrosis and inflammation in IOC with an accompanying decrease in cellular infiltration in tissue and an attenuation of WBC, monocytes, lymphocytes, and neutrophil numbers in blood, suggesting that leukocytes-cardiomycytes TXAS-TP signaling is sufficient to induce cardiac iron deposition and activate chronic inflammation in heart. They further discovered that the TXA_2 analogue, U46619, induces TNF-α production in which can be inhibited by NFAT-SiRNA, calcineurin inhibitor (CsA), or calcium chelator (BAPTA). These findings demonstrate a novel molecular mechanism of TXA_2 in mediating iron-overdosed cardiomyopathy and the involvement of calcineurin-NFAT signaling cascades (see Figure 1).

Because chronic iron loading may activate more than one signaling pathway that damaged the heart tissue; therefore, it is possible that iron may deposit on cardiac myocytes, and it may also stimulate macrophage infiltration and activate inflammation. In prior study by Lian et al., some of the IOC mice after G-CSF supplementation demonstrated increased ROS production with recruitment of macrophages, in which further aggravated inflammatory infiltration which eventually triggered cardiac thrombosis in the left ventricular chamber [41].

6. Novel Adiponectin Signaling Pathways Involved in IOC

Adiponectin (APN) is a circulating adipose-derived cytokine that may act as an antioxidative and anti-inflammatory protein. Although APN has been reported to confer cytoprotective effects in acute cardiac diseases, its effects in IOC are unknown. Recent studies have found a negative correlation between the levels of serum ferritin and APN [56–58], which suggests that adipocyte iron negatively regulates APN transcription via FOXO-1-mediated repression [59]. These data indicated that the increased tissue iron stores are sufficient to increase serum ferritin and decrease serum APN levels. Iron loading induced oxidative stress with the overexpression of proinflammatory molecules, such as IL-6, MCP-1, TNF-α, and ICAM-1, in heart or blood vasculature [60], leading to endothelial and cardiac dysfunction. Therefore, it is plausible that decreased APN levels are a risk index in cardiac inflammation and associated endothelial dysfunction.

Our recent study aimed to investigate whether APN offers beneficial effects in iron-induced chronic heart failure [61]. IOC mice exhibited decreased left ventricular contraction and decreased serum APN levels in which the phenotype can be rescued by in vivo cardiac AAV8-APN supplement. A further in vitro study showed that APN induced heme oxygenase-1 (HO-1) expression through the PPARα-HO-1 signaling pathway. In addition, the APN-mediated beneficial effects were PPARα-dependent as the APN-mediated protective effects on attenuating iron deposition were abolished in PPARα-knockout mice. Lastly, we demonstrated that PPARα-HO-1 signaling involved PPARα and PGC-1 binding and nuclear translocation, and their levels of expression can be increased after APN therapy. These data showed that APN ameliorated iron deposition in the heart through

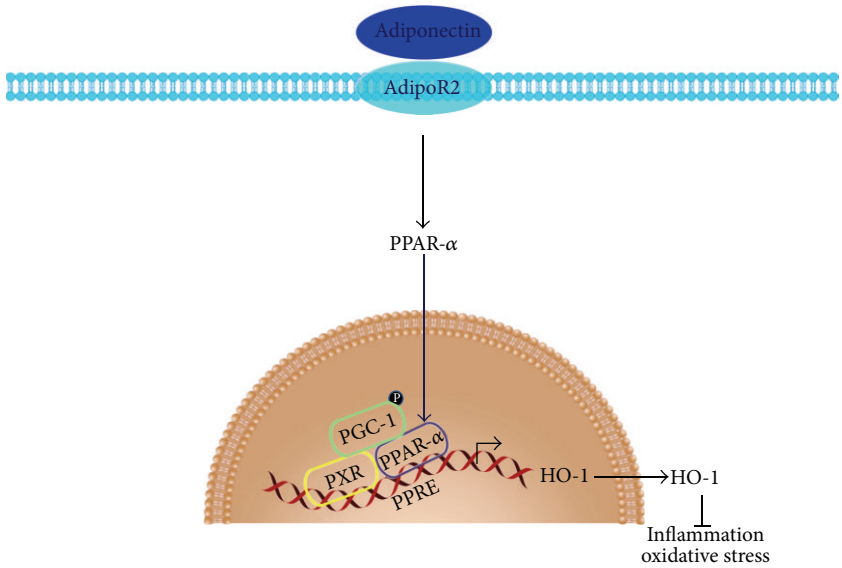

Figure 2: Adiponectin ameliorates cardiac inflammation in IOC through the PPARα-PGC1-dependent signaling pathway. The schematic diagram showing that adiponectin exerts its beneficial effects in cardiomyocytes through the PPARα-dependent HO-1 signaling pathway and requires PPARα-PGC-1 interaction. The adiponectin-AdipoR2-PPARα signaling may be the major pathway in exerting anti-inflammatory and antioxidative stress effects that ameliorate iron-overload cardiac dysfunction.

a PPARα-PGC-1-dependent mechanism and exert beneficial effects to IOC (see Figure 2).

7. Other Beneficial Effects against ROS and Inflammation in IOC

HMG-CoA reductase inhibitors, or statins, are known to improve cardiac dysfunction through their anti-inflammatory and antioxidative action. Statins also affect endothelial function through the production of nitric oxide [62, 63]. A recent study from Lian et al. demonstrates that simvastatin can reduce the myocardial iron depositionin G-CSF treated iron-overload heart [40]. Simvastatin administration also reduced the expression of the pro-inflammatory markers ICAM-1, tissue factor, MCP-1, and TNF-α. This study also revealed that simvastatin exerts their beneficial effects through elevation of both eNOS and phosphorylates Akt activity, thus ameliorates the inflammation-fibrosis found in the iron-overload heart.

A prior study by Grandel et al. showed that endotoxin depressed the contractility of isolated rat hearts by inducing TNF-α synthesis, and that TNF-α-induced microcirculatory dysfunction in mouse liver is dependent on TP receptor [64, 65]. These findings suggest that TXA_2 may act as a paracrine facilitator of TNF-α expression. A recent study from Lin et al. revealed that the addition of the TXA_2 agonist, U46619, to cardiac cultured cells can increase TNF-α expression [54]. This expression can be suppressed by BAPTA, CsA, and SQ29548, respectively. These results show that the TXA_2-mediated TP receptor-calcium/calcineurin signaling pathway activates the pro-inflammatory marker TNF-α. Iron-overloaded mice administered the TNF-α antibody infliximab showed decreased TXAS expression in the heart with improved left ventricular contractility. These data imply that blockade of TNF-α in vivo can decrease TXA_2 expression and attenuate IOC.

8. Conclusion

In this review, we delineated the multiple signaling pathways involved in IOC. These pathways may include organelles such as calcium channels, mitochondria, paracrine effects from both macrophages and fibroblast, and novel mediators such as thromboxane A2 and adiponectin. Because iron is a prooxidant, the involved signaling pathways were associated with increased oxidative stress and inflammation. A schematic diagram (Figure 3) was depicted to show these complex and interrelated molecular mechanisms: iron can enter the cardiomyocytes through both L-type and T-type calcium channels and increased the ROS within cardiac cells. These effects then inhibit the calcium influx, impaired the excitation-contraction coupling and myofilaments contractility, and damage the intracellular organelles, including mitochondria. In addition, iron can activate the TXA_2-TP receptor signaling pathway and promote cardiomyocyte-macrophage interaction. With G-CSF supplement, such macrophages recruitment and tissue factor induction will be enhanced, which further increased the ROS and gear up the inflammation-fibrosis circuit, result in aggravation of IOC and cardiac fibrosis. With further understanding on the molecular mechanisms involved in IOC, we propose the potential in using adiponectin, statins, and possible TNFα blockers for future therapeutic trials to ameliorate the cardiac toxicity induced by iron-overloading.

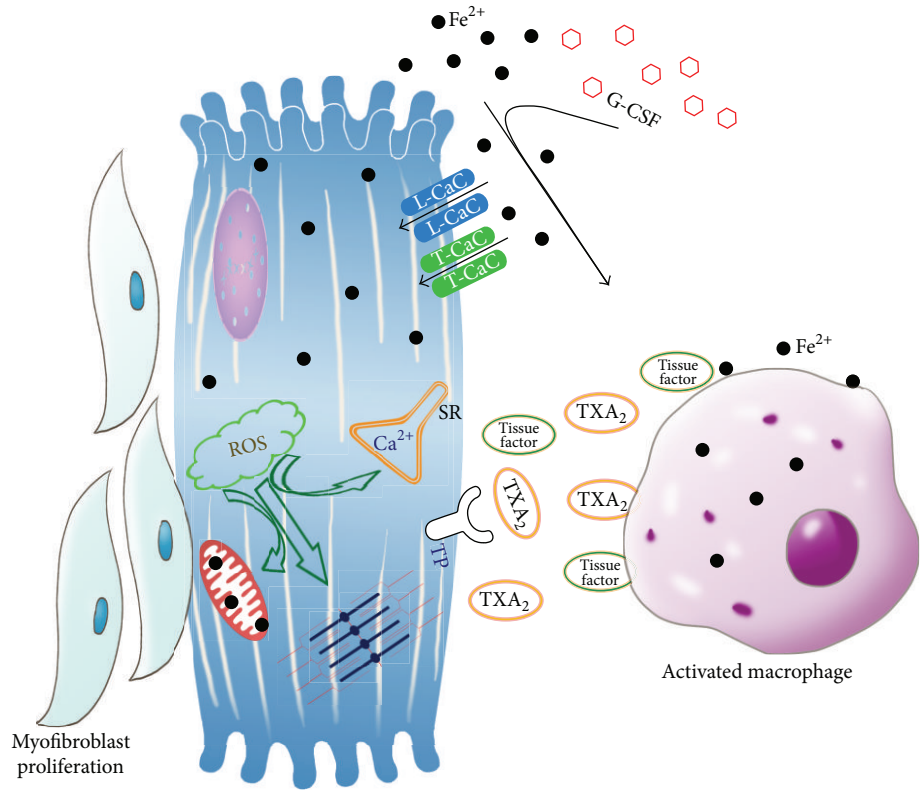

Figure 3: Involvement of multiple signaling pathways and cardiomyocyte-macrophage interactions in iron overload cardiomyopathy. The schematic diagram showed that iron can enter the cardiomyocytes through both L-type and T-type calcium channels and increased the ROS within cardiac cells. These effects then inhibit the calcium influx, impaired the excitation-contraction coupling and myofilaments contractility, and damage the intracellular organelles, including mitochondria. In addition, iron can activate the TXA_2-TP receptor signaling pathway and promote cardiomyocyte-macrophage interaction. With G-CSF supplement, such macrophages recruitment and tissue factor induction will be enhanced, which further increased the ROS and gear up the inflammation-fibrosis circuit, result in aggravation of IOC and cardiac fibrosis.

Acknowledgments

This work is supported by the Grants from Tzu Chi General Hospital (TCDR101-10, TCRDI-98-01, TCRDI-100-01-03), Tzu Chi University (TCIRP-99001), and the National Science Council (98-2314-B-303-001-MY3, 101-2325-B-303-001-) to Ching-Feng Cheng.

References

[1] M. G. Zurlo, D. P. Stefano, C. Borgna-Pignatti et al., "Survival and causes of death in thalassaemia major," *The Lancet*, vol. 2, no. 8653, pp. 27–30, 1989.

[2] N. F. Olivieri and G. M. Brittenham, "Iron-chelating therapy and the treatment of thalassemia," *Blood*, vol. 89, no. 3, pp. 739–761, 1997.

[3] E. D. Thomas, C. D. Buckner, and J. E. Sanders, "Marrow transplantation for thalassaemia," *The Lancet*, vol. 2, no. 8292, pp. 227–229, 1982.

[4] I. Roberts, "Current status of allogeneic transplantation for haemoglobinopathies," *British Journal of Haematology*, vol. 98, no. 1, pp. 1–7, 1997.

[5] "Third internationalsymposium on BMT in thalassemia," *Bone Marrow Transplant*, vol. 19, supplement 2, pp. 1–206, 1997.

[6] C. Giardini, M. Galimberti, G. Lucarelli et al., "Desferrioxamine therapy accelerates clearance of iron deposits after bone marrow transplantation for thalassaemia," *British Journal of Haematology*, vol. 89, no. 4, pp. 868–873, 1995.

[7] P. Liu and N. Olivieri, "Iron overload cardiomyopathies: new insights into an old disease," *Cardiovascular Drugs and Therapy*, vol. 8, no. 1, pp. 101–110, 1994.

[8] M. A. Aldouri, B. Wonke, A. V. Hoffbrand et al., "High incidence of cardiomyopathy in beta-thalassaemia patients receiving regular transfusion and iron chelation: reversal by intensified chelation," *Acta Haematologica*, vol. 84, no. 3, pp. 113–117, 1990.

[9] J. W. Hou, M. H. Wu, K. H. Lin, and H.-C. Lue, "Prognostic significance of left ventricular diastolic indexes in β- thalassemia major," *Archives of Pediatrics and Adolescent Medicine*, vol. 148, no. 8, pp. 862–866, 1994.

[10] M. A. Engle, M. Erlandson, and C. H. Smith, "Late cardiac complications of chronic, severe, refractory anemia with hemochromatosis," *Circulation*, vol. 30, pp. 698–705, 1964.

[11] W. J. Bartfay, F. Dawood, W. H. Wen et al., "Cardiac function and cytotoxic aldehyde production in a murine model of chronic iron-overload," *Cardiovascular Research*, vol. 43, no. 4, pp. 892–900, 1999.

[12] J. C. Wood, "Cardiac iron across different transfusion-dependent diseases," *Blood Reviews*, vol. 22, supplement 2, pp. S14–S21, 2008.

[13] J. B. Porter, "Concepts and goals in the management of transfusional iron overload," *American Journal of Hematology*, vol. 82, no. 12, pp. 1136–1139, 2007.

[14] G. Y. Oudit, M. G. Trivieri, N. Khaper, P. P. Liu, and P. H. Backx, "Role of L-type Ca2+ channels in iron transport and iron-overload cardiomyopathy," *Journal of Molecular Medicine*, vol. 84, no. 5, pp. 349–364, 2006.

[15] C. Hershko, G. Link, and I. Cabantchik, "Pathophysiology of iron overload," *Annals of the New York Academy of Sciences*, vol. 850, pp. 191–201, 1998.

[16] E. W. Randell, J. G. Parkes, N. F. Olivieri, and D. M. Templeton, "Uptake of non-transferrin-bound iron by both reductive and nonreductive processes is modulated by intracellular iron," *Journal of Biological Chemistry*, vol. 269, no. 23, pp. 16046–16053, 1994.

[17] R. G. Tsushima, A. D. Wickenden, R. A. Bouchard, G. Y. Oudit, P. P. Liu, and P. H. Backx, "Modulation of iron uptake in heart by L-type Ca2+ channel modifiers: possible implications in iron overload," *Circulation Research*, vol. 84, no. 11, pp. 1302–1309, 1999.

[18] G. Y. Oudit, H. Sun, M. G. Trivieri et al., "L-type Ca2+ channels provide a major pathway for iron entry into cardiomyocytes in iron-overload cardiomyopathy," *Nature Medicine*, vol. 9, no. 9, pp. 1187–1194, 2003.

[19] D. T. Kremastinos, D. P. Tsiapras, G. A. Tsetsos, E. I. Rentoukas, H. P. Vretou, and P. K. Toutouzas, "Left ventricular diastolic Doppler characteristics in β-thalassemia major," *Circulation*, vol. 88, no. 3, pp. 1127–1135, 1993.

[20] N. F. Olivieri, G. M. Brittenham, D. Matsui et al., "Iron-chelation therapy with oral deferipronein patients with thalassemia major," *New England Journal Medicine*, vol. 332, no. 14, pp. 918–922, 1995.

[21] S. Crowe and W. J. Bartfay, "Amlodipine decreases iron uptake and oxygen free radical production in the heart of chronically iron overloaded mice," *Biological Research for Nursing*, vol. 3, no. 4, pp. 189–197, 2002.

[22] S. Kumfu, S. Chattipakorn, K. Chinda, S. Fucharoen, and N. Chattipakorn, "T-type calcium channel blockade improves survival and cardiovascular function in thalassemic mice," *European Journal of Haematology*, vol. 88, no. 6, pp. 535–548, 2012.

[23] S. Kumfu, S. Chattipakorn, S. Fucharoen, and N. Chattipakorn, "Ferric iron uptake into cardiomyocytes of β-thalassemic mice is not through calcium channels," *Drug and Chemical Toxicology*, vol. 36, no. 3, pp. 329–334, 2013.

[24] A. O. Jorgensen, A. C.-Y. Shen, W. Arnold, P. S. McPherson, and K. P. Campbell, "The Ca2+-release channel/ryanodine receptor is localized in junctional and corbular sarcoplasmic reticulum in cardiac muscle," *Journal of Cell Biology*, vol. 120, no. 4, pp. 969–980, 1993.

[25] E. Kim, S. N. Giri, and I. N. Pessah, "Iron(II) is a modulator of ryanodine-sensitive calcium channels of cardiac muscle sarcoplasmic reticulum," *Toxicology and Applied Pharmacology*, vol. 130, no. 1, pp. 57–66, 1995.

[26] R. A. Rose, M. Sellan, J. A. Simpson et al., "Iron overload decreases CaV1.3-dependent L-type Ca2+ currents leading to bradycardia, altered electrical conduction, and atrial fibrillation," *Circulation*, vol. 4, no. 5, pp. 733–742, 2011.

[27] G. J. Quinlan, T. W. Evans, and J. M. C. Gutteridge, "Iron and the redox status of the lungs," *Free Radical Biology and Medicine*, vol. 33, no. 10, pp. 1306–1313, 2002.

[28] X. Gao, J. L. Campian, M. Qian, X. Sun, and J. W. Eaton, "Mitochondrial DNA damage in iron overload," *Journal of Biological Chemistry*, vol. 284, no. 8, pp. 4767–4775, 2009.

[29] X. Gao, M. Qian, J. L. Campian et al., "Mitochondrial dysfunction may explain the cardiomyopathy of chronic iron overload," *Free Radical Biology and Medicine*, vol. 49, no. 3, pp. 401–407, 2010.

[30] J. H. Jackson, I. U. Schraufstatter, P. A. Hyslop et al., "Role of oxidants in DNA damage. Hydroxyl radical mediates the synergistic DNA damaging effects of asbestos and cigarette smoke," *Journal of Clinical Investigation*, vol. 80, no. 4, pp. 1090–1095, 1987.

[31] I. Schraufstatter, P. A. Hyslop, J. H. Jackson, and C. G. Cochrane, "Oxidant-induced DNA damage of target cells," *Journal of Clinical Investigation*, vol. 82, no. 3, pp. 1040–1050, 1988.

[32] H. U. Enright, W. J. Miller, and R. P. Hebbel, "Nucleosomal histone protein protects DNA from iron-mediated damage," *Nucleic Acids Research*, vol. 20, no. 13, pp. 3341–3346, 1992.

[33] H. Enright, K. A. Nath, R. P. Hebbel, and S. L. Schrier, "Internucleosomal cleavage of DNA is insufficient evidence to conclude that cell death is apoptotic," *Blood*, vol. 83, no. 7, pp. 2005–2007, 1994.

[34] F. M. Yakes and B. Van Houten, "Mitochondrial DNA damage is more extensive and persists longer than nuclear DNA damage in human cells following oxidative stress," *Proceedings of the National Academy of Sciences of the United States of America*, vol. 94, no. 2, pp. 514–519, 1997.

[35] J. J. Salazar and B. Van Houten, "Preferential mitochondrial DNA injury caused by glucose oxidase as a steady generator of hydrogen peroxide in human fibroblasts," *Mutation Research*, vol. 385, no. 2, pp. 139–149, 1997.

[36] M. Shvartsman, R. Kikkeri, A. Shanzer, and Z. I. Cabantchik, "Non-transferrin-bound iron reaches mitochondria by a chelator-inaccessible mechanism: biological and clinical implications," *American Journal of Physiology*, vol. 293, no. 4, pp. C1383–C1394, 2007.

[37] M. Shvartsman, E. Fibach, and Z. I. Cabantchik, "Transferrin-iron routing to the cytosol and mitochondria as studied by live and real-time fluorescence," *Biochemical Journal*, vol. 429, no. 1, pp. 185–193, 2010.

[38] R. Bolli, B. S. Patel, W.-X. Zhu et al., "The iron chelator desferrioxamine attenuates postischemic ventricular dysfunction," *American Journal of Physiology*, vol. 253, no. 6, pp. H1372–H1380, 1987.

[39] A. M. M. van der Kraaij, H. G. van Eijk, and J. F. Koster, "Prevention of postischemic cardiac injury by the orally active iron chelator 1,2-dimethyl-3-hydroxy-4-pyridone (L1) and the antioxidant (+)-cyanidanol-3," *Circulation*, vol. 80, no. 1, pp. 158–164, 1989.

[40] W. S. Lian, H. Lin, W. T. K. Cheng, T. Kikuchi, and C. F. Cheng, "Granulocyte-CSF induced inflammation-associated cardiac thrombosis in iron loading mouse heart and can be attenuated by statin therapy," *Journal of Biomedical Science*, vol. 18, p. 26, 2011.

[41] M. Harada, Y. Qin, H. Takano et al., "G-CSF prevents cardiac remodeling after myocardial infarction by activating the Jak-Stat pathway in cardiomyocytes," *Nature Medicine*, vol. 11, no. 3, pp. 305–311, 2005.

[42] S. Minatoguchi, G. Takemura, X. Chen et al., "Acceleration of the healing process and myocardial regeneration may be important as a mechanism of improvement of cardiac function and

remodeling by postinfarction granulocyte colony-stimulating factor treatment," *Circulation*, vol. 109, no. 21, pp. 2572–2580, 2004.

[43] M. Ohtsuka, H. Takano, Y. Zou et al., "Cytokine therapy prevents left ventricular remodeling and dysfunction after myocardial infarction through neovascularization," *The FASEB Journal*, vol. 18, no. 7, pp. 851–853, 2004.

[44] E. Deindl, M. Zaruba, S. Brunner et al., "G-CSF administration after myocardial infarction in mice attenuates late ischemic cardiomyopathy by enhanced arteriogenesis," *The FASEB Journal*, vol. 20, no. 7, pp. 956–958, 2006.

[45] L. Li, G. Takemura, Y. Li et al., "Granulocyte colony-stimulating factor improves left ventricular function of doxorubicin-induced cardiomyopathy," *Laboratory Investigation*, vol. 87, no. 5, pp. 440–455, 2007.

[46] S. M. Day, D. Duquaine, L. V. Mundada et al., "Chronic iron administration increases vascular oxidative stress and accelerates arterial thrombosis," *Circulation*, vol. 107, no. 20, pp. 2601–2606, 2003.

[47] Z. Cheng, L. Ou, Y. Liu et al., "Granulocyte colony-stimulating factor exacerbates cardiac fibrosis after myocardial infarction in a rat model of permanent occlusion," *Cardiovascular Research*, vol. 80, no. 3, pp. 425–434, 2008.

[48] Z. Cheng, X. Liu, L. Ou et al., "Mobilization of mesenchymal stem cells by granulocyte colony-stimulating factor in rats with acute myocardial infarction," *Cardiovascular Drugs and Therapy*, vol. 22, no. 5, pp. 363–371, 2008.

[49] E. Stoyanova, G. Cloutier, H. Felfly, W. Lemsaddek, N. Ah-Son, and M. Trudel, "Evidence for a novel mechanism independent of myocardial iron in beta-thalassemia cardiac pathogenesis," *PloS ONE*, vol. 7, Article ID e52128, 2012.

[50] L. C. Skow, B. A. Burkhart, and F. M. Johnson, "A mouse model for β-thalassemia," *Cell*, vol. 34, no. 3, pp. 1043–1052, 1983.

[51] E. Stoyanova, M. Trudel, H. Felfly, D. Garcia, and G. Cloutier, "Characterization of circulatory disorders in β-thalassemic mice by noninvasive ultrasound biomicroscopy," *Physiological Genomics*, vol. 29, no. 1, pp. 84–90, 2007.

[52] R. Mattera, G. P. Stone, N. Bahhur, and Y. A. Kuryshev, "Increased release of arachidonic acid and eicosanoids in iron-overloaded cardiomyocytes," *Circulation*, vol. 103, no. 19, pp. 2395–2401, 2001.

[53] G. Johnson III, L. E. Furlan, N. Aoki, and A. M. Lefer, "Endothelium and myocardial protecting actions of taprostene, a stable prostacyclin analogue, after acute myocardial ischemia and reperfusion in cats," *Circulation Research*, vol. 66, no. 5, pp. 1362–1370, 1990.

[54] H. Lin, H. F. Li, W. S. Lian et al., "Thromboxan A2 mediates iron-overload cardiomyopathy in mice through calcinurin-NFAT signaling pathway," *Circulation Journal*, vol. 77, no. 10, pp. 2586–2595, 2013.

[55] T. Cyrus, T. Ding, and D. Praticò, "Expression of thromboxane synthase, prostacyclin synthase and thromboxane receptor in atherosclerotic lesions: correlation with plaque composition," *Atherosclerosis*, vol. 208, no. 2, pp. 376–381, 2010.

[56] N. G. Forouhi, A. H. Harding, M. Allison et al., "Elevated serum ferritin levels predict new-onset type 2 diabetes: results from the EPIC-Norfolk prospective study," *Diabetologia*, vol. 50, no. 5, pp. 949–956, 2007.

[57] O. A. Mojiminiyi, R. Marouf, and N. A. Abdella, "Body iron stores in relation to the metabolic syndrome, glycemic control and complications in female patients with type 2 diabetes," *Nutrition, Metabolism and Cardiovascular Diseases*, vol. 18, no. 8, pp. 559–566, 2008.

[58] B. J. Ku, S. Y. Kim, T. Y. Lee, and K. S. Park, "Serum ferritin is inversely correlated with serum adiponectin level: population-based cross-sectional study," *Disease Markers*, vol. 27, no. 6, pp. 303–310, 2009.

[59] J. S. Gabrielsen, Y. Gao, J. A. Simcox et al., "Adipocyte iron regulates adiponectin and insulin sensitivity," *The Journal of Clinical Investigation*, vol. 122, no. 10, pp. 3529–3540, 2012.

[60] E. Kahn, M. Baarine, S. Pelloux et al., "Iron nanoparticles increase 7-ketocholesterol-induced cell death, inflammation, and oxidation on murine cardiac HL1-NB cells," *International Journal of Nanomedicine*, vol. 5, no. 1, pp. 185–195, 2010.

[61] H. Lin, W. S. Lian, H. H. Chen, P. F. Lai, and C. F. Cheng, "Adiponectin ameliorates iron-overload cardiomyopathy through the PPARα-PGC-1-dependent signaling pathway," *Molecular Pharmacology*, vol. 84, no. 2, pp. 275–285, 2013.

[62] J. Davignon, "Beneficial cardiovascular pleiotropic effects of statins," *Circulation*, vol. 109, no. 23, pp. III39–III43, 2004.

[63] J. K. Liao and U. Laufs, "Pleiotropic effects of statins," *Annual Review of Pharmacology and Toxicology*, vol. 45, pp. 89–118, 2005.

[64] U. Grandel, L. Fink, A. Blum et al., "Endotoxin-induced myocardial tumor necrosis factor-α synthesis depresses contractility of isolated rat hearts: evidence for a role of sphingosine and cyclooxygenase-2-derived thromboxane production," *Circulation*, vol. 102, no. 22, pp. 2758–2764, 2000.

[65] H. Katagiri, Y. Ito, S. Ito et al., "TNF-α induces thromboxane receptor signaling-dependent microcirculatory dysfunction in mouse liver," *Shock*, vol. 30, no. 4, pp. 463–467, 2008.

Hindawi Publishing Corporation
BioMed Research International
Volume 2013, Article ID 839761, 7 pages
http://dx.doi.org/10.1155/2013/839761

Review Article

Role of NADPH Oxidase-Mediated Reactive Oxygen Species in Podocyte Injury

Shan Chen,[1] Xian-Fang Meng,[2] and Chun Zhang[1]

[1] *Department of Nephrology, Union Hospital, Tongji Medical College, Huazhong University of Science and Technology, Wuhan 430022, China*
[2] *Department of Neurobiology, Tongji Medical College, Huazhong University of Science and Technology, Wuhan 430030, China*

Correspondence should be addressed to Xian-Fang Meng; meng.xianfang@yahoo.com and Chun Zhang; drzhangchun@gmail.com

Received 10 June 2013; Revised 16 September 2013; Accepted 4 October 2013

Academic Editor: Maha Zaki Rizk

Proteinuria is an independent risk factor for end-stage renal disease (ESRD) (Shankland, 2006). Recent studies highlighted the mechanisms of podocyte injury and implications for potential treatment strategies in proteinuric kidney diseases (Zhang et al., 2012). Reactive oxygen species (ROS) are cellular signals which are closely associated with the development and progression of glomerular sclerosis. NADPH oxidase is a district enzymatic source of cellular ROS production and prominently expressed in podocytes (Zhang et al., 2010). In the last decade, it has become evident that NADPH oxidase-derived ROS overproduction is a key trigger of podocyte injury, such as renin-angiotensin-aldosterone system activation (Whaley-Connell et al., 2006), epithelial-to-mesenchymal transition (Zhang et al., 2011), and inflammatory priming (Abais et al., 2013). This review focuses on the mechanism of NADPH oxidase-mediated ROS in podocyte injury under different pathophysiological conditions. In addition, we also reviewed the therapeutic perspectives of NADPH oxidase in kidney diseases related to podocyte injury.

1. Introduction

Chronic kidney disease (CKD) is a major public health problem worldwide. Proteinuria is a common clinical signature and a potent predictor for the progression of CKD. Podocytes are highly differentiated glomerular epithelial cells which lie in the outmost layer of the glomerular filtration barrier. Podocyte foot processes interdigitate with the counterparts of neighboring cells to form the slit diaphragm, which constitutes the final barrier to prevent protein loss from vascular to urinary space. Podocyte injury has been considered as the most important early event initiating glomerulosclerosis in many proteinuric kidney diseases [1]. The slit diaphragm proteins, such as nephrin, podocin, CD2-associated protein (CD2AP), and canonical transient receptor potential-6 channel (TRPC6), have been proved to play key role in maintaining normal podocyte structure and function [2]. Podocyte injury is generally presented as slit diaphragm disruption, actin cytoskeleton rearrangement, podocyte foot processes effacement, and proteinuria.

2. Reactive Oxygen Species

Oxidative stress is a characteristic feature in many chronic and inflammatory diseases and indeed associated with the development and progression of CKD [3]. The imbalance between reactive oxygen species (ROS) production and antioxidant systems to scavenge the reactive intermediates will induce oxidative stress. ROS are oxygen-derived small molecules produced as intermediates in the redox processes, such as superoxide ($O_2^{\bullet -}$), hydroxyl ($^{\bullet}OH$), hypochlorous acid (HOCl), ozone (O_3), singlet oxygen ($^1O_2$), and hydrogen peroxide (H_2O_2) [4]. ROS play important roles in diverse physiological signaling processes but also trigger diseases.

Several oxidoreductases have been identified as potential sources of ROS, including cyclooxygenase, lipoxygenase, cytochrome P450 enzymes, nitric-oxide synthase, xanthine oxidase, mitochondrial NADH: ubiquinone oxidoreductase, and nicotinamide adenine dinucleotide phosphate (NADPH) oxidase. Unlike other enzymes that produce ROS secondary to their specific catalytic process, NADPH oxidase is the only

enzyme known to produce ROS as the primary function. And a previous study showed that the primary source of ROS generation in the renal cortex is NADPH oxidase [5].

ROS overproduction was found in many podocyte injury models in vitro and in experimental diseases such as diabetic nephropathy (DN), membranous nephropathy (MN), minimal change disease (MCD), and focal segmental glomerulosclerosis (FSGS) [3]. Oxidants in turn cause podocyte injury directly, including DNA damage and apoptosis. However, recent researches showed poor outcomes of antioxidant therapies in clinical studies. It implies that specifically targeting the enzymatic sources of pathophysiologically relevant ROS may be more effective [6].

3. NADPH Oxidase and ROS Production

NADPH oxidase is a cytoplasmic enzyme consisting of at least one catalytic, transmembrane-spanning NOX subunit, which produces ROS by transferring electrons from NADPH to molecular oxygen. To date, the NOX family consists of seven members, NOX1–5, and two NOX5-like dual oxidases, Duox1-2. All NOX subunits have been reported to bind one or more regulatory subunits, including $p22^{phox}$, NOXO1 localized in the membrane and cytosolic submits $p40^{phox}$, $p47^{phox}$, $p67^{phox}$, NOXA1, and Rac GTPases. It has long been accepted that the translocation and binding of $p47^{phox}$ with membrane complex of NOX2 and $p22^{phox}$ are the key events leading to the activation of NADPH oxidase and generation of ROS.

The phagocyte NADPH oxidase NOX2, also named $gp91^{phox}$, is the prototypical catalytic subunit of NADPH oxidase. And the backbone of the enzyme is cell membrane-bound cytochrome b558, which consists of NOX2 and $p22^{phox}$. NOX1, NOX3, and NOX4 share some similarities with NOX2, such as structural organization and molecular weight. NOX5 possess an extra aminoterminal calmodulin-like domain that contains four Ca^{2+}-binding EF-hands structures. Duox possess an extracellular peroxidase domain that uses the H_2O_2 generated by its NOX catalytic moiety in addition to the NOX5-based structure. All the NOX1–4 isoforms require the $p22^{phox}$ subunit, whereas NOX5 and Duox are activated directly by Ca^{2+}.

4. NADPH Oxidase-Mediated ROS Production and Podocyte Injury

NADPH oxidase plays a fundamental role in maintaining normal cell functions and can be activated by diverse stimuli, such as chemical, physical, environmental, and biological factors. Various NADPH oxidase components are found in the kidney and glomerular cells. NOX1, NOX2, NOX4, $p22^{phox}$, $p47^{phox}$, $p67^{phox}$, and Rac1/2 protein have been indentified within the kidney [7]. Greiber et al. have first demonstrated that in the primary cultured human podocytes, ROS are primarily generated by NADPH oxidases, and the NADPH oxidase subunits $p22^{phox}$, $p47^{phox}$, NOX2, and $p67^{phox}$ were expressed [8]. In addition, Whaley-Connell et al. reported that NOX2, NOX4, $p22^{phox}$, $p47^{phox}$, and Rac1 are expressed immortalized murine podocyte cells [9].

Growing evidence reveals that NADPH oxidase-derived ROS overproduction is importantly involved in the progression of podocyte injury associated with the upregulation of various NOX subtypes [10]. NADPH oxidase in the podocyte is activated by adenosine triphosphate (ATP) [8], chemokine [11], angiotensin II (ANG II) [9], aldosterone [12], high glucose [13–17], C5b-9 [18], advanced oxidation protein products (AOPPs) [29], hyperhomocysteinemia (hHcys) [19–21], insulin [22], puromycin aminonucleoside (PAN) [23, 24], and N-methyl-D-aspartate (NMDA) [25].

4.1. Primary Glomerular Nephritis. ROS-mediated glomerular injury was proved in many experimental studies, and ROS may play important roles in the pathogenesis of primary glomerular nephritis [3]. ROS generated from podocytes may trigger podocyte injury. Puromycin aminonucleoside (PAN) was widely used to establish animal models of podocyte injury, such as MCD and FSGS. Incubation of podocytes with puromycin (PAN) induced NOX4 expression and promoted superoxide generation [23, 24]. It led to the upregulation of TRPC6 and a loss of cell viability followed by an elevation in the gap junction protein connexin43 (Cx43) levels. It suggested that NADPH oxidase may promote the cellular structure destruction in podocytes. Known from the Heymann nephritis models of MN in rats, podocytes are the targets of the membrane attack complex C5b-9 [26]. Treatment of immortalized murine podocytes with C5b-9 complex increased ROS production. Immunostaining confirmed the presence of the subunit $p47^{phox}$ in podocytes and showed its translocation to the plasma membrane after C5b-9 assembly [18]. It implies that NADPH oxidase-mediated ROS induced podocyte injury in MN.

4.2. Diabetic Nephropathy. It is widely accepted that oxidative stress is a key component in the development of diabetic nephropathy. NADPH oxidases are the main source of ROS in the diabetic kidney. In rat models of streptozotocin-induced diabetic nephropathy, the expression of $p47^{phox}$, $p22^{phox}$, and NOX4 was found upregulated in glomeruli [27]. Podocyte injury has been intensively studied in diabetic nephropathy. Studies using an in vitro model show high glucose-induced NADPH oxidase level and activity elevation, NOX4 upregulation, SOD production, caspase-3 activation, and apoptosis induction in podocyte [13–17, 28]. The accumulation of plasma AOPPs is prevalent in diabetes. Increasing the amount of AOPPs in the media of conditionally immortalized podocytes rapidly triggered the production of intracellular superoxide by activation of NADPH oxidase, and led to podocyte apoptosis [29]. Interestingly, recent studies show that insulin treatment increased the generation of H_2O_2, the surface expression of the NADPH oxidase, NOX4, and TRPC6 channels in cultured podocytes [22, 30]. These results suggest that NOX4 may play a role in insulin signaling via TRPC6 channels and may induce insulin resistance in podocytes in diabetic nephropathy.

4.3. Hyperhomocysteinemia. Li's team and others have demonstrated that oxidative stress mediated by NADPH oxidase is importantly involved in the progression of glomerular injury associated with hyperhomocysteinemia (hHcys) [31, 32]. Recently, Li et al. found that hHcys induced NOX2 and $p47^{phox}$ expression, NADPH oxidase activation, and superoxide production in immortalized murine podocytes [20, 21, 33, 34]. In addition, hHcys activates lipid raft (LR) clustering which leads to aggregation and assembling of NADPH oxidase subunits to form an active enzyme complex to produce ROS [21].

4.4. Others. It was confirmed that NADPH oxidase-derived ROS was induced by NMDA receptor activation in neurons [35], and lately similar results were found in kidney [10]. Recent studies demonstrated that sustained application of NMDA triggered cultured immortalized mouse podocytes produce ROS, associated with increased cell surface expression of $p47^{phox}$ and TRPC6 channels and reduced total and cell surface expression of podocyte slit diaphragm proteins nephrin and podocin without loss of cells [25]. Since NMDA receptor and TRPC6 channels are related to calcium entry in podocytes [36], it is possible that elevation of the intracellular Ca^{2+} concentration may also activate NADPH oxidase in podocytes.

5. Role of NADPH Oxidase in Podocyte Injury

5.1. Renin-Angiotensin-Aldosterone System. It is noteworthy that podocytes express a functional intrinsic renin-angiotensin-aldosterone system (RAAS) characterized by neprilysin, aminopeptidase A, angiotensin converting enzyme (ACE), prorenin receptor (PRR), renin, and mineralocorticoid receptor (MR), implying a local RAAS in the glomerulus [12, 37]. Previous researches have addressed that ANG II activation of the angiotensin type 1 receptor (AT1R) leads to oxidative stress [38], which is linked to glomerular injury. Moreover, recent evidence indicates that NADPH oxidase was associated with RAAS-induced podocyte and filtration barrier injury [39]. TG (mRen2)27 (Ren2) transgenic rat is a rodent model that overexpresses the mouse rennin gene, exhibits increased RAAS activity, elevated ANG II levels, and oxidative stress [40, 41]. Whaley-Connell et al. demonstrated that increases in kidney cortical tissue ANG II, AT_1R, and total NADPH oxidase activity submits (NOX2, $p67^{phox}$, $p47^{phox}$, and Rac1) expression, ROS production, podocyte effacement, and loss of the slit-pore diaphragm integrity in Ren2 rats compared with age-matched Sprague-Dawley (S-D) rats [39, 42]. Furthermore, the same team found that direct rennin inhibition, AT_1R blockade, and MR antagonism could attenuate increased NADPH oxidase activity and submit expression, accompanied by restore podocyte slit diaphragm protein nephrin expression and ultrastructural changes in Ren2 rats [43, 44]. In addition, Fujita's team discovered aldosterone involved podocyte injury [45, 46]. They first explored the presence of MR in podocytes in vivo and in vitro [12]. To study aldosterone-induced podocyte injury, uninephrectomized rats were continuously infused with aldosterone and fed a high-salt diet. It was found that increased $p67^{phox}$, Rac1, NOX2, $p47^{phox}$, and $p22^{phox}$ gene expressions, ROS overproduction, decreased nephrin and podocin expressions, and enhanced expression of aldosterone effector kinase Sgk1 in aldosterone-infused rats could be prevented by treatment of eplerenone, a selective aldosterone receptor blocker [12]. Furthermore, spironolactone, a MR antagonist, inhibited aldosterone induced $p67^{phox}$ translocation and oxidative stress generation in cultured podocytes with consistent expression of MR [12]. Data from these investigations highlight the importance of NADPH oxidase in RAAS-mediated podocyte injury.

5.2. Epithelial-to-Mesenchymal Transition. Studies from different laboratories have demonstrated that podocytes could undergo an epithelial-to-mesenchymal transition (EMT) process when challenged by different injurious stimuli, such as transforming growth factor-β1 (TGF-β1) [47, 48], high glucose [49], adriamycin [47], hcys [19, 20], and mesangial medium from IgA nephropathy patients [50]. Recent studies showed that NOX2 [51], NOX1 [52], NOX4 [53], and Rac1b [54] were related to EMT in different types of epithelial cells, implying that NADPH oxidase-derived ROS may promote activation of the EMT program. Emerging evidence suggests that hHcys induces podocytes to undergo EMT through the activation of NADPH oxidase [19]. EMT in conditionally immortalized mouse podocytes was shown by marked decreases in slit diaphragm-associated protein P-cadherin and zonula occludens-1 (ZO-1) as epithelial markers and by dramatic increases in the expression of mesenchymal markers, fibroblast specific protein-1 and α-smooth muscle actin (α-SMA). These phenotype changes in podocytes induced by Hcys were accompanied by enhanced superoxide production, which was substantially suppressed by NADPH oxidase inhibition. In wild wildtype ($gp91^{+/+}$) mice, hHcys induced enhanced expression of mesenchymal markers but decreased expression of epithelial markers of podocytes in glomeruli, which were not observed in mice lacking NOX2 ($gp91^{-/-}$) [19]. Recently, Li et al. found that Hcys-induced superoxide production via NADPH oxidase was significantly inhibited by growth hormone (GH), and hcys failed to induce podocyte EMT by GH treatment [20]. These results indicated that NOX-mediated ROS generation is critically involved in mediating podocyte EMT and consequent glomerular functional impairment.

5.3. Inflammation. The phagocyte NADPH oxidase NOX2 was initially implicated in innate immunity and inflammation. NOX is recognized as a critical mediator of inflammatory responses in nonimmune systems, such as neuroinflammation, gastric inflammation, colon inflammation, lung inflammation, and vascular inflammation. An anti-inflammatory activity of NOX enzymes, also mentioned in NOX2- and $p47^{phox}$-dificient mice, found that LPS-induced systemic inflammatory responses were significantly enhanced by genetic deficiency of NOX [55]. However, the precise molecular mechanisms accountable for the installation of NADPH oxidase-mediated inflammation are still

an unsettled issue. Huber et al. reported that podocytes in culture and podocytes in human kidney sections express a set of chemokine receptors. And chemokine stimulation of the expressed CCRs (CCR4, CCR8, CCR9, and CCR10) and CXCRs (CXCR1, CXCR3, CXCR4, and CXCR5) increased activity of NADPH oxidase and formation of superoxide anions in cultured human podocytes [11]. Moreover, Hu et al. have examined oxidative stress and inflammation in kidney in rats that fed on high fructose, the results showed inflammatory cytokines tumor necrosis factor α (TNF-α) and interleukin 6 (IL-6); oxidative stress index NOX2 and $p22^{phox}$ were upregulated in kidney, which could be partly restored by farnesoid X receptor (FXR) agonist chenodeoxycholic acid (CDCA) treatment [56]. Induction of proinflammatory cytokine granulocyte macrophage-colony-stimulating factor (GM-CSF) was found in cultured podocytes exposed to ROS [57]. Recent observations from Zhang et al. indicated that NADPH oxidase-derived superoxide production may be an important mechanism mediating hHcys-induced NOD-like receptor protein (NALP3) inflammasome activation in podocytes [58, 59]. Since inflammasome formation and activation may be crucial mechanisms mediating a renal inflammatory response that may directly cause podocyte dysfunction, it is plausible that NADPH oxidase activation is an important early mechanism triggering or promoting podocyte inflammatory injury, leading to glomerularsclerosis.

6. Therapeutic Interventions of NADPH Oxidase

6.1. NADPH Oxidase Inhibitors. Pharmacological NADPH oxidase inhibitors have been used for many years, such as apocynin, diphenylene iodonium (DPI), and 4-(2-aminoethyl)-benzenesulfonylfluorid (AEBSF). NADPH oxidase inhibition by Apocynin or DPI could attenuate podocyte injury [18, 23, 59, 60]. However, these inhibitors are not specific for NADPH oxidase. Triazolo pyrimidines, represented by the commercially available VAS2870 and its derivative VAS3947, were the first reported selective NADPH oxidase inhibitors [61]. Furthermore, several NADPH oxidase subunit-specific inhibitors have been discovered [62, 63]. Vendrov et al. have shown that GKT136901, a specific inhibitor of NOX1 and NOX4, attenuates ROS generation and atherosclerosis in atherosclerotic lesions [64]. Recently, NOX4 inhibitors with good oral bioavailability were explored for the potential treatment of fibrotic diseases [65]. To date, no evidence shows podocyte protect effects of NADPH oxidase-specific inhibitors. It should be further investigated.

6.2. Statins. Statins, also known as 3-Hydroxy-3-methylglutaryl (HMG)-coenzyme A (CoA) reductase inhibitors, exert beneficial actions on oxidative stress independent cholesterol-lowering effects. Statins have an indirect NOX inhibitory action by preventing the isoprenylation of Rac1 [66]. In the Zucker obese rats, a homeostasis model includes assessment-insulin resistance index, rosuvastatin treatment improved albuminuria, podocyte foot process effacement, and NADPH oxidase activity via superoxide dismutase [67]. Moreover, rosuvastatin treatment normalized nephrin expression in Ren2 rats, and attenuated ANG II-dependent increases in NADPH oxidase activity and subunit expression (NOX2, NOX4, Rac1, and $p22^{phox}$) and ROS generation in cultured podocytes [9]. Pretreatment with pitavastatin showed similar podocyte protect effects in Dahl salt-sensitive rats and cultured podocytes via restoring NADPH subunits expression [68].

6.3. RAAS Inhibitors. Accumulating evidence reveals that drugs inhibit the RAAS system, including rennin inhibitors, ACE inhibitors (ACEI), AT1R blockers (ARB), aldosterone receptor blocker, and MR antagonist, reduce kidney oxidative stress by the inhibition of NADPH oxidase. Notably, recent study showed that losartan metabolite EXP3179 blocked NADPH oxidase-mediated ROS production [69]. The metabolite may confer to losartan the specific capacity of reduce oxidative stress through NADPH oxidase regulation.

6.4. Traditional Chinese Medicine. Triptolide, a major active component of Tripterygium wilfordii Hook F, has potent anti-inflammatory [70] and podocyte protect effects [71]. Recently, Chen et al. have shown that triptolide treatment restored the foot process effacement in PHN rats and inhibited ROS generation and $p47^{phox}$ migration to the podocyte cellular plasma after C5b-9 treatment in vitro [18]. It implyies triptolide interfere with NADPH oxidase activation or expression, thus supports the pleiotropy of the Chinese medicinal herb.

7. Conclusions

In conclusion, NADPH oxidase appears to be one of the most promising targets to attenuate podocyte injury. Oxidative stress is a common mechanism of CKD [72]. Restore podocyte injury in the early stage will be helpful to prevent CKD patients progress to ESRD. DATA from experimental models showed that the activation of NADPH oxidase in podocytes could be partly blocked by statins [9, 68], ARB [69], and triptolide [18]. It implies that the protection effects of such drugs in podocytes may include various mechanisms. Furthermore, tissue specific, isoform-selective NADPH oxidase inhibitors will be explored in elucidating the full therapeutic potential of NADPH oxidase in the progression of kidney diseases.

Conflict of Interests

The authors declare no conflict of interests.

Acknowledgments

This work was supported by Grants from the National Natural Science Foundation of China (no. 30871174, no. 81170662, no. 81170600, and no. 81300604), the Natural Science Foundation of Hubei Province (no. 2013CFA026), the Doctoral Fund of Ministry of Education of China (20130142110064), and a Young Teacher Grant from Huazhong University of Science and Technology (no. 2012QN226).

References

[1] S. J. Shankland, "The podocyte's response to injury: role in proteinuria and glomerulosclerosis," *Kidney International*, vol. 69, no. 12, pp. 2131–2147, 2006.

[2] K. Tryggvason, J. Patrakka, and J. Wartiovaara, "Hereditary proteinuria syndromes and mechanisms of proteinuria," *The New England Journal of Medicine*, vol. 354, no. 13, pp. 1387–1401, 2006.

[3] S. V. Shah, R. Baliga, M. Rajapurkar, and V. A. Fonseca, "Oxidants in chronic kidney disease," *Journal of the American Society of Nephrology*, vol. 18, no. 1, pp. 16–28, 2007.

[4] K. Bedard and K.-H. Krause, "The NOX family of ROS-generating NADPH oxidases: physiology and pathophysiology," *Physiological Reviews*, vol. 87, no. 1, pp. 245–313, 2007.

[5] D. Wang, Y. Chen, T. Chabrashvili et al., "Role of oxidative stress in endothelial dysfunction and enhanced responses to angiotensin II of afferent arterioles from rabbits infused with angiotensin II," *Journal of the American Society of Nephrology*, vol. 14, no. 11, pp. 2783–2789, 2003.

[6] S. Altenhofer, P. W. Kleikers, K. A. Radermacher et al., "The NOX toolbox: validating the role of NADPH oxidases in physiology and disease," *Cellular and Molecular Life Sciences*, vol. 69, pp. 2327–2343, 2012.

[7] P. Modlinger, T. Chabrashvili, P. S. Gill et al., "RNA silencing in vivo reveals role of $p22^{phox}$ in rat angiotensin slow pressor response," *Hypertension*, vol. 47, no. 2, pp. 238–244, 2006.

[8] S. Greiber, T. Münzel, S. Kästner, B. Müller, P. Schollmeyer, and H. Pavenstädt, "NAD(P)H oxidase activity in cultured human podocytes: effects of adenosine triphosphate," *Kidney International*, vol. 53, no. 3, pp. 654–663, 1998.

[9] A. Whaley-Connell, J. Habibi, R. Nistala et al., "Attenuation of NADPH oxidase activation and glomerular filtration barrier remodeling with statin treatment," *Hypertension*, vol. 51, no. 2, pp. 474–480, 2008.

[10] C. Zhang, F. Yi, M. Xia et al., "NMDA receptor-mediated activation of NADPH oxidase and glomerulosclerosis in hyperhomocysteinemic rats," *Antioxidants and Redox Signaling*, vol. 13, no. 7, pp. 975–986, 2010.

[11] T. B. Huber, H. C. Reinhardt, M. Exner et al., "Expression of functional CCR and CXCR chemokine receptors in podocytes," *Journal of Immunology*, vol. 168, no. 12, pp. 6244–6252, 2002.

[12] S. Shibata, M. Nagase, S. Yoshida, H. Kawachi, and T. Fujita, "Podocyte as the target for aldosterone: roles of oxidative stress and Sgk1," *Hypertension*, vol. 49, no. 2, pp. 355–364, 2007.

[13] J. Xu, Z. Li, P. Xu, and Z. Yang, "Protective effects of leukemia inhibitory factor against oxidative stress during high glucose-induced apoptosis in podocytes," *Cell Stress Chaperones*, vol. 17, pp. 485–493, 2012.

[14] J. Toyonaga, K. Tsuruya, H. Ikeda et al., "Spironolactone inhibits hyperglycemia-induced podocyte injury by attenuating ROS production," *Nephrology Dialysis Transplantation*, vol. 26, no. 8, pp. 2475–2484, 2011.

[15] A. A. Eid, B. M. Ford, K. Block et al., "AMP-activated Protein Kinase (AMPK) negatively regulates Nox4-dependent activation of p53 and epithelial cell apoptosis in diabetes," *The Journal of Biological Chemistry*, vol. 285, no. 48, pp. 37503–37512, 2010.

[16] A. Piwkowska, D. Rogacka, M. Jankowski, M. H. Dominiczak, J. K. Stepiński, and S. Angielski, "Metformin induces suppression of NAD(P)H oxidase activity in podocytes," *Biochemical and Biophysical Research Communications*, vol. 393, no. 2, pp. 268–273, 2010.

[17] K. Susztak, A. C. Raff, M. Schiffer, and E. P. Böttinger, "Glucose-induced reactive oxygen species cause apoptosis of podocytes and podocyte depletion at the onset of diabetic nephropathy," *Diabetes*, vol. 55, no. 1, pp. 225–233, 2006.

[18] Z.-H. Chen, W.-S. Qin, C.-H. Zeng et al., "Triptolide reduces proteinuria in experimental membranous nephropathy and protects against C5b-9-induced podocyte injury in vitro," *Kidney International*, vol. 77, no. 11, pp. 974–988, 2010.

[19] C. Zhang, M. Xia, K. M. Boini et al., "Epithelial-to-mesenchymal transition in podocytes mediated by activation of NADPH oxidase in hyperhomocysteinemia," *Pflügers Archiv—European Journal of Physiology*, vol. 462, no. 3, pp. 455–467, 2011.

[20] C.-X. Li, M. Xia, W.-Q. Han et al., "Reversal by growth hormone of homocysteine-induced epithelial-to- mesenchymal transition through membrane raft-redox signaling in podocytes," *Cellular Physiology and Biochemistry*, vol. 27, no. 6, pp. 691–702, 2011.

[21] C. Zhang, J.-J. Hu, M. Xia, K. M. Boini, C. Brimson, and P.-L. Li, "Redox signaling via lipid raft clustering in homocysteine-induced injury of podocytes," *Biochimica et Biophysica Acta*, vol. 1803, no. 4, pp. 482–491, 2010.

[22] E. Y. Kim, M. Anderson, and S. E. Dryer, "Insulin increases surface expression of TRPC6 channels in podocytes: role of NADPH oxidases and reactive oxygen species," *American Journal of Physiology—Renal Physiology*, vol. 302, no. 3, pp. F298–F307, 2012.

[23] Q. Yan, K. Gao, Y. Chi et al., "NADPH oxidase-mediated upregulation of connexin43 contributes to podocyte injury," *Free Radical Biology and Medicine*, vol. 53, pp. 1286–1297, 2012.

[24] Z. Wang, X. Wei, Y. Zhang et al., "NADPH oxidase-derived ROS contributes to upregulation of TRPC6 expression in puromycin aminonucleoside-induced podocyte injury," *Cellular Physiology and Biochemistry*, vol. 24, no. 5-6, pp. 619–626, 2009.

[25] E. Y. Kim, M. Anderson, and S. E. Dryer, "Sustained activation of N-methyl-D-aspartate receptors in podoctyes leads to oxidative stress, mobilization of transient receptor potential canonical 6 channels, nuclear factor of activated T cells activation, and apoptotic cell death," *Molecular Pharmacology*, vol. 82, no. 4, pp. 728–737, 2012.

[26] C. Ponticelli, "Membranous nephropathy," *Journal of Nephrology*, vol. 20, no. 3, pp. 268–287, 2007.

[27] T. Etoh, T. Inoguchi, M. Kakimoto et al., "Increased expression of NAD(P)H oxidase subunits, NOX4 and $p22^{phox}$, in the kidney of streptozotocin-induced diabetic rats and its reversibity by interventive insulin treatment," *Diabetologia*, vol. 46, no. 10, pp. 1428–1437, 2003.

[28] A. A. Eid, Y. Gorin, B. M. Fagg et al., "Mechanisms of podocyte injury in diabetes role of cytochrome P450 and NADPH oxidases," *Diabetes*, vol. 58, no. 5, pp. 1201–1211, 2009.

[29] L. L. Zhou, F. F. Hou, G. B. Wang et al., "Accumulation of advanced oxidation protein products induces podocyte apoptosis and deletion through NADPH-dependent mechanisms," *Kidney International*, vol. 76, no. 11, pp. 1148–1160, 2009.

[30] A. M. Johnson and J. M. Olefsky, "The origins and drivers of insulin resistance," *Cell*, vol. 152, pp. 673–684, 2013.

[31] F. Yi, M. Xia, N. Li, C. Zhang, L. Tang, and P.-L. Li, "Contribution of guanine nucleotide exchange factor Vav2 to hyperhomocysteinemic glomerulosclerosis in rats," *Hypertension*, vol. 53, no. 1, pp. 90–96, 2009.

[32] Z.-Z. Yang and A.-P. Zou, "Homocysteine enhances TIMP-1 expression and cell proliferation associated with NADH oxidase

in rat mesangial cells," *Kidney International*, vol. 63, no. 3, pp. 1012–1020, 2003.

[33] C. Zhang, J.-J. Hu, M. Xia et al., "Protection of podocytes from hyperhomocysteinemia-induced injury by deletion of the gp91^{phox} gene," *Free Radical Biology and Medicine*, vol. 48, no. 8, pp. 1109–1117, 2010.

[34] K. M. Boini, M. Xia, C. Li et al., "Acid sphingomyelinase gene deficiency ameliorates the hyperhomocysteinemia- induced glomerular injury in mice," *American Journal of Pathology*, vol. 179, no. 5, pp. 2210–2219, 2011.

[35] A. M. Brennan, S. W. Suh, S. J. Won et al., "NADPH oxidase is the primary source of superoxide induced by NMDA receptor activation," *Nature Neuroscience*, vol. 12, no. 7, pp. 857–863, 2009.

[36] S. Chen, F.-F. He, H. Wang et al., "Calcium entry via TRPC6 mediates albumin overload-induced endoplasmic reticulum stress and apoptosis in podocytes," *Cell Calcium*, vol. 50, no. 6, pp. 523–529, 2011.

[37] J. C. Q. Velez, A. M. Bland, J. M. Arthur, J. R. Raymond, and M. G. Janech, "Characterization of renin-angiotensin system enzyme activities in cultured mouse podocytes," *American Journal of Physiology—Renal Physiology*, vol. 293, no. 1, pp. F398–F407, 2007.

[38] K. K. Griendling and M. Ushio-Fukai, "Reactive oxygen species as mediators of angiotensin II signaling," *Regulatory Peptides*, vol. 91, no. 1–3, pp. 21–27, 2000.

[39] A. T. Whaley-Connell, N. A. Chowdhury, M. R. Hayden et al., "Oxidative stress and glomerular filtration barrier injury: role of the renin-angiotensin system in the Ren2 transgenic rat," *American Journal of Physiology—Renal Physiology*, vol. 291, no. 6, pp. F1308–F1314, 2006.

[40] M. C. Blendea, D. Jacobs, C. S. Stump et al., "Abrogation of oxidative stress improves insulin sensitivity in the Ren-2 rat model of tissue angiotensin II overexpression," *American Journal of Physiology—Endocrinology and Metabolism*, vol. 288, no. 2, pp. E353–E359, 2005.

[41] D. J. Campbell, P. Rong, A. Kladis, B. Rees, D. Ganten, and S. L. Skinner, "Angiotensin and bradykinin peptides in the TGR(mRen-2)27 rat," *Hypertension*, vol. 25, no. 5, pp. 1014–1020, 1995.

[42] A. Whaley-Connell, J. Habibi, M. Johnson et al., "Nebivolol reduces proteinuria and renal NADPH oxidase-generated reactive oxygen species in the transgenic Ren2 rat," *American Journal of Nephrology*, vol. 30, no. 4, pp. 354–360, 2009.

[43] A. Whaley-Connell, R. Nistala, J. Habibi et al., "Comparative effect of direct renin inhibition and AT1R blockade on glomerular filtration barrier injury in the transgenic Ren2 rat," *American Journal of Physiology—Renal Physiology*, vol. 298, no. 3, pp. F655–F661, 2010.

[44] A. Whaley-Connell, J. Habibi, Y. Wei et al., "Mineralocorticoid receptor antagonism attenuates glomerular filtration barrier remodeling in the transgenic Ren2 rat," *American Journal of Physiology—Renal Physiology*, vol. 296, no. 5, pp. F1013–F1022, 2009.

[45] M. Nagase, H. Matsui, S. Shibata, T. Gotoda, and T. Fujita, "Salt-induced nephropathy in obese spontaneously hypertensive rats via paradoxical activation of the mineralocorticoid receptor: role of oxidative stress," *Hypertension*, vol. 50, no. 5, pp. 877–883, 2007.

[46] M. Nagase and T. Fujita, "Aldosterone and glomerular podocyte injury," *Clinical and Experimental Nephrology*, vol. 12, no. 4, pp. 233–242, 2008.

[47] Y. S. Kang, Y. Li, C. Dai, L. P. Kiss, C. Wu, and Y. Liu, "Inhibition of integrin-linked kinase blocks podocyte epithelial-mesenchymal transition and ameliorates proteinuria," *Kidney International*, vol. 78, no. 4, pp. 363–373, 2010.

[48] R. Sam, L. Wanna, K. P. Gudehithlu et al., "Glomerular epithelial cells transform to myofibroblasts: early but not late removal of TGF-β1 reverses transformation," *Translational Research*, vol. 148, no. 3, pp. 142–148, 2006.

[49] H.-Y. Dai, M. Zheng, L.-L. Lv et al., "The roles of connective tissue growth factor and integrin-linked kinase in high glucose-induced phenotypic alterations of podocytes," *Journal of Cellular Biochemistry*, vol. 113, no. 1, pp. 293–301, 2012.

[50] C. Wang, X. Liu, Z. Ke et al., "Mesangial medium from IgA nephropathy patients induces podocyte epithelial-to-mesenchymal transition through activation of the phosphatidyl inositol-3-kinase/Akt signaling pathway," *Cellular Physiology and Biochemistry*, vol. 29, pp. 743–752, 2012.

[51] A. Djamali, S. Reese, O. Hafez et al., "Nox2 is a mediator of chronic CsA nephrotoxicity," *American Journal of Transplantation*, vol. 12, no. 8, pp. 1997–2007, 2012.

[52] F. Liu, A. M. Gomez Garcia, and F. L. Meyskens Jr., "NADPH oxidase 1 overexpression enhances invasion via matrix metalloproteinase-2 and epithelial-mesenchymal transition in melanoma cells," *Journal of Investigative Dermatology*, vol. 132, pp. 2033–2041, 2012.

[53] H. E. Boudreau, B. W. Casterline, B. Rada, A. Korzeniowska, and T. L. Leto, "Nox4 involvement in TGF-beta and SMAD3-driven induction of the epithelial-to-mesenchymal transition and migration of breast epithelial cells," *Free Radical Biology and Medicine*, vol. 53, pp. 1489–1499, 2012.

[54] K. Lee, Q. K. Chen, C. Lui, M. A. Cichon, D. C. Radisky, and C. M. Nelson, "Matrix compliance regulates Rac1b localization, NADPH oxidase assembly, and epithelial-mesenchymal transition," *Molecular Biology of the Cell*, vol. 23, no. 20, pp. 4097–4108, 2012.

[55] W.-J. Zhang, H. Wei, and B. Frei, "Genetic deficiency of NADPH oxidase does not diminish, but rather enhances, LPS-induced acute inflammatory responses in vivo," *Free Radical Biology and Medicine*, vol. 46, no. 6, pp. 791–798, 2009.

[56] Z. Hu, L. Ren, C. Wang, B. Liu, and G. Song, "Effect of chenodeoxycholic acid on fibrosis, inflammation and oxidative stress in kidney in high-fructose-fed Wistar rats," *Kidney & Blood Pressure Research*, vol. 36, no. 1, pp. 85–97, 2012.

[57] S. Greiber, B. Müller, P. Daemisch, and H. Pavenstädt, "Reactive oxygen species alter gene expression in podocytes: induction of granulocyte macrophage-colony-stimulating factor," *Journal of the American Society of Nephrology*, vol. 13, no. 1, pp. 86–95, 2002.

[58] C. Zhang, K. M. Boini, M. Xia et al., "Activation of Nod-like receptor protein 3 inflammasomes turns on podocyte injury and glomerular sclerosis in hyperhomocysteinemia," *Hypertension*, vol. 60, pp. 154–162, 2012.

[59] J. M. Abais, C. Zhang, M. Xia et al., "NADPH oxidase-mediated triggering of inflammasome activation in mouse podocytes and glomeruli during hyperhomocysteinemia," *Antioxidants & Redox Signaling*, vol. 18, no. 13, pp. 1537–1548, 2013.

[60] S. Kinugasa, A. Tojo, T. Sakai et al., "Selective albuminuria via podocyte albumin transport in puromycin nephrotic rats is attenuated by an inhibitor of NADPH oxidase," *Kidney International*, vol. 80, no. 12, pp. 1328–1338, 2011.

[61] S. Wind, K. Beuerlein, T. Eucker et al., "Comparative pharmacology of chemically distinct NADPH oxidase inhibitors,"

British Journal of Pharmacology, vol. 161, no. 4, pp. 885–898, 2010.

[62] D. Gianni, N. Taulet, H. Zhang et al., "A novel and specific NADPH oxidase-1 (Nox1) small-molecule inhibitor blocks the formation of functional invadopodia in human colon cancer cells," *ACS Chemical Biology*, vol. 5, no. 10, pp. 981–993, 2010.

[63] S. S. Bhandarkar, M. Jaconi, L. E. Fried et al., "Fulvene-5 potently inhibits NADPH oxidase 4 and blocks the growth of endothelial tumors in mice," *The Journal of Clinical Investigation*, vol. 119, no. 8, pp. 2359–2365, 2009.

[64] A. E. Vendrov, N. R. Madamanchi, X.-L. Niu et al., "NADPH oxidases regulate CD44 and hyaluronic acid expression in thrombin-treated vascular smooth muscle cells and in atherosclerosis," *The Journal of Biological Chemistry*, vol. 285, no. 34, pp. 26545–26557, 2010.

[65] B. Laleu, F. Gaggini, M. Orchard et al., "First in class, potent, and orally bioavailable NADPH oxidase isoform 4 (Nox4) inhibitors for the treatment of idiopathic pulmonary fibrosis," *Journal of Medicinal Chemistry*, vol. 53, no. 21, pp. 7715–7730, 2010.

[66] A. Manea, "NADPH oxidase-derived reactive oxygen species: involvement in vascular physiology and pathology," *Cell and Tissue Research*, vol. 342, no. 3, pp. 325–339, 2010.

[67] A. Whaley-Connell, V. G. Demarco, G. Lastra et al., "Insulin resistance, oxidative stress, and podocyte injury: role of rosuvastatin modulation of filtration barrier injury," *American Journal of Nephrology*, vol. 28, no. 1, pp. 67–75, 2007.

[68] X. W. Cheng, M. Kuzuya, T. Sasaki et al., "Inhibition of mineralocorticoid receptor is a renoprotective effect of the 3-hydroxy-3-methylglutaryl-coenzyme A reductase inhibitor pitavastatin," *Journal of Hypertension*, vol. 29, no. 3, pp. 542–552, 2011.

[69] A. Fortuno, J. Bidegain, P. A. Robador et al., "Losartan metabolite EXP3179 blocks NADPH oxidase-mediated superoxide production by inhibiting protein kinase C: potential clinical implications in hypertension," *Hypertension*, vol. 54, pp. 744–750, 2009.

[70] D. Qui and P. N. Kao, "Immunosuppressive and anti-inflammatory mechanisms of triptolide, the principal active diterpenoid from the Chinese medicinal herb Tripterygium wilfordii Hook. f," *Drugs in R and D*, vol. 4, no. 1, pp. 1–18, 2003.

[71] C.-X. Zheng, Z.-H. Chen, C.-H. Zeng, W.-S. Qin, L.-S. Li, and Z.-H. Liu, "Triptolide protects podocytes from puromycin aminonucleoside induced injury in vivo and in vitro," *Kidney International*, vol. 74, no. 5, pp. 596–612, 2008.

[72] N. D. Vaziri, "Roles of oxidative stress and antioxidant therapy in chronic kidney disease and hypertension," *Current Opinion in Nephrology and Hypertension*, vol. 13, no. 1, pp. 93–99, 2004.

Hindawi Publishing Corporation
BioMed Research International
Volume 2013, Article ID 824656, 12 pages
http://dx.doi.org/10.1155/2013/824656

Research Article

Oxidative Damage and Mutagenic Potency of Fast Neutron and UV-B Radiation in Pollen Mother Cells and Seed Yield of *Vicia faba* L.

Ekram Abdel Haliem,[1,2] Hanan Abdullah,[3] and Asma A. AL-Huqail[2]

[1] *Plant Cytogenetic and Molecular Biology, Botany Department, Science College, Zagazig University, P.O. Box 44519, Zagazig 308213, Egypt*
[2] *Plant Physiology, Botany and Microbiology Department, Science College, King Saud University, P.O. Box 22452, Riyadh 11495, Saudi Arabia*
[3] *Plant Physiology, Botany Department, Science College, Zagazig University, P.O. Box 44519, Zagazig 308213, Egypt*

Correspondence should be addressed to Ekram Abdel Haliem; ekram.esa@gmail.com

Received 11 May 2013; Revised 11 June 2013; Accepted 2 July 2013

Academic Editor: Afaf K. El-Ansary

In recent years, there has been a great deal of attention toward free radicals, reactive oxygen species (ROS) generated by exposure of crop plant cells to physical radiations. Henceforth, the current study was planned to compare oxidative stress and mutagenic potential of different irradiation doses of fast neutron (FN) and UV-B on meiotic-pollen mother cells (PMCs), pollen grains (PGs) and seeds yielded from irradiated faba beans seedlings. On the cytogenetic level, each irradiation type had special interference with DNA of PMC and exhibited wide range of mutagenic action on the frequency and type of chromosomal anomalies, fertility of PGs and seed yield productivity based on the irradiation exposure dose and radiation sensitivity of faba bean plants compared with un-irradiated ones. On the molecular level, SDS-PAGE and RPAD-PCR analyses of seeds yielded from irradiated seedlings exhibited distinctive polymorphisms based on size, intensity, appearance, and disappearance of polypeptides bands compared with un-irradiated ones. The total values of protein and DNA polymorphisms reached 88% and 90.80% respectively. The neutron fluency (2.3×10^6 n/cm^2) and UV-B dose for 1 hr were recorded as bio-positive effects. The present study proved that genetic variations revealed by cytogenetic test could be supported by gene expression (alterations in RAPD and protein profiles).

1. Introduction

It has been known for many years that exposure of crop plant cells under natural conditions of growth and development to physical radiations such as ionizing FN and nonionizing UV-B resulted in excessive production of free radicals ROS [1, 2], respectively. These radiolytic ROS include a wide range of oxygen-radicals, such as superoxide anion ($O_2^{\bullet -}$), hydroxyl radical ($^{\bullet}OH$), perhydroxyl radical ($HO_2^{\bullet}$), and hydrogen peroxide (H_2O_2) [3]. They are highly reactive due to the presence of unpaired valence shell electrons [4] and can result in noncontrolled oxidation in cells, cellular macromolecules compartments including DNA, proteins, lipids, and enzymes [5]. On the other hand, ROS-induced genotoxic damage can induce structural changes in DNA, such as chromosomal rearrangement, strand breaks, base deletions, pyrimidine dimers, cross-links and base modifications, mutations, and other genotoxic effects [5, 6].

Despite the ROS destructive activity, their production in plant tissues is controlled by the very efficient enzymatic and nonenzymatic antioxidant defense systems which serve to keep down the levels of free radicals, permitting them to perform useful biological functions without too much damage and act as a cooperative network employing a series of redox reactions [5, 7]. From these plants, leguminous especially faba bean plant which proved that it has high antioxidant activity due to that they contained phenolic and flavonoid compounds [8–10]. On the other hand, it has a diploid ($2n = 12$) and relatively large chromosomes.

Therefore, it is important model system among the plant bioassays for monitoring or testing environmental pollutants as reviewed by the US Environmental Protection Agency (EPA) Gene Tox program [11] and can detect a wide range of genetic damage, including gene mutations, chromosome aberrations, and DNA strand breaks [12].

Biologically, FN differs from UV-B radiation in the way in which energy is distributed in irradiated tissues and their biological effects in the living cell [1]. Each type of these radiations can induce ROS in cell by special interference with cellular macromolecules (DNA and protein). The effects of these radiations vary depending on the applied dose and sensitivity of living plant cell to the action of radiation type [13]. The biological irradiation by FN based on the interaction with atoms or molecules in living cell, particularly water, to produce free radicals, which induce DNA deletions in nucleus and chromosome that range in size from a few base pairs to several megabases [14]. It is a potent DNA-damaging agent and more efficient in inducing biochemical modification of bases and double strand breaks in DNA by directly ionizing DNA itself or by indirect processes in which DNA reacts with numerous radiolytic reactive products that are generated in aqueous fluid surrounding DNA causing DNA base oxidation and DNA breaks formation (i.e., single-strand breaks, SSBs and double-strand breaks, DSBs) [13, 14]. All these modifications lead to protein denaturation which causes a conformational change in the structure and render them inactive [1]. On the other hand, the strong absorption of the UV-B at (280–320 nm) by DNA and protein in plant cells [15] based on photons which have enough energy to destroy chemical bonds between these macromolecules, causing a photochemical reaction which lead to generation of highly toxic reactive oxygen species (ROS) in cells [2]. Radiolytic ROS induce oxidative DNA damage by oxidative cross linking between adjacent pyrimidine bases forming cyclobutane-pyrimidine dimers (CPDs), 6-4 photoproducts (6-4PPs) and their Dewar valence isomers, that ultimately block the movement of DNA polymerases on DNA template [16–18] and also induce oxidative protein cross-links by alteration of the expression of several genes through nonspecific signaling pathways leading to protein destruction which often causes heritable mutations affecting various physiological processes [5].

It is important for detection of oxidative stress and mutagenic potential of various types of radiations on crop plants, to understand their biological consequences and their molecular action on chromosome, protein, and DNA of plant cell by introducing cytogenetic and molecular assays. Cytogenetic tests are considered to be indicator of cytotoxicity, genotoxicity, genetic variability, and estimation of the mutagen potency in meiotic PMCs and PGs [12, 19]. On the other hand, proteins being primary gene products of plant's DNA hence, any observed variation in protein systems induced by oxidative stresses or any mutagen is considered as a mirror for genetic variations [20]. Determination of protein MWs via polyacrylamide gel electrophoresis in the presence of sodium dodecyl sulfate (SDS-PAGE) is a universally used method in biomedical research [21]. Some studies used SDS-PAGE for detection of alterations in protein profiles occurring during irradiation by UV-B [15, 22]. Furthermore, DNA alterations based on random amplification of polymorphic DNA (RAPD) profiles are a useful biomarker assay for the evaluation of genotoxic and mutagenic effects of radiations on plants especially when the nucleotide sequence is not known [23]. The advantage of RAPD relies on its simplicity, rapidity, a small quantity of DNA, and its ability to generate more number of polymorphic bands, numerous polymorphisms [24], and the observation of the specific band pattern from each primer [25]. Some previous studies used RAPD markers for detection of high levels of genetic polymorphisms by the used radiations [23, 26, 27]. In relation to fast neutron, there are no previous studies that dealt SDS-PAGE and RAPD-PCR for detection of its mutagenic effects and oxidative potential in crop plants.

In light of the previously mentioned, the main goal of this study is to evaluate and compare the effects of various levels of ROS generated by different irradiation doses of FN and UV-B on PMCs, PGs, and seeds yield of irradiated *Vicia faba* seedling on the cytogenetic and molecular levels for a better understanding of their oxidative stress and mutagenic potential in case of accidental or occupational exposure.

2. Materials and Methods

2.1. Plant Material and Germination. Faba bean seeds (*Vicia faba* L. variety Giza 2) were obtained from the Agriculture Research Center in Cairo, Egypt. Seeds were screened for viability and uniformity size and divided into three groups (A, B, and C). Seeds of all groups were sterilized and germinated until seven-day-old seedlings. Seedling of groups (A and B) is irradiated with FN and UV-B (280–320 nm) radiations, respectively, while seedling of group (C) was maintained without irradiation (un-irradiated samples).

2.2. Irradiation Processes. The seedling of group (A) is packed regularly in polyethylene high-density bags and irradiated by fission neutrons from Cf^{252} point source using four fluencies (2.5×10^5, 2.3×10^6, 3×10^7, and 1.5×10^8 n/cm^2). The source was manufactured by Radiochemical Center Amersham, England, and presented at Biophysics Department, Faculty of science, Zagazig University, Egypt. On the other hand, the seedling of group (B) was exposed to a standard laboratory UV-B (280–320 nm) sterile fluorescent lamp of 500/630 μW/cm^2 for different time periods (1/2, 1, 2, 3 hours) at a distance of 30 cm from the irradiated seedling. After irradiation processes, groups (A, B, and C) were subdivided and prepared for cytogenetic and molecular analyses.

2.3. Cytogenetic Analysis of Meiotic PMCs and PGs. Irradiated and un-irradiated seedlings were transferred immediately to soil and sown in rows under field conditions. A spacing of 30 cm row to row and 15 cm plant to plant were maintained. At maturity, ten flower buds from ten plants for each irradiation dose in addition to un-irradiated ones were collected, fixed immediately in Carnoy's fixative (3 : 1) absolute ethyl alcohol : glacial acetic acid for 24 hours and then stored in refrigerator in 70% ethyl alcohol and finally stained using

acido-carmin smear method [28]. Cytogenetic analyses of PMCs selected from six randomly flower buds were scored for 1st and 2nd meiotic anomalies. On the other hand, the pollen fertility test was carried out using the same acido-carmin stain of matured anthers. Pollen grains, which took stain and had a regular outline, were considered as fertile, while empty and unstained ones as sterile [29].

2.4. Seed Yield Measurements. Quantitative parameters of six plants irradiated by the various irradiation doses of FN and UV-B radiation mentioned previously were measured as mean number of pods/plant, mean number of seeds/plant, and mean dry weight of 100 seeds compared with those of un-irradiated one. Seeds yielded from irradiated and un-irradiated plants were harvested and analyzed on molecular level using SDS-PAGE analysis of seed storage proteins and RAPD analysis of seed DNA via the polymerase chain reaction (PCR).

2.5. SDS-PAGE Analysis of Seed Storage Proteins of M_1 Progeny. Seeds yielded from all irradiated faba beans seedlings by FN and UV-B were used for SDS-PAGE analysis.

2.5.1. Seed Cake and Defatted Meal Preparation. Sterilized seeds were milled and defatted according to [30].

2.5.2. Extraction of Seed Storage Proteins and SDS-PAGE Analysis. The protein extraction technique was employed according to [31]. Sample buffer was added to 0.2 g of seed flour as extraction liquid and mixed thoroughly in an Eppendorf tube by vortex. The extraction buffer contained the following final concentration: 0.5 M Tris-HCl, PH 6.8, 2.5% SDS, 5% urea, and 5% 2-mercaptoethanol. Before centrifugation at 10,000 g for 5 min at 4°C, the sample buffer was boiled for 5 min. SDS-PAGE was performed by a standard method on a vertical slab gel. Bromophenol blue was added to the supernatant as tracking dye to watch the movement of protein in the gel. Proteins profiling of samples was performed using SDS-polyacrylamide gels as described by [32]. Seed proteins were analyzed by SDS-PAGE using 10% polyacrylamide gel. After electrophoresis, the protein bands were visualized by staining with Coomassie brilliant blue G-250. Marker proteins (Fermentas) were used as references. The bands produced in the electropherogram were scored, and their molecular weights were compared to the standard Pharmacia protein marker.

2.5.3. Protein Imaging and Data Analysis. Gel photographing and documentation were carried out using Bio-Rad gel documentation system. The number of bands revealed in each gel lane were counted and compared with each other's using Gel Pro-Analyzer. Quantitative variations in band number as well as band concentration were estimated using BIO-RAD Video densitometer, Model Gel Doc 2000.

2.6. RAPD Analysis of Seeds Yield of Irradiated Vicia faba. Seeds yielded from irradiated faba beans seedlings by stimulatory FN fluency 2.3×10^6 and UV-B doses for 1 h and inhibitory FN fluency 1.5×10^8 and UV-B doses for 3 h were used for RAPD analysis.

2.6.1. Isolation of Genomic DNA. Fifty grams of dried seeds of both two doses of FN and UV-B was crushed in a mill and powdered by using a domestic grinder. The powder was sieved using thin mesh and only finely ground powder was kept in refrigerator until DNA extraction. One gram of finely sieved seed powder was taken, and genomic DNA was isolated using Hexadecyl trimethyl ammonium bromide (CTAB) as described by [33].

2.6.2. Quantity and Quality of Isolated DNA. The yield of DNA per gram of seed material extracted was measured by using UV spectrophotometer (Perkin Elmer) at 260 nm and A280 nm. Thepurity of DNA was determined by calculating the ratio of absorbanceat 260/280 nm. For quality and yield assessments, electrophoresis was done of all DNA samples on 0.8% agarose gel, stained with ethidium bromide, and bands were observed in gel documentation system (Alpha Innotech) and compared with the known standard Lambda DNA marker. The gels were visualized and photographed under UV light (Gel documentation system, Bio-Rad).

2.6.3. PCR Amplification Using Random Primers (RAPD). Briefly, the PCR reaction mixture contains 2.5 μL 10x buffer with 15 mM $MgCl_2$ (Fermentas), with 0.25 mM each of dNTP (Sigma), 0.3 μM of the primer, 0.5 unit of Taq DNA polymerase (Sigma), and 50 ng of template DNA. PCR reaction was performed in Palm Cycler (Corbett Research) using the following profile with initial denaturation of 4 min at 95°C followed by 40 cycles of 1 min at 95°C, 1 min at 38°C, and 2 min at 72°C with final extension at 72°C for 10 min and a hold temperature of 4°C at the end. A total of twenty random DNA oligonucleotide primers (10 mer) were independently used in the PCR reactions (UBC, University of British Columbia, Canada) according to [34] with some modifications. Only six primers (A-02, 03, 10, 12, 15, and 17) succeeded to generate reproducible amplified DNA products. The code and sequences of these primers were listed in (Table 4). The amplification products were electrophoresed on 1.5% Agarose gel (Sigma) in TAE buffer (0.04 M Tris-acetate, 1 Mm EDTA, pH 8). The run was performed at 100 V constant voltagesfor one hour. Gels were stained with 0.2 μg/mL ethidium bromide. Bands were detected on UV-transilluminator and photographed by a Polaroid camera.

2.6.4. Data Analysis. Gels were visualized with Photo Print (Vilber Lourmat, France) imaging system, and analysis of RAPD bands was performed by BioOne D++ software (Vilber Lourmat, France). The RAPD bands (markers) were scored as 1 if present and 0 if absent.

3. Results

3.1. Cytogenetic Analysis of Meiotic PMCs and PGs. The ability of fast neutron and UV-B radiation to exert genotoxic action on PMCs DNA in 1st and 2nd meiotic divisions was observed in spite of long period of recovery (Table 1) and (Figure 1,

Table 1: Number, frequencies of abnormal PMCs in 1st and 2nd meiotic divisions, frequencies of meiotic abnormalities, types of abnormal meiotic PMCs, and percentages of fertile PGs after irradiation of *Vicia faba* seedlings by various irradiation doses of FN and UV-B.

Irradiation types	Doses	1st meiotic Division		2nd meiotic division		Total no. of PMCs	Total no. of abnormal PMCs	% of abnormal PMCs ± SE	Types and frequency of meiotic abnormalities of PMCs								PGs	
		Total no. of PMCs	% of abnormal cells	Total no. of PMCs	% of abnormal cells				Stickiness	Disturbed	Unorient.	Micronuclei + fragments	Lagging + free	Bridge	Tripolar	Multipolar	No. of PGs	Mean % of fertility
Un-irradiated	0.00	835	0.00	1050	0.00	1885	0	0	0.00	0.00	0.00	0.00	0.00	0.00	0.00	0.00	600	99.98 ± 0.12
FN fluencies (Φ) n/cm^2	2.5×10^5	541	38.26	339	47.79	880	369	38.80 ± 0.54	19.56	30.37	14.43	13.90	8.52	2.64	9.13	1.60	600	88.90 ± 1.40
	2.3×10^6	446	15.47	505	14.85	951	145	14.23 ± 0.95	25.06	37.95	12.51	5.82	6.71	6.26	3.58	1.12	600	99.96 ± 0.12
	3.0×10^7	515	58.64	440	42.50	955	498	52.15 ± 2.17	25.56	27.37	10.30	13.73	4.61	8.40	7.59	2.44	600	65.10 ± 0.06
	1.5×10^8	412	66.50	336	65.18	748	493	65.91 ± 1.00	41.92	12.47	11.86	15.75	6.95	3.48	4.94	2.69	600	35.88 ± 0.12
UV-B doses μw/cm^2	1/2 h	526	33.08	435	38.39	955	341	35.71 ± 0.79	12.00	7.84	20.85	42.22	3.82	10.04	0.88	2.35	600	81.99 ± 0.02
	1 h	459	21.70	435	19.06	1158	236	20.38 ± 0.54	22.40	5.91	8.93	33.20	4.48	19.55	3.26	3.26	600	96.72 ± 0.25
	2 h	424	49.06	450	43.55	874	404	46.22 ± 1.12	31.68	4.70	8.17	25.57	6.44	20.96	1.49	1.00	600	57.77 ± 0.23
	3 h	680	49.71	421	49.64	1101	607	55.13 ± 0.18	37.50	8.25	10.51	31.16	3.44	6.34	1.27	1.74	600	25.54 ± 0.26

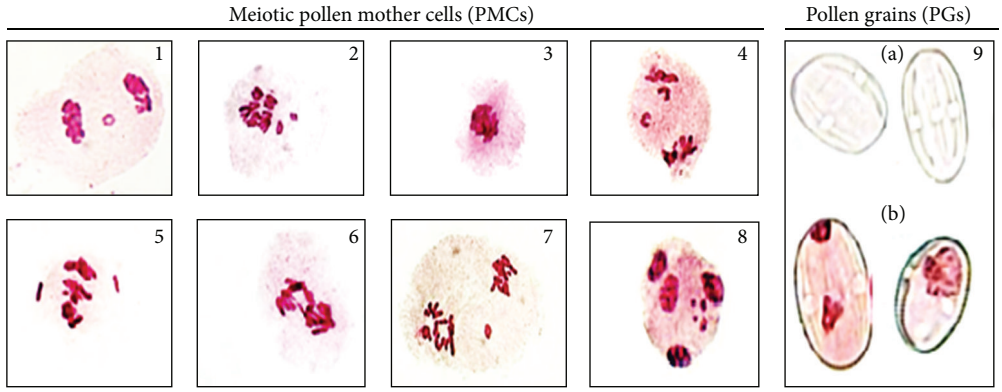

Figure 1: The most common meiotic chromosomal aberrations induced by fast neutron ((1)–(4)) and UV-B radiation ((5)–(8)). (1) Telophase I with micronucleus, (2) disturbed anaphase, (3) sticky metaphase I, (4) sticky anaphase II with two lagging chromosomes, (5) metaphase I with two unoriented chromosomes, (6) sticky anaphase I with bridges, (7) metaphase II with sticky fragment, (8) four micronuclei with sticky telophase II, (9) (a) sterile Pollen grains (colorless), and (b) fertile one (color).

(1)–(8)). Both radiations induced a wide range of meiotic abnormalities extended in 1st and 2nd meiotic divisions after all irradiation doses are compared to un-irradiated samples. Moreover, the types and frequencies of anomalies in meiotic PMCs were linearly linked to the irradiation exposure doses. The maximum values of meiotic-PMCs abnormalities were 65.91 ± 1.00% at FN fluency (1.5×10^8 n/cm^2) and 55.13 ± 0.18% at UV-B dose after 3 hours. The most frequent types of PMCs abnormalities induced by various fluencies of FN were stickiness, chromosomal disturbances, unoriented chromosomes, and chromosomal fragmentation, whereas the anomalies induced by irradiation doses of UV-B were meiotic micronuclei, chromosomal fragmentation, stickiness, and bridges (Figure 1). On the other hands, the pollen grains fertility was dose dependent as evident from its reduction by all irradiation doses of FN and UV-B expect FN fluency (2.3×10^6) and UV-B dose for 1 h compared to un-irradiated one (Table 1) and (Figure 1 (a) and (b)). The maximum reduction of PGs fertility was observed at FN fluency (2.3×10^8) and UV-B dose for 3 h which reached the values of (35.88 ± 0.12% and 25.54±0.26%), respectively; this indicated that the irradiation exposure doses of UV-B were more effectiveness in reduction of PGs fertility than irradiation fluencies of FN. On the other hand, FN fluency (2.3×10^6) and UV-B dose for 1 h showed improvement in the values of PGs fertility reaching (96.95 ± 0.12% and 93.72 ± 0.25%), respectively, nearly similar to the value of un-irradiated sample which reached (99.98 ± 0.12%).

3.2. Parameters of Seed Yield Productivity. The different parameters of seeds yield productivity of irradiated faba beans seedlings that were represented in the mean number of pods/plant, number of seeds/pod, and average weight of 100 seeds/gm were dose-dependent as evident from their reduction by most irradiation doses of FN and UV-B radiations expect FN fluency (2.3×10^6) and UV-B dose after 1 h that showed improvement in parameters of seeds yield productivity (Table 2). This indicated that these doses may be having bio-positive or stimulation effects that can be useful in induction of mutations in faba beans plants.

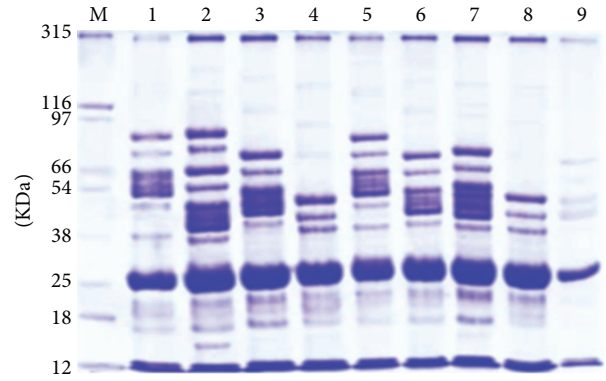

Figure 2: SDS-PAGE banding patterns of storage protein in seeds yielded from irradiated *Vicia faba* seedlings by various doses of fast neutron and UV-B. M: Protein marker, (1) (2.5×10^5 n/cm^2), (2) (2.3×10^6 n/cm^2), (3) (3×10^7 n/cm^2), (4) (1.5×10^8 n/cm^2), (5) un-irradiated seeds, (6) UV-B dose for 1/2 hour, (7) UV-B dose for 1 hour, (8) UV-B dose for 2 hours, and (9) UV-B dose for 3 hours.

3.3. SDS-PAGE Analysis. Each irradiation dose of FN and UV-B used in the current study exhibited distinctive quantitative and qualitative alterations in electrophoretic banding pattern of total seed proteins yielded from irradiated faba bean seedlings compared to un-irradiated ones. These protein alterations are based on changes in bands molecular weights (MWs), bands intensities, fractionation of some bands, appearance of new bands (unique bands), and disappearance of some bands (polymorphic bands) as shown in (Table 3) and (Figure 2). SDS-PAGE analysis revealed total of (111) polypeptides bands with different MWs that ranged from 315 to 12 KDa. Out of which, 22, 3, and 3 bands were polymorphic, unique, and monomorphic bands, respectively. Two unique bands with MWs (175 and 29 KDa) were recorded at FN fluency (2.3×10^6), while one unique band with MW (120 KDa) was observed only at UV-B dose for 1 h. These unique bands can be used as markers for these irradiation

Table 2: The productivity parameters of seeds yielded from irradiated *Vicia faba* seedlings by various irradiation doses of FN and UV-B.

Irradiation types	Doses	Seed yield parameters		
		No. of pods/plant	No. of seeds/plant	Average wt. of 100 seeds/gm
FN fluencies (Φ) n/cm^2	0.00	21 ± 1.90	62 ± 2.23	72.80 ± 1.30
	2.5×10^5	14 ± 2.10	53 ± 1.20	65.60 ± 1.17
	2.3×10^6	28 ± 1.2	70 ± 2.00	80.60 ± 2.30
	3.0×10^7	12 ± 3.10	33 ± 3.21	56.20 ± 3.00
	1.5×10^8	10 ± 1.50	19 ± 1.60	40.20 ± 1.72
UV-B doses μw/cm^2	0.00	21 ± 1.00	62 ± 2.23	72.80 ± 1.30
	1/2 h	15 ± 1.7	45 ± 1.2	56.00 ± 2.33
	1 h	23 ± 2.50	68 ± 2.30	75.43 ± 1.76
	2 h	12 ± 1.5	27 ± 1.50	44.12 ± 2.00
	3 h	8 ± 1.10	11 ± 1.76	28.45 ± 1.66

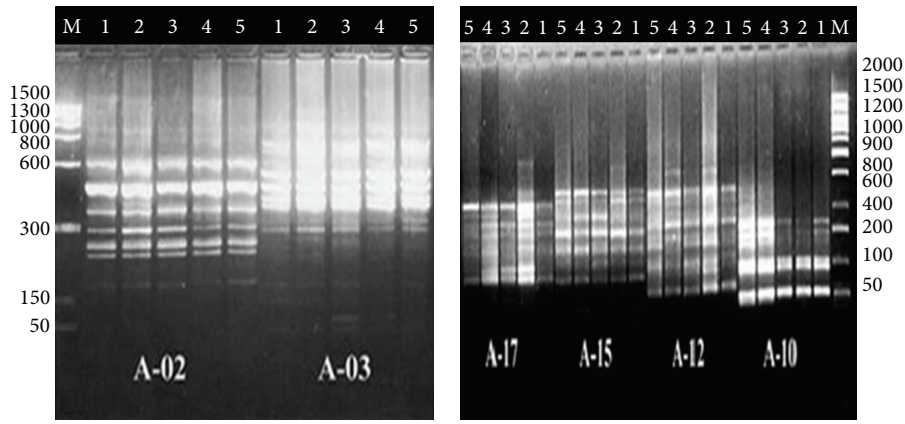

(a) (b)

Figure 3: (a) and (b) DNA banding pattern of RAPD analysis of seeds yielded from irradiated *Vicia faba* seedlings generated by the six primers; (1) (1.5×10^8 n/cm^2), (5) UV-B dose for 3 h as bio-negative irradiation doses, (2) (2.5×10^6 n/cm^2), (4) UV-B dose for 1 h as bio-positive irradiation doses of each FN and UV-B, respectively, and (3) un-irradiated sample. M: Lambda DNA marker.

doses. The total value of polymorphism revealed by SDS-PAGE was (88%). On the other hands, the maximum number of polypeptide bands was (18 bands) with value (16.22%) observed at FN fluency (2.3×10^6), whereas the minimum number of bands was (7 bands) with value (6.31%) observed at UV-B dose for 3 h compared with number of polypeptides bands in un-irradiated sample which reached (14 bands) with value (12.61%).

3.4. RAPD-PCR Analysis. RAPD analysis was employed in the present study to evaluate the extent of the DNA alterations in seeds yielded from irradiated faba beans seedlings by the two bio-positive doses (FN fluency (2.3×10^6) and UV-B dose for 1 h) and the two negative doses (FN fluency (2.3×10^8) and UV-B dose for 3 h). Twenty random primers were used for the RAPD analysis, in which only six primers of them (A-02, 03, 10, 12, 15, and 17) succeeded to produce clear reproducible DNA bands and gave satisfactory results with many alterations in the RAPD profiles as shown in (Table 4) and (Figure 3). In total, two hundred forty-eight (248) reproducible DNA bands were scored after using the six primers (with an average of 41 bands/primer). Out of which 76 bands were polymorphic with value (30.65%), 27 bands were unique with value (10.89%), and 8 bands were monomorphic with value (3.23%). Moreover, the total value of polymorphism generated by six primers reached the value of (90.80%). The maximum number of gene products (60 bands) with value (24.19%) was observed at FN fluency (2.3×10^6), whereas the minimum number of bands (45) with value (18.15%) was at UV-B dose for 3 h. On the other hand, the highest number of gene products (60 bands) was generated by primer A-03, whereas the lowest number (31 bands) was generated by the primer A-17. Furthermore, the highest value of polymorphism (100%) was revealed by the primer A-03, whereas the lowest one (58.82%) is revealed by the primer A-02.

4. Discussion

4.1. Cytogenetic Analysis of Meiotic PMCs, PGs, and Seed Yield Productivity. Cytogenetic test is considered to be indicator of oxidative potential, genotoxicity, and estimation of the mutagen potency in meiotic PMCs and PGs [12, 19]. The present investigation observed that all irradiation exposure

Table 3: Electrophoretic banding analysis of seeds storage proteins yielded from irradiated *Vicia faba* plant by various doses of FN and UV-B.

No.	MW/KDa	Protein marker		Fluencies of FN radiation (n/cm^2)								Un-irritated sample		Various doses of UV-B radiation (μw/cm^2)								Polymorphism types
		Lane M		2.5×10^5 Lane 1		2.3×10^6 Lane 2		3.0×10^7 Lane 3		1.5×10^8 Lane 4		Lane 5		1/2 h Lane 6		1 h Lane 7		2 h Lane 8		3 h Lane 9		
		KDa	%	KDa	%	KDa	%	KDa	%	KDa	%	KDa	%	KDa	%	KDa	%	KDa	%	KDa	%	
1	315	+	+	+	32.77	+	106.58	+	106.84	+	66.82	+	87.95	+	90.73	+	101.3	+	96.49	+	52.91	M
2	181	–	–			–	–	–	–	–	–	+	32.69	–	–	–	–	–	–	–	–	P
3	175	–	–	–	–	+	17.83	–	–	–	–	–	–	–	–	–	–	–	–	–	–	U
4	158	–	–	–	–	–	–	+	16.35	–	–	–	–	+	11.28	+	17.83	+	12.57	–	–	P
5	145	–	–	–	–	–	–	–	–	+	14.3	–	–	–	–	+	10.37	–	–	–	–	P
6	128	–	–	–	–	+	17.83	–	–	–	–	+	15.39	–	–	–	–	–	–	–	–	P
7	120	–	–	–	–	–	–	–	–	–	–	–	–	–	–	+	9.43	–	–	–	–	U
8	116	116	8.86	–	–	+	10.54	+	15.16	–	–	–	–	+	11.28	+	12.48	–	–	–	–	P
9	97	97	29.84	–	–	–	–	–	–	+	9.23	–	–	–	–	–	–	+	9.43	–	–	P
10	86	–	–			+	106.00	+	125.86	+	5.34	+	99.46	–	–	–	–	–	–	–	–	P
11	75	–	–	+	81.51	+	103.47	–	–	–	–	+	99.23	+	114.7	+	118.96	–	–	+	9.22	P
12	66	66	33.00	+	77.69	+	118.97	+	106.00	–	–	+	105.23	+	111.6	+	118.96	–	–	+	–	P
13	60	–	–	–	–	–	–	–	–	–	–	+	128.02	–	–	–	–	–	–	–	7.22	p
14	54	–	–	+	77.69	+	95.21	–	–	–	–	+	126.51	–	–	+	–	–	–	–	–	P
15	50	–	–	+	91.41	+	94.02	+	86.79	–	–	+	117.37	–	–	+	126.51	–	–	–	–	P
16	45	–	–	+	52.69	+	101.95	+	125.54	+	100.21	+	138.29	+	109.63	+	77.41	+	58.55	+	14.84	M
17	40	–	–	+	14.84	–	–	+	38.65	+	73.35	+	56.23	+	55.71	+	77.19	–	–	+	28.59	P
18	38	38	32.88	+	21.36	+	14.57	–	–	–	–	–	–	–	–	–	–	–	–	–	–	P
19	29	–	–	–	–	+	11.62	–	–	–	–	–	–	–	–	–	–	–	–	–	–	U
20	25	–	–	+	225.17	+	232.77	+	266.37	+	256.43	+	267.16	+	261.93	+	237.79	+	231.78	+	–	p
21	23	–	–	–	–	+	19.42	+	41.76	+	77.98	–	–	+	78.44	+	35.64	+	36.11	–	118.23	P
22	18	18	43.44	+	41.76	+	56.82	+	94.7	+	44.88	–	–	+	61.21	–	–	+	29.95	–	–	P
23	16	–	–	+	16.23	+	26.58	+	17.85	+	17.34	+	9.28	+	12.48	+	10.46	+	29.95	–	–	P
24	14	–	–	–	–	+	26.58	–	–	–	–	–	–	–	–	+	11.07	–	–	–	–	P
25	12	12	103.15	+	134.29	+	173.34	+	188.58	+	174.19	+	177.85	+	179.34	+	137.12	+	146.44	+	128.09	M
Total bands of each lane				12		18		13		11		14		12		15		9		7		
% Total bands				10.81		16.22		11.71		9.91		12.61		10.81		13.51		8.11		6.31		

Total protein bands of all lanes = 111	Polymorphic bands		Unique bands		Monomorphic bands		% of polymorphism
	No. of bands	%	No. of bands	%	No. of bands	%	
	22	19.82	3	2.70	3	2.70	88

Table 4: RAPD-PCR amplification products of DNA extracted from seeds yielded from irradiated *Vicia faba* by FN and UV-B using six random primers.

Primers	Sequence of primers from 5′ → 3′	Amplicon lengths (pb)	Total no. of scorable bands					Polymorphic bands									
			Fluencies of fast neutrons radiation (n/cm^2)		Control	Various doses of UV-B radiation (μw/cm^2)		Total no.	% of total bands	No. of unique bands	% of unique bands	No. of nonunique bands	% of nonunique bands	% of polymorphic bands	No. of monomorphic bands	% of monomorphic	% of Total polymorphism
			1.5×10^8 Lane 1	2.3×10^6 Lane 2	Lane 3	1 h Lane 4	3 h Lane 5										
A-02	TGCCGAGCTG	1500–50	12	13	10	10	12	57	22.98	4	7.02	9	15.79	17.54	4	7.02	58.82
A-03	AGTCAGCCAC	1300–50	11	15	13	11	10	61	24.60	6	9.83	15	24.59	34.43			100.00
A-10	GTGATCGCAG	550–50	6	5	4	9	6	30	12.10	3	10.00	4	13.33	20.00	1	3.33	75.00
A-12	TCGGCGATAG	900–65	5	8	7	7	9	35	14.11	4	11.43	7	20.00	31.43	1	2.86	91.67
A-15	TTCCGAACCC	700–75	8	8	7	6	5	34	13.71	5	14.71	5	14.71	23.53	1	2.94	72.73
A-17	GACCGCTTGT	800–65	5	11	5	7	3	31	12.50	5	16.13	9	29.03	45.16	1	3.23	93.33
	Overall total DNA bands		47	60	46	50	45	248		27	10.89	49	19.78	30.65	8	3.23	90.80
	%Total DNA bands		18.95	24.19	18.55	20.16	18.15										

doses of FN and UV-B exhibited special interference with meiotic PMC and PGs leading to genotoxic effects except two doses (FN fluency (2.3×10^6) and UV-B dose for 1 h) that showed improvement in meiotic PMC, pollen fertility, and consequently, parameters of seed yield productivity. This improvement may be due to the antioxidant defense system of *Vicia faba* plant which allows the toxic-free radical oxygen intermediates to perform useful biological functions without too much damage [5, 7]. Therefore, these irradiation doses may be having bio-positive or stimulation effects that may lead to inducing useful mutations as a new source of altered *Vicia faba* germplasm. In this respect, some previous studies indicated that the FN and UV-B irradiations had bio-positive effects at specific dose [35, 36], respectively. On the contrary, the remained irradiation doses of FN and UV-B induced genotoxic and oxidative action in meiotic-PMC and PGs of faba beans. These actions may be due to the induction of oxidative damage in these cells by production of the free radical oxygen that lead to higher frequency of chromosomal aberrations and DNA damage which in turn can affect the vigor, pollen grains fertility and likely to persist in seeds yield or even longer due to the accumulative genotoxicity and chromosomal aberrations [37]. Moreover, pollen grains which have no cytoplasm content and fail to pick up the acido-carmin stain were sterile [29]. Each of FN and UV-B radiations can induce ROS in PMCs by special interference with DNA leading to induction of structural changes in DNA, such as chromosomal rearrangement, strand breaks, base deletions, pryrimidine dimers, cross-links and base modifications, mutations, and other genotoxic effects [5, 6]. These DNA damages may influence the expression of a number of genes leading to alteration in proteins that control many metabolic processes like plant development, cell cycle, fertilization, and seed formation [2].

4.2. SDS-PAGE Analysis of Seed Storage Proteins of M_1 Progeny. The present study observed that SDS-PAGE analysis exhibited distinctive qualitative and quantitative alterations in electrophoretic SDS-proteins stored in seeds yielded from irradiated faba beans seedlings. These alterations are based on variations in molecular weights and intensities of polypeptides bands as well as gain or loss of protein bands that led to highly levels of protein polymorphism. Electrophoretic analysis of protein provides information concerning the structural genes and their regulatory systems that control the biosynthetic pathways of that protein. Each polypeptide band represents the final products of a transcriptional and translational events occurring due to active structural genes [38]. The changed protein products caused by dependent-irradiation exposure doses may result from base changes in DNA or altering protein sites or changes in amino acid sequences or frame shift mutations. Additionally, they may serve as genetic markers because they can be quite polymorphic and their variability is generally highly heritable [39].

The appearance of new bands (unique bands) may be explained on the basis of mutational events at the regulatory system of unexpected gene(s) or on the basis of band subfractionation which could be attributed to the cytological anomalies in PMCs leading to gene duplication followed by the occurrence of point mutation that encoded the fractionated band [40] or result from different DNA structural changes (breaks, transpositions, deletion, etc.) which led to change in amino acids and consequently protein formed [39]. On the other hand, the disappearance of some protein bands which led to formation of polymorphic bands could be attributed to the loss of genetic material which may be due to the cytogenetic anomalies in PMCs such as chromosomal laggards, free, fragmentations, bridges, micro- and multinucleate, or the breaking of a small number of peptide bonds to form polypeptides of shorter length than the original protein [38]. Furthermore, the changes in band intensity could be interpreted on the basis of gene duplication or point mutation that leads to production of shorter and longer polypeptide chains and alteration in the structural genes which may be due to the changes in regulator gene(s) expression [41]. The distinction protein polymorphisms shown between irradiated samples in the present study may be resulted from insertions or deletions between mutated sites of protein bands and could be used as biomarkers for identification of irradiated plants [39]. Additionally, high radionuclide content of plants causes alterations in the relative mobility of bands, intensities, expression of new proteins, and suppression of some proteins.

The result obtained in this study indicated that the UV-B doses for (2 and 3 h) may cause highly oxidative protein cross-links due to alteration of the expression of several genes that leading to proteins denaturation and disappearance of numerous bands due to aggregation or cross linking of individual polypeptide chains [42] or alteration of the expression of several genes through nonspecific signaling pathways [5]. On the other hand, the neutron fluency (2.3×10^6 n/cm^2) could show bio-positive (stimulation) effects by appearance of numerous new bands which can be valuable in the fields of genetic as mutant lines.

4.3. RAPD-PCR Analysis of DNA of Seed Yield of M_1 Progeny. RAPD assay used in the current study showed that various irradiation doses of the FN and UV-B exhibited distinctive qualitative and quantitative alterations in the RAPD profiles based on gene products, the amplified DNA sizes, their intensities, and appearance or disappearance of DNA bands that led to generation highly levels of DNA polymorphism. Variations in the characteristic DNA banding pattern generated by RAPD analysis may be caused by rearrangements of the genomic DNA, base pair deletions, mutations, inversions, translocations, and transpositions within base pair sequences of DNA which result in the loss or gain of DNA bands resulting in different DNA lengths and consequently highly level polymorphisms [43]. In this regard, [44] revealed that highly level of DNA polymorphisms generated by RAPD are the reflection of structural changes in the genomic DNA that alter the distance between two annealing sites and delete an existing site of new one or reflection of variation in gene expression which would be a better parameter to measure the pattern of genetic variations. They also concluded that deletion or insertion of the amplified regions or changes of nitrogenous base that alter primer binding sites will result polymorphisms in RAPD profile. On the other hand, appearance of new DNA bands is usually resulting from

different DNA structural changes (breaks, transpositions, deletion, etc.), while disappearance of some bands and band intensity may correlate with the level of photoproducts in DNA template after irradiation which can reduce the number of binding sites for Taq polymerase and the starting copy number of a particular DNA sequence within genome [26]. Furthermore, the disappeared DNA bands in some irradiated samples may be due to deletion of DNA segments that is the predominant radiation-oxidative damage in irradiated plant cells. This DNA deletion may be caused by (1) misrepair of two separate double-strand breaks in a DNA molecule with joining of the two outer ends and loss of the fragment between the breaks or (2) the process of cleaning (enzyme digestion of nucleotides, the component molecules of DNA) the broken ends before rejoining to repair one double-strand break [44].

The current study investigated that DNA alterations in RAPD profile could be explained on the basis of the biological way by which the radiation type interacts with DNA, by producing their own ROS through the direct and/or indirect effect in the irradiated cells. In relation to ROS generated in faba bean seedlings by bio-negative fluencies of FN can induce DNA deletions in nucleus and chromosome that range in size from a few base pairs to several megabases [14]. These DNA deletions can lead to increasing of the level of DNA break formation by producing different intragenic mutations with respect to the size of deletions that reflect differences in the nature of the DNA damage by generating oxygen species such as hydroxyl (OH) in aqueous media [14, 26]. Whereas ROS generated by bio-negative doses of UV-B radiation is capable of inducing several major types of DNA lesions such as DNA strand breaks, deletion or insertion of base pairs, pyrimidine dimers, cross-links, and base modification, such as alkylation and oxidation. Additionally, these DNA breaks can result from DNA damage by free radicals or from DNA replication, repair, transcription processes, and chromatin condensation and decondensation [2]. The breaks and perturbation of the molecular structures of deoxyribonucleic acids are manifested as chromosomal aberrations in meiotic-PMCs. UV-B can influence metabolic processes of plants either through direct damage including DNA damage and protein denaturation, which often cause heritable mutations affecting various metabolic processes or via various regulatory effects. These effects could adversely affect plant growth, development, and morphology, especially the productivity of sensitive crop species [45].

5. Conclusions

The present study observed that the cytogenetic analysis of meiotic PMCs and PGs in addition to SDS-PAGE and RAPD analyses of proteins and DNA of seeds yielded from irradiated faba beans seedlings by neutron fluency (2.3×10^6) and UV-B dose for 1 h was recorded as stimulatory effects for PMCs, PGs viability and parameters of seed productivity. These data are supported and confirmed by generation of numerous protein bands and high number of gene products generated from appearance of new protein and DNA bands, respectively, at these doses. Moreover, neutron fluency (2.3×10^6) was more stimulatory and effective as compared with UV-B dose for 1 h which in turn was higher than un-irradiated ones. In view of this, the current study proved that cytogenetic analysis alone cannot reveal alterations at the genome level; therefore it must be augmented with gene expression analyses represented in alteration in electrophoretic SDS-protein profiles using SDS-PAGE and DNA levels, changes in RAPD profiles using RAPD-PCR techniques that offered a useful molecular marker for evaluation of oxidative stress and mutagenic effects of various levels of ROS induced by irradiation exposure doses of FN and UV-B in faba beans cells. Finally, the current study proved that neutron fluency (2.3×10^6) and UV-B dose for 1 h were recorded as bio-positive or stimulation effects. Therefore, they may lead to induction of useful mutation in crop plants and can be useful as a new source of altered germplasm which may be valuable in the field of genetic and crop improvements.

Acknowledgments

The authors would like to extend their sincere appreciation to the deanship of Scientific Research at King Saud University for funding this research through the Research Group Project no. RGP-VPP-231. They also wish to express their deep thanks to Professor Magda Hanafy, Biophysics Department, Science College, Zagazig University, for her effort in performing the fast neutron irradiation and estimation of FN fluencies.

References

[1] G. M. Nabil, A. M. M. Attia, and M. A. Elhag, "Radioprotective effects of dietary ginger (*Zingiber officinales* Rosc.) against fast neutron-induced oxidative stress in rats," *World Applied Sciences Journal*, vol. 6, no. 4, pp. 494–498, 2009.

[2] S. B. Agrawal, S. Singh, and M. Agrawal, "Chapter 3 ultraviolet-B induced changes in gene expression and antioxidants in plants," *Advances in Botanical Research C*, vol. 52, pp. 47–86, 2009.

[3] G. Scandalios, "Oxidative stress: molecular perception and transduction of signals triggering antioxidant gene defenses," *Brazilian Journal of Medical and Biological Research*, vol. 38, no. 7, pp. 995–1014, 2005.

[4] M. D. Vishal-Tandon, B. M. Gupta, and R. Tandon, "Free radicals/reactive oxygen species," *JK Practitioner*, vol. 12, no. 3, pp. 143–148, 2005.

[5] S. S. Gill and N. Tuteja, "Reactive oxygen species and antioxidant machinery in abiotic stress tolerance in crop plants," *Plant Physiology and Biochemistry*, vol. 48, no. 12, pp. 909–930, 2010.

[6] P. Ahmad, M. Sarwat, and S. Sharma, "Reactive oxygen species, antioxidants and signaling in plants," *Journal of Plant Biology*, vol. 51, no. 3, pp. 167–173, 2008.

[7] T. Karuppanapandian, J. Moon, C. Kim, K. Manoharan, and W. Kim, "Reactive oxygen species in plants: their generation, signal transduction, and scavenging mechanisms," *Australian Journal of Crop Science*, vol. 5, no. 6, pp. 709–725, 2011.

[8] A. A. Aly and H. E. S. El-Beltagi, "Influence of ionizing irradiation on the antioxidant enzymes of *Vicia faba* L.," *Grasas Y Aceites*, vol. 61, no. 3, pp. 288–294, 2010.

[9] N. Chaieb, J. L. González, M. López-Mesas, M. Bouslama, and M. Valiente, "Polyphenols content and antioxidant capacity of thirteen faba bean (*Vicia faba* L.) genotypes cultivated in

Tunisia," *Food Research International*, vol. 44, no. 4, pp. 970–977, 2011.

[10] D. S. Ismael, M. Timoracká, A. Vollmannová et al., "Influence of variety, locality and soil contamination on total polyphenol content and antioxidant activity of faba bean grains," *Journal of Microbiology, Biotechnology and Food Sciences*, vol. 2012, no. 1, pp. 931–941, 2012.

[11] T. H. Ma, G. L. Cabrera, and E. Owens, "Genotoxic agents detected by plant bioassays," *Reviews on Environmental Health*, vol. 20, no. 1, pp. 1–13, 2005.

[12] J. Maluszynska and J. Juchimiuk, "Plant genotoxicity: a molecular cytogenetic approach in plant bioassays," *Arhiv za Higijenu Rada i Toksikologiju*, vol. 56, no. 2, pp. 177–184, 2005.

[13] M. A. da Silva, P. R. P. Coelho, P. Bartolini et al., "Induction of chromosomal aberrations in human lymphocytes by fission neutrons," in *Proceedings of the International Nuclear Atlantic Conference (INAC '09)*, pp. 1–9, 2009.

[14] R. Yoshihara, Y. Hase, R. Sato, K. Takimoto, and I. Narumi, "Mutational effects of different LET radiations in rpsL transgenic Arabidopsis," *International Journal of Radiation Biology*, vol. 86, no. 2, pp. 125–131, 2010.

[15] A. J. de Britto, M. Jeevitha, and T. L. S. Raj, "Alterations of protein and DNA profiles of *Zea mays* L. under UV- B radiation," *Journal of Stress Physiology & Biochemistry*, vol. 7, no. 4, pp. 232–240, 2011.

[16] R. P. Sinha and D. Häder, "UV-induced DNA damage and repair: a review," *Photochemical and Photobiological Sciences*, vol. 1, no. 4, pp. 225–236, 2002.

[17] D. Häder and R. P. Sinha, "Solar ultraviolet radiation-induced DNA damage in aquatic organisms: potential environmental impact," *Mutation Research*, vol. 571, no. 1-2, pp. 221–233, 2005.

[18] S. Kumari, R. P. Rastogi, K. L. Singh et al., "DNA damage: detection strategies," *EXCLI Journal*, vol. 7, pp. 44–62, 2008.

[19] S. Husain, M. I. Kozgar, I. F. Jafrey et al., "Meiotic changes in *Vicia faba* L. subsequent to treatments of hydrazine hydrate and maleic hydrazide," *Journal of BioScience and Biotechnology*, vol. 2, no. 1, pp. 33–38, 2013.

[20] R. K. Yadav, "Seed protein electrophoresis studies in cucurbits-a review," *Agricultural Revolution*, vol. 29, no. 1, pp. 21–30, 2008.

[21] A. Rath, M. Glibowicka, V. G. Nadeau, G. Chen, and C. M. Deber, "Detergent binding explains anomalous SDS-PAGE migration of membrane proteins," *Proceedings of the National Academy of Sciences of the United States of America*, vol. 106, no. 6, pp. 1760–1765, 2009.

[22] W. Mäueler, A. Kyas, F. Brocker, and J. T. Epplen, "Altered electrophoretic behavior of DNA due to short-time UV-B irradiation," *Electrophoresis*, vol. 15, no. 12, pp. 1499–1505, 1994.

[23] B. S. Selvi, V. Ponnywarni, and T. Sumathi, "Identification of DNA polymorphism induced by gamma ray irradiation iun Amla (Emblia officinalis Gaertn) grafts of V1M1 and V2 M1 generation," *Journal of Applied Sciences Research*, vol. 3, pp. 1933–1935, 2007.

[24] P. Kumar, V. K. Gupta, A. K. Misra et al., "Potential molecular markers in plant biotechnology," *Plant Omics Journal*, vol. 2, pp. 141–162, 2009.

[25] T. Taryono, P. Cahyaningrum, and S. Human, "The detection of mutational changes in Sorghum using RAPD," *Indonesian Journal of Biotechnology*, vol. 16, no. 1, pp. 66–70, 2011.

[26] O. Danylchenko and B. Sorochinsky, "Use of RAPD assay for the detection of mutation changes in plant DNA induced by UV-B and R-rays," *BMC Plant Biology*, vol. 5, no. 1, p. 59, 2005.

[27] F. El-Sherif, S. Khattab, E. Goniam et al., "The effect of gamma irradiation on enhancement of some economic traits and molecular changes in *Hibiscus Sabdariffa* L.," *Life Science Journal*, vol. 8, no. 3, pp. 220–229, 2011.

[28] R. Snow, "Alcoholic hydrochloric acid-carmine as a stain for chromosomes in squash preparations," *Stain Technology*, vol. 38, pp. 9–13, 1963.

[29] N. Awasthi and D. Dubey, "Effects of some phytogametcides on growth fertility and yield of lentil," *Lens Newslett*, vol. 12, pp. 16–22, 1985.

[30] M. P. Hojilla-Evangelista and R. L. Evangelista, "Effects of cooking and screw-pressing on functional properties of Cuphea PSR23 seed proteins," *Journal of the American Oil Chemists' Society*, vol. 83, no. 8, pp. 713–718, 2006.

[31] R. Saraswati, T. Matoh, P. Phupaibul et al., "Identification of Sesbania species from electrophoretic patterns of seed protein," *Journal of Tropical Agriculture*, vol. 70, pp. 282–285, 1993.

[32] U. K. Laemmli, "Cleavage of structural proteins during the assembly of the head of bacteriophage T4," *Nature*, vol. 227, no. 5259, pp. 680–685, 1970.

[33] M. K. Mishra, N. S. Rani, A. S. Ram, H. L. Sreenath, and J. Jayarama, "A simple method of DNA extraction from coffee seeds suitable for PCR analysis," *African Journal of Biotechnology*, vol. 7, no. 4, pp. 409–413, 2008.

[34] J. G. K. Williams, A. R. Kubelik, K. J. Livak, J. A. Rafalski, and S. V. Tingey, "DNA polymorphisms amplified by arbitrary primers are useful as genetic markers," *Nucleic Acids Research*, vol. 18, no. 22, pp. 6531–6535, 1990.

[35] O. A. Falusi, O. A. Y. Daudu, T. Thomas et al., "Further observations on the effects of fast neutron irradiation on morphological and yield traits of M1 and M2 generation of African wrinkled pepper (Capsicum annuum var abbreviatum Fingerh)," *Advances in Bioscience and Bioengineering*, vol. 1, no. 1, pp. 25–34, 2013.

[36] C. D. Leasure, H. Tong, G. Yuen, X. Hou, X. Sun, and Z. He, "Root UV-B sensitive2 acts with root UV-B sensitive1 in a root ultraviolet B-sensing pathway," *Plant Physiology*, vol. 150, no. 4, pp. 1902–1915, 2009.

[37] M. Uhl, M. J. Plewa, B. J. Majer et al., "Basic principles of genetic toxicology with an emphasis on plant bioassays," in *Bioassays in Plant Cells For Improvement of Ecosystem and Human Health*, J. Maluszynska and M. Plewa, Eds., pp. 11–30, Wydawnictwo Uniwersytetu Śląskiego, Katowice, Poland, 2003.

[38] M. I. Soliman and G. T. Ghoneam, "The mutagenic potentialities of some herbicides using Viciafaba as a biological system," *Biotechnology*, vol. 3, no. 2, pp. 140–154, 2004.

[39] L. Mondini, A. Noorani, and M. A. Pagnotta, "Assessing plant genetic diversity by molecular tools," *Diversity*, vol. 1, no. 1, pp. 19–35, 2009.

[40] N. Shikazono, C. Suzuki, S. Kitamura, H. Watanabe, S. Tano, and A. Tanaka, "Analysis of mutations induced by carbon ions in Arabidopsis thaliana," *Journal of Experimental Botany*, vol. 56, no. 412, pp. 587–596, 2005.

[41] C. R. Azzam, S. N. Zein, and S. M. Abbas, "Biochemical genetic markers for levels of resistance to cowpea aphid borne mosaic poty virus in sesame irradiated with gamma rays," *Egypt Journal Plant Breed*, vol. 11, no. 2, pp. 861–885, 2007.

[42] R. P. Sinha and D. Häder, "UV-induced DNA damage and repair: a review," *Photochemical and Photobiological Sciences*, vol. 1, no. 4, pp. 225–236, 2002.

[43] K. Semagn, A. Bjørnstad, and M. N. Ndjiondjop, "An overview of molecular marker methods for plants," *African Journal of Biotechnology*, vol. 5, pp. 2540–2568, 2006.

[44] D. Dhakshanamoorthy, R. Selvaraj, and A. L. A. Chidambaram, "Induced mutagenesis in *Jatropha curcas* L. using gamma rays and detection of DNA polymorphism through RAPD marker," *Comptes Rendus-Biologies*, vol. 334, no. 1, pp. 24–30, 2011.

[45] Z. S. Zlatev, F. J. C. Lidon, and M. Kaimakanova, "Plant physiological responses to UV-B radiation," *Emirates Journal of Food and Agriculture*, vol. 24, no. 6, pp. 481–501, 2012.

Hindawi Publishing Corporation
BioMed Research International
Volume 2013, Article ID 942916, 15 pages
http://dx.doi.org/10.1155/2013/942916

Review Article

Mechanisms of Nanoparticle-Induced Oxidative Stress and Toxicity

Amruta Manke,[1] Liying Wang,[2] and Yon Rojanasakul[1]

[1] *Department of Pharmaceutical Sciences and Mary Babb Randolph Cancer Center, West Virginia University, Morgantown, WV 26506, USA*
[2] *Physiology and Pathology Research Branch, National Institute for Occupational Safety and Health, Morgantown, WV 26505, USA*

Correspondence should be addressed to Yon Rojanasakul; yrojan@hsc.wvu.edu

Received 9 May 2013; Accepted 16 July 2013

Academic Editor: Nikhat J. Siddiqi

The rapidly emerging field of nanotechnology has offered innovative discoveries in the medical, industrial, and consumer sectors. The unique physicochemical and electrical properties of engineered nanoparticles (NP) make them highly desirable in a variety of applications. However, these novel properties of NP are fraught with concerns for environmental and occupational exposure. Changes in structural and physicochemical properties of NP can lead to changes in biological activities including ROS generation, one of the most frequently reported NP-associated toxicities. Oxidative stress induced by engineered NP is due to acellular factors such as particle surface, size, composition, and presence of metals, while cellular responses such as mitochondrial respiration, NP-cell interaction, and immune cell activation are responsible for ROS-mediated damage. NP-induced oxidative stress responses are torch bearers for further pathophysiological effects including genotoxicity, inflammation, and fibrosis as demonstrated by activation of associated cell signaling pathways. Since oxidative stress is a key determinant of NP-induced injury, it is necessary to characterize the ROS response resulting from NP. Through physicochemical characterization and understanding of the multiple signaling cascades activated by NP-induced ROS, a systemic toxicity screen with oxidative stress as a predictive model for NP-induced injury can be developed.

1. Introduction

The growing field of nanotechnology has transformed many sectors of the industrial field with their breakthrough applications in the areas of biotechnology, electronics, medicinal drug delivery, cosmetics, material science, aerospace engineering, and biosensors. Manufactured nanomaterials (NM) have gained commercial interest in a variety of consumer products. Their novel physicochemical, thermal, and electrical properties facilitate their application in clothing, medicine, and cosmetics thereby increasing the probability for human and environmental contact with these NM [1–3]. Of all the NM, carbon nanotubes (CNT) and metal-based nanoparticles (NP) have generated considerable commercial interest owing to their remarkable intrinsic properties such as high tensile strength and conductivity, which in turn meet the needs of the specific application for which these NP are designed [4, 5]. Their widespread use raises concerns of their inadvertent exposure in humans and the consequent deleterious health effects [6]. As compared to the growing commercial interest of NM, modest research effort has been invested in evaluating the potential adverse effects of these engineered NM. The sheer multiplicity of the physicochemical parameters of NM such as size, shape, structure, and elemental constituents makes the investigation of their toxic effects complex and challenging [7]. Some of the paradigms for NP-mediated toxicity include oxidative stress, inflammation, genetic damage, and the inhibition of cell division and cell death [8–11]. Most work to date has suggested that ROS generation (which can be either protective or harmful during biological interactions) and consequent oxidative stress are frequently observed with NP toxicity [3, 9]. The physicochemical characterization of NP including particle size, surface charge, and chemical composition is a key indicator for the resulting ROS response and NP-induced injury since many of these NP intrinsic properties can catalyze the

ROS production [6]. NP-mediated ROS responses have been reported to orchestrate a series of pathological events such as genotoxicity, inflammation, fibrosis, and carcinogenesis. For instance, CNT-induced oxidative stress triggers cell signaling pathways resulting in increased expression of proinflammatory and fibrotic cytokines [12]. Some NP have been shown to activate inflammatory cells such as macrophages and neutrophils which can result in the increased production of ROS [13–15]. Other NP such as titanium dioxide (TiO_2), zinc oxide (ZnO), cerium oxide (CeO_2), and silver NP have been shown to deposit on the cellular surface or inside the subcellular organelles and induce oxidative stress signaling cascades that eventually result in oxidative stress to the cell [16]. The mechanism for ROS generation is different for each NP and to date the exact underlying cellular mechanism for ROS generation is incompletely understood and remains to be elucidated. Most of the metal-based NP elicit free radical-mediated toxicity via Fenton-type reactions [4, 17], whereas mitochondrial damage plays a major role in CNT-mediated ROS generation [18]. However, it is inaccurate to assume that ROS generation is a prerequisite to NP-induced toxicity since a few studies have reported the direct toxicity of NP without causing ROS [19]. Nevertheless, ROS generation is a major event during NP-induced injury that needs to be thoroughly characterized in order to predict NP-induced toxicity. This review will focus on oxidative stress as a mechanism for understanding NP-induced toxicity. For this paper, we have considered metal-based NP and CNT in the light of oxidative stress. The relationship between different NP characteristics and resulting oxidative stress is discussed.

1.1. Generation of ROS. ROS, key signaling molecules during cell signaling and homeostasis, are reactive species of molecular oxygen. ROS constitute a pool of oxidative species including superoxide anion ($O_2^{\bullet -}$), hydroxyl radical ($OH^{\bullet}$), hydrogen peroxide (H_2O_2), singlet oxygen ($^1O_2$), and hypochlorous acid (HOCl). ROS are generated intrinsically or extrinsically within the cell. Molecular oxygen generates $O_2^{\bullet -}$, the primary ROS via one-electron reduction catalyzed by nicotinamide adenine dinucleotide phosphate (NADPH) oxidase. Further reduction of oxygen may either lead to H_2O_2 or $OH^{\bullet}$ via dismutation and metal-catalyzed Fenton reaction, respectively [20, 21]. Some of the endogenous sources of ROS include mitochondrial respiration, inflammatory response, microsomes, and peroxisomes, while engineered NM, environmental pollutants act as exogenous ROS inducers. Physiologically, ROS are produced in trace amounts in response to various stimuli. Free radicals occur as essential byproducts of mitochondrial respiration and transition metal ion-catalyzed Fenton-type reactions [20]. Inflammatory phagocytes such as neutrophils and macrophages induce oxidative outburst as a defense mechanism towards environmental pollutants, tumor cells, and microbes. A variety of NP including metal oxide particles induce ROS as one of the principal mechanisms of cytotoxicity [22]. NP have been reported to influence intracellular calcium concentrations, activate transcription factors, and modulate cytokine production via generation of free radicals [12, 23].

1.2. Oxidative Stress. Abundance of ROS can have potentially damaging biological responses resulting in oxidative stress phenomenon. It results from an imbalance between the production of ROS and a biological system's ability to readily detoxify the reactive intermediates or repair the resulting damage. To overcome the excess ROS response, cells can activate enzymatic and nonenzymatic antioxidant systems [24]. The hierarchical model of oxidative stress was proposed to illustrate a mechanism for NP-mediated oxidative stress [4, 9]. According to this model, cells and tissues respond to increasing levels of oxidative stress via antioxidant enzyme systems upon NP exposure. During conditions of mild oxidative stress, transcriptional activation of phase II antioxidant enzymes occurs via nuclear factor (erythroid-derived 2)-like 2 (Nrf2) induction. At an intermediate level, redox-sensitive mitogen-activated protein kinase (MAPK) and nuclear factor kappa-light-chain enhancer of activated Bcells (NF-κB) cascades mount a proinflammatory response. However, extremely toxic levels of oxidative stress result in mitochondrial membrane damage and electron chain dysfunction leading to cell death. Some of the key factors favoring the prooxidant effects of engineered NM include either the depletion of antioxidants or the increased production of ROS. Perturbation of the normal redox state contributes to peroxide and free radical production that has adverse effects on cell components including proteins, lipids, and DNA [23]. Given its chemical reactivity, oxidative stress can amount to DNA damage, lipid peroxidation, and activation of signaling networks associated with loss of cell growth, fibrosis, and carcinogenesis [16, 25, 26]. Besides cellular damage, ROS can result from interactions of NP with several biological targets as an effect of cell respiration, metabolism, ischemia/reperfusion, inflammation, and metabolism of various NM [22]. Most significantly, the oxidative stresses resulting from occupational NM exposures as well as experimental challenge with various NP lead to airway inflammation and interstitial fibrosis [27–30].

1.3. Nanoparticle-Induced Oxidative Stress. Nanomaterials of varying chemical composition such as fullerenes, CNT, and metal oxides have been shown to induce oxidative stress [20, 31]. The key factors involved in NP-induced ROS include (i) prooxidant functional groups on the reactive surface of NP; (ii) active redox cycling on the surface of NP due to transition metal-based NP; and (iii) particle-cell interactions [22, 25]. From a mechanistic point of view, we discuss the sources of ROS based on the physicochemical parameters and particle-cell interactions.

Several studies demonstrate the significance of reactive particle surface in ROS generation [20, 32]. Free radicals are generated from the surface of NP when both the oxidants and free radicals bound to the particle surface. Surface bound radicals such as $SiO^{\bullet}$ and $SiO_2^{\bullet}$ present on quartz particles are responsible for the formation of ROS such as $OH^{\bullet}$ and $O_2^{\bullet -}$ [17, 25]. Ambient matter such as ozone and nitrogen dioxide (NO_2) adsorbed on the particle surface is capable of inducing oxidative damage [16]. Reduced particle size results in structural defects and altered electronic properties

on the particle surface creating reactive groups on the NP surface [27, 33]. Within these reactive sites, the electron donor or acceptor active sites interact with molecular O_2 to form $O_2^{\bullet-}$ which in turn can generate additional ROS via Fenton-type reactions [3]. For instance, NP such as Si and Zn with identical particle size and shape lead to diverse cytotoxicity responses due to their surface properties. ZnO being more chemically active than SiO_2, led to increased $O_2^{\bullet-}$ formation resulting in oxidative stress. Free radicals are either directly bound to the NP surface or may be generated as free entities in an aqueous suspension [17]. Dissolution of NP and subsequent release of metal ions can enhance the ROS response [25]. For instance, aqueous suspensions of quartz particles generate H_2O_2, $OH^{\bullet}$, and $^1O_2$ [17, 20, 32].

Apart from surface-dependent properties, metals and chemical compounds on the NP surface accelerate the ROS response [34]. Transition metals including iron (Fe), copper (Cu), chromium (Cr), vanadium (V), and silica (Si) are involved in ROS generation via mechanisms such as Haber-Weiss and Fenton-type reactions [25]. Fenton reactions usually involve a transition metal ion that reacts with H_2O_2 to yield $OH^{\bullet}$ and an oxidized metal ion. For example, the reduction of H_2O_2 with ferrous iron (Fe^{2+}) results in the formation of $OH^{\bullet}$ that is extremely reactive and toxic to biological molecules [21]. Cu and Fe metal NP have been reported to induce oxidative stress ($O_2^{\bullet-}$ and $OH^{\bullet}$) via Fenton-type reaction [26], while the Haber-Weiss-type reaction involves a reaction between oxidized metal ion and H_2O_2 to induce $OH^{\bullet}$ [21, 35]. NP including chromium, cobalt, and vanadium can catalyze both Fenton and Haber-Weiss-type reactions [26]. Glutathione reductase, an antioxidant enzyme, reduces metal NP into intermediates that potentiate the ROS response. In addition, some metal NP (Ar, Be, Co, and Ni) promote the activation of intercellular radical-inducing system such as the MAPK and NF-κB pathways [36].

In addition to the prooxidant effect of NP, ROS are also induced endogenously where the mitochondrion is a major cell target for NP-induced oxidative stress. Once NP gain access into the mitochondria, they stimulate ROS via impaired electron transport chain, structural damage, activation of NADPH-like enzyme system, and depolarization of the mitochondrial membrane [37, 38]. For instance, cationic polystyrene nanospheres induce $O_2^{\bullet-}$ mediated apoptosis in murine macrophages based on their ability to target mitochondria [38].

Cellular internalization of NP has been shown to activate immune cells including macrophages and neutrophils, contributing to ROS/RNS [22, 25]. This process usually involves the activation of NADPH oxidase enzymes. *In vivo* particle exposures such as silica activate the rich pool of inflammatory phagocytes within the lung causing them to induce oxidative outburst [39]. NP with smaller particle size are reported to induce higher ROS owing to their unique characteristics such as high surface to volume ratio and high surface charge. Particle size determines the number of reactive groups/sites on the NP surface [34, 37, 40]. The pulmonary responses induced by inhaled NP are considered to be greater than those produced by micron-sized particles because of the increased surface area to particle mass ratio [28]. Larger surface area ensures that the majority of the molecules are exposed to the surface than the interior of the NM [3]. Accordingly, nano-sized SiO_2 and TiO_2 and MWCNT induce greater ROS as compared to their larger counterparts [41]. Additionally, a study with cobalt/chromium NP exposure demonstrated particle size dependent ROS-mediated genotoxicity [42].

2. Oxidant Generation via Particle-Cell Interactions

Besides being self-oxidative in nature, NP react with cells and induce their prooxidant effects via intracellular ROS generation involving mitochondrial respiration and activation of NADPH-like enzyme systems [43]. NP can activate the cellular redox system specifically in the lungs where immune cells including alveolar macrophages (AM) and neutrophils act as direct ROS inducers. Professional phagocytic cells including neutrophils and AM of the immune system induce substantial ROS upon internalization of NP via the NADPH oxidase enzyme system [44]. The phagocytic oxidative outburst is attributable to some of the NP physicochemical properties. In case of silica and quartz particles, inflammation-induced ROS was associated with the surface-based radical-generating properties of the particles [45]. Additionally, NP from the residual oily fly ash and diesel exhaust activate the pool of inflammatory phagocytes resulting in massive ROS release [46]. Furthermore, adsorption of chemicals such as organic matter onto the NP surface may drive the inflammation-induced oxidative stress [24].

2.1. Lung Injury Caused by Nanoparticle-Induced Reactive Nitrogen Species. Besides oxidative damage, NP exposure within the lung is reported to induce reactive nitrogen species (RNS). Particle deposition in the lung causes recruitment of inflammatory cells that generate ROS, clastogenic factors, and cytokines either harming or stimulating resident lung cells [31]. Inflammatory phagocytes are an important source of RNS/ROS generation within the lung. Owing to their inducible nitric oxide synthase (iNOS) activity, phagocytes can produce a large amount of genotoxic RNS, including nitric oxide ($NO^{\bullet}$) and the highly reactive peroxynitrite ($ONOO^-$). $ONOO^-$ formed by the reaction of $NO^{\bullet}$ and $O_2^{\bullet-}$ causes DNA fragmentation, lipid oxidation, and protein dysfunction consequently contributing to particle-induced lung injury [47]. *In vivo* exposure to SiO_2 and quartz NP elicited an RNS response characterized by increased iNOS and $NO^{\bullet}$ within the lung as a result of phagocyte influx [48, 49].

2.2. Mechanisms of ROS Production and Apoptosis within Metal Nanoparticles. Apoptosis has been implicated as a major mechanism of cell death caused by NP-induced oxidative stress [50–52]. Among the different apoptotic pathways, the intrinsic mitochondrial apoptotic pathway plays a major role in metal oxide NP-induced cell death since mitochondria are one of the major target organelles for NP-induced oxidative stress [38]. High levels of ROS in the mitochondria can

result in damage to membrane phospholipids inducing mitochondrial membrane depolarization [53]. Small proportion of electrons escapes the mitochondrial chain and interacts with molecular oxygen to form $O_2^{\bullet -}$ which later gives rise to H_2O_2 or partially reduces to the damaging $OH^{\bullet}$. NP can catalyze the $O_2^{\bullet -}$ generation either by blocking the electron transport chain or accelerating electron transfer to molecular oxygen [54, 55]. Various metal oxide NP including Zn, Cu, Ti, and Si elicit ROS-mediated cell death via mitochondrial dysfunction [56–59].

3. Introduction to Transition Metals

Transition metal oxide particles have been used to revolutionize several fields including catalysis, sensors, optoelectronic materials, drug delivery, automobile, and material science engineering. Apart from industrial scale applications, metal NP are increasingly used in a variety of consumer products such as cosmetics, sunscreens, textiles, and food products. Among the transition metal oxides, titanium dioxide, cupric oxide, and zinc oxide have gained attention owing to their commercial usage [60]. Metal oxide particles can undergo surface modification for better stability and binding to other substrates. Such widespread applications are attributable to their electrochemical and physical properties reflecting their small sizes and reactive surfaces. For example, a relatively inert metal or metal oxide may become a highly effective catalyst when manufactured as NP. Their fixed particle mass, high aspect ratio, and particle surface bioreactivity tailor them to meet the needs of specific application. However, a high surface-to-volume ratio makes NP reactive and exposes them to environmental stressors, particularly free radical generation [61, 62]. Besides, the nanoscale dimensions enhance their cellular uptake and interaction with biological tissues. Metals can generate free radicals via the Fenton-type reactions that react with cellular macromolecules and induce oxidative stress [63]. The toxicity of metallic NP including Zn, Ti, Si, Fe, and Ce has been characterized by increased ROS generation and oxidative stress and apoptosis [61, 64–66]. The oxidative stress mediated outcomes of various metal NP are summarized in Table 1.

4. Prooxidant Effects of Metal Oxide Nanoparticles

To overcome the overwhelming ROS production, cells trigger either a defensive or an injurious response eliciting a chain of adverse biological responses. Free radicals are potentially damaging to cellular macromolecules including lipids, proteins, and nucleic acids. DNA is one of the major targets for oxidative stress and represents the first step involved in mutagenesis, carcinogenesis, and aging. ROS/RNS cause oxidative DNA damage in the form of DNA strand breaks, DNA protein cross-links, and alkali-labile sites [67, 68], and given their characteristic nature free radicals appear as one of the likely carcinogens [25, 69]. Testing the genotoxic potential is essential for carcinogenic risk assessment of NP. Genotoxic effects may be produced either by direct interaction of particles with genetic material or by secondary damage from particle-induced ROS. Transition metal NP induce chromosomal aberrations, DNA strand breaks, oxidative DNA damage, and mutations [70]. $OH^{\bullet}$, one of the highly potent radicals, is known to react with all components of DNA causing DNA single strand breakage via formation of 8-hydroxyl-2′-deoxyguanosine (8-OHdG) DNA adduct [71, 72]. 8-OHdG is a biomarker of $OH^{\bullet}$-mediated DNA lesions. NP exposure significantly elevated 8-OHdG levels both *in vivo* [73] and *in vitro* [74], demonstrating their mutagenic behavior. A recent study comparing metal oxide NP including Cu, Fe, Ti, and Ag reported ROS-mediated genotoxicity characterized by micronuclei and DNA damage *in vivo* [75].

Along with chromosomal damage, free radicals also interact with lipids and proteins, abundantly present in biomembranes, to yield lipid peroxidation products associated with mutagenesis. Polyunsaturated fatty acids are subject to oxidation giving rise to lipid hydroperoxides as the initial step in ROS generation [25, 76]. Prooxidant metals such as Cu and Fe react with these lipid hydroperoxides to induce DNA damaging end-products malondialdehyde (MDA) and 4-hydroxynonenal that act as inflammatory mediators and risk factors for carcinogenesis. Exposures to metal oxide NP of Ti, Cu, Si, and Fe were reported to induce tissue damage, abnormal cellular stress response via lipid peroxidation [77–79].

Alterations within the antioxidant defense system pose as a risk factor for carcinogenesis [68]. Glutathione, (GSH) a potent free-radical scavenger, is responsible for maintaining the cellular redox state and protecting cells from oxidative damage [80, 81]. NP-triggered free radicals reduce GSH into its oxidized form glutathione disulfide (GSSG), thereby contributing to oxidative stress, apoptosis, and sensitization to oxidizing stimuli [82, 83]. Apart from GSH, NP-induced ROS modulate the antioxidant activities of ROS-metabolizing enzymes including NADPH-dependent flavoenzyme, catalase, glutathione peroxidase, and superoxide dismutase [84].

It is well established that uncontrolled generation of ROS triggers a cascade of proinflammatory cytokines and mediators via activation of redox sensitive MAPK and NF-κB signaling pathways that control transcription of inflammatory genes such as IL-1β, IL-8, and TNF-α [21]. Oxidative stress plays a key role in NP-induced airway hypersensitivity and respiratory inflammation [85]. A study involving coexposure of metal oxide NP with a bacterial endotoxin demonstrated exaggerated lung inflammation and pulmonary edema [86]. Additionally, studies with different metal oxide NP have demonstrated ROS-mediated inflammatory response. For instance, SiO_2 and TiO_2 NP induce an elevated inflammatory response through the underlying mechanism of ROS generation [64, 85, 87]. Pulmonary inflammation may induce changes in membrane permeability, facilitating NP distribution beyond the lung and indirectly affecting cardiovascular performance [88].

Metal ion-induced free radicals can activate oncogenes such as Ras [25]. Excess amounts of NP have been associated with skin, bladder, liver, lung, and respiratory tract cancers [7]. Transition metals in trace amounts are introduced during the manufacture and preparation of CNT. Given

Table 1: List of studies describing the ROS-dependent effects of metal-based NP.

Nanoparticles	ROS-dependent effect	Reference
	Iron oxide	
Iron oxide	Necrosis and apoptosis in murine macrophage (J774) cells	[61]
Zero-valent iron	Acute cytotoxicity in human bronchial epithelial cells	[140]
Iron oxide	Human microvascular endothelial cell permeability	[141]
SPIONS	Activation of NF-κB and AP-1, inflammation in human epidermal keratinocytes (HEK) and murine epidermal cells (JB6 P(+))	[142]
	Copper oxide	
Copper oxide	Genotoxicity in human lung epithelial cells	[143]
Copper oxide	Mitochondrial dysfunction, oxidative DNA damage, cell death in A549 cell line	[144]
Copper oxide	Cytotoxicity *in vitro* in Hep-2 cell line	[145]
Copper oxide	Nephrotoxicity and hepatotoxicity *in vivo*	[146]
	Cerium oxide	
Cerium oxide	Lung inflammation and alveolar macrophage apoptosis *in vivo*	[147]
Cerium oxide	Apoptosis via caspase-3 activation and chromatin condensation *in vitro* in BEAS-2B cells	[64]
Cerium oxide	HO-1 induction via the p38-Nrf-2 signaling pathway *in vitro* in BEAS-2B cell line	[148]
Cerium oxide	Lipid peroxidation and membrane damage *in vitro* in lung cancer cells	[149]
	Zinc oxide	
Zinc oxide	Mitochondrial dysfunction, morphological modification, and apoptosis *in vitro* in human fetal lung fibroblasts	[59]
Zinc oxide	Cellular oxidant injury, excitation of inflammation, and cell death in BEAS-2B and RAW 264.7 cells	[150]
Zinc oxide	Mitochondrial damage, apoptosis, and IL-8 release *in vitro* in LoVo human colon carcinoma cell line	[151]
Zinc oxide	Mitochondrial damage, genotoxic and apoptotic cell effects *in vitro* human liver cells	[152]
Zinc oxide	Genotoxic and apoptotic responses *in vitro* in human skin melanoma cell line (A375)	[153]
Zinc oxide	Endoplasmic reticulum stress, apoptosis, and necrosis in rat retinal ganglion cells	[154]
Zinc oxide nanorods	Apoptosis in human alveolar adenocarcinoma cells via p53, surviving, and bax/bcl-2 pathways	[155]
	Nanosilica	
Nanosilica	Cytotoxicity and apoptosis via activation of p53 and Bax *in vitro* in human hepatic cell line p53 and p21 mediated G1 phase arrest *in vitro* myocardial H9c2 (2-1) cells	[156] [157]
Nanosilica	Cell cycle arrest and apoptosis *in vitro* human embryonic kidney cell line	[158]
Nanosilica	Hepatotoxicity *in vitro* in Kupffer cells and ROS-mediated cell death, oxidative DNA damage	[159]
	Nickel oxide	
Nickel oxide	Lipid peroxidation, apoptosis *in vivo* in human epithelial airway cells	[160]
Nickel ferrite	Apoptosis in A549 cells through oxidative stress via p53, survivin, bax/bcl-2, and caspase pathways in normal Chang (normal human liver), MCF10A (normal breast epithelial), and WI38 (normal lung fibroblast) cell lines	[161]
	Titanium dioxide	
Titanium dioxide	Apoptotic cell death through ROS-mediated Fas upregulation and Bax activation	[162]
Titanium dioxide	Cytotoxic and genotoxic effects *in vitro* in human amnion epithelial (WISH) cell line	[163]
Titanium dioxide	Cytotoxicity and apoptotic cell death *in vitro* in HeLa cell line	[164]
	Aluminum oxide	
Aluminium oxide	Mitochondria mediated oxidative stress and cytotoxicity in human mesenchymal stem cells	[165]
	Gold	
Gold	Lipid peroxidation and autophagy *in vitro* in MRC-5 lung fibroblasts	[166]
	Silver	
Ag-NP	Mitochondrial damage and genotoxicity in human lung fibroblast cells (IMR-90) and human glioblastoma cells (U251)	[167]
Ag-NP	JNK-mediated mitochondrial apoptosis in NIH3T3 fibroblasts	[50]
Ag-NP	Mitochondrial damage, apoptosis *in vitro* in A549 cells	[168]
	Cobalt-chromium (Co-Cr)	
Co-Cr NP	Oxidative DNA damage, micronuclei induction, reduced cell viability in human dermal fibroblasts	[169]

their oxidizable nature, studies suggest that metals including Fe, Co, and Ni are more toxic and fibrogenic upon their interaction with CNT as compared to pure CNT [89–93]. Vanadium pentoxide (V_2O_5), a transition metal byproduct of petrochemicals, is associated with fibrosis via generation of H_2O_2 and other ROS [94]. Occupational exposures to combustion-derived NP such as welding fumes consisting of metals such as Fe, Mn, Si, Cr, and Ni induce fibrogenic responses [95]. Metal containing welding fume NP elicited ROS-dependent lipid peroxidation and inflammation *in vivo* [96, 97].

5. Cellular Signaling Affected by Metal Nanoparticles

The prooxidant effects of NP result in the activation of signaling pathways, transcription factors, and cytokine cascade contributing to a diverse range of cellular responses. The regulation of redox homeostasis entails signaling cascades such as HIF-1, NF-κB, PI3 K, and MAPK which control proliferation, metastasis, cell growth, apoptosis, survival, and inflammation [7, 12]. At an intermediate level of oxidative stress, proinflammatory pathways are activated in an attempt to maintain the redox equilibrium. The inflammatory cascade involves profibrotic mediators such as TNF-α, IL-1β, and TGF-β which have been implicated in the pathogenesis of fibrosis. Cells are known to counteract the overwhelming oxidative stress response via increased cytokine expression such as interleukins and TNF-α, activation of kinases, and inhibition of phosphatases thereby influencing the phosphorylation cascade. Protein phosphorylation is involved in the regulation of critical cellular responses including mitogenesis, cell adhesion, oncogenic transformation, and apoptosis. Thus, ROS response appears to be closely related to factors driving carcinogenesis [98].

5.1. NF-κB. The NF-κB group of proteins activates genes responsible for defense mechanisms against cellular stress and regulates miscellaneous functions such as inflammation, immune response, apoptosis, and cell proliferation. Prooxidant H_2O_2-mediated NF-κB activation through the classical IKK-dependent pathway is well established. ROS such as $OH^{\bullet}$, HOCl, and $^1O_2$ and RNS such as $ONOO^-$ activate NF-κB via the release of IκBs resulting in the nuclear translocation of NF-κB [99, 100]. Once inside the nucleus, NF-κB induces transcription of proinflammatory mediators resulting in inflammation and oxidative stress. During NP-mediated lung injury, ROS activate NF-κB to modulate the production of proinflammatory TNF-α, IL-8, IL-2, and IL-6 from macrophages and lung epithelial cells [101]. Several metal oxide NP such as Zn, Cd, Si, and Fe exert their toxic effects via ROS-dependent NF-κB activation [62, 102, 103].

5.2. AP-1. Activator protein (AP)-1 is a transcription factor activated in response to oxidants, cytokines, growth factors, and bacterial and viral infections. It is responsible for regulation of cell proliferation, differentiation, and apoptosis, thereby it is a key factor in carcinogenesis [104]. Activation of AP-1 under oxidative conditions is believed to be mediated via phosphorylation of protooncogene c-jun [68]. Metal NP including Cr, Ni, and Fe have been shown to activate AP-1 via ROS generation [60].

5.3. MAPK. MAPK are serine-threonine protein kinases that control a diverse range of cellular responses including proliferation, gene expression, differentiation, mitosis, cell survival, and apoptosis. MAPK consist of growth factor-regulated extracellular signal-related kinases (ERK) and the stress-activated MAPK, c-jun NH_2-terminal kinases (JNK), and p38 MAPK. Once ROS production exceeds the capacity of the antioxidant proteins, free radicals may induce oxidative modification of MAPK signaling proteins (e.g., RTK and MAP3 K), thereby leading to MAPK activation. ROS may activate MAPK pathways via inhibition and/or degradation of MAPK phosphatases (MKP) [105, 106]. Finally, the site of ROS production and the concentration and kinetics of ROS production as well as cellular antioxidant pools and redox state are most likely to be important factors in determining the effects of ROS on activation of MAPK pathways [107]. Ag-NP activate JNK protein signaling and apoptosis in a variety of cells [50], whereas CeO_2 NP trigger p38 MAPK signaling in bronchoalveolar cells [64].

5.4. PTP. Protein tyrosine phosphatases (PTP) are key regulatory components in signal transduction pathways involved in cell growth, differentiation, proliferation, and transformation. The highly reactive cysteine residues of PTP are predisposed to oxidative stress in the form of H_2O_2, free radicals or changes in intracellular thiol/disulfide redox state [98, 108]. Metal NP including Zn^{2+} and V^{5+} may be critical in redox regulation of PTP via the inhibition of MAPK and EGFR [109, 110].

5.5. Src. Src kinases belong to the nonreceptor tyrosine kinase family involved in the regulation of cell growth. Mild oxidative stress is sufficient to activate Src kinase which later triggers a cell signaling cascade [111]. This may explain the low dose of metal NP-induced lymphocyte cell death via ROS-dependent activation of Src kinases [112].

6. Carbon Nanotubes

One of the most promising materials in the field of nanotechnology is CNT, and their widespread applications are attributable to the diverse physical, chemical, and electrical characteristics they possess. CNT are high aspect ratio nanomaterials (HARN) having at least one of their dimensions in the order of 100 nm or less according to the British Standards Institute Report [113]. CNT are made of either single-walled (SW) or multiwalled (MW) graphite layers. With unique properties such as high tensile strength and conductivity, they have been explored in the areas of electronics, biotechnology, medicinal drug delivery, cosmetics, material science, and aerospace engineering. CNT structure facilitates their entry, deposition, and residence in the lungs and pleura, resulting in incomplete phagocytosis and clearance from the lungs [5].

Owing to their biopersistent and nonbiodegradable nature, and particularly their resemblance to needle-like asbestos fibers, CNT are believed to induce biologically harmful effects [89]. Physicochemical parameters such as particle size, surface modification, presence of metals, surface reactivity, and surface charge are responsible for the prooxidant effects of CNT. Frustrated phagocytosis of CNT has been implied in CNT-induced oxidative stress.

7. Carbon Nanotube-Induced Oxidative Stress

One of the most frequently reported toxicity endpoints for CNT is the formation of ROS which can be either protective or harmful during biological interactions. Oxidative stress may be caused directly by CNT-induced ROS in the vicinity or inside the cell or could arise more indirectly due to the effects of internalized CNT on mitochondrial respiration [114] or in depletion of antioxidant species within the cell [64]. Moreover, NADPH-mediated ROS are critical for SWCNT-induced pulmonary responses [91]. The most likely mechanism for CNT-induced oxidative stress and lung toxicity involves mitochondrial dysfunction. Incomplete phagocytosis of CNT, presence of transition metals and specific reactive groups on the CNT surface are key drivers of ROS generation. Metal impurities such as Fe, Co, and Ni introduced within the CNT during their synthesis are key factors driving CNT-mediated ROS response [115, 116]. CNT-induced oxidative stress mediates important cellular processes including inflammation, cell injury, apoptosis, and activation of cellular signaling pathways such as MAPK and NF-κB which are implicated in the pathogenesis of lung fibrosis [31, 117]. For instance, SWCNT dependent $OH^{\bullet}$ generation leads to activation of molecular pathways MAPK, AP-1, NF-κB, and Akt associated with cell proliferation and tumor progression *in vitro* [93]. Several studies demonstrate SWCNT-induced oxidative stress [118–120]. Similarly, MWCNT exposures have been reported to induce ROS both *in vitro* and *in vivo* [18, 121–123]. Interestingly, oxidative stress is reported to be a mechanism for biodegradation of CNT. SWCNT undergoes oxidative biodegradation via myeloperoxidase, a prooxidant enzyme involved in host defense responses [120]. Table 2 summarizes the different studies that report ROS-dependent effects of CNT.

8. Role of ROS in CNT-Induced Inflammation

ROS and inflammation demonstrate an interdependent relationship in the case of exposure to NP. Inflammatory cells such as macrophages and neutrophils induce enormous ROS release in order to get rid of the NP. However, NP exposure-mediated oxidative stress leads to activation of RTK, MAPK, Akt, and NF-κB contributing to the proinflammatory cascade [124]. Accordingly, CNT-induced ROS were reported to elicit pro-inflammatory transcription factors such as NF-κB, AP-1 and MAPK *in vivo*. This was found to be an inflammation dependent response [93]. MWCNT treatment in macrophages mediates ROS-dependent activation of NF-κB pathway, thereby inducing the expression of chemokines and cytokines such as TNF-α, IL-1β, IL-6, IL-10, and MCP-1 [18]. Likewise, MWCNT-induced nitrosative stress *in vivo* is associated with pulmonary inflammation [125].

9. Role of ROS in CNT-Induced Genotoxicity

CNT elicit genotoxic effects through direct interaction with DNA or indirectly via CNT-induced oxidative stress and inflammatory responses. CNT-induced sustained oxidative stress can result in DNA damage and abnormal cell growth, possibly leading to carcinogenesis and fibrogenesis [126, 127]. A plethora of studies demonstrate the genotoxic potential of both MWCNT and SWCNT [128–131]. ROS can activate cellular signaling pathways resulting in cell cycle arrest and apoptosis. CNT induce a multitude of genotoxic responses including DNA strand breakage, oxidation, micronuclei induction, chromosomal aberrations, formation of γH2AX foci, and mutant frequencies [132]. Oxidative stress-dependent DNA breakage and repair and activation of signaling pathways including poly-ADP-ribose polymerase (PARP), AP-1, NF-κB, p38, and Akt were reported in human mesothelial cells exposed to SWCNT [93]. CNT induce ROS-dependent lipid peroxidation both *in vitro* and *in vivo* [133, 134]. A number of studies account for mitochondrial membrane depolarization, damage, and oxidative stress upon CNT exposure [92, 135, 136]. Unlike the traditional prooxidant effect of NP, CNT have been reported to sequester ROS which in turn is associated with their structural defects [83]. This quenching is reported to be related to the genotoxic and inflammatory effects observed with CNT [137].

10. Role of ROS in CNT-Induced Fibrosis

Increased ROS has been implicated in lung inflammation and fibrosis. The inflammatory cascade is reported to contribute to oxidative stress mediated lung injury [138]. Exposure to CNT results in expression of genes responsible for inflammation and fibrosis via the activation of cell signaling pathways and transcription factors including NF-κB, STAT-1, MAPK, and RTK [31]. ROS-dependent p38-MAPK has been shown to be responsible for CNT-induced collagen and angiogenic responses [118]. Additionally, SWCNT induce fibrogenic effects via ROS-mediated NF-κB activation [139], whereas MWCNT induce fibroblast to myofibroblast differentiation via ROS-dependent NF-κB activation [18].

11. Oxidative Stress as an Underlying Mechanism for NP Toxicity

Findings from several studies have pointed out that ROS generation and oxidative stress occur as an early event leading to NP-induced injury. Oxidative stress corresponds with the physicochemical reactivity of NP including metal-based particles as well as the fibrous CNT. Oxidative stress related to NP exposure involves mitochondrial respiration, mitochondrial apoptosis, activation of NADPH oxidase system, alteration of calcium homeostasis, and depletion of antioxidant enzymes; all of which are associated with tissue injury. NP-driven ROS

Table 2: List of studies describing the ROS-dependent effects of CNT.

	CNT	
SWCNT with 30% iron by mass	Lipid peroxidation, reduced cell viability, and antioxidant reserve in human keratinocytes	[170]
Acid treated MWCNTs with Co and Ni	Decreased cell viability, altered mitochondrial membrane potential in rat macrophages (NR8383) and human A549 lung cells	[92]
SWCNT	Reduced cell viability and antioxidant reserve in rat lung epithelial cells	[171]
SWCNT	Increased apoptosis, DNA damage, activated MAPKs, AP-1, NF-κB, and Akt in normal and malignant human mesothelial cells	[93]
SWCNT	Reduced cell proliferation, activation of NF-κB in human keratinocytes	[119]
Unpurified SWCNT (30% w/w iron)	Activation of AP-1 and NF-κB, cytotoxicity, and proinflammatory response *in vitro* and *in vivo*	[172]
Unpurified SWCNT (17.7% w/w iron)	Lipid peroxidation, acute inflammatory response, decreased respiratory function in adult C57BL/6 mice	[91]
Raw MWCNT	Dose-dependent cytotoxicity in RAW 264.7 macrophages and A549 cells: cell inflammation, membrane leakage, lipid peroxidation, and protein release	[173]
MWCNT	Increase in cell permeability, cell migration, and endothelial permeability in human microvascular endothelial cells (HMVEC)	[174]
SWCNT	Activation of p38 MAPK in CNT mediated fibrogenic and angiogenic responses *in vitro* in human lung fibroblasts	[118]
MWCNT	Activation of NF-κB, fibroblast-myofibroblast transformation, profibrogenic cytokine, and growth factor induction *in vitro* (BEAS-2B, WI-38, and A549 cell lines)	[18]

response contributes to activation of cell signaling pathways, inflammatory cytokine and chemokine expressions, and specific transcription factor activation. Activation of these cellular mechanisms is closely associated with transcription of genes involved in inflammation, genotoxicity, fibrosis, and cancer. Thus, the pathological consequences observed during NP exposure could be attributable to ROS generation. It is essential to incorporate these adverse biological responses as a screening tool for toxic effects of NP. For instance, overexpression of antioxidant enzymes is indicative of the mild oxidative stress, whereas mitochondrial apoptosis occurs during conditions of toxic oxidative stress. The hierarchical model of ROS response provides a scale to gauge the adverse health effects upon NP exposures. A NP exposure study must collectively involve rigorous characterization of NP and assign *in vitro* and *in vivo* oxidative stress markers as toxicity endpoints as a predictive paradigm for risk assessment [6, 9, 12]. Figure 1 summarizes the key findings regarding the oxidative effects of NP and resulting toxicity.

12. Conclusion

This paper reviews the cellular mechanisms of NP-induced oxidative stress and toxicity. We focus on the toxicity of metal oxide NP and CNT with respect to the oxidative stress paradigm. The principal factors for NP-induced oxidative stress involve (a) the oxidative properties of the NP themselves and (b) oxidant generation upon interaction of NP with cellular material. The direct prooxidant effects of NP are attributable to their physicochemical properties including surface reactivity, particle size, surface charge, chemical composition, and the presence of transition metals. Therefore, it is necessary to ensure extensive characterization of the physicochemical properties for safer design and manufacture of NP. Whereas, ROS mediated via NP-cell interaction involve mechanisms including immune cell activation, mitochondrial respiration, and NADPH oxidase system. Apart from ROS, NP also arbitrate RNS-mediated injury. Given their chemical reactivity, metal-based NP induce oxidative damage to cellular macromolecules such as proteins, lipids, and DNA via Fenton-type and Haber Weiss-type reactions. The key pathophysiological outcomes of oxidative insults during metal NP exposures involve cell membrane damage, lipid peroxidation, protein denaturation, and alteration of calcium homeostasis. Furthermore, the findings in the review article suggest that CNT-induced oxidative stress is indicative of the pulmonary toxicity of CNT. Metal-based NP and fibrous CNT-mediated ROS result in activation of cell signaling pathways, transcription factor activation, cytokine mediator release, and apoptosis. The persistent activation of these signaling cascades has some clinical ramifications. Redox imbalance via engineered NP exerts undesirable pathophysiological outcomes such as genotoxicity, inflammation, fibrosis, and carcinogenesis. It is of utmost importance to understand the molecular and cellular mechanisms of NP-induced oxidative stress which in turn will yield novel strategies to mitigate the toxicity of engineered NP. Moreover, it necessitates the establishment of stringent procedures for testing the oxidative potential of manufactured NP prior to their commercialization. Identifying the major cellular targets for NP-induced ROS will facilitate safer design and manufacture of NM in the market place.

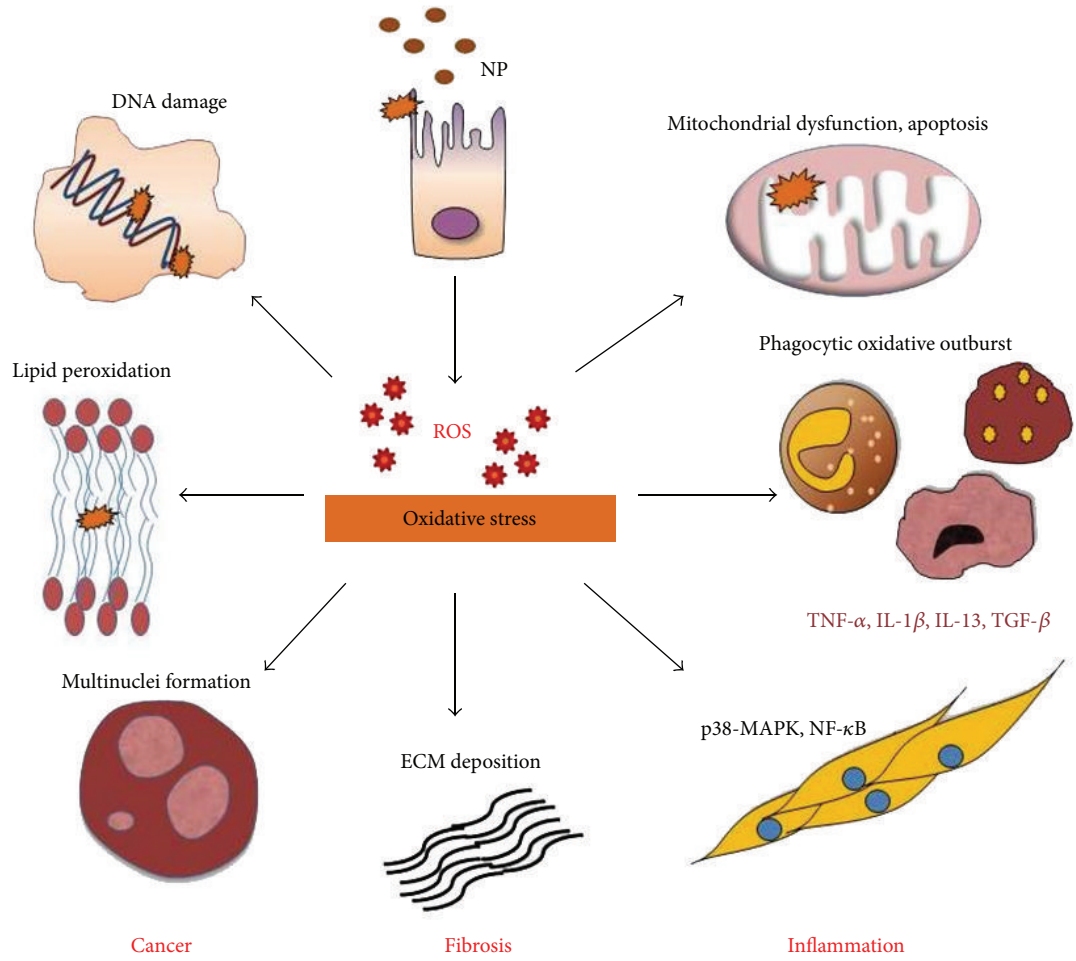

Figure 1: Prooxidant pathway for NP-induced toxicity: various NP exhibit oxidative stress dependent toxicity. Upon NP exposure, ROS generation is capable of inducing oxidative DNA damage, strand breaks, protein denaturation, and lipid peroxidation thereby demonstrating the mutagenic and carcinogenic characteristics associated with NP. Excess free radical production leads to mitochondrial membrane damage causing necrosis and cell death. Phagocytes including neutrophils and macrophages generate massive ROS upon incomplete phagocytosis of NP through the NADPH-oxidase enzyme system whereas NP-induced ROS triggers an inflammatory cascade of chemokine and cytokine expression via activation of cell signaling pathways such as MAPK, NF-κB, Akt, and RTK. Furthermore, oxidative stress mediated stimulation of these cellular mechanisms results in transcription of genes responsible for fibrosis, EMT, and carcinogenesis. NP-elicited ROS is at the center stage for majority of the ensuing adverse outcomes.

Abbreviations

ROS: Reactive oxygen species
NP: Nanoparticles
NM: Nanomaterials
RNS: Reactive nitrogen species
CNT: Carbon nanotubes
H_2O_2: Hydrogen peroxide
$O_2^{\bullet-}$: Superoxide anion
$OH^{\bullet}$: Hydroxyl radical
$^1O_2$: Singlet oxygen
HOCl: Hypochlorous acid
$ONOO^-$: Peroxynitrite
AM: Alveolar macrophages
NADPH: Nicotinamide adenine dinucleotide phosphate
Nrf2: Nuclear factor (erythroid-derived 2)-like 2
MAPK: Mitogen activated protein kinase
NF-κB: Nuclear factor kappa-light-chain enhancer of activated B cells
iNOS: Inducible nitric oxide synthase
IL-1β: Interleukin-1beta
ERKs: Extracellular signal-related kinases
GSH: Glutathione
GSSG: Glutathione disulfide
8-OHdG: 8-Hydroxyl-2′-deoxyguanosine
AP-1: Activator protein-1
STAT-1: Signal transducer and activator of transcription-1
RTK: Receptor tyrosine kinases
PTP: Protein tyrosine phosphatases
HARN: High aspect ratio nanomaterials
PARP: Poly-ADP-ribose polymerase

TNF-α: Tumor necrosis factor-alpha
TGF-β: Transforming growth factor-beta
EMT: Epithelial-mesenchymal transition.

Disclaimer

Research findings and conclusions are those of the authors and do not necessarily represent the views of the National Institute for Occupational Safety and Health.

Conflict of Interests

The authors report no conflict of interests.

Acknowledgments

This work is supported by the National Institutes of Health Grant R01-HL076340 and by the National Science Foundation Grant EPS-1003907.

References

[1] A. D. Maynard, P. A. Baron, M. Foley, A. A. Shvedova, E. R. Kisin, and V. Castranova, "Exposure to carbon nanotube material: aerosol release during the handling of unrefined single-walled carbon nanotube material," *Journal of Toxicology and Environmental Health A*, vol. 67, no. 1, pp. 87–107, 2004.

[2] K. Donaldson, F. A. Murphy, R. Duffin, and C. A. Poland, "Asbestos, carbon nanotubes and the pleural mesothelium: a review of the hypothesis regarding the role of long fibre retention in the parietal pleura, inflammation and mesothelioma," *Particle and Fibre Toxicology*, vol. 7, article 5, 2010.

[3] A. Nel, T. Xia, L. Mädler, and N. Li, "Toxic potential of materials at the nanolevel," *Science*, vol. 311, no. 5761, pp. 622–627, 2006.

[4] Y. Huang, C. Wu, and R. Aronstam, "Toxicity of transition metal oxide nanoparticles: recent insights from in vitro Studies," *Materials*, vol. 3, no. 10, pp. 4842–4859, 2010.

[5] G. M. Stella, "Carbon nanotubes and pleural damage: perspectives of nanosafety in the light of asbestos experience," *Biointerphases*, vol. 6, no. 2, pp. P1–P17, 2011.

[6] A. A. Shvedova, A. Pietroiusti, B. Fadeel, and V. E. Kagan, "Mechanisms of carbon nanotube-induced toxicity: focus on oxidative stress," *Toxicology and Applied Pharmacology*, vol. 261, no. 2, pp. 121–133, 2012.

[7] M. Pojlak-Blazi, M. Jaganjac, and N. Zarkovic, "Cell oxidative stress: risk of metal nanoparticles," in *Handbook of Nanophysics: Nanomedicine and Nanorobotics*, pp. 1–17, CRC Press, New York, NY, USA, 2010.

[8] Y. Ju-Nam and J. R. Lead, "Manufactured nanoparticles: an overview of their chemistry, interactions and potential environmental implications," *Science of the Total Environment*, vol. 400, no. 1–3, pp. 396–414, 2008.

[9] N. Li, T. Xia, and A. E. Nel, "The role of oxidative stress in ambient particulate matter-induced lung diseases and its implications in the toxicity of engineered nanoparticles," *Free Radical Biology and Medicine*, vol. 44, no. 9, pp. 1689–1699, 2008.

[10] V. Stone, H. Johnston, and M. J. D. Clift, "Air pollution, ultrafine and nanoparticle toxicology: cellular and molecular interactions," *IEEE Transactions on Nanobioscience*, vol. 6, no. 4, pp. 331–340, 2007.

[11] H. J. Johnston, G. Hutchison, F. M. Christensen, S. Peters, S. Hankin, and V. Stone, "A review of the in vivo and in vitro toxicity of silver and gold particulates: particle attributes and biological mechanisms responsible for the observed toxicity," *Critical Reviews in Toxicology*, vol. 40, no. 4, pp. 328–346, 2010.

[12] J. J. Li, S. Muralikrishnan, C. T. Ng, L. Y. Yung, and B. H. Bay, "Nanoparticle-induced pulmonary toxicity," *Experimental Biology and Medicine*, vol. 235, no. 9, pp. 1025–1033, 2010.

[13] Z. Zhang, A. Berg, H. Levanon, R. W. Fessenden, and D. Meisel, "On the interactions of free radicals with gold nanoparticles," *Journal of the American Chemical Society*, vol. 125, no. 26, pp. 7959–7963, 2003.

[14] I. M. Kennedy, D. Wilson, and A. I. Barakat, "Uptake and inflammatory effects of nanoparticles in a human vascular endothelial cell line," *Research Report*, no. 136, pp. 3–32, 2009.

[15] H. Lee, D. Shin, H. Song et al., "Nanoparticles up-regulate tumor necrosis factor-α and CXCL8 via reactive oxygen species and mitogen-activated protein kinase activation," *Toxicology and Applied Pharmacology*, vol. 238, no. 2, pp. 160–169, 2009.

[16] C. Buzea, I. I. Pacheco, and K. Robbie, "Nanomaterials and nanoparticles: sources and toxicity," *Biointerphases*, vol. 2, no. 4, pp. MR17–MR71, 2007.

[17] B. Fubini and A. Hubbard, "Reactive oxygen species (ROS) and reactive nitrogen species (RNS) generation by silica in inflammation and fibrosis," *Free Radical Biology and Medicine*, vol. 34, no. 12, pp. 1507–1516, 2003.

[18] X. He, S. Young, D. Schwegler-Berry, W. P. Chisholm, J. E. Fernback, and Q. Ma, "Multiwalled carbon nanotubes induce a fibrogenic response by stimulating reactive oxygen species production, activating NF-κB signaling, and promoting fibroblast-to-myofibroblast transformation," *Chemical Research in Toxicology*, vol. 24, no. 12, pp. 2237–2248, 2011.

[19] L. Wang, R. R. Mercer, Y. Rojanasakul et al., "Direct fibrogenic effects of dispersed single-walled carbon nanotubes on human lung fibroblasts," *Journal of Toxicology and Environmental Health A*, vol. 73, no. 5-6, pp. 410–422, 2010.

[20] V. Vallyathan and X. Shi, "The role of oxygen free radicals in occupational and environmental lung diseases," *Environmental Health Perspectives*, vol. 105, supplement 1, pp. 165–177, 1997.

[21] V. J. Thannickal and B. L. Fanburg, "Reactive oxygen species in cell signaling," *American Journal of Physiology*, vol. 279, no. 6, pp. L1005–L1028, 2000.

[22] L. Risom, P. Møller, and S. Loft, "Oxidative stress-induced DNA damage by particulate air pollution," *Mutation Research*, vol. 592, no. 1-2, pp. 119–137, 2005.

[23] C. Huang, R. S. Aronstam, D. Chen, and Y. Huang, "Oxidative stress, calcium homeostasis, and altered gene expression in human lung epithelial cells exposed to ZnO nanoparticles," *Toxicology in Vitro*, vol. 24, no. 1, pp. 45–55, 2010.

[24] H. Sies, "Oxidative stress: introduction," in *Oxidative Stress Oxidants and Antioxidants*, H. Sies, Ed., pp. 15–22, Academic Press, London, UK, 1991.

[25] A. M. Knaapen, P. J. A. Borm, C. Albrecht, and R. P. F. Schins, "Inhaled particles and lung cancer, part A: mechanisms," *International Journal of Cancer*, vol. 109, no. 6, pp. 799–809, 2004.

[26] M. Valko, C. J. Rhodes, J. Moncol, M. Izakovic, and M. Mazur, "Free radicals, metals and antioxidants in oxidative stress-induced cancer," *Chemico-Biological Interactions*, vol. 160, no. 1, pp. 1–40, 2006.

[27] K. Donaldson and C. L. Tran, "Inflammation caused by particles and fibers," *Inhalation Toxicology*, vol. 14, no. 1, pp. 5–27, 2002.

[28] K. Donaldson, V. Stone, A. Clouter, L. Renwick, and W. MacNee, "Ultrafine particles," *Occupational and Environmental Medicine*, vol. 58, no. 3, pp. 211–216, 2001.

[29] K. Donaldson, V. Stone, C. L. Tran, W. Kreyling, and P. J. A. Borm, "Nanotoxicology," *Occupational and Environmental Medicine*, vol. 61, no. 9, pp. 727–728, 2004.

[30] A. Nel, "Air pollution-related illness: effects of particles," *Science*, vol. 308, no. 5723, pp. 804–806, 2005.

[31] J. C. Bonner, "Lung fibrotic responses to particle exposure," *Toxicologic Pathology*, vol. 35, no. 1, pp. 148–153, 2007.

[32] R. P. F. Schins, "Mechanisms of genotoxicity of particles and fibers," *Inhalation Toxicology*, vol. 14, no. 1, pp. 57–78, 2002.

[33] G. Oberdörster, A. Maynard, K. Donaldson et al., "Principles for characterizing the potential human health effects from exposure to nanomaterials: elements of a screening strategy," *Particle and Fibre Toxicology*, vol. 2, article 8, 2005.

[34] M. R. Wilson, J. H. Lightbody, K. Donaldson, J. Sales, and V. Stone, "Interactions between ultrafine particles and transition metals in vivo and in vitro," *Toxicology and Applied Pharmacology*, vol. 184, no. 3, pp. 172–179, 2002.

[35] S. D. Aust, C. F. Chignell, T. M. Bray, B. Kalyanaraman, and R. P. Mason, "Free radicals in toxicology," *Toxicology and Applied Pharmacology*, vol. 120, no. 2, pp. 168–178, 1993.

[36] K. R. Smith, L. R. Klei, and A. Barchowsky, "Arsenite stimulates plasma membrane NADPH oxidase in vascular endothelial cells," *American Journal of Physiology*, vol. 280, no. 3, pp. L442–L449, 2001.

[37] C. Sioutas, R. J. Delfino, and M. Singh, "Exposure assessment for atmospheric Ultrafine Particles (UFPs) and implications in epidemiologic research," *Environmental Health Perspectives*, vol. 113, no. 8, pp. 947–955, 2005.

[38] T. Xia, M. Kovochich, J. Brant et al., "Comparison of the abilities of ambient and manufactured nanoparticles to induce cellular toxicity according to an oxidative stress paradigm," *Nano Letters*, vol. 6, no. 8, pp. 1794–1807, 2006.

[39] T. Coccini, S. Barni, R. Vaccarone, P. Mustarelli, L. Manzo, and E. Roda, "Pulmonary toxicity of instilled cadmium-doped silica nanoparticles during acute and subacute stages in rats," *Histology and Histopathology*, vol. 28, no. 2, pp. 195–209, 2013.

[40] V. Stone, J. Shaw, D. M. Brown, W. Macnee, S. P. Faux, and K. Donaldson, "The role of oxidative stress in the prolonged inhibitory effect of ultrafine carbon black on epithelial cell function," *Toxicology in Vitro*, vol. 12, no. 6, pp. 649–659, 1998.

[41] S. K. Sohaebuddin, P. T. Thevenot, D. Baker, J. W. Eaton, and L. Tang, "Nanomaterial cytotoxicity is composition, size, and cell type dependent," *Particle and Fibre Toxicology*, vol. 7, article 22, 2010.

[42] V. K. Raghunathan, M. Devey, S. Hawkins et al., "Influence of particle size and reactive oxygen species on cobalt chrome nanoparticle-mediated genotoxicity," *Biomaterials*, vol. 34, no. 14, pp. 3559–3570, 2013.

[43] K. E. Driscoll, B. W. Howard, J. M. Carter, Y. M. W. Janssen, B. T. Mossman, and R. J. Isfort, "Mitochondrial-derived oxidants and quartz activation of chemokine gene expression," *Advances in Experimental Medicine and Biology*, vol. 500, pp. 489–496, 2001.

[44] B. Fadeel and V. E. Kagan, "Apoptosis and macrophage clearance of neutrophils: regulation by reactive oxygen species," *Redox Report*, vol. 8, no. 3, pp. 143–150, 2003.

[45] A. Deshpande, P. K. Narayanan, and B. E. Lehnert, "Silica-induced generation of extracellular factor(s) increases reactive oxygen species in human bronchial epithelial cells," *Toxicological Sciences*, vol. 67, no. 2, pp. 275–283, 2002.

[46] I. Berg, T. Schluter, and G. Gercken, "Increase of bovine alveolar macrophage superoxide anion and hydrogen peroxide release by dusts of different origin," *Journal of Toxicology and Environmental Health*, vol. 39, no. 3, pp. 341–354, 1993.

[47] W. A. Pryor, K. Stone, C. E. Cross, L. Machlin, and L. Packer, "Oxidants in cigarette smoke: radicals, hydrogen peroxide, peroxynitrate, and peroxynitrite," *Annals of the New York Academy of Sciences*, vol. 686, pp. 12–28, 1993.

[48] V. Castranova, L. J. Huffman, D. J. Judy et al., "Enhancement of nitric oxide production by pulmonary cells following silica exposure," *Environmental Health Perspectives*, vol. 106, supplement 5, pp. 1165–1169, 1998.

[49] J. M. Carter and K. E. Driscoll, "The role of inflammation, oxidative stress, and proliferation in silica-induced lung disease: a species comparison," *Journal of Environmental Pathology, Toxicology and Oncology*, vol. 20, supplement 1, pp. 33–43, 2001.

[50] Y. Hsin, C. Chen, S. Huang, T. Shih, P. Lai, and P. J. Chueh, "The apoptotic effect of nanosilver is mediated by a ROS- and JNK-dependent mechanism involving the mitochondrial pathway in NIH3T3 cells," *Toxicology Letters*, vol. 179, no. 3, pp. 130–139, 2008.

[51] P. J. A. Borm, D. Robbins, S. Haubold et al., "The potential risks of nanomaterials: a review carried out for ECETOC," *Particle and Fibre Toxicology*, vol. 3, article 11, 2006.

[52] H. Eom and J. Choi, "p38 MAPK activation, DNA damage, cell cycle arrest and apoptosis as mechanisms of toxicity of silver nanoparticles in Jurkat T cells," *Environmental Science and Technology*, vol. 44, no. 21, pp. 8337–8342, 2010.

[53] G. Lenaz, "The mitochondrial production of reactive oxygen species: mechanisms and implications in human pathology," *IUBMB Life*, vol. 52, no. 3–5, pp. 159–164, 2001.

[54] J. F. Turrens, "Mitochondrial formation of reactive oxygen species," *Journal of Physiology*, vol. 552, no. 2, pp. 335–344, 2003.

[55] J. Boonstra and J. A. Post, "Molecular events associated with reactive oxygen species and cell cycle progression in mammalian cells," *Gene*, vol. 337, pp. 1–13, 2004.

[56] L. Wang, L. Bowman, Y. Lu et al., "Essential role of p53 in silica-induced apoptosis," *American Journal of Physiology*, vol. 288, no. 3, pp. L488–L496, 2005.

[57] Y. Shi, F. Wang, J. He, S. Yadav, and H. Wang, "Titanium dioxide nanoparticles cause apoptosis in BEAS-2B cells through the caspase 8/t-Bid-independent mitochondrial pathway," *Toxicology Letters*, vol. 196, no. 1, pp. 21–27, 2010.

[58] P. Manna, M. Ghosh, J. Ghosh, J. Das, and P. C. Sil, "Contribution of nano-copper particles to in vivo liver dysfunction and cellular damage: role of IκBα/NF-κB, MAPKs and mitochondrial signal," *Nanotoxicology*, vol. 6, no. 1, pp. 1–21, 2012.

[59] X. Q. Zhang, L. H. Yin, M. Tang, and Y. P. Pu, "ZnO, TiO_2, SiO_2, and Al_2O_3 nanoparticles-induced toxic effects on human fetal lung fibroblasts," *Biomedical and Environmental Sciences*, vol. 24, no. 6, pp. 661–669, 2011.

[60] M. Poljak-Blazi, M. Jaganjac, M. Mustapic, N. Pivac, and D. Muck-Seler, "Acute immunomodulatory effects of iron polyisomaltosate in rats," *Immunobiology*, vol. 214, no. 2, pp. 121–128, 2009.

[61] S. Naqvi, M. Samim, M. Z. Abdin et al., "Concentration-dependent toxicity of iron oxide nanoparticles mediated by increased oxidative stress," *International Journal of Nanomedicine*, vol. 5, no. 1, pp. 983–989, 2010.

[62] I. Pujalté, I. Passagne, B. Brouillaud et al., "Cytotoxicity and oxidative stress induced by different metallic nanoparticles on human kidney cells," *Particle and Fibre Toxicology*, vol. 8, article 10, 2011.

[63] H. A. Jeng and J. Swanson, "Toxicity of metal oxide nanoparticles in mammalian cells," *Journal of Environmental Science and Health A*, vol. 41, no. 12, pp. 2699–2711, 2006.

[64] E. Park, J. Choi, Y. Park, and K. Park, "Oxidative stress induced by cerium oxide nanoparticles in cultured BEAS-2B cells," *Toxicology*, vol. 245, no. 1-2, pp. 90–100, 2008.

[65] A. Kumar, A. K. Pandey, S. S. Singh, R. Shanker, and A. Dhawan, "Engineered ZnO and TiO_2 nanoparticles induce oxidative stress and DNA damage leading to reduced viability of *Escherichia coli*," *Free Radical Biology and Medicine*, vol. 51, no. 10, pp. 1872–1881, 2011.

[66] I. Kim, M. Baek, and S. Choi, "Comparative cytotoxicity of Al_2O_3, CeO_2, $TiO_2$and ZnO nanoparticles to human lung cells," *Journal of Nanoscience and Nanotechnology*, vol. 10, no. 5, pp. 3453–3458, 2010.

[67] S. Kawanishi, Y. Hiraku, M. Murata, and S. Oikawa, "The role of metals in site-specific DNA damage with reference to carcinogenesis," *Free Radical Biology and Medicine*, vol. 32, no. 9, pp. 822–832, 2002.

[68] H. Shi, L. G. Hudson, and K. J. Liu, "Oxidative stress and apoptosis in metal ion-induced carcinogenesis," *Free Radical Biology and Medicine*, vol. 37, no. 5, pp. 582–593, 2004.

[69] H. Wiseman and B. Halliwell, "Damage to DNA by reactive oxygen and nitrogen species: role in inflammatory disease and progression to cancer," *Biochemical Journal*, vol. 313, part 1, pp. 17–29, 1996.

[70] H. Xie, M. M. Mason, and J. P. Wise Sr., "Genotoxicity of metal nanoparticles," *Reviews on Environmental Health*, vol. 26, no. 4, pp. 251–268, 2011.

[71] A. Pilger and H. W. Rüdiger, "8-Hydroxy-2′-deoxyguanosine as a marker of oxidative DNA damage related to occupational and environmental exposures," *International Archives of Occupational and Environmental Health*, vol. 80, no. 1, pp. 1–15, 2006.

[72] A. Valavanidis, T. Vlachogianni, and C. Fiotakis, "8-hydroxy-2′-deoxyguanosine (8-OHdG): a critical biomarker of oxidative stress and carcinogenesis," *Journal of Environmental Science and Health C*, vol. 27, no. 2, pp. 120–139, 2009.

[73] K. Inoue, H. Takano, R. Yanagisawa et al., "Effects of airway exposure to nanoparticles on lung inflammation induced by bacterial endotoxin in mice," *Environmental Health Perspectives*, vol. 114, no. 9, pp. 1325–1330, 2006.

[74] K. E. Eblin, M. E. Bowen, D. W. Cromey et al., "Arsenite and monomethylarsonous acid generate oxidative stress response in human bladder cell culture," *Toxicology and Applied Pharmacology*, vol. 217, no. 1, pp. 7–14, 2006.

[75] M. Song, Y. Li, H. Kasai, and K. Kawai, "Metal nanoparticle-induced micronuclei and oxidative DNA damage in mice," *Journal of Clinical Biochemistry and Nutrition*, vol. 50, no. 3, pp. 211–216, 2012.

[76] P. J. Howden and S. P. Faux, "Fibre-induced lipid peroxidation leads to DNA adduct formation in Salmonella typhimurium TA104 and rat lung fibroblasts," *Carcinogenesis*, vol. 17, no. 3, pp. 413–419, 1996.

[77] R. K. Shukla, V. Sharma, A. K. Pandey, S. Singh, S. Sultana, and A. Dhawan, "ROS-mediated genotoxicity induced by titanium dioxide nanoparticles in human epidermal cells," *Toxicology in Vitro*, vol. 25, no. 1, pp. 231–241, 2011.

[78] D. Napierska, V. Rabolli, L. C. J. Thomassen et al., "Oxidative stress induced by pure and iron-doped amorphous silica nanoparticles in subtoxic conditions," *Chemical Research in Toxicology*, vol. 25, no. 4, pp. 828–837, 2012.

[79] M. L. Turski and D. J. Thiele, "New roles for copper metabolism in cell proliferation, signaling, and disease," *The Journal of Biological Chemistry*, vol. 284, no. 2, pp. 717–721, 2009.

[80] I. Rahman, S. K. Biswas, L. A. Jimenez, M. Torres, and H. J. Forman, "Glutathione, stress responses, and redox signaling in lung inflammation," *Antioxidants and Redox Signaling*, vol. 7, no. 1-2, pp. 42–59, 2005.

[81] G. M. Habib, Z. Shi, and M. W. Lieberman, "Glutathione protects cells against arsenite-induced toxicity," *Free Radical Biology and Medicine*, vol. 42, no. 2, pp. 191–201, 2007.

[82] K. Rahman, "Studies on free radicals, antioxidants, and co-factors," *Clinical Interventions in Aging*, vol. 2, no. 2, pp. 219–236, 2007.

[83] I. Fenoglio, I. Corazzari, C. Francia, S. Bodoardo, and B. Fubini, "The oxidation of glutathione by cobalt/tungsten carbide contributes to hard metal-induced oxidative stress," *Free Radical Research*, vol. 42, no. 8, pp. 737–745, 2008.

[84] C. Stambe, R. C. Atkins, G. H. Tesch, T. Masaki, G. F. Schreiner, and D. J. Nikolic-Paterson, "The role of p38alpha mitogen-activated protein kinase activation in renal fibrosis," *Journal of the American Society of Nephrology*, vol. 15, no. 2, pp. 370–379, 2004.

[85] E. Park, J. Yoon, K. Choi, J. Yi, and K. Park, "Induction of chronic inflammation in mice treated with titanium dioxide nanoparticles by intratracheal instillation," *Toxicology*, vol. 260, no. 1–3, pp. 37–46, 2009.

[86] C. Moon, H. Park, Y. Choi, E. Park, V. Castranova, and J. L. Kang, "Pulmonary inflammation after intraperitoneal administration of ultrafine titanium dioxide (TiO_2) at rest or in lungs primed with lipopolysaccharide," *Journal of Toxicology and Environmental Health A*, vol. 73, no. 5-6, pp. 396–409, 2010.

[87] M. A. Maurer-Jones, Y. Lin, and C. L. Haynes, "Functional assessment of metal oxide nanoparticle toxicity in immune cells," *ACS Nano*, vol. 4, no. 6, pp. 3363–3373, 2010.

[88] M. Zhu, W. Feng, Y. Wang et al., "Particokinetics and extrapulmonary translocation of intratracheally instilled ferric oxide nanoparticles in rats and the potential health risk assessment," *Toxicological Sciences*, vol. 107, no. 2, pp. 342–351, 2009.

[89] C. Lam, J. T. James, R. McCluskey, and R. L. Hunter, "Pulmonary toxicity of single-wall carbon nanotubes in mice 7 and 90 days after intractracheal instillation," *Toxicological Sciences*, vol. 77, no. 1, pp. 126–134, 2004.

[90] A. A. Shvedova, E. R. Kisin, R. Mercer et al., "Unusual inflammatory and fibrogenic pulmonary responses to single-walled carbon nanotubes in mice," *American Journal of Physiology*, vol. 289, no. 5, pp. L698–L708, 2005.

[91] A. A. Shvedova, E. Kisin, A. R. Murray et al., "Inhalation vs. aspiration of single-walled carbon nanotubes in C57BL/6 mice: inflammation, fibrosis, oxidative stress, and mutagenesis," *American Journal of Physiology*, vol. 295, no. 4, pp. L552–L565, 2008.

[92] K. Pulskamp, S. Diabaté, and H. F. Krug, "Carbon nanotubes show no sign of acute toxicity but induce intracellular reactive oxygen species in dependence on contaminants," *Toxicology Letters*, vol. 168, no. 1, pp. 58–74, 2007.

[93] M. Pacurari, X. J. Yin, J. Zhao et al., "Raw single-wall carbon nanotubes induce oxidative stress and activate MAPKs, AP-1,

NF-κB, and Akt in normal and malignant human mesothelial cells," *Environmental Health Perspectives*, vol. 116, no. 9, pp. 1211–1217, 2008.

[94] J. L. Ingram, A. B. Rice, J. Santos, B. Van Houten, and J. C. Bonner, "Vanadium-induced HB-EGF expression in human lung fibroblasts is oxidant dependent and requires MAP kinases," *American Journal of Physiology*, vol. 284, no. 5, pp. L774–L782, 2003.

[95] J. M. Antonini, "Health effects of welding," *Critical Reviews in Toxicology*, vol. 33, no. 1, pp. 61–103, 2003.

[96] P. D. Blanc, H. A. Boushey, H. Wong, S. F. Wintermeyer, and M. S. Bernstein, "Cytokines in metal fume fever," *American Review of Respiratory Disease*, vol. 147, no. 1, pp. 134–138, 1993.

[97] M. D. Taylor, J. R. Roberts, S. S. Leonard, X. Shi, and J. M. Antonini, "Effects of welding fumes of differing composition and solubility on free radical production and acute lung injury and inflammation in rats," *Toxicological Sciences*, vol. 75, no. 1, pp. 181–191, 2003.

[98] M. Genestra, "Oxyl radicals, redox-sensitive signalling cascades and antioxidants," *Cellular Signalling*, vol. 19, no. 9, pp. 1807–1819, 2007.

[99] J. Ye, X. Zhang, H. A. Young, Y. Mao, and X. Shi, "Chromium(VI)-induced nuclear factor-κB activation in intact cells via free radical reactions," *Carcinogenesis*, vol. 16, no. 10, pp. 2401–2405, 1995.

[100] R. G. Allen and M. Tresini, "Oxidative stress and gene regulation," *Free Radical Biology and Medicine*, vol. 28, no. 3, pp. 463–499, 2000.

[101] J. D. Byrne and J. A. Baugh, "The significance of nanoparticles in particle-induced pulmonary fibrosis," *McGill Journal of Medicine*, vol. 11, no. 1, pp. 43–50, 2008.

[102] A. R. Murray, E. R. Kisin, A. V. Tkach et al., "Factoring-in agglomeration of carbon nanotubes and nanofibers for better prediction of their toxicity versus asbestos," *Particle and Fibre Toxicology*, vol. 9, article 10, 2012.

[103] A. K. Hubbard, C. R. Timblin, A. Shukla, M. Rincón, and B. T. Mossman, "Activation of NF-κB-dependent gene expression by silica in lungs of luciferase reporter mice," *American Journal of Physiology*, vol. 282, no. 5, pp. L968–L975, 2002.

[104] M. Ding, X. Shi, Y. Lu et al., "Induction of activator protein-1 through reactive oxygen species by crystalline silica in JB6 cells," *The Journal of Biological Chemistry*, vol. 276, no. 12, pp. 9108–9114, 2001.

[105] K. Z. Guyton, Y. Liu, M. Gorospe, Q. Xu, and N. J. Holbrook, "Activation of mitogen-activated protein kinase by H2O2: role in cell survival following oxidant injury," *The Journal of Biological Chemistry*, vol. 271, no. 8, pp. 4138–4142, 1996.

[106] C. Tournier, G. Thomas, J. Pierre, C. Jacquemin, M. Pierre, and B. Saunier, "Mediation by arachidonic acid metabolites of the H2O2-induced stimulation of mitogen-activated protein kinases (extracellular-signal-regulated kinase and c-Jun NH2-terminal kinase)," *European Journal of Biochemistry*, vol. 244, no. 2, pp. 587–595, 1997.

[107] Y. Son, Y. Cheong, N. Kim, H. Chung, D. G. Kang, and H. Pae, "Mitogen-activated protein kinases and reactive oxygen species: how can ROS activate MAPK pathways?" *Journal of Signal Transduction*, vol. 2011, Article ID 792639, 6 pages, 2011.

[108] D. M. Barrett, S. M. Black, H. Todor, R. K. Schmidt-Ullrich, K. S. Dawson, and R. B. Mikkelsen, "Inhibition of protein-tyrosine phosphatases by mild oxidative stresses is dependent on S-nitrosylation," *The Journal of Biological Chemistry*, vol. 280, no. 15, pp. 14453–14461, 2005.

[109] Y. Kim, W. Reed, W. Wu, P. A. Bromberg, L. M. Graves, and J. M. Samet, "Zn^{2+}-induced IL-8 expression involves AP-1, JNK, and ERK activities in human airway epithelial cells," *American Journal of Physiology*, vol. 290, no. 5, pp. L1028–L1035, 2006.

[110] T. L. Tal, L. M. Graves, R. Silbajoris, P. A. Bromberg, W. Wu, and J. M. Samet, "Inhibition of protein tyrosine phosphatase activity mediates epidermal growth factor receptor signaling in human airway epithelial cells exposed to Zn^{2+}," *Toxicology and Applied Pharmacology*, vol. 214, no. 1, pp. 16–23, 2006.

[111] F. Esposito, G. Chirico, N. M. Gesualdi et al., "Protein kinase B activation by reactive oxygen species is independent of tyrosine kinase receptor phosphorylation and requires Src activity," *The Journal of Biological Chemistry*, vol. 278, no. 23, pp. 20828–20834, 2003.

[112] K. Balamurugan, R. Rajaram, T. Ramasami, and S. Narayanan, "Chromium(III)-induced apoptosis of lymphocytes: death decision by ROS and Src-family tyrosine kinases," *Free Radical Biology and Medicine*, vol. 33, no. 12, pp. 1622–1640, 2002.

[113] British Standard Institute (BSI), "Nanotechnologies—part 2: guide to safe handling and disposal of manufactured nanomaterials," Tech. Rep. PD, 6699-2, British Standard Institute (BSI), London, UK, 2007.

[114] T. Xia, M. Kovochich, M. Liong, J. I. Zink, and A. E. Nel, "Cationic polystyrene nanosphere toxicity depends on cell-specific endocytic and mitochondrial injury pathways," *ACS Nano*, vol. 2, no. 1, pp. 85–96, 2008.

[115] A. Le Goff, M. Holzinger, and S. Cosnier, "Enzymatic biosensors based on SWCNT-conducting polymer electrodes," *Analyst*, vol. 136, no. 7, pp. 1279–1287, 2011.

[116] D. B. Warheit, B. R. Laurence, K. L. Reed, D. H. Roach, G. A. M. Reynolds, and T. R. Webb, "Comparative pulmonary toxicity assessment of single-wall carbon nanotubes in rats," *Toxicological Sciences*, vol. 77, no. 1, pp. 117–125, 2004.

[117] J. C. Bonner, "The epidermal growth factor receptor at the crossroads of airway remodeling," *American Journal of Physiology*, vol. 283, no. 3, pp. L528–L530, 2002.

[118] N. Azad, A. K. Iyer, L. Wang, Y. Liu, Y. Lu, and Y. Rojanasakul, "Reactive oxygen species-mediated p38 MAPK regulates carbon nanotube-induced fibrogenic and angiogenic responses," *Nanotoxicology*, vol. 7, no. 2, pp. 157–168, 2012.

[119] S. K. Manna, S. Sarkar, J. Barr et al., "Single-walled carbon nanotube induces oxidative stress and activates nuclear transcription factor-κB in human keratinocytes," *Nano Letters*, vol. 5, no. 9, pp. 1676–1684, 2005.

[120] A. A. Shvedova, A. A. Kapralov, W. H. Feng et al., "Impaired clearance and enhanced pulmonary inflammatory/fibrotic response to carbon nanotubes in myeloperoxidase-deficient mice," *PLoS ONE*, vol. 7, no. 3, Article ID e30923, 2012.

[121] A. R. Reddy, D. R. Krishna, Y. N. Reddy, and V. Himabindu, "Translocation and extra pulmonary toxicities of multi wall carbon nanotubes in rats," *Toxicology Mechanisms and Methods*, vol. 20, no. 5, pp. 267–272, 2010.

[122] L. A. Mitchell, J. Gao, R. V. Wal, A. Gigliotti, S. W. Burchiel, and J. D. McDonald, "Pulmonary and systemic immune response to inhaled multiwalled carbon nanotubes," *Toxicological Sciences*, vol. 100, no. 1, pp. 203–214, 2007.

[123] S. Clichici, A. R. Biris, F. Tabaran, and A. Filip, "Transient oxidative stress and inflammation after intraperitoneal administration of multiwalled carbon nanotubes functionalized with single strand DNA in rats," *Toxicology and Applied Pharmacology*, vol. 259, no. 3, pp. 281–292, 2012.

[124] K. Donaldson and C. A. Poland, "Inhaled nanoparticles and lung cancer—what we can learn from conventional particle toxicology," *Swiss Medical Weekly*, vol. 142, Article ID w13547, 2012.

[125] M. Pacurari, Y. Qian, D. W. Porter et al., "Multi-walled carbon nanotube-induced gene expression in the mouse lung: association with lung pathology," *Toxicology and Applied Pharmacology*, vol. 255, no. 1, pp. 18–31, 2011.

[126] M. C. Jaurand, "Mechanisms of fiber-induced genotoxicity," *Environmental Health Perspectives*, vol. 105, supplement 5, pp. 1073–1084, 1997.

[127] M. F. Jaurand, A. Renier, and J. Daubriac, "Mesothelioma: do asbestos and carbon nanotubes pose the same health risk?" *Particle and Fibre Toxicology*, vol. 6, article 16, 2009.

[128] A. K. Patlolla, S. M. Hussain, J. J. Schlager, S. Patlolla, and P. B. Tchounwou, "Comparative study of the clastogenicity of functionalized and nonfunctionalized multiwalled carbon nanotubes in bone marrow cells of Swiss-Webster mice," *Environmental Toxicology*, vol. 25, no. 6, pp. 608–621, 2010.

[129] A. Patlolla, B. Knighten, and P. Tchounwou, "Multi-walled carbon nanotubes induce cytotoxicity, genotoxicity and apoptosis in normal human dermal fibroblast cells," *Ethnicity & Disease*, vol. 20, supplement 1, pp. 65–72, 2010.

[130] E. R. Kisin, A. R. Murray, L. Sargent et al., "Genotoxicity of carbon nanofibers: are they potentially more or less dangerous than carbon nanotubes or asbestos?" *Toxicology and Applied Pharmacology*, vol. 252, no. 1, pp. 1–10, 2011.

[131] E. R. Kisin, A. R. Murray, M. J. Keane et al., "Single-walled carbon nanotubes: geno- and cytotoxic effects in lung fibroblast V79 cells," *Journal of Toxicology and Environmental Health A*, vol. 70, no. 24, pp. 2071–2079, 2007.

[132] D. van Berlo, M. J. Clift, C. Albrecht, and R. P. Schins, "Carbon nanotubes: an insight into the mechanisms of their potential genotoxicity," *Swiss Medical Weekly*, vol. 142, Article ID w13698, 2012.

[133] Y. Guo, J. Zhang, Y. Zheng, J. Yang, and X. Zhu, "Cytotoxic and genotoxic effects of multi-wall carbon nanotubes on human umbilical vein endothelial cells in vitro," *Mutation Research*, vol. 721, no. 2, pp. 184–191, 2011.

[134] A. R. N. Reddy, M. V. Rao, D. R. Krishna, V. Himabindu, and Y. N. Reddy, "Evaluation of oxidative stress and anti-oxidant status in rat serum following exposure of carbon nanotubes," *Regulatory Toxicology and Pharmacology*, vol. 59, no. 2, pp. 251–257, 2011.

[135] F. Zhou, D. Xing, B. Wu, S. Wu, Z. Ou, and W. R. Chen, "New insights of transmembranal mechanism and subcellular localization of noncovalently modified single-walled carbon nanotubes," *Nano Letters*, vol. 10, no. 5, pp. 1677–1681, 2010.

[136] P. Ravichandran, S. Baluchamy, B. Sadanandan et al., "Multi-walled carbon nanotubes activate NF-κB and AP-1 signaling pathways to induce apoptosis in rat lung epithelial cells," *Apoptosis*, vol. 15, no. 12, pp. 1507–1516, 2010.

[137] J. Muller, I. Decordier, P. H. Hoet et al., "Clastogenic and aneugenic effects of multi-wall carbon nanotubes in epithelial cells," *Carcinogenesis*, vol. 29, no. 2, pp. 427–433, 2008.

[138] T. Kisseleva and D. A. Brenner, "Mechanisms of fibrogenesis," *Experimental Biology and Medicine*, vol. 233, no. 2, pp. 109–122, 2008.

[139] X. He, S. Young, J. E. Fernback, and Q. Ma, "Single-walled carbon nanotubes induce fibrogenic effect by disturbing mitochondrial oxidative stress and activating NF-κB signaling," *Journal of Clinical Toxicology*, supplement S5, article 005, 2012.

[140] C. R. Keenan, R. Goth-Goldstein, D. Lucas, and D. L. Sedlak, "Oxidative stress induced by zero-valent iron nanoparticles and Fe(II) in human bronchial epithelial cells," *Environmental Science and Technology*, vol. 43, no. 12, pp. 4555–4560, 2009.

[141] P. L. Apopa, Y. Qian, R. Shao et al., "Iron oxide nanoparticles induce human microvascular endothelial cell permeability through reactive oxygen species production and microtubule remodeling," *Particle and Fibre Toxicology*, vol. 6, article 1, 2009.

[142] A. R. Murray, E. Kisin, A. Inman et al., "Oxidative stress and dermal toxicity of iron oxide nanoparticles in vitro," *Cell Biochemistry and Biophysics*. In press.

[143] M. Ahamed, M. A. Siddiqui, M. J. Akhtar, I. Ahmad, A. B. Pant, and H. A. Alhadlaq, "Genotoxic potential of copper oxide nanoparticles in human lung epithelial cells," *Biochemical and Biophysical Research Communications*, vol. 396, no. 2, pp. 578–583, 2010.

[144] H. L. Karlsson, J. Gustafsson, P. Cronholm, and L. Möller, "Size-dependent toxicity of metal oxide particles—a comparison between nano- and micrometer size," *Toxicology Letters*, vol. 188, no. 2, pp. 112–118, 2009.

[145] B. Fahmy and S. A. Cormier, "Copper oxide nanoparticles induce oxidative stress and cytotoxicity in airway epithelial cells," *Toxicology in Vitro*, vol. 23, no. 7, pp. 1365–1371, 2009.

[146] R. Lei, C. Wu, B. Yang et al., "Integrated metabolomic analysis of the nano-sized copper particle-induced hepatotoxicity and nephrotoxicity in rats: a rapid in vivo screening method for nanotoxicity," *Toxicology and Applied Pharmacology*, vol. 232, no. 2, pp. 292–301, 2008.

[147] J. Y. Ma, H. Zhao, R. R. Mercer et al., "Cerium oxide nanoparticle-induced pulmonary inflammation and alveolar macrophage functional change in rats," *Nanotoxicology*, vol. 5, no. 3, pp. 312–325, 2011.

[148] H. Eom and J. Choi, "Oxidative stress of CeO_2 nanoparticles via p38-Nrf-2 signaling pathway in human bronchial epithelial cell, Beas-2B," *Toxicology Letters*, vol. 187, no. 2, pp. 77–83, 2009.

[149] W. Lin, Y. Huang, X. Zhou, and Y. Ma, "Toxicity of cerium oxide nanoparticles in human lung cancer cells," *International Journal of Toxicology*, vol. 25, no. 6, pp. 451–457, 2006.

[150] T. Xia, M. Kovochich, M. Liong et al., "Comparison of the mechanism of toxicity of zinc oxide and cerium oxide nanoparticles based on dissolution and oxidative stress properties," *ACS Nano*, vol. 2, no. 10, pp. 2121–2134, 2008.

[151] B. De Berardis, G. Civitelli, M. Condello et al., "Exposure to ZnO nanoparticles induces oxidative stress and cytotoxicity in human colon carcinoma cells," *Toxicology and Applied Pharmacology*, vol. 246, no. 3, pp. 116–127, 2010.

[152] V. Sharma, D. Anderson, and A. Dhawan, "Zinc oxide nanoparticles induce oxidative DNA damage and ROS-triggered mitochondria mediated apoptosis in human liver cells (HepG2)," *Apoptosis*, vol. 17, no. 8, pp. 852–870, 2012.

[153] S. Alarifi, D. Ali, S. Alkahtani et al., "Induction of oxidative stress, DNA damage, and apoptosis in a malignant human skin melanoma cell line after exposure to zinc oxide nanoparticles," *International Journal of Nanomedicine*, vol. 8, pp. 983–993, 2013.

[154] D. Guo, H. Bi, B. Liu, Q. Wu, D. Wang, and Y. Cui, "Reactive oxygen species-induced cytotoxic effects of zinc oxide nanoparticles in rat retinal ganglion cells," *Toxicology in Vitro*, vol. 27, no. 2, pp. 731–738, 2013.

[155] M. Ahamed, M. J. Akhtar, M. Raja et al., "ZnO nanorod-induced apoptosis in human alveolar adenocarcinoma cells via p53, survivin and bax/bcl-2 pathways: role of oxidative stress," *Nanomedicine*, vol. 7, no. 6, pp. 904–913, 2011.

[156] Y. Ye, J. Liu, J. Xu, L. Sun, M. Chen, and M. Lan, "Nano-SiO_2 induces apoptosis via activation of p53 and Bax mediated by oxidative stress in human hepatic cell line," *Toxicology in Vitro*, vol. 24, no. 3, pp. 751–758, 2010.

[157] Y. Ye, J. Liu, M. Chen, L. Sun, and M. Lan, "In vitro toxicity of silica nanoparticles in myocardial cells," *Environmental Toxicology and Pharmacology*, vol. 29, no. 2, pp. 131–137, 2010.

[158] F. Wang, F. Gao, M. Lan, H. Yuan, Y. Huang, and J. Liu, "Oxidative stress contributes to silica nanoparticle-induced cytotoxicity in human embryonic kidney cells," *Toxicology in Vitro*, vol. 23, no. 5, pp. 808–815, 2009.

[159] Q. Chen, Y. Xue, and J. Sun, "Kupffer cell-mediated hepatic injury induced by silica nanoparticles in vitro and in vivo," *International Journal of Nanomedicine*, vol. 8, pp. 1129–1140, 2013.

[160] M. A. Siddiqui, M. Ahamed, J. Ahmad et al., "Nickel oxide nanoparticles induce cytotoxicity, oxidative stress and apoptosis in cultured human cells that is abrogated by the dietary antioxidant curcumin," *Food and Chemical Toxicology*, vol. 50, no. 3-4, pp. 641–647, 2012.

[161] M. Ahamed, M. J. Akhtar, M. A. Siddiqui et al., "Oxidative stress mediated apoptosis induced by nickel ferrite nanoparticles in cultured A549 cells," *Toxicology*, vol. 283, no. 2-3, pp. 101–108, 2011.

[162] K. C. Yoo, C. H. Yoon, D. Kwon, K. H. Hyun, S. J. Woo, R. K. Kim et al., "Titanium dioxide induces apoptotic cell death through reactive oxygen species-mediated fas upregulation and bax activation," *International Journal of Nanomedicine*, vol. 7, pp. 1203–1214, 2012.

[163] Q. Saquib, A. A. Al-Khedhairy, M. A. Siddiqui, F. M. Abou-Tarboush, A. Azam, and J. Musarrat, "Titanium dioxide nanoparticles induced cytotoxicity, oxidative stress and DNA damage in human amnion epithelial (WISH) cells," *Toxicology in Vitro*, vol. 26, no. 2, pp. 351–361, 2012.

[164] K. M. Ramkumar, C. Manjula, G. GnanaKumar et al., "Oxidative stress-mediated cytotoxicity and apoptosis induction by TiO_2 nanofibers in HeLa cells," *European Journal of Pharmaceutics and Biopharmaceutics*, vol. 81, no. 2, pp. 324–333, 2012.

[165] A. A. Alshatwi, P. V. Subbarayan, E. Ramesh, A. A. Al-Hazzani, M. A. Alsaif, and A. A. Alwarthan, "Aluminium oxide nanoparticles induce mitochondrial-mediated oxidative stress and alter the expression of antioxidant enzymes in human mesenchymal stem cells," *Food Additives and Contaminants A*, vol. 30, no. 1, pp. 1–10, 2013.

[166] J. J. Li, D. Hartono, C. Ong, B. Bay, and L. L. Yung, "Autophagy and oxidative stress associated with gold nanoparticles," *Biomaterials*, vol. 31, no. 23, pp. 5996–6003, 2010.

[167] P. V. AshaRani, G. L. K. Mun, M. P. Hande, and S. Valiyaveettil, "Cytotoxicity and genotoxicity of silver nanoparticles in human cells," *ACS Nano*, vol. 3, no. 2, pp. 279–290, 2009.

[168] P. Chairuangkitti, S. Lawanprasert, S. Roytrakul, S. Aueviriyavit, D. Phummiratch, K. Kulthong et al., "Silver nanoparticles induce toxicity in A549 cells via ROS-dependent and ROS-independent pathways," *Toxicology in Vitro*, vol. 27, no. 1, pp. 330–338, 2013.

[169] I. Papageorgiou, C. Brown, R. Schins et al., "The effect of nano- and micron-sized particles of cobalt-chromium alloy on human fibroblasts in vitro," *Biomaterials*, vol. 28, no. 19, pp. 2946–2958, 2007.

[170] A. A. Shvedova, V. Castranova, E. R. Kisin et al., "Exposure to carbon nanotube material: assessment of nanotube cytotoxicity using human keratinocyte cells," *Journal of Toxicology and Environmental Health A*, vol. 66, no. 20, pp. 1909–1926, 2003.

[171] C. S. Sharma, S. Sarkar, A. Periyakaruppan et al., "Single-walled carbon nanotubes induces oxidative stress in rat lung epithelial cells," *Journal of Nanoscience and Nanotechnology*, vol. 7, no. 7, pp. 2466–2472, 2007.

[172] A. R. Murray, E. Kisin, S. S. Leonard et al., "Oxidative stress and inflammatory response in dermal toxicity of single-walled carbon nanotubes," *Toxicology*, vol. 257, no. 3, pp. 161–171, 2009.

[173] B. Chen, Y. Liu, W. M. Song, Y. Hayashi, X. C. Ding, and W. H. Li, "In vitro evaluation of cytotoxicity and oxidative stress induced by multiwalled carbon nanotubes in murine RAW 264.7 macrophages and human A549 Lung cells," *Biomedical and Environmental Sciences*, vol. 24, no. 6, pp. 593–601, 2011.

[174] M. Pacurari, Y. Qian, W. Fu et al., "Cell permeability, migration, and reactive oxygen species induced by multiwalled carbon nanotubes in human microvascular endothelial cells," *Journal of Toxicology and Environmental Health A*, vol. 75, no. 2, pp. 112–128, 2012.

Hindawi Publishing Corporation
BioMed Research International
Volume 2013, Article ID 329058, 9 pages
http://dx.doi.org/10.1155/2013/329058

Research Article

1H NMR Based Targeted Metabolite Profiling for Understanding the Complex Relationship Connecting Oxidative Stress with Endometriosis

Saikat K. Jana,[1] Mainak Dutta,[1] Mamata Joshi,[2] Sudha Srivastava,[2] Baidyanath Chakravarty,[3] and Koel Chaudhury[1]

[1] *School of Medical Science and Technology, Indian Institute of Technology, Kharagpur 721302, India*
[2] *National Facility for High-Field NMR, Tata Institute of Fundamental Research, Mumbai 400005, India*
[3] *Institute of Reproductive Medicine, Kolkata 700106, India*

Correspondence should be addressed to Koel Chaudhury; koeliitkgp@gmail.com

Received 28 April 2013; Accepted 3 July 2013

Academic Editor: Nikhat J. Siddiqi

Accumulating evidence indicates the active role of oxidative stress in the development of endometriosis; however, the mechanism of reactive oxygen species generation is poorly understood. Metabonomics/metabolomics is a scientific discipline that can be used to study changes in metabolite ensembles associated with disease pathophysiology. The present study focuses on the use of proton nuclear magnetic resonance spectroscopy based targeted metabolite profiling approach to explore dysregulation in metabolites expression in women with endometriosis. Further, association of oxidative stress with the metabolite ensembles, if any, is investigated. Using multivariate statistics, partial least square discriminant analysis model was generated which could classify endometriosis patients with sensitivity and specificity of 92.83% and 100%, respectively, and with a classification rate of 96.4%. In conjunction with increased glucose metabolism, citrate and succinate were found to be elevated in endometriosis patients. Higher levels of reactive oxygen species, lipid peroxidation, and advanced oxidation protein products and lower levels of total antioxidant capacity, superoxide dismutase, catalase, and glutathione were also observed. Increased glucose metabolism and defects in the mitochondrial respiratory system are suggested to be the possible sources of excessive reactive oxygen species generation in endometriosis.

1. Introduction

Endometriosis is classically defined as the growth of endometrial glands and stroma at extrauterine sites, most commonly implanted over visceral and peritoneal surfaces within the female pelvis. In India, approximately 1% women undergoing major gynecological surgery, 6%–43% undergoing sterilization, 12%–32% undergoing laparoscopy for pelvic pain, of 21%–48% undergoing laparoscopy for infertility are diagnosed with endometriosis [1]. From a global perspective, it is a fairly common gynecological disorder affecting almost 10% of women of reproductive age [2]. The correct approach for endometriosis management is still unclear. The risks and the diagnostic limitations of laparoscopy and the inaccuracy of clinical examination justify the considerable efforts made to improve the diagnosis with noninvasive techniques. In our previously published paper, we have reported a metabolic fingerprint which may be used for non-invasive diagnosis of the disease [3]. Also, the therapeutic approach still focuses on management of clinical symptoms of the disease rather than on the disease itself. A thorough understanding of the pathophysiology of endometriosis is therefore essential to the development of novel diagnostic and treatment approaches for this debilitating condition.

Several early studies in 1990s showed no significant correlation between oxidative stress (OS) and endometriosis [4–6]. Murphy and coworkers, way back in late 1990s, were one of the first groups to emphasize on the active role of OS in the pathogenesis and development of endometriosis [7]. Since then there has been increasing evidence suggesting

that OS plays a key role in the pathogenesis and progression of endometriosis [8, 9]. Recently, a systematic review of 19 original articles from 1990 to 2011 on OS biomarkers in patients with endometriosis has been reported [10]. Despite such long-term research activity in this field, it is still not very clear as to when and why OS may occur and its relation to endometriosis, possibly because of limited data and complex environment of the peritoneal cavity.

During OS, in addition to insufficient antioxidants, oxygen radicals are also formed at a rate greater than the rate of consumption. Changes in the composition of metabolite ensembles are responsible for physiological changes associated with OS. Thus, it is reasonable to conjecture that targeted metabolite profiling will provide information on quantitative changes in metabolites of interest based on prior knowledge of the biological function or metabolic pathway.

Metabolomic profiling has emerged as a powerful and reliable tool for the identification of total metabolites present in the biological system under a given physiological condition. Metabolites represent the final products of cells' regulatory processes and act as communicators between information-rich genome and the functional phenotype of the cell. Nuclear magnetic resonance (NMR) spectroscopy is the only technique which can identify and quantify complex mixtures of metabolites with little or no sample preparation [11]. Furthermore, only small sample volumes are required, and the analysis is nondestructive [12]. An added advantage of this technique is that the metabolite profile of a biological sample can be acquired rapidly (1–15 min) with sufficient sensitivity to differentiate even subtle biological differences. Chemometrics and targeted profiling are the two distinct approaches that have been established for processing NMR spectra. Chemometrics involves separation of NMR spectra into different groups with no assumptions about the identity and quantity of metabolites in the spectra while targeted profiling involves the identification and quantification of each metabolite in every NMR spectrum, so that metabolite concentrations are the variables [13]. In both the approaches, various multivariate statistical methods such as principal components analysis (PCA) partial least squares discriminant analysis (PLS-DA) are used to search for meaningful differences among the spectra.

Herein, we have used 1H NMR based targeted metabolite profiling followed by multivariate statistical analysis to explore metabolite imbalances, which in turn, would provide a better understanding of oxidative protection, injury, and recovery in endometriosis. Further, association of OS with the metabolite ensembles, if any, is investigated, and a probable mechanism of ROS generation in endometriosis is hypothesized.

2. Material and Methods

2.1. Subject Selection and Sample Collection. One hundred and thirty five women (24–40 years, BMI < 25) reporting at the Institute of Reproductive Medicine, Salt Lake, Kolkata, India, for infertility treatment volunteered to participate in this study. The study group consisted of 75 women with endometriosis confirmed by diagnostic laparoscopy, and 60 women with tubal factor infertility were considered as controls. Tubal factor infertility refers to women who had salpingectomy for ectopic pregnancy and proximal tubal obstruction because of low-grade infection or fimbrial occlusion with or without mild peritubal adhesions. Tubal infertility associated with gross hydrosalpingeal changes, dense pelvic adhesions because of endometriosis or pelvic inflammatory diseases were excluded. As such, in this study, tubal factor infertility refers to women who had fallopian tube(s) removed for tubal pregnancy. Women included in the study did not receive any kind of medical or hormonal treatment during the last three months. Women with history of removal of chocolate cysts, previous history of any kind of gynecological surgery including lower pelvic and abdominal surgery, with other possible causes of pain or pelvic pathology including pelvic tuberculosis were excluded. The study was approved by the Institutional ethics committee, and written informed consent was taken from all women enrolled in the study.

Venous blood was drawn in sterile containers from all women during the day time in fasting state and in their early follicular phase. Based on the effects of estrogen, it was hypothesized that the magnitude of the responses would be greater when measured during the early follicular phase compared to the rest of the menstrual cycle. The blood were then allowed to clot and serum separated by centrifugation at 3,000 rpm for 5 min at 4°C. ROS was measured immediately in the serum of all subjects. Remaining serum samples were stored at −20°C until further analysis for total antioxidant capacity (TAC), lipid peroxidation (LPO), superoxide dismutase (SOD), glutathione (GSH), and catalase levels. Further, 26 samples from endometriosis cases and 24 from controls were randomly selected from these stored serum samples and used for metabolic profiling using NMR.

2.2. Measurement of Reactive Oxygen Species. Free radicals generation was determined in serum samples from endometriosis and controls by monitoring luminol (5-amino-2,3-dihydro-1,4-phthalazinedione)-mediated chemiluminescence (CL) [14]. Luminol reacts with reactive oxygen species (ROS) present in serum resulting in a luminophore that has an emission peak at ~425 nm. The intensity of the CL is proportional to the amount of ROS in the serum. The reaction mixture contained 25 μL of serum and 0.1 mM luminol in 10 mM sodium phosphate buffer (pH 7.4). The reaction was initiated by the addition of H_2O_2 at a final concentration of 1 mM. CL was measured for 10 min using a luminometer (Berthold, Sirius Single tube Luminometer, Model no. 0727). H_2O_2 was added as an activator of luminol. Background (blank) was determined in each experiment utilizing H_2O_2, luminol, and sodium phosphate buffer without samples. The reaction was performed at 37°C and expressed in relative light units (cps).

2.3. Measurement of Lipid Peroxidation. The slightly modified thiobarbituric acid (TBA) method [15] was used to measure malonaldehyde (MDA) content in the serum sample.

Fifty microliter aliquot of frozen serum was thawed and immediately used for lipid peroxidation (LPO) estimation. Hundred microliter of stock reagent (12%, w/v trichloroacetic acid, 0.375%, w/v TBA and 0.25 mol/L HCl warmed to dissolve the TBA) was mixed thoroughly with 50 μL of the sample and heated for 15 min in a boiling water bath. After cooling, the flocculent precipitate was removed by centrifugation at 1000 ×g for 10 min and the OD of the supernatant determined at 535 nm in multiplate reader (Victor X3, Perkin Elmer, USA) against a blank containing all the reagents. LPO values were expressed as μM MDA.

2.4. Measurement of Total Antioxidant Capacity. TAC was measured in serum using a modified enhanced CL assay [16]. Serum was thawed at room temperature and diluted 1 : 10 with deionized water. Signal reagent was prepared using a CL kit (GE Healthcare, UK). A constant peak of ROS was produced using HRP conjugated IgG (Santa Cruz Biotechnology, Santa Cruz, CA). HRP was diluted with deionized water to give a desired CL output. Luminometer was set in the kinetic mode, and 900 μL of reaction mixture (100 μL signal reagent + 700 μL deionized water + 100 μL 1 : 350 diluted HRP) was added to the cuvette. After 100 seconds of reaction mixture addition, 50 μL of the diluted serum sample was added to the mixture, and 10% recovery of CL was recorded. Trolox, a water soluble tocopherol analogue, was used as a standard. The antioxidant capacity of serum samples was expressed in μM Trolox equivalents.

2.5. Determination of the Superoxide Dismutase Enzymatic Activity. Serum superoxide dismutase (SOD) activity was measured utilizing the inhibition of auto-oxidation of pyrogallol by SOD [17]. Tris buffer (containing 50 mM of Tris buffer and 1 mM of ethylene diamine tetraacetic acid, EDTA) was prepared, and pH was adjusted to 8.5 using hydrochloric acid. One hundred microliter of 20 mM pyrogallol solution was added to 2.9 mL of Tris buffer and mixed for controls measurement. Reading was taken at 420 nm after 1 min 30 s and 3 min 30 s using a UV-visible spectrophotometer (Perkin Elmer, USA). Serum SOD activity was measured by adding 0.1 mL of diluted serum sample to 2.8 mL of Tris buffer. The reaction was started by adding 0.1 mL of 20 mM pyrogallol solution. Reading was taken at 420 nm exactly after 1 min 30 s and 3 min 30 s and the absorbance recorded per 2 min. The percentage of inhibition of pyrogallol autoxidation was calculated, and 1 unit of enzymatic activity was defined as the quantity of enzyme necessary to achieve a 50% inhibition of autoxidation at 25°C.

2.6. Determination of the Catalase Enzymatic Activity. The activity of catalase enzyme was determined according to Aebi [18]. The capacity of catalase to transform H_2O_2 was measured by monitoring the decomposition of H_2O_2 at 240 nm. The final reaction volume of 3 mL contained 0.05 M Tris-buffer, 5 mM EDTA (pH 7.0), and 10 mM H_2O_2 (in 0.1 M potassium phosphate buffer, pH 7.0). Fifty microliter of serum sample was added to the above mixture. One unit of enzymatic activity was considered as the quantity of enzyme necessary to transform 1 μmol of H_2O_2 in 1 min at 37°C. Catalase activity was calculated using the molar extinction coefficient of $0.0436\,(\text{mmol L}^{-1})^{-1}\,\text{cm}^{-1}$ and expressed in terms of mM H_2O_2 consumed/min/mg protein used.

2.7. Determination of the Glutathione. Glutathione (GSH) in the serum samples was estimated by the method of Moron et al. [19]. The required amount of serum was mixed with 25% of trichloroacetic acid (TCA) and centrifuged at 2000 ×g for 15 min to settle the precipitated proteins. The supernatant was aspirated and diluted to 1 mL with 0.2 M sodium phosphate buffer (pH 8.0). Later, 2 mL of 0.6 mM 5,5′-dithiobis-2-nitrobenzoic acid (DTNB) was added. After 10 min, the OD of the yellow-colored complex formed by the reaction of GSH and DTNB was measured at 405 nm. A standard curve was obtained with standard GSH. The levels of GSH were expressed as μmol/mL.

2.8. Determination of Advanced Oxidation Protein Products. Determination of advanced oxidation protein products (AOPP) was based on spectrophotometric detection according to Witko-Sarsat et al. [20]. Two hundred microliter of serum diluted 1 : 5 in PBS, 200 μL of chloramine-T standard solution (0 to 100 μmol/liter) for calibration, and 200 μL of PBS as blank were placed in each well of a 96-well microliter plate (PerkinElmer, USA). Ten microliter of 1.16 M potassium iodide (KI, Sigma) was then added, followed by 20 μL of acetic acid. The absorbance of the reaction mixture was immediately read at 340 nm in a microplate reader against a blank. The chloramine-T absorbance at 340 nm was linear within the range of 0 to 100 μmol/liter. AOPP concentrations were expressed in μmol/liter of chloramine-T equivalents.

2.9. Nuclear Magnetic Resonance Analysis. Prior to nuclear magnetic resonance (NMR) analysis, serum samples were thawed and homogenized using a vortex mixer. Two hundred microliter of serum was mixed with 400 μL deuterium oxide (D_2O) containing 1 mM sodium salt of 3-(trimethylsilyl)propionic-2,2′,3,3′,d4 acid (TSP). After centrifugation (8000 rpm, 5 min), 600 μL of each sample was transferred to 5 mm NMR tubes. Proton NMR spectra were recorded at 298 K using a 700 MHz Bruker Avance AV III spectrometer. The resulting spectra were phased and baseline corrected by Bruker TOPSPIN 2.1 software. Individual metabolites were identified from various sources, including earlier published articles and literature, and cross checked from the Human Metabolome Database (HMDB).

2.10. Statistical Analysis. Two types of statistical analysis were performed for analysis of the entire data presented in this paper.

2.10.1. Student t-Test. Data were analyzed using analysis of t-test, as appropriate. Data analyses were performed with (GraphPad QuickCalcs, 2002–2005, GraphPad Software, Inc., USA). Statistical significance was defined as $P \leq 0.05$.

2.10.2. Multivariate Statistical Analysis. Expression of different metabolites in endometriosis compared to controls was analyzed using multivariate statistical analysis. The analysis was applied to a total of 50 spectra from 26 endometriosis and 24 control serum samples. After acquisition, data matrix of peak integral values corresponding to identified compounds was built. Data were preprocessed using normalization and scaling to remove possible bias arising due to sample handling and sample variability. Normalization (by sum) was performed in order to minimize possible differences in concentration between samples. Following normalization, scaling (mean-centering and division by the square root of standard deviation of each variable) was done to give all variables equal weight regardless of their absolute value. After data preprocessing, PCA and PLS-DA were performed using web-based metabolomic data processing tool MetaboAnalyst 2.0 (Canada) (accessible at http://www.metaboanalyst.ca/) [21]. In MetaboAnalyst, statistical computing and visualization operations are performed using functions from the R and Bioconductor packages [22, 23]. PCA is used to detect intrinsic clusters and outliers within the data set, while PLS-DA maximizes class discrimination. Model robustness was assessed using another web-based ROC curve analysis tool, ROCCET (accessible at http://www.roccet.ca/). ROC curves in ROCCET are generated by Monte Carlo Cross Validation (MCCV) [24] using balanced subsampling. In each MCCV, two-third (2/3) of the samples were used to evaluate the feature importance. The top 100 important features were then used to build classification models which were validated on one-third of the samples that were left out. The procedures were repeated multiple times to calculate the performance of the PLS-DA model. Sensitivity and specificity of the model were calculated from the confusion matrix generated from the multiple MCCV iterations. Further validation was performed with MetaboAnalyst 2.0, using permutation tests consisting of 1000 permutations.

2.10.3. Metabolic Pathway Analysis. Detailed analysis of the most relevant metabolic pathways and networks in women with endometriosis was performed by MetaboAnalyst that combines results from powerful pathway enrichment analysis involved in the conditions under study. MetaboAnalyst uses high-quality KEGG metabolic pathways as the back end knowledge base. It integrates many well-established methods (i.e., univariate analysis, over-representation analysis), and novel algorithms and concepts (i.e., Global Test, Global-Ancova, network topology analysis) with pathway analysis [25].

3. Results

OS markers in serum of women with endometriosis and controls are summarized in Table 1. ROS, LPO, and AOPP were observed to be increased significantly whereas TAC, SOD, catalase, and GSH levels were significantly less in endometriosis women as compared to controls. Several amino acids, organic acids, and other molecules were identified in serum using 1H NMR metabolic profiling. A representative metabolic fingerprint of serum from women with endometriosis is shown in Supplementary Figure 1 in Supplementary Materials available online at http://dx.doi.org/10.1155/2013/329058. Exploratory PCA of identified metabolites was employed to detect intrinsic clustering and possible outliers. Figure 1(a) depicting PC1 versus PC2 scores scatter plot shows a trend for unsupervised separation between endometriosis and controls. PLS-DA further maximized the group separation (Figure 1(b)). Leave one out cross-validation (LOOCV) was employed from which Q^2 and R^2 values (representing the predictive capability and the explained variance, resp.) were extracted. The model with R^2 close to 0.83 and Q^2 well above 0.82 showed a very good predictive ability. To better assess the predictive ability of the PLS-DA classification model, MCCV was applied as discussed in Section 2. Sensitivity (percentage of endometriosis samples correctly classified as true positives) and specificity (percentage of control samples correctly classified as true negatives) of the PLS-DA model were found to be 100% and 91.67%, respectively, with a classification rate (total number of samples correctly classified) of 95.83%. Area under the ROC curve (Figure 1(c)) was found to be 0.99, denoting high predictive accuracy of the model. Further, model validation relied on permutation analysis. The analysis was performed only for the best model. If the performance score of the original data lies outside the distribution, then the result is significant. Using 1000 permutation tests, the P value is reported as $P \leq 0.001$, denoting that none of the results are better than the original one (Figure 1(d)). The further away from the plot origin a variable lies, the stronger impact the variable has on the model. From PLS-DA loading plot, metabolites with higher loadings were identified (Supplementary Figure 2). On comparing the loading and scores plot, it becomes evident that lactate, 2-hydroxybutyrate, succinate, lysine, glycerophosphocholine, citric acid, pyruvate, adipic acid and lipids are overexpressed in endometriosis whereas isoleucine, arginine, asparagine, glucose, creatine, alanine, leucine and fatty acid have higher expression in controls. Signals with high VIP values (Supplementary Figure 3) are considered to be significant and therefore validated using t-test (Table 2). With pattern recognition analysis of profiles of metabolites, a clear separation between endometriosis and controls was achieved. As a consequence of dysregulation of specific metabolites, metabolic pathway analysis was performed using MetaboAnalyst. The affected pathways (Impact-value ≥ 0.10) in women with endometriosis are represented in Supplementary Figure 4.

4. Discussion

The present study is an attempt to measure levels of various OS parameters in serum of endometriosis patients and identify differently expressed metabolites using 1H-NMR based targeted profiling to have an improved understanding of the disease pathophysiology.

Several studies have reported ROS concentration to be higher in women with endometriosis [6, 26] which is in agreement with our findings. Endometriosis has also been associated with significantly higher levels of lipid peroxide-modified rabbit serum albumin, malondialdehyde-modified

Table 1: Levels of oxidative stress parameters in endometriosis and controls.

Parameters	Endometriosis ($n = 60$)	Controls ($n = 60$)	P value
ROS (cps)	129.5 ± 1.9	73.84 ± 1.7	$P \leq 0.001$
LPO (μM MDA)	1.366 ± 0.04372	1.014 ± 0.03146	$P \leq 0.001$
TAC (μM Trolox equivalent)	733.6 ± 4.989	936.3 ± 4.141	$P \leq 0.001$
SOD (units/mL)	23.19 ± 0.43	39.23 ± 0.48	$P \leq 0.001$
Catalase (nmol/min/mg)	30.63 ± 0.7389	49.09 ± 1.148	$P \leq 0.001$
GSH (μmol/mL)	3.06 ± 0.06898	7.01 ± 0.08175	$P \leq 0.001$
AOPP (μmol/L)	155.1 ± 4.250	90.60 ± 3.445	$P \leq 0.001$

Mean ± SEM.

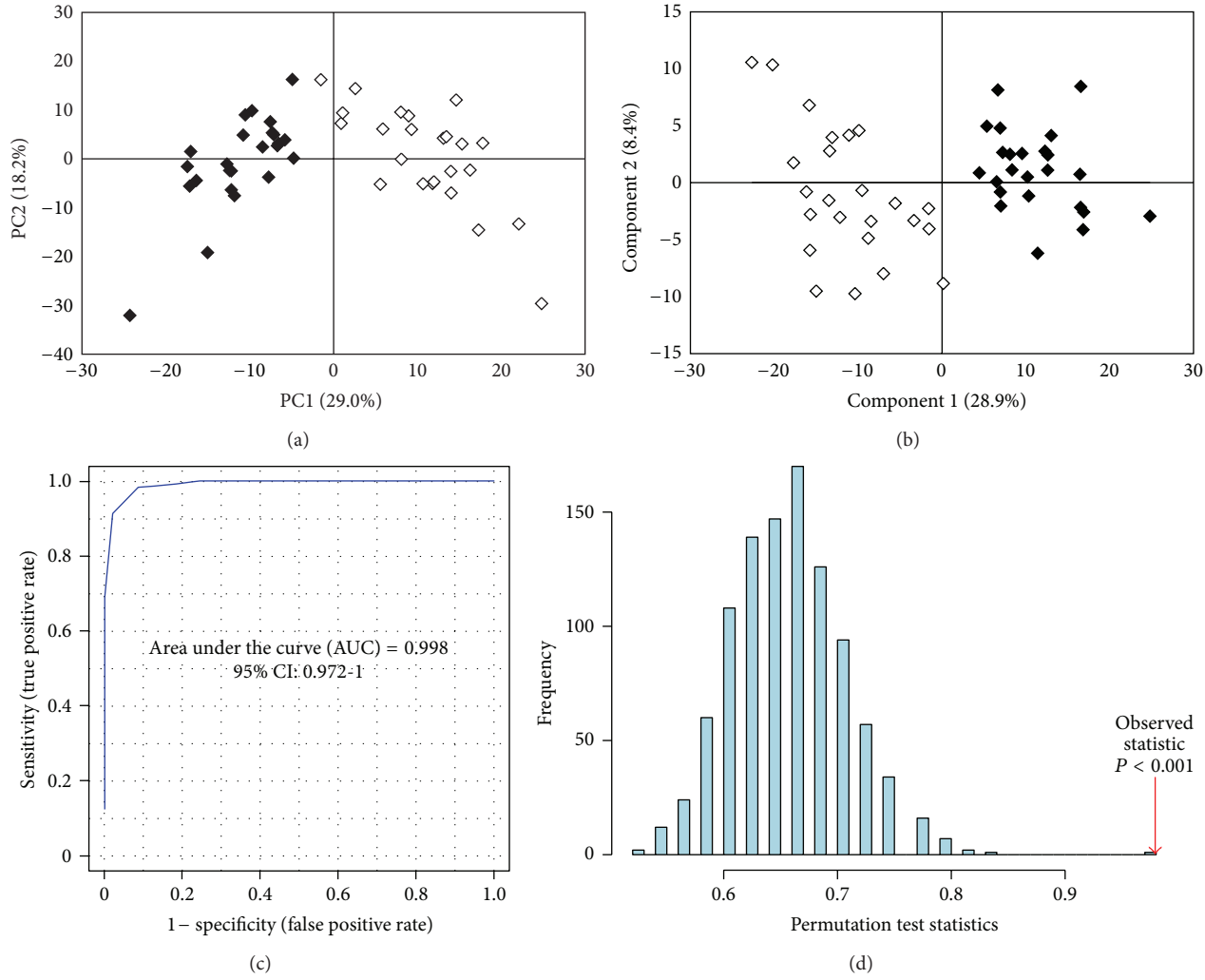

Figure 1: Scores scatter plot of (a) PC1 versus PC2 and (b) component 1 versus component 2 resulting from PCA and PLS-DA, respectively, applied to 1H NMR spectra of serum of endometriosis patients (black diamond) and controls (white diamond). Validation of the PLS-DA model was performed by (c) receiver operating characteristic (ROC) analysis where area under the curve (AUC) was found to be 0.99 (d) Permutation test statistics at 1000 permutations with observed statistic at $P < 0.001$.

low-density lipoprotein, and oxidized low-density lipoprotein as measured in serum and compared to tubal ligation cases [27]. Furthermore, lipid peroxide concentrations have been reported to be highest in women with endometriosis indicating the involvement of ROS in the development of the disease [9]. These observations support the results of the present study where significant increase in LPO levels in endometriosis women is observed.

Catalase, SOD and GSH are utilized to keep ROS in check. It is thus imperative that lower levels of these enzymes

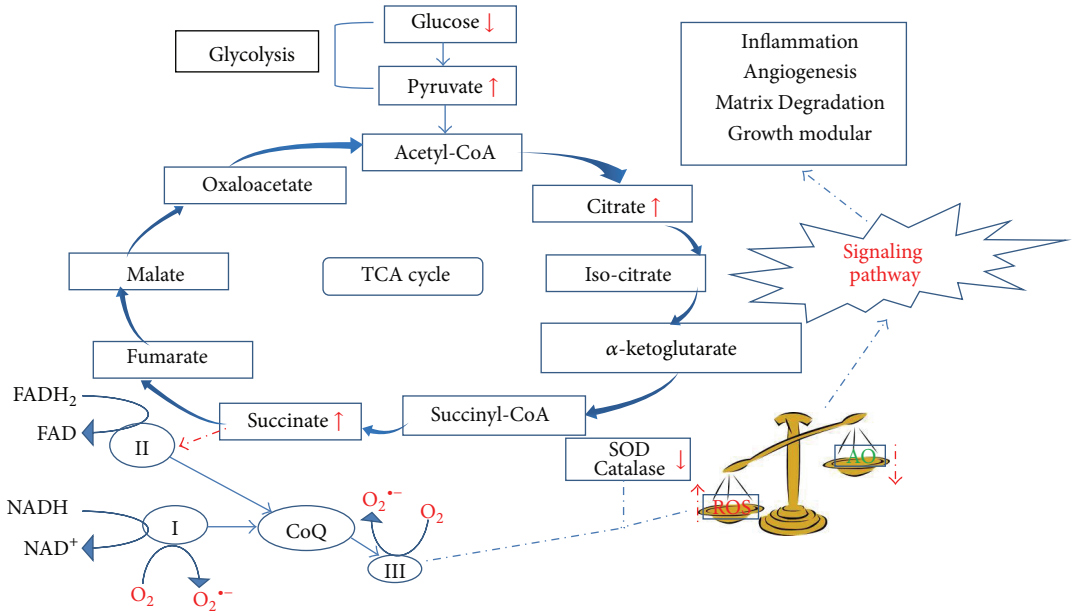

Figure 2: Figure depicting the role of metabolites in generation of free radicals. Lower levels of glucose along with elevated levels of pyruvate, citrate, and succinate indicate enhanced glucose metabolism along with impaired mitochondrial respiration. I, II, and III represent complex I, II, and III, respectively, of electron transport chain. Complex I and III are the primary sites of free radical generation. Elevated levels of succinate indicate complex III to be the most probable site for ROS generation in endometriosis. These free radicals are further removed from the system by various ROS scavengers such as SOD and catalase. An imbalance in the rate of formation and removal of free radicals results in oxidative stress. In endometriosis, lower levels of these enzymes lead to continued prevalence of oxidative stress.

Table 2: Main serum metabolites contributing towards discrimination between endometriosis and controls.

Metabolites	δ 1H (ppm)	Fold changes (relative to controls)
Glucose	3.26	0.26
Alanine	1.5	0.32
Creatine	3.06	0.13
2-hydroxybutyrate	3.96	1.55
Lactate	4.11	1.92
L-lysine	3.04	1.72
Pyruvate	2.47	1.58
Succinic acid	2.39	1.48
Adipic acid	1.54	1.61
L-leucine	0.99	0.51
Citric acid	2.54	1.67
L-iso leucine	1.03	0.82
Glycerophosphocholine	3.66	1.85
L-asparagine	2.84	0.41
L-arginine	1.64	0.94

would indicate increased ROS production which is evidenced by the findings of the present study (Table 1). A significant decrease in TAC level in endometriosis women was also observed in the present study (Table 1). This is in accordance with the findings of Szczepańska and coworkers who have documented that mean activity of SOD and total antioxidant status are lowest among infertile patients with endometriosis [9]. Ota et al. reported a higher expression of SOD in endometrial tissues of endometriotic women as compared to controls by immunohistochemistry, which is a semiquantitative method [28]. On the contrary, Szczepańska et al. observed reduced SOD level in peritoneal fluid in endometriosis as compared to controls using quantitative spectrophotometric assay [9]. This is in accordance with our present study, where reduced SOD level were observed in serum of endometriotic women. From the present study, OS condition is indicated in endometriosis, as evidenced by lower expression of TAC, SOD, GSH, catalase, and higher ROS generation.

Protein cross-linking products formed due to oxidation of amino acids by ROS in the plasma are designated as AOPP [29]. AOPP are formed during OS by the action of chlorinated oxidants, mainly hypochlorous acid and chloramines [30]. AOPP are predominantly aggregates of albumin damaged by OS [29]. Increased levels of AOPP in endometriosis observed in the present study are in agreement with increased OS reported in these women.

Multivariate analysis of the identified NMR spectra clearly distinguishes endometriosis cases from the controls. On plotting PC1 (29.0%) × PC2 (18.2%), the plots for endometriosis are observed to lie in a principal component plane which is significantly different from the plane where plots for controls are clustered (Figure 1(a)). As evidenced in Figure 1(b), PLS-DA shows statistically significant separation between endometriosis and control cases. Our values corresponding to R^2 and Q^2 close to 0.8 indicate that the

model is valid and can predict better than chance. Sensitivity, specificity and classification rates of 100%, 91.67%, and 95.83%, respectively, further validate the model robustness. Also, permutation test statistics result ($P < 0.001$) validates the predictive ability of the real model. Metabolites with high VIP scores including lactate, L-alanine, glycerophosphocholine, glucose, L-leucine, L-lysine, creatine, L-arginine, succinic acid, adipic acid, lipid, pyruvate, 2-hydroxybutyrate, L-isoleucine, L-asparagine, and citric acid were considered as significant.

The tripeptide glutathione is reported to be critical in the detoxification of ROS [31]. Glutathione is considered as one of the most abundant antioxidants present in cells [32, 33]. Reduced glutathione donates electron to ROS and gets oxidized, thus helping in scavenging unstable ROS. Increased GSSG/GSH ratio is indicative of OS [34]. This is in agreement with our results which indicate a significant decrease in GSH. Ophthalmate has been indicated as a biomarker of OS as insufficient levels of GSH results in ophthalmate synthesis [35]. 2-hydroxybutyrate is released as a by-product during ophthalmate synthesis. Metabolite profiling of serum revealed increased levels of 2-hydroxybutyrate which further support the prevalence of OS in endometriosis. Unlike ROS detoxifying agents like SOD and catalase that only decompose ROS without having an impact on their production, the TCA cycle can regulate both, their formation and decomposition [35]. Glucose levels were found to be significantly less in endometriosis as compared to controls. Increased metabolism of glucose in conjunction with up-regulation of pyruvate suggests enhanced glycolysis in these women. It is well known that all aerobic organisms rely predominantly on the TCA cycle to generate NADH and FADH2 from acetyl CoA for the synthesis of ATP during oxidative phosphorylation. Other than the production of ATP, mitochondria are also involved in the cell's response to OS. Several steps in the path of oxygen reduction in mitochondria have the potential to produce highly reactive free radicals that can damage cells. 0.1%–4% of the O_2 used by actively respiring mitochondria forms $^{\bullet}O_2^-$ which can have lethal effects on a cell unless the free radical is quickly disposed of. In the present study, in conjunction with increased glucose metabolism, citrate and succinate, two TCA cycle intermediate products, were also found to be elevated in endometriosis patients. These data support the notion that a possible defect is associated with the mitochondrial respiratory system with an increased probability of ROS generation from the ETC. A probable hypothesis summarizing the possible route of free radical generation in endometriosis patients is depicted in Figure 2. While in normal cells various antioxidants dispose of ROS from the system, insufficient levels of SOD and catalase in endometriosis are indicative of inefficient scavenging effect leading to a continued prevalence of ROS in the system.

Leucine and isoleucine are essential amino acids. Leucine catabolism terminates at acetyl CoA whereas isoleucine gives rise to acetyl CoA and propionyl CoA. Moreover, acetyl CoA provides the carbon atoms of its acetyl group to the TCA cycle for energy production. Decreased serum levels of both leucine and isoleucine indicate enhanced catabolism of these amino acids leading to elevated TCA cycle intermediates.

Adipic acid is a byproduct of LPO which is nonenzymatically mediated by ROS. NMR metabonomic data indicating a significant decrease in lipid and increase in adipic acid levels supported by the higher levels of LPO estimated biochemically reconfirms the involvement of OS. L-lysine is an essential amino acid which is known to reduce OS [35]. Since lysine uses the same intracellular transporter system as arginine, hence lysine competes with arginine for its transport within the cells. Elevated lysine and lower arginine levels in serum of women in endometriosis may be attributed to increased uptake of arginine by the cells.

Glycerophosphocholine (GPC) plays a pivotal role as an osmotic pressure regulator and metabolic antitoxin. It is a major reservoir for cell membrane omega-3 phospholipids, the major building blocks for cell membranes. It helps in supporting membrane fluidity, enabling membrane proteins to perform with better efficiency. Under OS condition, GPC is reported to get oxidized [36] and reduced GPC levels in serum may lead to reduced cell membrane fluidity and efficiency.

Asparaginase is an enzyme which converts asparagine into ammonia and aspartate. Aspartate transaminates to oxaloacetate, which follows the gluconeogenic pathway to form glucose. Lower serum levels of gluconeogenic amino acids including asparagine and alanine in endometriosis may be due to its increased utilization as a major gluconeogenic precursor, to meet the high glucose uptake and demand by fast growing endometrial cells outside the uterus.

5. Conclusion

This is the first attempt to identify the potential causes of ROS generation in women with endometriosis. NMR based targeted metabolic profiling method was used for this purpose. The preliminary findings suggest increased glucose metabolism and defects in the mitochondrial respiratory system to be possible sources of excessive ROS generation in these women. It may be argued that these preliminary results are not reliable enough to functionally associate OS with metabolite pathways. Follow-up laboratory efforts leading to experimental validation targeted specifically to the predicted pathway are, therefore, necessary.

6. Limitation

Multivariate statistical analysis is useful in providing association between multiple risk factors and disease condition. It was, therefore, used to identify the potential causes of ROS generation in endometriosis cases. However, these preliminary results require further validation to functionally associate OS with the proposed metabolite pathway.

Abbreviations

OS: Oxidative stress
ROS: Reactive oxygen species
LPO: Lipid peroxidation
OD: Optical density
TBA: 3-(methyl thio)butyric acid

MDA: Malondialdehyde
TAC: Total antioxidant capacity
HRP: Horseradish peroxidase
SOD: Superoxide dismutase
GPC: Glycerophosphocholine
GSH: Glutathione
AOPP: Advanced oxidation protein products
NMR: Nuclear magnetic resonance
D_2O: Heavy water.

Conflict of Interests

Authors have no conflict of interests.

Authors' Contribution

Saikat K. Jana and Koel Chaudhury conceived and designed the experiments. Saikat K. Jana, Mainak Dutta, and Mamata Joshi performed the experiments. Saikat K. Jana and Mainak Dutta analyzed the data. Koel Chaudhury and Sudha Srivastava contributed in providing reagents/materials/analysis tools. Baidyanath Chakravarty and Saikat K. Jana contributed in patient selection and sample collection. Saikat K. Jana, Mainak Dutta, and Koel Chaudhury drafted the paper. The authors Saikat K. Jana and Mainak Dutta have contributed equally to the work and may be considered as joint first authors.

Acknowledgments

The authors would like to acknowledge Department of Science and Technology, Government of India, India (research project SR/SO/HS-0022/2008) for funding. The authors are grateful to all the volunteers who participated in this study, as well as to Shanawaz Yasmin from IRM, Kolkata and IIT Kharagpur, respectively, for helping in the collection of samples. The facilities provided by the National Facility for High Field NMR located at TIFR and supported by the Department of Science and Technology (DST) are also gratefully acknowledged.

References

[1] S. Mittal, "Endometriosis-clinical perspectives," in *Proceedings of the INDO—US Workshop on Microarray in Endometriosis: Clinics to Research Laboratory*, All India Institute of Medical Sciences, New Delhi, India, 2009.

[2] L. C. Giudice and L. C. Kao, "Endometriosis," *The Lancet*, vol. 364, no. 9447, pp. 1789–1799, 2004.

[3] M. Dutta, M. Joshi, S. Srivastava, I. Lodh, B. Chakravarty, and K. Chaudhury, "A metabonomics approach as a means for identification of potential biomarkers for early diagnosis of endometriosis," *Molecular BioSystems*, vol. 8, pp. 3281–3287, 2012.

[4] K. Arumugam and Y. C. Y. Dip, "Endometriosis and infertility: the role of exogenous lipid peroxides in the peritoneal fluid," *Fertility and Sterility*, vol. 63, no. 1, pp. 198–199, 1995.

[5] H.-N. Ho, M.-Y. Wu, S.-U. Chen, K.-H. Chao, C.-D. Chen, and Y.-S. Yang, "Total antioxidant status and nitric oxide do not increase in peritoneal fluids from women with endometriosis," *Human Reproduction*, vol. 12, no. 12, pp. 2810–2815, 1997.

[6] Y. Wang, J. Goldberg, R. K. Sharma, A. Agarwal, and T. Falcone, "Importance of reactive oxygen species in the peritoneal fluid of women with endometriosis or idiopathic infertility," *Fertility and Sterility*, vol. 68, no. 5, pp. 826–830, 1997.

[7] A. A. Murphy, N. Santanam, and S. Parthasarathy, "Endometriosis: a disease of oxidative stress?" *Seminars in Reproductive Endocrinology*, vol. 16, no. 4, pp. 263–273, 1998.

[8] A. Agarwal, A. Aponte-Mellado, B. J. Premkumar, A. Shaman, and S. Gupta, "The effects of oxidative stress on female reproduction: a review," *Reproductive Biology and Endocrinology*, vol. 10, article 49, 2012.

[9] M. Szczepańska, J. Koźlik, J. Skrzypczak, and M. Mikołajczyk, "Oxidative stress may be a piece in the endometriosis puzzle," *Fertility and Sterility*, vol. 79, pp. 1288–1293, 2003.

[10] L. F. Carvalho, A. N. Samadder, A. Agarwal, L. F. Fernandes, and M. S. Abrão, "Oxidative stress biomarkers in patients with endometriosis: systematic review," *Archives of Gynecology and Obstetrics*, vol. 286, pp. 1033–1040, 2012.

[11] O. Beckonert, H. C. Keun, T. M. D. Ebbels et al., "Metabolic profiling, metabolomic and metabonomic procedures for NMR spectroscopy of urine, plasma, serum and tissue extracts," *Nature protocols*, vol. 2, no. 11, pp. 2692–2703, 2007.

[12] W. S. Price, "Applications of pulsed gradient spin-echo NMR diffusion measurements to solution dynamics and organization," in *Diffusion Fundamentals*, J. Karger, F. Grinberg, and P. Heitjans, Eds., pp. 490–508, Leipzig University Press, Leipzig, Germany, 2005.

[13] J. Liu, L. Litt, M. R. Segal, M. J. S. Kelly, J. G. Pelton, and M. Kim, "Metabolomics of oxidative stress in recent studies of endogenous and exogenously administered intermediate metabolites," *International Journal of Molecular Sciences*, vol. 12, no. 10, pp. 6469–6501, 2011.

[14] K. Chaudhury, K. N. Babu, A. K. Singh, S. Das, A. Kumar, and S. Seal, "Mitigation of endometriosis using regenerative cerium oxide nanoparticles," *Nanomedicine*, vol. 9, pp. 439–448, 2012.

[15] J. A. Buege and S. D. Aust, "Microsomal lipid peroxidation," *Methods in Enzymology*, vol. 52, pp. 302–310, 1978.

[16] I. L. C. Chapple, "Reactive oxygen species and antioxidants in inflammatory diseases," *Journal of Clinical Periodontology*, vol. 24, no. 5, pp. 287–296, 1997.

[17] S. Marklund and G. Marklund, "Involvement of the superoxide anion radical in the autoxidation of pyrogallol and a convenient assay for superoxide dismutase," *European Journal of Biochemistry*, vol. 47, no. 3, pp. 469–474, 1974.

[18] H. Aebi, "Catalase in vitro," *Methods in Enzymology*, vol. 105, pp. 121–126, 1984.

[19] M. S. Moron, J. W. Depierre, and B. Mannervik, "Levels of glutathione, glutathione reductase and glutathione S-transferase activities in rat lung and liver," *Biochimica et Biophysica Acta*, vol. 582, no. 1, pp. 67–78, 1979.

[20] V. Witko-Sarsat, M. Friedlander, C. Capeillere-Blandin et al., "Advanced oxidation protein products as a novel marker of oxidative stress in uremia," *Kidney International*, vol. 49, pp. 1304–1313, 1996.

[21] J. Xia, R. Mandal, I. V. Sinelnikov, D. Broadhurst, and D. S. Wishart, "MetaboAnalyst 2. 0—a comprehensive server for metabolomic data analysis," *Nucleic Acids Research*, vol. 40, pp. 127–133, 2012.

[22] J. Xia and D. S. Wishart, "Chapter 14: metabolomic data processing, analysis, and interpretation using MetaboAnalyst," in *Current Protocols in Bioinformatics*, 2011.

[23] J. Xia, N. Psychogios, N. Young, and D. S. Wishart, "MetaboAnalyst: a web server for metabolomic data analysis and interpretation," *Nucleic Acids Research*, vol. 37, no. 2, pp. W652–W660, 2009.

[24] J. Carrola, C. M. Rocha, A. S. Barros et al., "Metabolic signatures of lung cancer in biofluids: NMR-based metabonomics of urine," *Journal of Proteome Research*, vol. 10, no. 1, pp. 221–230, 2011.

[25] J. Xia and D. S. Wishart, "Web-based inference of biological patterns, functions and pathways from metabolomic data using MetaboAnalyst," *Nature Protocols*, vol. 6, no. 6, pp. 743–760, 2011.

[26] M. A. Bedaiwy, T. Falcone, R. K. Sharma et al., "Prediction of endometriosis with serum and peritoneal fluid markers: a prospective controlled trial," *Human Reproduction*, vol. 17, no. 2, pp. 426–431, 2002.

[27] A. Shanti, N. Santanam, A. J. Morales, S. Parthasarathy, and A. A. Murphy, "Autoantibodies to markers of oxidative stress are elevated in women with endometriosis," *Fertility and Sterility*, vol. 71, no. 6, pp. 1115–1118, 1999.

[28] H. Ota, S. Igarashi, J. Hatazawa, and T. Tanaka, "Immunohistochemical assessment of superoxide dismutase expression in the endometrium in endometriosis and adenomyosis," *Fertility and Sterility*, vol. 72, no. 1, pp. 129–134, 1999.

[29] F. Yuan, S.-X. Liu, and J.-W. Tian, "Advanced oxidation protein products induce reactive oxygen species production in endothelial cells," *Di Yi Jun Yi Da Xue Xue Bao*, vol. 24, no. 12, pp. 1350–1352, 2004.

[30] V. Witko-Sarsat, V. Gausson, A.-T. Nguyen et al., "AOPP-induced activation of human neutrophil and monocyte oxidative metabolism: a potential target for N-acetylcysteine treatment in dialysis patients," *Kidney International*, vol. 64, no. 1, pp. 82–91, 2003.

[31] D. M. Townsend, K. D. Tew, and H. Tapiero, "The importance of glutathione in human disease," *Biomedicine and Pharmacotherapy*, vol. 57, no. 3, pp. 145–155, 2003.

[32] A. Meister and M. E. Anderson, "Glutathione," *Annual Review of Biochemistry*, vol. 52, pp. 711–760, 1983.

[33] C. Kerksick and D. Willoughby, "The antioxidant role of glutathione and N-acetyl-cysteine supplements and exercise-induced oxidative stress," *Journal of the International Society of Sports Nutrition*, vol. 2, pp. 38–44, 2005.

[34] J. B. Owen and D. A. Butterfield, "Measurement of oxidized/reduced glutathione ratio," *Methods in Molecular Biology*, vol. 648, pp. 269–277, 2010.

[35] T. Soga, R. Baran, M. Suematsu et al., "Differential metabolomics reveals ophthalmic acid as an oxidative stress biomarker indicating hepatic glutathione consumption," *Journal of Biological Chemistry*, vol. 281, no. 24, pp. 16768–16776, 2006.

[36] I. Milic, M. Fedorova, K. Teuber, J. Schiller, and R. Hoffmann, "Characterization of oxidation products from 1-palmitoyl-2-linoleoyl-sn- glycerophosphatidylcholine in aqueous solutions and their reactions with cysteine, histidine and lysine residues," *Chemistry and Physics of Lipids*, vol. 165, no. 2, pp. 186–196, 2012.

Hindawi Publishing Corporation
BioMed Research International
Volume 2013, Article ID 152909, 9 pages
http://dx.doi.org/10.1155/2013/152909

Research Article

The Effect of *Msh2* Knockdown on Toxicity Induced by *tert*-Butyl-hydroperoxide, Potassium Bromate, and Hydrogen Peroxide in Base Excision Repair Proficient and Deficient Cells

N. Cooley,[1] R. H. Elder,[2] and A. C. Povey[1]

[1] *Centre for Occupational and Environmental Health, Institute of Population Health, Faculty of Medical and Human Sciences, University of Manchester, Manchester M13 9PT, UK*
[2] *School of Environment and Life Sciences, Cockcroft Building, University of Salford, Salford M5 4WT, UK*

Correspondence should be addressed to A. C. Povey; apovey@manchester.ac.uk

Received 18 April 2013; Revised 3 July 2013; Accepted 10 July 2013

Academic Editor: Nikhat J. Siddiqi

The DNA mismatch repair (MMR) and base excision repair (BER) systems are important determinants of cellular toxicity following exposure to agents that cause oxidative DNA damage. To examine the interactions between these different repair systems, we examined whether toxicity, induced by *t*-BOOH and $KBrO_3$, differs in BER proficient ($Mpg^{+/+}$, $Nth1^{+/+}$) and deficient ($Mpg^{-/-}$, $Nth1^{-/-}$) mouse embryonic fibroblasts (MEFs) following *Msh2* knockdown of between 79 and 88% using an shRNA expression vector. *Msh2* knockdown in $Nth1^{+/+}$ cells had no effect on *t*-BOOH and $KBrO_3$ induced toxicity as assessed by an MTT assay; knockdown in $Nth1^{-/-}$ cells resulted in increased resistance to *t*-BOOH and $KBrO_3$, a result consistent with Nth1 removing oxidised pyrimidines. *Msh2* knockdown in $Mpg^{+/+}$ cells had no effect on *t*-BOOH toxicity but increased resistance to $KBrO_3$; in $Mpg^{-/-}$ cells, *Msh2* knockdown increased cellular sensitivity to $KBrO_3$ but increased resistance to t-BOOH, suggesting a role for *Mpg* in removing DNA damage induced by these agents. MSH2 dependent and independent pathways then determine cellular toxicity induced by oxidising agents. A complex interaction between MMR and BER repair systems, that is, exposure dependent, also exists to determine cellular toxicity.

1. Introduction

Reactive oxygen species (ROS) can induce a wide range of DNA base lesions [1], and different ROS can modify DNA in different ways [2]. Furthermore, given that the biological potency of only a minority of these lesions has been characterised, the precise role, if any, of an individual lesion in inducing toxicity can be unclear. 8-oxoguanine (8-oxoG) is one of the most studied lesions, being formed in high amounts in DNA by ROS, and is potentially mutagenic [3]. 8-oxoG is formed upon exposure to a wide range of agents including hydrogen peroxide (H_2O_2; [4]), *tert*-butyl-hydroperoxide (*t*-BOOH; [5]), and potassium bromate ($KBrO_3$; [6]), though other DNA base modifications will also be formed [6, 7].

ROS induced damage can be repaired by a number of different DNA repair systems including those involving base excision repair (BER; [8]) and mismatch repair (MMR: [9]). BER of oxidative base damage is initiated by the action of a number of different DNA glycosylases that can excise a spectrum of different oxidised DNA lesions. NTH1, for example, removes oxidised pyrimidines as well as 2,6-diamino-4-hydroxy-5-formamidopyrimidine (FapyG) and 4,6-diamino-5-formamidopyrimidine (FapyA: [10, 11]). Loss of hNTH1 increases levels of FapyG and FapyA [11] as well as sensitivity to γ-rays and H_2O_2 [12]. In human cells, MMR is initiated through the binding of a heterodimer of hMSH2 with either hMSH6 (hMutSα) or hMSH3 (hMutSβ) to the site of the mismatch or base insertion/deletion [13]. Loss of hMSH2 results in an increase in steady state levels of 8-oxoG [14, 15] and increased levels following exposure to H_2O_2 [14, 16], methotrexate [17], or ionising radiation [18]. Loss of hMSH2 can also increase other forms of oxidative damage such as 8-oxoadenine and thymine glycol or clustered DNA

base lesions following treatment with ionising radiation [18, 19].

Though, *Msh2*$^{-/-}$ cells can show a strong mutator phenotype (e.g., at the *hprt* gene [20]) and have an increased mutation frequency after treatment, for example, with ionising radiation [18], the effects of MSH2 deficiency appear to be cell specific. Thus, there was no evidence of an increased mutation rate or microsatellite instability in *Msh2*$^{-/-}$ murine embryonic fibroblast (MEF) clones overexpressing hNOX1, despite an increased level of 8-oxodG [16]. Initially, it was also reported that *Msh2*$^{-/-}$ cells have an increased resistance to the toxic effects of ionising radiation [18, 19] especially at low doses [18], though subsequent work suggests that MMR is not involved in ionising radiation induced cell death [21]. MMR sensitisation may arise through futile cycling of DNA damage or indirectly by generating signals that drive cell fate pathways [18]. However, increased resistance following MSH2 loss is not universally described as it has been reported that methotrexate and H_2O_2 treatment resulted in increased sensitivity in clonogenic assays using tumour cells lacking MSH2 [17].

Hence, there are a number of unresolved issues regarding the role of MSH2 in removing oxidative DNA damage. Firstly, the effects of MSH2 deficiency appear cell specific for as yet unknown reasons but could include the relative levels of other DNA repair proteins involved in removing oxidative DNA damage. Secondly, although it has been reported that MSH2 has broad substrate specificity, there is a relative lack of information regarding the effects of MSH2 deficiency in cells treated with differing forms of oxidative stress. To address these issues, we have investigated the effects of MSH2 on toxicity induced by $KBrO_3$ and *t*-BOOH, in cells proficient and deficient in BER proteins that either remove oxidative DNA damage (NTH1) or alkylated DNA or DNA damaged by lipid peroxidation products (MPG).

2. Methods

2.1. Cells. BER proficient (*Mpg*$^{+/+}$, *Nth1*$^{+/+}$) and deficient MEF cell lines (*Mpg*$^{-/-}$, *Nth1*$^{-/-}$) were used as the parental cells for gene silencing [22]. All cells were grown in DMEM-F12 supplemented with 10% fetal bovine serum, 2 mM L-glutamine, and 0.12% sodium bicarbonate, at 37°C in a 5% CO_2 and 3% O_2 humidified atmosphere. Stable *Msh2* knockdown cell lines were generated by transfection of the parental cell lines with an shRNA expression vector (pshRNA) containing oligonucleotide inserts specifically designed to knockdown *Msh2* expression. These were 5′-GATGAACTTTGAGTCTTTCG-3′ (*Msh2*^{283},[22]). A pshRNA vector containing no target sequence was used as a control.

2.2. Determination of Msh2 Expression Levels. *Msh2* expression levels in individual clones were determined by quantitative real-time PCR using a standard curve generated using varying amounts of cDNA from a nontransfected, parental cell line [22]. Total RNA was extracted from confluent cell pellets using an RNeasy Mini Kit (Qiagen), purified by treatment with RNase-free DNase (Promega), and first strand cDNA was synthesised using AMV-reverse transcriptase (Promega). Oligonucleotide sequences used were 5′-TCTTCTTCTGGTTCGCCAGT-3′ (*Msh2* forward primer), 5′-TGATCATTCTCGGGGAACTC-3′ (*Msh2* reverse primer); 5′-AACTTTGGCATTGTGGAAGG-3′ (*Gapdh* forward primer), 5′-ACACATTGGGGGTAGGAACA-3′ (*Gapdh* reverse primer); *Actin* forward primer, 5′-TGTTACCAACTGGGACGACA-3′, *Actin* reverse primer: 5′-GGGGTGTTGAAGGTCTCAAA-3′. The real-time PCR reaction was performed using the following protocol: 1 cycle of 95°C for 10 min, 40 cycles of 95°C for 15 s, 57°C for 15 s, and 72°C for 30 s followed by a fluorescence reading and 1 cycle of 72°C for 1 min. Finally, a fluorescence reading was taken every 0.2°C between 75°C and 92°C to ensure the presence of a single PCR product. *Msh2* expression in each sample was normalized to the housekeeping gene (Gapdh or actin) expression. Finally, the fold change in the target gene of the sample was expressed as a ratio compared to the target gene expression in the empty vector control.

2.3. Western Blot Analysis of MSH2 Protein Levels. Western blot analysis was carried out as described previously [22]. Briefly, proteins obtained from extracts of the cell lines were separated by SDS-PAGE, electrophoretically transferred to nitrocellulose membranes and the membranes blocked with nonfat milk (Marvel) prior to incubation with anti-MSH2 (1 : 2000 dilution, Abcam). HRP-conjugated secondary antibodies (Dako) and the SuperSignal West Dura detection system (Pierce) were used to detect proteins of interest. To ensure equal loading of proteins, the membrane was reprobed with a primary antibody (1 : 4000) against a housekeeping gene or loading control (Gapdh, actin, or α-tubulin; Abcam).

2.4. MTT Cytotoxicity Assay. MEFs (typically 500 cells) were plated in a 96-well tissue culture plate, treated with *t*-BOOH (0.1 mM) and $KBrO_3$ (0–2 mM) for 72 h, and then 3-(4,5-dimethylthiazol-2-yl)-2,5-diphenyltetrazolium bromide (MTT) was added, and incubation continued for a further 3 h [22]. The medium was removed, and the cells were lysed with DMSO. Formazan formation was determined by absorbance at 590 nm, and the background correction was measured at 690 nm. The number of surviving cells at each concentration was calculated as a percentage of the absorbance from untreated control cells. Results are presented as means ± SEM.

2.5. Clonogenic Survival Assay. The clonogenic survival assay was carried out as described previously [22]. Briefly MEFs (typically 250 cells/well) were plated in a 6-well tissue culture plate, treated every 3-4 days with *t*-BOOH (0–15 μM) or $KBrO_3$ (0–250 μM) for 2-3 weeks until cell colonies of greater than 50 cells could be seen in the control wells. After staining with crystal violet, cell colonies (nucleus of >50 cells) were counted under a microscope. Clonogenic survival was calculated as the number of colonies observed after treatment divided by the number of cells initially plated after adjustment for the survival fraction (viz., the number of

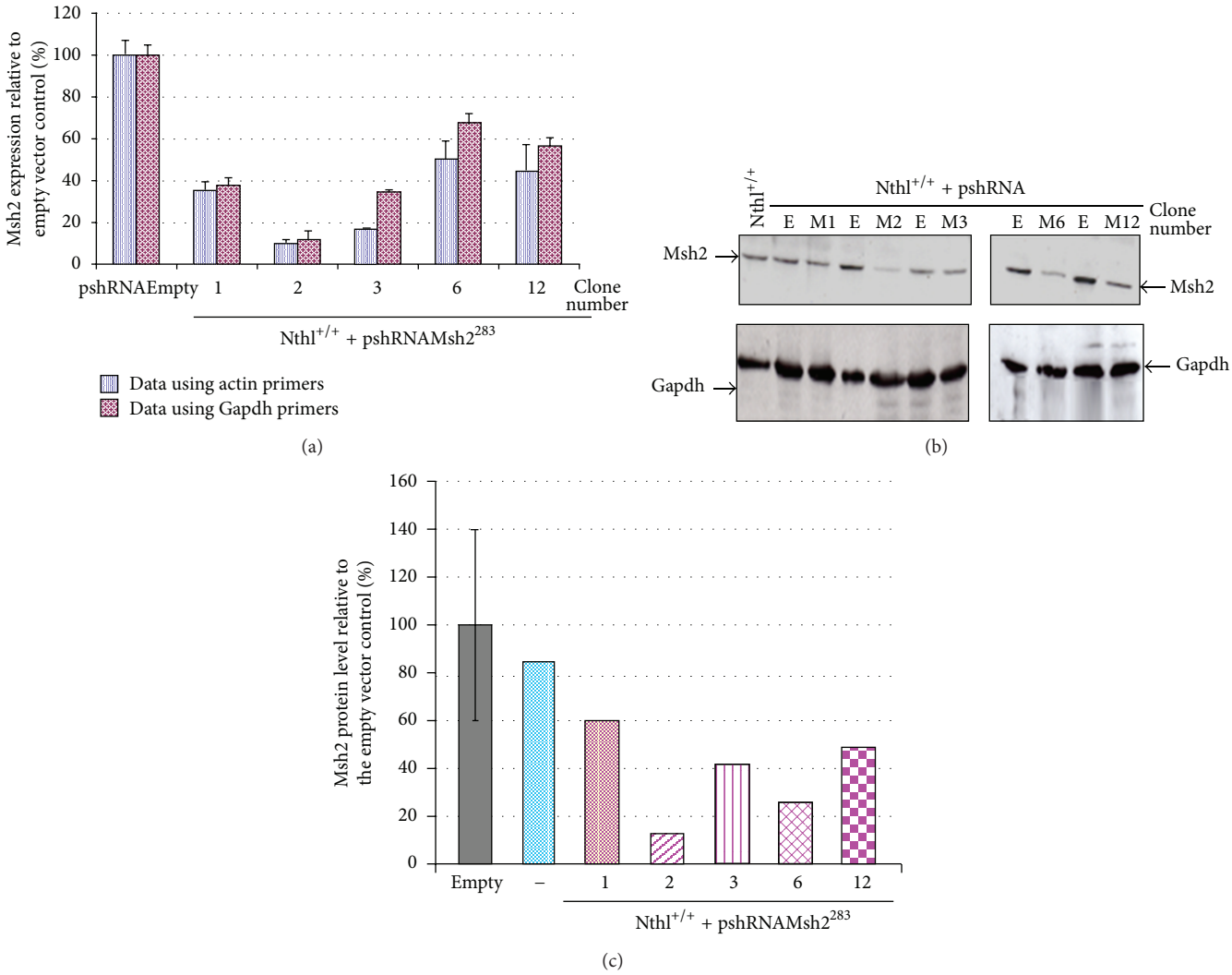

FIGURE 1: *Msh2* silencing in *Nth1*$^{+/+}$ cells. (a) Real-time data analysis for *Msh2* gene expression in *Nth1*$^{+/+}$ clones identified by screening. The data is an average of two real-time PCR reactions (each in triplicate) and analyzed using either *Actin* or *Gapdh* as the reference gene. (b) Western blot analysis for MSH2 and Gapdh protein expression using whole cell extracts. E is the empty vector control and M1, M2, M3, M6, and M12 are different clones. (c) Quantification of the Western blot band intensity and the data expressed as a percentage of the pshRNAEmpty cell extract. The second blue column marked (–) is *Nth1*$^{+/+}$ cells.

colonies observed without treatment divided by the number of cells plated). Results are presented as means ± SEM.

2.6. Statistical Analysis. Data was analyzed by repeated measures ANOVA using STATA 8. Linear regression was used to examine the relationship between treatment and cell line with the untreated cell line transfected with pshRNAEmpty used as the reference. The date the experiment was performed was included in the linear regression model.

3. Results

3.1. Msh2 Expression. The pshRNA*Msh2283* vector was used to transfect MEFs, and a reduction in *Msh2* expression was observed, using either *Gapdh* or *Actin* as the reference genes when compared to the empty vector control as shown in Figure 1 for *Nth1*$^{+/+}$ MEFs. Different clones were isolated from *Mpg*$^{+/+}$, *Mpg*$^{-/-}$, *Nth1*$^{+/+}$, and *Nth1*$^{-/-}$ MEFs, and cell lines chosen for the cytotoxic assays (*Mpg*$^{+/+}$ clone 9, *Mpg*$^{-/-}$ clone 1 *Nth1*$^{+/+}$ clone 2, and *Nth1*$^{-/-}$ clone 1) all had high levels of MSH2 knockdown as estimated by either real-time PCR (mean 84 ± 4% range 79–88%) or western analysis (mean 76 ± 4% range 73–80%).

3.2. Treatment with t-BOOH. *Msh2* knockdown in *Nth1*$^{+/+}$ cells had little effect on cellular resistance to *t*-BOOH as assessed by the MTT assay (Figure 2(a)), but there was evidence of increased resistance using the clonogenic assay (Figure 2(b)). In *Nth1*$^{-/-}$ MEFs, *Msh2* knockdown increased resistance as assessed by the MTT assay (Figure 2(c)) but not the clonogenic assay (Figure 2(d)).

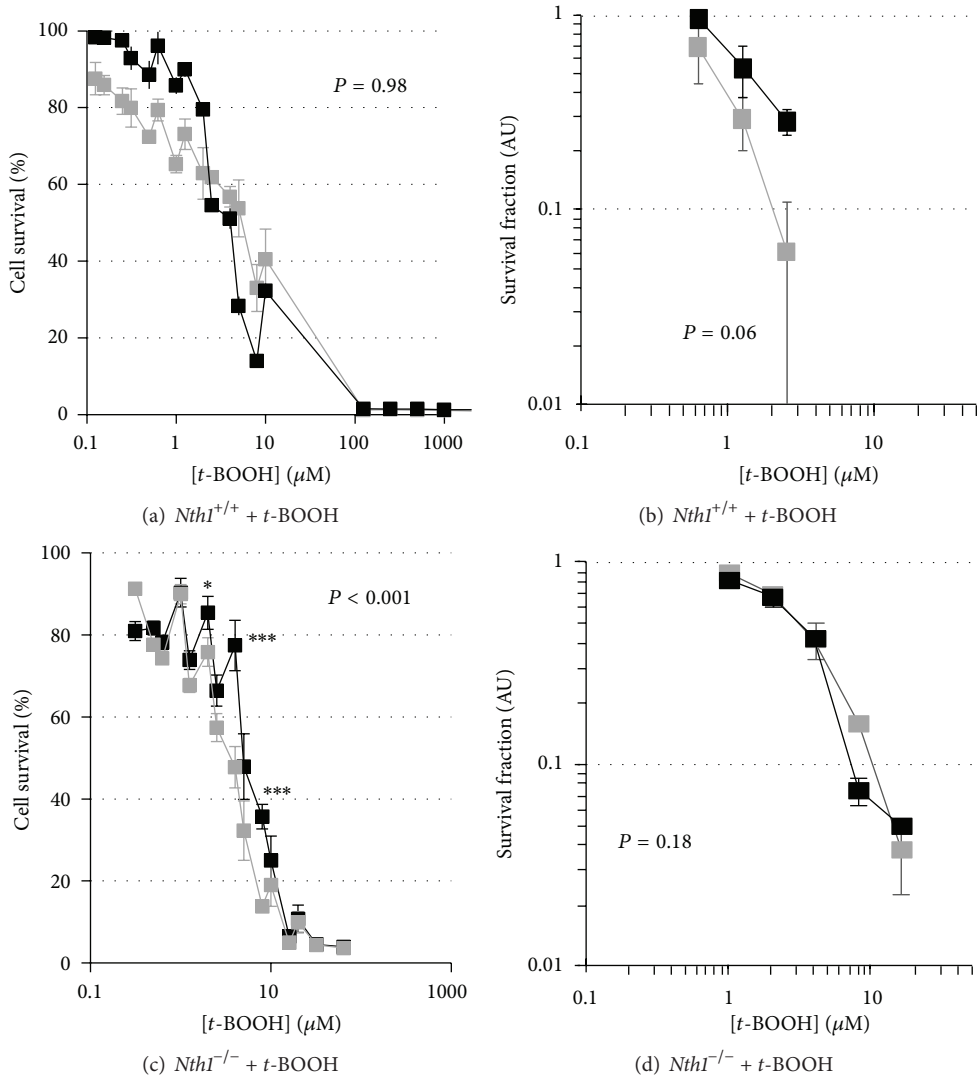

Figure 2: MTT and clonogenic survival curves for *t*-BOOH treatment of $Nth1^{+/+}$ and $Nth1^{-/-}$ MEFs with and without reduced *Msh2* expression. MTT (a) and clonogenic survival (b) curves for $Nth1^{+/+}$ + pshRNA*Msh2283*, clone 2 (88% *Msh2* gene silencing; black square) and $Nth1^{+/+}$ + pshRNA empty (grey square) treated with *t*-BOOH. MTT (c) and clonogenic survival (d) curves for $Nth1^{-/-}$ + pshRNA*Msh2283*, clone 1 (85% *Msh2* gene silencing; solid square), or $Nth1^{-/-}$ + pshRNA empty (grey square) treated with *t*-BOOH. Results are expressed as mean ± SEM; $^{*}P < 0.05$, $^{**}P < 0.01$, and $^{***}P < 0.001$.

Reduction in *Msh2* expression in $Mpg^{+/+}$ cells had little on cellular sensitivity to *t*-BOOH using either the MTT (Figure 3(a)) or clonogenic assay (Figure 3(b)), whereas in $Mpg^{-/-}$ cells, *Msh2* knockdown increased resistance in the MTT assay (Figure 3(c)) but not the clonogenic assay (Figure 3(d)).

3.3. Treatment with $KBrO_3$. Reduction in *Msh2* gene expression in $Nth1^{+/+}$ MEFs did not alter $KBrO_3$ toxicity (Figures 4(a) and 4(b)) but resulted in increased resistance in $Nth1^{-/-}$ MEFs using both the MTT (Figure 4(c)) and clonogenic (Figure 4(d)) assays. Decreased MSH2 expression in $Mpg^{+/+}$ cells resulted in increased resistance as assessed using the MTT (Figure 5(a)) and the clonogenic assay (Figure 5(b)) whereas such reduction decreased resistance in $Mpg^{-/-}$ cells using the MTT assay (Figure 5(c)) but not the clonogenic assay (Figure 5(d)).

4. Discussion

Results of this study reveal a complex interaction between oxidative DNA damage, MSH2 function, and the activity of NTH1 and MPG that helps to determine cellular toxicity. Interestingly, results suggest that, whilst the presence or absence of NTH1 activity can influence MSH2 dependent toxicity induced by ROS (which is predictable as NTH1 removes oxidative DNA base lesions [10]), loss of MPG activity also reveals toxicity, that is, MSH2, and exposure dependent implying MSH2 also acts upon MPG substrate

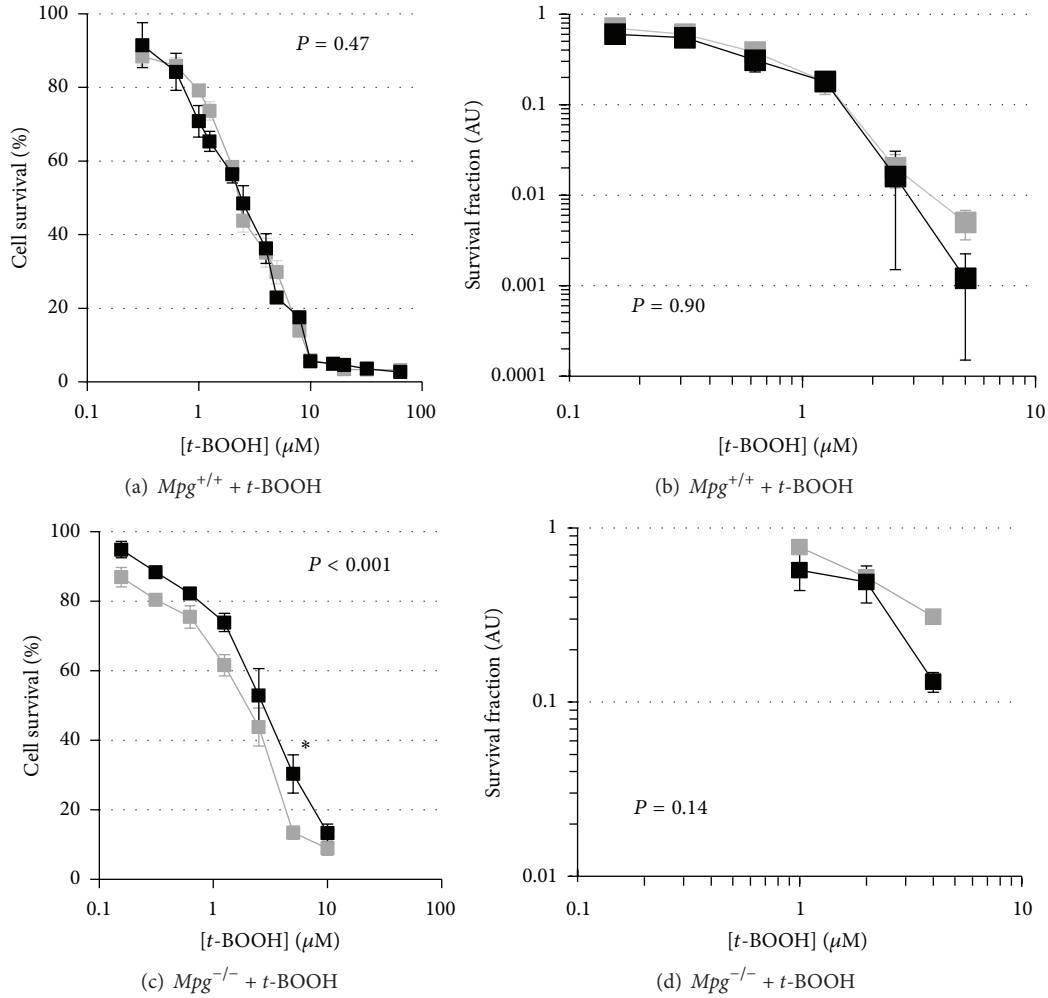

Figure 3: MTT and clonogenic survival curves for *t*-BOOH treatment of $Mpg^{+/+}$ and $Mpg^{-/-}$ MEFs with and without reduced *Msh2* expression. MTT (a) and clonogenic survival (b) curves for $Mpg^{+/+}$ + pshRNA*Msh2283*, clone 9 (85% *Msh2* gene silencing; black square), or $Mpg^{+/+}$ + pshRNA empty (grey square) cells treated with *t*-BOOH. MTT (c) and clonogenic survival (d) curves for $Mpg^{-/-}$ + pshRNA*Msh2283*, clone 1 (79% *Msh2* gene silencing; solid square), or $Mpg^{-/-}$ + pshRNA empty (grey square) cells treated with *t*-BOOH. Results are expressed as mean ± SEM; $^{*}P < 0.05$, $^{**}P < 0.01$, and $^{***}P < 0.001$.

lesions. Loss of MSH2 typically results in increased resistance to DNA damaging agents, and our results are in general consistent with this model (Table 1). However, loss of MSH2 in $Mpg^{-/-}$ MEFs resulted in increased sensitivity to $KBrO_3$ consistent with previously published data reporting that cells lacking MSH2 are more sensitive to methotrexate [17] or cytarabine and similar nucleoside analogs [23].

These results also provide a demonstration of both MSH2 dependent and independent toxicity pathways. In $Nth1^{+/+}$ cells, there was little evidence for MSH2 dependent pathways as MSH2 deficiency has no effect either on *t*-BOOH and $KBrO_3$ toxicity (Table 1). However, in $Nth1^{-/-}$ cells, there was an MSH2 dependent pathway that acts on DNA damage, presumably oxidised pyrimidines induced by both *t*-BOOH and $KBrO_3$. Similarly, MLH1 deficient cells are more resistant to *t*-BOOH than MLH1 proficient cells although the same level of DNA damage was observed in both cell lines [24].

Table 1: Changes in resistance[a] to *t*-BOOH and $KBrO_3$ in cell lines as a result of *Msh2* knockdown in $Nth1^{+/+}$, $Nth1^{-/-}$, $Mpg^{+/+}$, and $Mpg^{-/-}$ MEFs.

Cell line	% *Msh2* gene silencing	*t*-BOOH		$KBrO_3$	
		MTT	Clonogenic	MTT	Clonogenic
$Nth1^{+/+}$	88%	—	$\sim\uparrow^{\ddagger}$	—	—
$Nth1^{-/-}$	85%	$\uparrow^{***}$	—	$\uparrow^{***}$	$\uparrow^{*}$
$Mpg^{+/+}$	85%	—	—	$\uparrow^{***}$	$\uparrow^{*}$
$Mpg^{-/-}$	79%	$\uparrow^{***}$	—	$\downarrow^{**}$	—

[a]Assessed by MTT and clonogenic assays.
$^{*}P \leq 0.05$; $^{**}P \leq 0.01$; $^{***}P \leq 0.001$; $^{\ddagger}P = 0.06$.

In $Mpg^{+/+}$ cells, there was an MSH2 dependent pathway for $KBrO_3$ but not *t*-BOOH induced toxicity (Table 1). Interestingly, Msh2 knockdown in $Mpg^{-/-}$ cells increased resistance

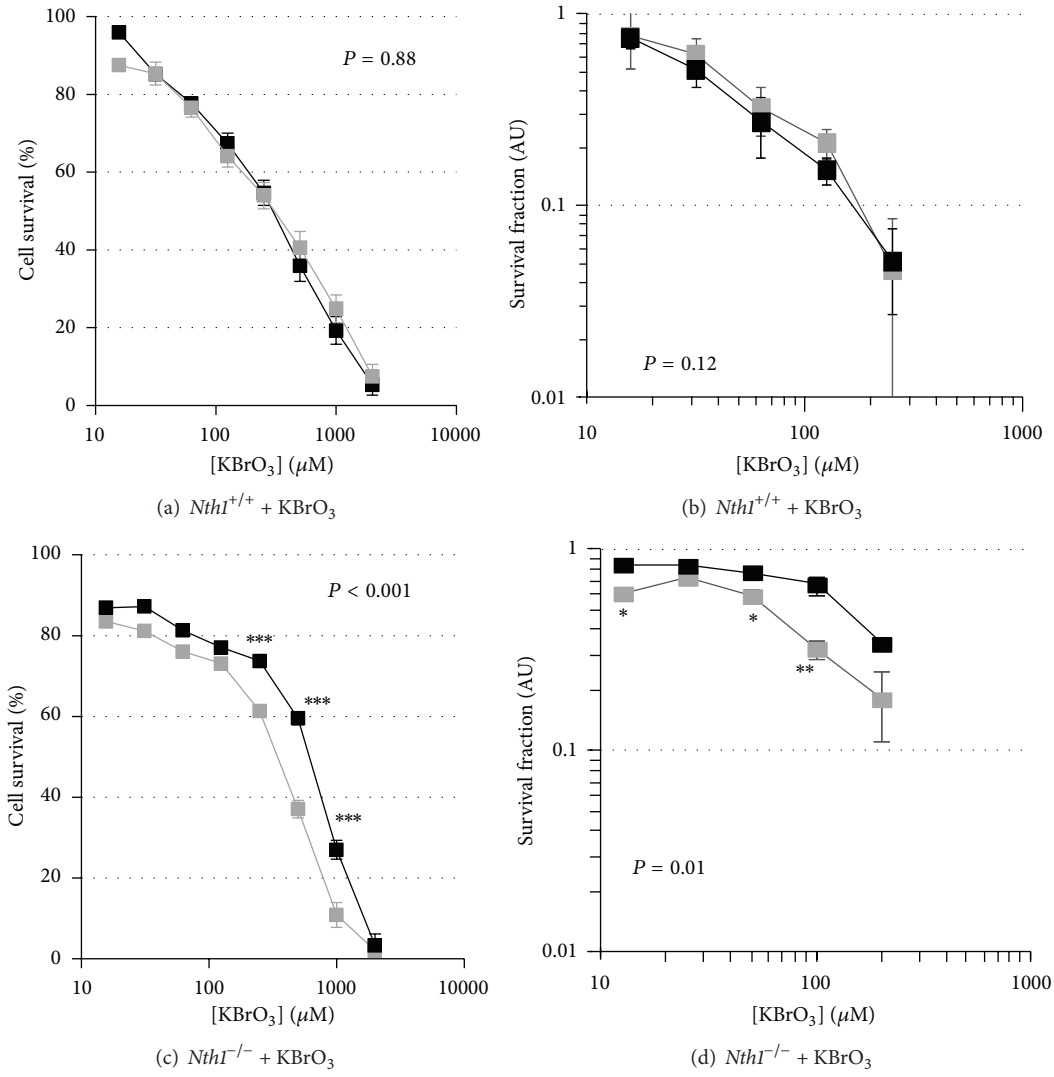

Figure 4: MTT and clonogenic survival curves for $KBrO_3$ treatment of $Nth1^{+/+}$ and $Nth1^{-/-}$ MEFs with and without reduced *Msh2* expression. MTT (a) and clonogenic survival (b) curves for $Nth1^{+/+}$ + pshRNA*Msh2283*, clone 2 (88% *Msh2* gene silencing; black square), and $Nth1^{+/+}$ + pshRNA empty (grey square) treated with $KBrO_3$. MTT (c) and clonogenic survival (d) curves for $Nth1^{-/-}$ + pshRNA*Msh2283*, clone 1 (85% *Msh2* gene silencing; solid square), or $Nth1^{-/-}$ + pshRNA empty (grey square) treated with $KBrO_3$.

to *t*-BOOH but increased sensitivity to $KBrO_3$ suggesting that these agents induce different types (or levels) of adducts.

It is currently unclear why the loss of both MPG and MSH2 should differently alter the sensitivity to $KBrO_3$ and *t*-BOOH. MPG removes alkyl DNA base products such as 7-methylguanine and 3-methyladenine [25] and also removes DNA toxic lesions induced by lipid peroxidation such as the etheno adduct 1,N^6-ethenoadenine [26]. However, MSH2 knockdown in $Mpg^{-/-}$ cells did not alter cellular toxicity induced by alkylating agents such as temozolomide and MMS, suggesting that alkyl adducts are not substrates for MSH2 [22]. Furthermore, alkyl DNA damage is unlikely to be induced by the agents used in this study. This then potentially implicates etheno or indeed other MPG substrates [27] as lesions that may be recognised by, the MutS homolog, MSH2 as MutS from *Escherichia coli* recognises exocyclic adducts arising from exposure to malondialdehyde [28]. Both *t*-BOOH [29] and $KBrO_3$ [30] treatments can increase lipid peroxidation and potentially increase etheno DNA adducts, so that there does not seem to be a simple correlation between the persistence or absence of etheno DNA adducts and cellular response following Msh2 knockdown. However, this does not rule out the possibility that the different treatments used result in differing levels of etheno adducts and/or that $KBrO_3$ results in a lesion whose persistence is directly cytotoxic irrespective of MSH2 function, whereas *t*-BOOH forms predominantly lesions whose toxicity is MSH2 dependent. The identity of these substrates is unclear.

The extent of *Msh2* knockdown in the cell lines used was between ~80 and 90%. It is then possible that remaining MSH2 could have been sufficient to accomplish basic repair tasks, and though the results implicate DNA damage,

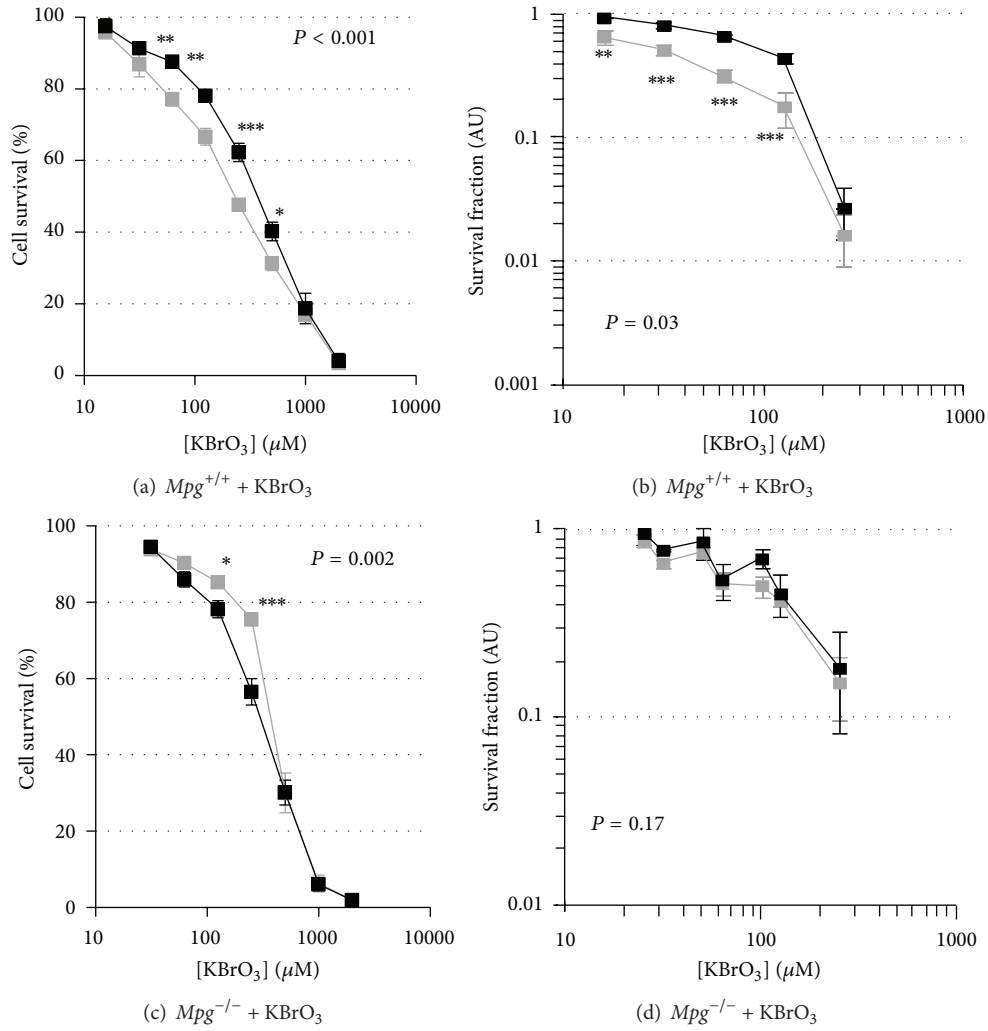

FIGURE 5: MTT and clonogenic survival curves for $KBrO_3$ treatment of $Mpg^{+/+}$ and $Mpg^{-/-}$ MEFs with and without reduced *Msh2* expression. MTT (a) and clonogenic survival (b) curves for $Mpg^{+/+}$ + pshRNA*Msh2283*, clone 9 (85% *Msh2* gene silencing; black square), or $Mpg^{+/+}$ + pshRNA empty (grey square) cells treated with $KBrO_3$. MTT (c) and clonogenic survival (d) curves for $Mpg^{-/-}$ + pshRNA*Msh2283*, clone 1 (79% *Msh2* gene silencing; solid square), or $Mpg^{-/-}$ + pshRNA empty (grey square) cells treated with $KBrO_3$. Results are expressed as mean ± SEM; $^{*}P < 0.05$, $^{**}P < 0.01$, and $^{***}P < 0.001$.

the observed difference in sensitivity to *Msh2* knockdown may then have resulted from other mechanisms [31]. However, we have already shown that similar residual levels of MSH2 are not sufficient to prevent knockdown induced alterations in alkylating agent or 6-thioguanine induced cytotoxicity [22]. Other studies have also shown that a decrease in MSH2 expression of similar magnitude can have functional effects. For example, transfection of shRNA against *Msh2* into CCD34-Lu/hTERT cells resulted in a 35–90% reduction in MSH2 protein level. Mean telomere shortening rate was significantly greater in those shMSH2 clones having between a 50 and 90% reduction in MSH2 protein level [32]. We cannot rule out, however, that residual MSH2 protein can be active in the repair of at least some of the types of DNA damage induced by the oxidising agents used particularly as the DNA damage induced is not fully characterised.

Differences between clonogenic and MTT assays have been reported previously [33–35]; these differences are often compound and cell line specific and have been ascribed to differences in length of treatment allowing mechanistic differences between compounds to become apparent [33]. It is also possible that the MTT assay can reflect decreased mitochondrial function and not necessarily cell death [35]. In this study results for the MTT and clonogenic assays were consistent in three out of four cell lines following $KBrO_3$ treatment. However, in contrast to the MTT results, the ability of the MEFs to proliferate in the presence of *t*-BOOH was largely unaffected by both the BER status and *Msh2* status. The increased resistance to *t*-BOOH in BER deficient cells seen with the MTT assay was not observed in the clonogenic assay. It is possible that, in the BER deficient cells, the reduction in cell cycle arrest is temporary, and, as the cells

accumulate more oxidative damage, from persistent exposure to *t*-BOOH, MMR-independent signals are sent for the cells to undergo apoptosis, such as from single- or double-strand DNA breaks, or that the damage is repaired by another DNA repair pathway such as nucleotide excision repair after the initial recognition by MMR. Therefore, in short-term MTT experiments a difference can be seen in cell survival, yet the cells that survive in the short-term are unable to proliferate in long-term experiments. In support of this, Chinese hamster B14 cells that survived treatment with *t*-BOOH were unable to proliferate after being replenished with fresh medium [29].

5. Conclusions

Results suggest the presence of MSH2 dependent and independent pathways to determine cellular toxicity induced by oxidising agents and a complex interaction between MMR and BER repair systems in determining cellular toxicity that is exposure dependent. A DNA repair gene-exposure interaction may then in humans help to determine susceptibility to ROS induced toxicity.

Conflict of Interests

The authors declare that there is no conflict of interests.

Acknowledgment

This work was funded by the European Chemical Industry Council (Grant code LRI-CC2.001-UMAN).

References

[1] M. S. Cooke, M. D. Evans, M. Dizdaroglu, and J. Lunec, "Oxidative DNA damage: mechanisms, mutation, and disease," *The FASEB Journal*, vol. 17, no. 10, pp. 1195–1214, 2003.

[2] H. Wiseman and B. Halliwell, "Damage to DNA by reactive oxygen and nitrogen species: role in inflammatory disease and progression to cancer," *Biochemical Journal*, vol. 313, no. 1, pp. 17–29, 1996.

[3] A. Valavanidis, T. Vlachogianni, and C. Fiotakis, "8-hydroxy-2′-deoxyguanosine (8-OHdG): a critical biomarker of oxidative stress and carcinogenesis," *Journal of Environmental Science and Health. Part C*, vol. 27, no. 2, pp. 120–139, 2009.

[4] J. Rivière, J.-L. Ravanat, and J. R. Wagner, "Ascorbate and H_2O_2 induced oxidative DNA damage in Jurkat cells," *Free Radical Biology and Medicine*, vol. 40, no. 12, pp. 2071–2079, 2006.

[5] C. Tormos, F. J. Chaves, M. J. Garcia et al., "Role of glutathione in the induction of apoptosis and c-fos and c-jun mRNAs by oxidative stress in tumor cells," *Cancer Letters*, vol. 208, no. 1, pp. 103–113, 2004.

[6] D. Ballmaier and B. Epe, "Oxidative DNA damage induced by potassium bromate under cell-free conditions and in mammalian cells," *Carcinogenesis*, vol. 16, no. 2, pp. 335–342, 1995.

[7] J. Termini, "Hydroperoxide-induced DNA damage and mutations," *Mutation Research*, vol. 450, no. 1-2, pp. 107–124, 2000.

[8] D. Svilar, E. M. Goellner, K. H. Almeida, and R. W. Sobol, "Base excision repair and lesion-dependent subpathways for repair of oxidative DNA damage," *Antioxidants and Redox Signaling*, vol. 14, no. 12, pp. 2491–2507, 2011.

[9] M. T. Russo, G. De Luca, P. Degan, and M. Bignami, "Different DNA repair strategies to combat the threat from 8-oxoguanine," *Mutation Research*, vol. 614, no. 1-2, pp. 69–76, 2007.

[10] M. Dizdaroglu, B. Karahalil, S. Sentürker, T. J. Buckley, and T. Roldán-Arjona, "Excision of products of oxidative DNA base damage by human NTH1 protein," *Biochemistry*, vol. 38, no. 1, pp. 243–246, 1999.

[11] J. Hu, N. C. De Souza-Pinto, K. Haraguchi et al., "Repair of formamidopyrimidines in DNA involves different glycosylases: role of the OGG1, NTH1, and NEIL1 enzymes," *Journal of Biological Chemistry*, vol. 280, no. 49, pp. 40544–40551, 2005.

[12] N. Yang, M. A. Chaudhry, and S. S. Wallace, "Base excision repair by hNTH1 and hOGG1: a two edged sword in the processing of DNA damage in γ-irradiated human cells," *DNA Repair*, vol. 5, no. 1, pp. 43–51, 2006.

[13] G.-M. Li, "Mechanisms and functions of DNA mismatch repair," *Cell Research*, vol. 18, no. 1, pp. 85–98, 2008.

[14] C. Colussi, E. Parlanti, P. Degan et al., "The Mammalian Mismatch Repair pathway removes DNA 8-oxodGMP incorporated from the oxidized dNTP pool," *Current Biology*, vol. 12, no. 11, pp. 912–918, 2002.

[15] M. T. Russo, G. De Luca, P. Degan et al., "Accumulation of the oxidative base lesion 8-hydroxyguanine in DNA of tumor-prone mice defective in both the Myh and Ogg1 DNA glycosylases," *Cancer Research*, vol. 64, no. 13, pp. 4411–4414, 2004.

[16] F. Chiera, E. Meccia, P. Degan et al., "Overexpression of human NOX1 complex induces genome instability in mammalian cells," *Free Radical Biology and Medicine*, vol. 44, no. 3, pp. 332–342, 2008.

[17] S. A. Martin, A. McCarthy, L. J. Barber et al., "Methotrexate induces oxidative DNA damage and is selectively lethal to tumour cells with defects in the DNA mismatch repair gene MSH2," *EMBO Molecular Medicine*, vol. 1, no. 6-7, pp. 323–337, 2009.

[18] T. L. DeWeese, J. M. Shipman, N. A. Larrier et al., "Mouse embryonic stem cells carrying one or two defective Msh2 alleles respond abnormally to oxidative stress inflicted by low-level radiation," *Proceedings of the National Academy of Sciences of the United States of America*, vol. 95, no. 20, pp. 11915–11920, 1998.

[19] S. M. Holt, J.-L. Scemama, M. I. Panayiotidis, and A. G. Georgakilas, "Compromised repair of clustered DNA damage in the human acute lymphoblastic leukemia MSH2-deficient NALM-6 cells," *Mutation Research*, vol. 674, no. 1-2, pp. 123–130, 2009.

[20] M. T. Russo, G. De Luca, I. Casorelli et al., "Role of MUTYH and MSH2 in the control of oxidative DNA damage, genetic instability, and tumorigenesis," *Cancer Research*, vol. 69, no. 10, pp. 4372–4379, 2009.

[21] E. Papouli, P. Cejka, and J. Jiricny, "Dependence of the cytotoxicity of DNA-damaging agents on the mismatch repair status of human cells," *Cancer Research*, vol. 64, no. 10, pp. 3391–3394, 2004.

[22] N. Cooley, R. H. Elder, and A. C. Povey, "The effect of Msh2 knockdown on methylating agent induced toxicity in DNA glycosylase deficient cells," *Toxicology*, vol. 268, no. 1-2, pp. 111–117, 2010.

[23] S. E. Fordham, E. C. Matheson, K. Scott, J. A. E. Irving, and J. M. Allan, "DNA mismatch repair status affects cellular response to Ara-C and other anti-leukemic nucleoside analogs," *Leukemia*, vol. 25, no. 6, pp. 1046–1049, 2011.

[24] R. A. Hardman, C. A. Afshari, and J. C. Barrett, "Involvement of mammalian MLH1 in the apoptotic response to peroxide-induced oxidative stress," *Cancer Research*, vol. 61, no. 4, pp. 1392–1397, 2001.

[25] G. Ibeanu, B. Hartenstein, W. C. Dunn et al., "Overexpression of human DNA repair protein N-methylpurine-DNA glycosylase results in the increased removal of N-methylpurines in DNA without a concomitant increase in resistance to alkylating agents in Chinese hamster ovary cells," *Carcinogenesis*, vol. 13, no. 11, pp. 1989–1995, 1992.

[26] B. Hang, B. Singer, G. P. Margison, and R. H. Elder, "Targeted deletion of alkylpurine-DNA-N-glycosylase in mice eliminates repair of 1,N6-ethenoadenine and hypoxanthine but not of 3,N4-ethenocytosine or 8-oxoguanine," *Proceedings of the National Academy of Sciences of the United States of America*, vol. 94, no. 24, pp. 12869–12874, 1997.

[27] C.-Y. I. Lee, J. C. Delaney, M. Kartalou et al., "Recognition and processing of a new repertoire of DNA substrates by human 3-methyladenine DNA glycosylase (AAG)," *Biochemistry*, vol. 48, no. 9, pp. 1850–1861, 2009.

[28] K. A. Johnson, M. L. Mierzwa, S. P. Fink, and L. J. Marnett, "MutS recognition of exocyclic DNA adducts that are endogenous products of lipid oxidation," *Journal of Biological Chemistry*, vol. 274, no. 38, pp. 27112–27118, 1999.

[29] E. A. Lapshina, I. B. Zavodnik, M. Labieniec, K. Rękawiecka, and M. Bryszewska, "Cytotoxic and genotoxic effects of *tert*-butyl hydroperoxide on Chinese hamster B14 cells," *Mutation Research*, vol. 583, no. 2, pp. 189–197, 2005.

[30] I. A. Blair, "Lipid hydroperoxide-mediated DNA damage," *Experimental Gerontology*, vol. 36, no. 9, pp. 1473–1481, 2001.

[31] X. Zhang, D. De Silva, B. Sun et al., "Cellular and molecular mechanisms of bromate-induced cytotoxicity in human and rat kidney cells," *Toxicology*, vol. 269, no. 1, pp. 13–23, 2010.

[32] A. Mendez-Bermudez and N. J. Royle, "Deficiency in DNA mismatch repair increases the rate of telomere shortening in normal human cells," *Human Mutation*, vol. 32, no. 8, pp. 939–946, 2011.

[33] K. Kawada, T. Yonei, H. Ueoka et al., "Comparison of chemosensitivity tests: clonogenic assay versus MTT assay," *Acta Medica Okayama*, vol. 56, no. 3, pp. 129–134, 2002.

[34] M. Bačkorová, M. Bačkor, J. Mikeš, R. Jendželovský, and P. Fedoročko, "Variable responses of different human cancer cells to the lichen compounds parietin, atranorin, usnic acid and gyrophoric acid," *Toxicology in Vitro*, vol. 25, no. 1, pp. 37–44, 2011.

[35] M. V. Berridge, P. M. Herst, and A. S. Tan, "Tetrazolium dyes as tools in cell biology: new insights into their cellular reduction," *Biotechnology Annual Review*, vol. 11, pp. 127–152, 2005.

Hindawi Publishing Corporation
BioMed Research International
Volume 2013, Article ID 180156, 4 pages
http://dx.doi.org/10.1155/2013/180156

Research Article

Bioremediation of Direct Blue 14 and Extracellular Ligninolytic Enzyme Production by White Rot Fungi: *Pleurotus* Spp.

M. P. Singh, S. K. Vishwakarma, and A. K. Srivastava

Department of Biotechnology, VBS Purvanchal University, Jaunpur, UP 222001, India

Correspondence should be addressed to M. P. Singh; mpsingh.16@gmail.com

Received 13 April 2013; Accepted 26 May 2013

Academic Editor: Nikhat J. Siddiqi

In the present investigation, four species of white rot fungi (*Pleurotus*), that is, *P. flabellatus, P. florida, P. ostreatus* and *P. sajor-caju* were used for decolorization of direct blue 14 (DB14). Among all four species of *Pleurotus*, *P. flabellatus* showed the fastest decolorization in petri plates on different concentration, that is, 200 mg/L, 400 mg/L, and 600 mg/L. All these four species were also evaluated for extracellular ligninolytic enzymes (laccase and manganese peroxidase) production and it was observed that the twelve days old culture of *P. flabellatus* showed the maximum enzymatic activity, that is, 915.7 U/mL and 769.2 U/mL of laccase and manganese peroxidase, respectively. Other three *Pleurotus* species took more time for dye decolorization and exhibited less enzymatic activities. The rate of decolorization of DB14 dye solution (20 mg/L) by crude enzymes isolated from *P. flabellatus* was very fast, and it was observed that up to 90.39% dye solution was decolorized in 6 hrs of incubation.

1. Introduction

Azo dyes are the largest class of synthetic dyes used for textile dyeing, paper printing, and other industrial applications. During the dyeing process, 5–20% of the used dyestuffs are released into the processed water [1, 2]. It was estimated that only textile industries alone generate about 4500 million kiloliters of wastewaters annually. As these dyes are synthetic, they contain toxic content in the effluents because partial degradation of these dyes results in aromatic amines that are toxic to aquatic life and mutagenic and carcinogenic to humans [3]. There is a big challenge to remove dye content from industrial effluents. Various physical, chemical, and biological methods have been proposed [4] among these, microbiological and enzymatic decomposition have received much attention in recent years [5–7]. Although, many reports are available for dye decolorization and degradation by bacteria, the reductive products of dye degradation are generally aromatic amines which are potentially hazardous to living organisms [8, 9] and due to larger size of dyes, bacteria are unable to degrade these dyes efficiently.

White rot fungi degrade lignin because they secrete oxidoreductases including lignin peroxidase (1,2-bis (3,4-dimethoxyphenyl) propene-1,3-diol:hydrogen-peroxide-Lip EC 1.1.1.14), manganese peroxidase (Mn(II):hydrogen-peroxide oxidoreductase EC 1.11.1.13), and laccase (benzenediol:oxygen reductase EC 1.10.3.2). These enzymes oxidise in a nonspecific way both phenolic and nonphenolic lignin derivatives and thus are promising candidates for the degradation of environmental pollutants, for example, phenols, anilines, dyes, lignocelluloses [10–14] and highly recalcitrant compounds such as polychlorinated biphenyls (PCBs) and polycyclic aromatic hydrocarbons (PAHs) [15]. Biodegradation of several persistent compounds such as dyes, pesticides and lignin derivatives has been attributed to the oxidative enzymes, especially laccase [16, 17]. The present research work is undertaken to evaluate the potentialities of *Pleurotus* species for dye decolorization.

2. Materials and Methods

2.1. Cultures and Their Maintenance. The pure cultures of *Pleurotus* species, that is, *P. flabellatus*, *P. florida*, *P. ostreatus,* and *P. sajor-caju* were obtained from Directorate of Mushroom Research, Solan (Himachal Pradesh), India. Throughout the study, cultures were maintained on MEA (Malt extract agar) medium at 28°C and subcultured at the regular interval of three weeks.

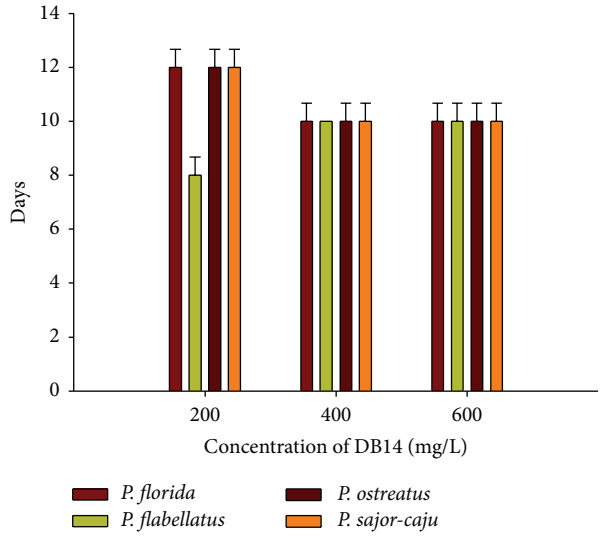

Figure 1: Decolorization of DB14 by *Pleurotus* spp.

2.2. Screening of Species for Dye Decolorization. DB14 (direct blue 14) was used as reference dye for group of azo dye. Inoculums of four *Pleurotus* spp. (*P. flabellatus*, *P. florida*, *P. ostreatus* and *P. sajor-caju*) were inoculated on MEA plate containing 200 mg/L, 400 mg/L, and 600 mg/L of DB14. These plates were incubated on 28 ± 2°C.

2.3. Production of Enzymes. The medium for enzyme production contained 2% wheat bran and 2.5% malt extract, and the pH was adjusted to 6.0 by using NaOH or HCl. Incubation was carried out at 28°C in biological oxygen demand BOD incubator in cotton-plugged 250 mL Erlenmeyer flasks containing 50 mL of media. Flasks were inoculated with 1 cm^2 agar pieces from actively growing fungus on malt extract agar plate.

2.4. Extraction of Extracellular Enzymes. Samples of substrate were collected at regular interval of 3 days and extracted in phosphate buffer (pH 6.0) for ligninolytic enzymes. Filtrate of extraction was used for enzyme assay.

2.5. Enzyme Assay. Laccase activity was determined *via* the oxidation of o-methoxyphenol catechol monomethylether (guaiacol) as substrate. The reaction mixture contained 1 mL of 1 mM guaiacol in 0.1 M sodium phosphate buffer (pH 6.0) and 1 mL of crude enzyme solution was incubated at 30°C for 10 min. The oxidation was followed by the increase in absorbance at 495 nm. One activity unit was defined as 1 μmol of guaiacol oxidised per minute [18].

Manganese peroxidase (MnP) activity was determined using guaiacol as substrate. The reaction mixture contained 0.2 mL of 0.5 M Na-tartrate buffer (pH 5.0), 0.1 mL of 1 mM $MnSO_4$, 0.1 mL of 1 mM H_2O_2, 0.25 mL of 1 mM guaiacol and 0.3 mL of crude enzymes. The oxidation of substrate at 30°C was followed spectrophotometrically at (A_{465}) [19].

2.6. Decolorization of Synthetic Dye by Crude Enzyme Solution. Decolorization of the azo dye direct blue 14 was monitored in a mixture containing 1.4 mL DB14 solution (20 mg L^{-1}), 0.2 mL 0.5 M sodium acetate buffer pH 3.5, 0.2 mL crude enzyme, 0.2 mL of deionised water, 0.1 M H_2O_2, 0.1 M $MnSO_4$ or 5.5 mM ABTS solutions, at 25 ± 2°C [20].

Visible spectra were recorded with a UV-visible (Elico-SL191) spectrophotometer at λ = 595 nm. The rate of decolorization was expressed as the percentage decrease in absorbance at the peak wavelength. Control tests were conducted with crude enzyme replaced by deionised water. Experiments were performed in triplicate, and results were expressed as the mean values.

3. Results and Discussion

All four species of *Pleurotus* selected in the present work showed different rate of decolorization of DB14. Among the four species of *Pleurotus, P. flabellatus* showed the fastest decolorization of DB14 followed by *P. florida*, *P. sajor-caju,* and *P. ostreatus* on 200 mg/L of DB14 (Figure 1). *P. flabellatus* completely decolorized DB14 within 8 days. *P. flabellatus* effectively decolorized the dye at the concentration of 400 mg/L and also at 600 mg/L. At 400 mg/L concentration complete decolorization occurred in 10 days and other species took almost the similar time, but the rate of decolorization and mycellial growth were better in case of *P. flabellatus*. Same results were observed at 600 mg/L concentration. The degrees of decolorization of different dyes such as malachite green, indigo carmine, xylidine ponceau, Bismarck brown and methyl orange using the white rot fungus *P. ostreatus* were previously evaluated by Neelamegam *et al.* [21]. This study demonstrated the potentialities of white rot fungi in bioremediation of dye contaminated ecosystems.

The time course of laccase and MnP activity was followed in the wheat bran supplemented liquid media over a period of 21 days. Initially, it was observed that amongst the four species of *Pleurotus, P. flabellatus* showed the highest laccase activities on all days evaluated, reaching maximum levels of 915.7 U/mL in 12 days of culture of *P. flabellatus* on wheat bran containing media. This was followed by *P. sajor-caju* which showed maximum laccase activity (608.6 U/mL) in 12 days. Subsequently, *P. ostreatus* and *P. florida* showed maximum laccase activity, that is, 436.3 U/mL and 353.3 U/mL in 9 days and 21 days, respectively (Figure 2). MnP activities were detected at levels of up to 769.2 U/mL by *P. flabellatus* in 12 days old culture followed by *P. Sajor-caju*, *P. ostreatus,* and *P. florida* that is, 407.4 U/mL, 241.8 U/mL, and 329 U/mL on 9, 9, and 15 days old culture, respectively (Figure 3).

Every species showed maximum enzymatic activity on the 9th day or after the 9th day of incubation, which might be due to the occurrence of initial lag phase when species try to establish it in new medium. When cultures are established in the culture medium, they enter into log phase, and metabolically this is the most active phase where species show maximum enzymatic activity. Cereal bran was reported to increase ligninolytic enzyme production of the white rot fungi *Coriolopsis gallica* and *Bjerkandera adusta* [22]. In the beginning of the experiment, on day 3, different *Pleurotus*

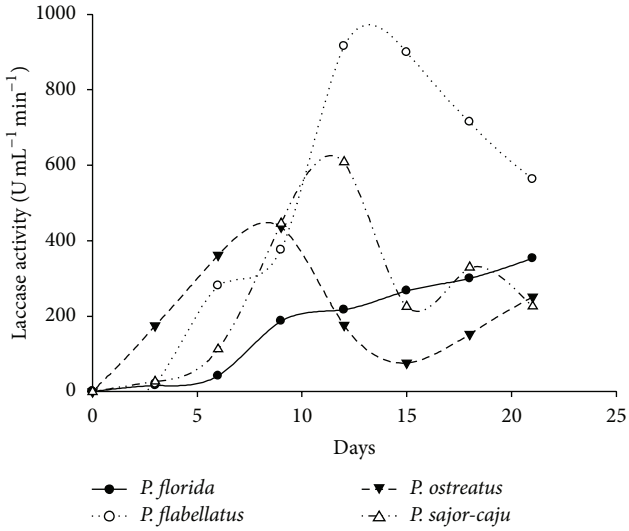

Figure 2: Laccase production by different *Pleurotus* species in submerged condition.

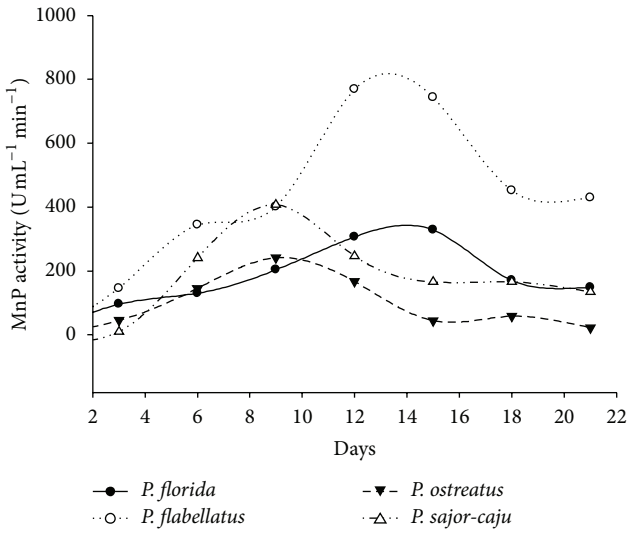

Figure 3: MnP production by different *Pleurotus* species in submerged condition.

species showed low enzymatic activities. This was followed by sharp increase up to 12 days in *P. flabellatus* and *P. sajor-caju,* whereas in case *P. ostreatus* and *P. florida* it took 9 and 21 days for laccase. *P. flabellatus* and *P. florida,* showed maximum MnP activities in 12 days whereas *P. ostreatus* and *P. sajor-caju* showed the maximum MnP activities in 9 days, respectively. Laccase and MnP both are oxidative enzyme and have broad range of substrate specificity.

Several authors have discussed the role of lignicolous fungal enzymes in the decolorization of dyes [14, 23, 24]. Crude enzymes obtained from cultures of *P. flabellatus* on wheat bran containing malt extract media were tested for decolorization of DB14. Figure 4 shows the percent decolorization during various periods. The decolorization of the dye using crude enzyme was 46.49% in the first hour,

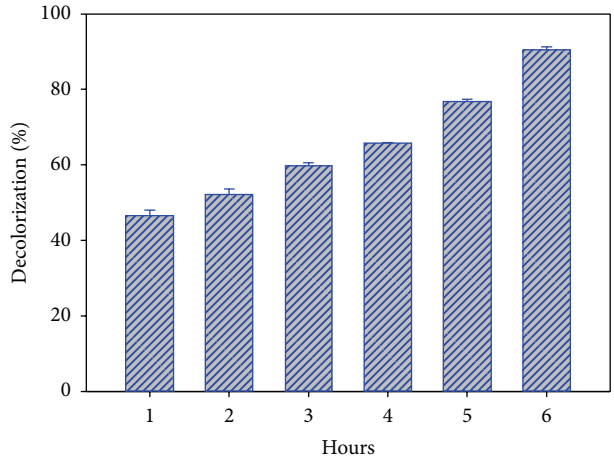

Figure 4: Decolorization of DB14 by crude extracellular enzymes of *P. flabellatus*.

in present investigation. 90.39% DB14 decolorization was reported in 6 hrs at room temperature (30°C).

The laccase [16] and MnP [25] play a major role in complete oxidation of DB14. It was observed that laccase and peroxidases can act as starters of a chain reaction which leads to dye degradation by generating highly active free radicals (e.g., Mn^{3+}, lipid, hydroxyl, and peroxy-radicals) [26, 27]. According to Meyer [28], because of the structural variety of azo dyes, they are not uniformly susceptible to biodegradation. It was demonstrated that substituent groups such as nitro and sulpho are frequently recalcitrant to biodegradation, whereas 2-methyl, 2-methoxy, 2,6-dimethyl and 2,6-dimethoxy-substituted 4-(4-sulfophenylazo)-phenol were preferred for azo-dye degradation by peroxidase from *Streptomyces* spp. and *Phanerochaete chrysosporium* [29]. The breaking down of the dye into smaller fragments, including the breakage of the azo bond, can lead to a decrease in the absorbance of the visible spectra and in a colorless solution [30].

4. Conclusion

The present investigation suggests that the white rot fungus *Pleurotus flabellatus* can be used in bioremediation of dye-contaminated ecosystems. This is because of the presence of powerful enzymatic machinery which can effectively degrade the recalcitrant and toxic dyes. Out of four species investigated, *P. flabellatus* showed the maximum enzymatic activity. Extracellular enzymes extracted from 12 days old culture of *P. flabellatus* decolorized the DB14 to maximum extent. For better enzyme production the wheat bran can be used as supplement in liquid media. Decolorized effluent after enzymatic treatment can be reused by industries and also in agriculture.

Abbreviations

DB14: Direct blue 14
MnP: Manganese peroxidase
hrs: Hours.

References

[1] G. M. B. Soares, M. Costa-Ferreira, and M. T. Pessoa de Amorim, "Decolorization of an anthraquinone-type dye using a laccase formulation," *Bioresource Technology*, vol. 79, no. 2, pp. 171–177, 2001.

[2] Y. Wong and J. Yu, "Laccase-catalyzed decolorization of synthetic dyes," *Water Research*, vol. 33, no. 16, pp. 3512–3520, 1999.

[3] H. M. Pinheiro, E. Touraud, and O. Thomas, "Aromatic amines from azo dye reduction: status review with emphasis on direct UV spectrophotometric detection in textile industry wastewaters," *Dyes and Pigments*, vol. 61, no. 2, pp. 121–139, 2004.

[4] E. Forgacs, T. Cserháti, and G. Oros, "Removal of synthetic dyes from wastewaters: a review," *Environment International*, vol. 30, no. 7, pp. 953–971, 2004.

[5] E. P. Chagas and L. R. Durrant, "Decolorization of azo dyes by *Phanerochaete chrysosporium* and *Pleurotus sajorcaju*," *Enzyme and Microbial Technology*, vol. 29, no. 8-9, pp. 473–477, 2001.

[6] K. Murugesan, I.-H. Nam, Y.-M. Kim, and Y.-S. Chang, "Decolorization of reactive dyes by a thermostable laccase produced by *Ganoderma lucidum* in solid state culture," *Enzyme and Microbial Technology*, vol. 40, no. 7, pp. 1662–1672, 2007.

[7] Z. Zheng and J. P. Obbard, "Oxidation of polycyclic aromatic hydrocarbons (PAH) by the white rot fungus, *Phanerochaete chrysosporium*," *Enzyme and Microbial Technology*, vol. 31, no. 1-2, pp. 3–9, 2002.

[8] M. Chivukula and V. Renganathan, "Phenolic azo dye oxidation by laccase from *Pyricularia oryzae*," *Applied and Environmental Microbiology*, vol. 61, no. 12, pp. 4374–4377, 1995.

[9] C. O'Neill, A. Lopez, S. Esteves, F. R. Hawkes, D. L. Hawkes, and S. Wilcox, "Azo-dye degradation in an anaerobic-aerobic treatment system operating on simulated textile effluent," *Applied Microbiology and Biotechnology*, vol. 53, no. 2, pp. 249–254, 2000.

[10] K. Fahr, H.-G. Wetzstein, R. Grey, and D. Schlosser, "Degradation of 2,4-dichlorophenol and pentachlorophenol by two brown rot fungi," *FEMS Microbiology Letters*, vol. 175, no. 1, pp. 127–132, 1999.

[11] V. S. Ferreira-Leitão, M. E. A. de Carvalho, and E. P. S. Bon, "Lignin peroxidase efficiency for methylene blue decolouration: comparison to reported methods," *Dyes and Pigments*, vol. 74, no. 1, pp. 230–236, 2007.

[12] V. K. Pandey, M. P. Singh, A. K. Srivastava, S. K. Vishwakarma, and S. Takshak, "Biodegradation of sugarcane bagasse by white rot fungus *Pleurotus citrinopileatus*," *Cellular and Molecular Biology*, vol. 58, no. 1, pp. 8–14, 2012.

[13] M. P. Singh, V. K. Pandey, A. K. Srivastava, and S. K. Viswakarma, "Biodegradation of Brassica haulms by white rot fungus *Pleurotus eryngii*," *Cellular and Molecular Biology*, vol. 57, no. 1, pp. 47–55, 2011.

[14] S. K. Vishwakarma, M. P. Singh, A. K. Srivastava, and V. K. Pandey, "Azo dye (direct blue) decolorization by immobilized extracellular enzymes of *Pleurotus* species," *Cellular and Molecular Biology*, vol. 58, no. 1, pp. 21–25, 2012.

[15] K. Svobodová, A. Majcherczyk, Č. Novotný, and U. Kües, "Implication of mycelium-associated laccase from *Irpex lacteus* in the decolorization of synthetic dyes," *Bioresource Technology*, vol. 99, no. 3, pp. 463–471, 2008.

[16] M. S. Revankar and S. S. Lele, "Synthetic dye decolorization by white rot fungus, *Ganoderma* sp. WR-1," *Bioresource Technology*, vol. 98, no. 4, pp. 775–780, 2007.

[17] C. Riccardi, M. Papacchini, A. Mansi et al., "Characterization of bacterial population coming from a soil contaminated by polycyclic aromatic hydrocarbons (PAHs) able to degrade pyrene in slurry phase," *Annals of Microbiology*, vol. 55, no. 2, pp. 85–90, 2005.

[18] R. P. S. Dhaliwal, H. S. Garcha, and P. K. Khanna, "Regulation of lignocellulotic enzyme system in *Pleurotus ostreatus*," *Indian Journal of Microbiology*, vol. 31, no. 2, pp. 181–184, 1991.

[19] J. Putter, "Peroxidases," in *Methods of Enzymatic Analysis*, H. U. Bergmeyer, Ed., vol. 2, pp. 685–690, Academic Press, NewYork, NY, USA, 1974.

[20] M. C. Abrahão, A. De Mello Gugliotta, R. Da Silva, R. J. Y. Fujieda, M. Boscolo, and E. Gomes, "Ligninolytic activity from newly isolated basidiomycete strains and effect of these enzymes on the azo dye orange II decolourisation," *Annals of Microbiology*, vol. 58, no. 3, pp. 427–432, 2008.

[21] R. Neelamegam, V. Baskaran, R. Dhanasekar, and T. Viruthagiri, "Decolourization of synthetic dyes using rice straw attached *Pleurotus ostreatus*," *Indian Journal of Chemical Technology*, vol. 11, no. 5, pp. 622–625, 2004.

[22] M. A. Pickard, H. Vandertol, R. Roman, and R. Vazquez-Duhalt, "High production of ligninolytic enzymes from white rot fungi in cereal bran liquid medium," *Canadian Journal of Microbiology*, vol. 45, no. 7, pp. 627–631, 1999.

[23] M. P. Singh, A. K. Pandey, S. K. Vishwakarma, A. K. Srivastava, and V. K. Pandey, "Extracellular Xylanase Production by *Pleurotus* species on Lignocellulosic Wastes under *in vivo* Condition using Novel Pretreatment," *Cellular and Molecular Biology*, vol. 58, no. 1, pp. 170–173, 2012.

[24] M. P. Singh, V. K. Pandey, A. K. Pandey, A. K. Srivastava, N. K. Vishwakarma, and V. K. Singh, "Production of xylanase by white rot fungi on wheat straw," *Asian Journal of Microbiology, Biotechnology and Environmental Sciences*, vol. 10, no. 4, pp. 859–862, 2008.

[25] T. Tsukihara, Y. Honda, R. Sakai, T. Watanabe, and T. Watanabe, "Mechanism for oxidation of high-molecular-weight substrates by a fungal versatile peroxidase, MnP^{2+}," *Applied and Environmental Microbiology*, vol. 74, no. 9, pp. 2873–2881, 2008.

[26] M. Hofrichter, "Review: lignin conversion by manganese peroxidase (MnP)," *Enzyme and Microbial Technology*, vol. 30, no. 4, pp. 454–466, 2002.

[27] M. L. Rabinovich, A. V. Bolobova, and L. G. Vasil'chenko, "Fungal decomposition of natural aromatic structures and xenobiotics: a review," *Applied Biochemistry and Microbiology*, vol. 40, no. 1, pp. 1–17, 2004.

[28] U. Meyer, "Biodegradation of synthetic organic colorants," *FEMS Symposium*, vol. 12, pp. 371–385, 1981.

[29] T. Suzuki, S. Timofei, L. Kurunczi, U. Dietze, and G. Schüürmann, "Correlation of aerobic biodegradability of sulfonated azo dyes with the chemical structure," *Chemosphere*, vol. 45, no. 1, pp. 1–9, 2001.

[30] A. Zille, T. Tzanov, G. M. Gübitz, and A. Cavaco-Paulo, "Immobilized laccase for decolourization of reactive Black 5 dyeing effluent," *Biotechnology Letters*, vol. 25, no. 17, pp. 1473–1477, 2003.

Hindawi Publishing Corporation
BioMed Research International
Volume 2013, Article ID 276524, 5 pages
http://dx.doi.org/10.1155/2013/276524

Research Article

Impact of Ciprofloxacin and Chloramphenicol on the Lipid Bilayer of *Staphylococcus aureus*: Changes in Membrane Potential

Paulina L. Páez, María C. Becerra, and Inés Albesa

Departamento de Farmacia, Facultad de Ciencias Químicas, Universidad Nacional de Córdoba, Haya de la Torre y Medina Allende, Ciudad Universitaria, IMBIV-CONICET, 5000 Córdoba, Argentina

Correspondence should be addressed to Paulina L. Páez; plpaez@fcq.unc.edu.ar

Received 18 March 2013; Revised 16 April 2013; Accepted 7 May 2013

Academic Editor: Afaf K. El-Ansary

The present study was undertaken to explore the interaction of ciprofloxacin and chloramphenicol with bacterial membranes in a sensitive and in a resistant strains of *Staphylococcus aureus* by using 1-anilino-8-naphthalene sulfonate (ANS). The binding of this probe to the cell membrane depends on the surface potential, which modulates the binding constant to the membrane. We observed that these antibiotics interacted with the bilayer, thus affecting the electrostatic surface potential. Alterations caused by antibiotics on the surface of the bacteria were accompanied by a reduction in the number of binding sites and an increase in the ANS dissociation constant in the sensitive strain, whereas in the ciprofloxacin-resistant strain no significant changes were detected. The changes seen in the electrostatic surface potential generated in the membrane of *S. aureus* by the antibiotics provide new aspects concerning their action on the bacterial cell.

1. Introduction

The plasmatic membrane is a chemoosmotic barrier that provides an interface between the organism and the environment. This bilayer presents an electrochemical potential (negative in the interior) which plays a basic role in the control of the exchange of solutes. Disturbances in the membrane potential can provide a rapid and sensitive indication of those stimuli that lead to physiological functionally important changes with respect to bacterial viability [1].

Fluorescent molecules have been extensively used as probes of biological membranes. These hydrophobic and amphiphilic probes are associated with membranes when added to cells or artificial systems, and their resultant fluorescence properties can be used to monitor a variety of membrane characteristics. In general, the addition of effectors results in the deenergization of cells, which leads to increased fluorescence from the probes present in the cell suspension, such as negatively charged 8-anilino-1-naphthalenesulfonate (ANS) [2].

ANS binding and fluorescence strongly respond to modulation of the surface potential, with the energy-dependent quenching being largely due to the generation of $\Delta\Psi$ and being accounted for by the movement of the anion across the membrane and from intramembrane sites in response to membrane potential [3].

It has been demonstrated that the determination of the membrane potential based on fluorochromes provides a useful and sensitive approximation for the monitoring of the cellular stresses in bacteria [4–6], since both oxidative and nitrosative stress are able to depolarize the plasmatic membrane [7].

The effect of the oxidative stress generated by reactive oxygen species (ROS) has been described as one of the most important sources of metabolic disturbance and the cellular damage. These agents are involved in the first important changes in the plasmatic membrane, and consequently at the beginning of cellular death [8–10].

Bacterial gyrase inhibitors, including synthetic quinolone antibiotics, induce a breakdown in iron regulatory dynamics, which promotes the formation of the ROS that contribute to cell death [11].

Bactericidal antibiotic killing mechanisms are currently attributed to the class of specific drug-target interactions.

However, the understanding of many of the bacterial responses that occur as a consequence of the primary drug-target interaction remains incomplete. It is known that oxidative stress in bacteria can be caused by exogenous agents that originate toxic effects, and our previous studies have shown that ciprofloxacin (CIP) and chloramphenicol (CMP), among others, can stimulate the induction of ROS in different bacterial species [12–16].

The aim of the present study was to explore the effects of clinically used antibiotics such as CIP and CMP on the lipid surface and to estimate the variation in the membrane potential in *Staphylococcus aureus* strains.

2. Materials and Methods

2.1. Susceptibility Determination. The antimicrobial activities of CIP and CMP were evaluated in two strains, one standard strain *S. aureus* ATCC 29213 and other clinical strain *S. aureus* by using the standard tube dilution method following the indications of the Clinical and Laboratory Standards Institute [17]. The strains were maintained by culture in trypticase soy broth (TSB) for 24 h at 37°C, and the minimum inhibitory concentration (MIC) was determined by using the standard tube dilution method. Cultures of 24 h in Mueller-Hinton medium were diluted to 10^6 CFU/mL, incubated for 10 min at 37°C, and then the antibiotics were added at different concentrations (0.125 μg/mL–512 μg/mL). Bacterial growth was observed at 24 h of incubation. MIC was determined as the lowest antibiotic concentrations at which growth was completely inhibited after overnight incubation of the tubes at 37°C. MICs were determined three times and the median values are taken.

2.2. ANS Binding Studies. Overnight cultures of *S. aureus* ATCC 29213 and clinical strain *S. aureus* were prepared in trypticase soy broth. Suspensions were centrifuged, and the pellets were resuspended in saline phosphate buffer (PBS) pH 7.4 at an optical density of 0.4 at 600 nm. Then, 50 μL of these suspensions was incubated with 256 μg/mL of CIP, 4 μg/mL of CMP, or without antibiotic (control) in a total volume of 1 mL in PBS.

The suspensions were centrifuged, and 1 mL of Triton 1% V/V in NaCl 10% was added to the pellet. Then, 20 μL of ANS 60 μM was added to 50 μL of bacterial suspensions and PBS to a total volume of 3 mL. The assay mixture for the standard curve consisted of 1 mL of bacterial suspensions and different concentrations of ANS, ranging from 0 to 120 μM. The structural changes on the membrane potential were studied by using L-anilino naphthalene-8-sulphonate as the fluorescent probe by the method of Verma et al. [18] and Robertson and Rottenberg [19]. The fluorescence emission was recorded on a Spectrofluorometer PTI (Photon Technology International) Model Quanta Master 2 QM2, with phosphorescence lifetime measurements taken at excitation and emission wavelengths of 360 nm and 516 nm, respectively. These experiments were performed at room temperature (23°C).

2.3. Measurement of K_d and n from ANS by Fluorescence Emission in Bacteria. The approach used to determine the dissociation constant (K_d) and the number of binding sites (n) from the fluorescence yield was as previously reported by Verma et al. [18] and Robertson and Rottenberg [19]. The fluorescence developed is recorded, and the data is plotted as the reciprocal of the fluorescence signal (arbitrary units) versus the reciprocal of the concentration of ANS. This produces a straight line whose extrapolation with the ordinate gives the reciprocal of the limiting fluorescence of ANS ($F_{\max}$). The number of binding sites for ANS was calculated by plotting the bound ANS per mg protein/free ANS versus bound ANS per mg protein.

2.4. Statistical Analysis. The assays were carried out at least in triplicate. Data were expressed as mean ± SD and analyzed by the Student's t-test. $P < 0.05$ was used as the level of statistical significance.

3. Results and Discussion

S. aureus ATCC 29213 exhibited sensitivity to CIP and CMP, with MICs of 0.5 μg/mL for CIP and 1 μg/mL for CMP. In addition, the clinical strain *S. aureus* MICs obtained were 32 μg/mL for CIP and 8 μg/mL for CMP; according to these results, the strain was resistant to CIP but sensitive to CMP. The fluorescence emission of ANS at 516 nm in the presence of 256 μg/mL of CIP, 4 μg/mL of CMP or in the absence of antibiotic was determined with *S. aureus* ATCC 29213 and clinical strain *S. aureus*.

Data were plotted as the reciprocal of the fluorescence signal (1/F) versus the reciprocal of the concentration of free ANS (1/ANS), as the reciprocal of the intercept gives the limit of the ANS fluorescence ($F_{\max}$), a parameter related to the maximum concentration of bound ANS. From the slope, the K_d was obtained from which the affinity of the fluorescent probe for binding sites on the bilayer could be inferred.

The values of bound ANS and free ANS were calculated from (1), where

$$\text{ANS bound (nmol)} = \frac{1/F_{\max}}{1/F} \times 100,$$
$$\text{ANS}_{\text{free}}\ \text{(nmol)} = \text{ANS}_{\text{total}} - \text{ANS}_{\text{bound}}. \quad (1)$$

The surface potential (Ψ) was calculated according to (2):

$$\Psi = 59 \log\left(F/F_o\right), \quad (2)$$

where F corresponds to the fluorescence in the presence of each antibiotic and F_o corresponds to the fluorescence obtained when $\Psi = 0$.

The change in membrane potential ($\Delta\Psi$) in the presence of antibiotic with respect to the control without antibiotic was obtained from the difference between Ψ with and without antibiotic (3):

$$\Delta\Psi = \Psi - \Psi_{\text{control}}. \quad (3)$$

The number of binding sites for ANS was calculated by using (4), in which the intercept represents the value of the

Table 1: Parameters obtained from the ANS binding studies in *S. aureus* ATCC 29213 and clinical strain *S. aureus*.

	F_{max}	K_d	n	Ψ (mV)	ΔΨ (mV)
S. aureus ATCC 29213 sensitive to CIP and CMP					
Control without antibiotic	143	251	603028	−306	—
Ciprofloxacin 256 μg/mL	70	927	52983	−406	−100
Chloramphenicol 4 μg/mL	62	846	48332	−331	−25
Clinical strain *S. aureus* resistant to CIP					
Control without antibiotic	77	902	45110	−287	—
Ciprofloxacin 256 μg/mL	77	937	46865	−302	−15

F_{max} is the fluorescence intensity (related to the maximum concentration of bound ANS), n is the number of binding sites of ANS to the membrane, K_d is the dissociation constant, Ψ is the potential at the surface of the membrane and ΔΨ is the change in surface potential of the membrane in the control without antibiotic.

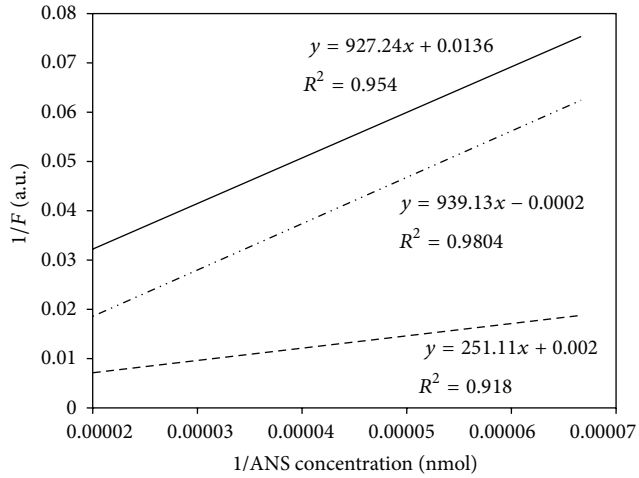

Figure 1: Scatchard plots of ANS interaction with *S. aureus* ATCC 29213 control (- - -), treated with ciprofloxacin (—) and treated with CMP (-···-).

reciprocal of q (a constant of proportionality), with the value of n being obtained from the slope (K_d/qn):

$$\frac{\text{ANS}_{\text{free}}}{F} = \frac{K_d}{qn} \times \frac{1}{[\text{bacteria}]} + \frac{1}{q}. \quad (4)$$

The same procedure was performed to determine the number of binding sites for ANS when the bacterial suspensions were incubated with the antibiotics studied, where a decrease in the number of binding sites for ANS with antibiotic would suggest changes in the cell surface.

Any alteration in the binding of ANS to the membrane of *S. aureus* in the presence of antibiotics was tested by a decrease in the number of binding sites for ANS compared with control. When ANS bounds to phospholipids, the fluorescence intensity increased with high concentrations of ANS. However, in the presence of CMP or CIP, the ANS fluorescence decreased, with this behavior reflecting competition between CMP and the ANS binding site that might have been located at the interface of the membrane. By comparing the values of K_d, we were able to infer that the affinity of the probe sites of the bilayer was affected by the two antibiotics. Moreover, differences in the values of the electric potentials indicated alterations in the bacterial membranes.

The fluorescence of ANS emission was determined at 516 nm in the presence of CIP and CMP and in the absence of antibiotic. The data were plotted as the reciprocal of the fluorescence signal ($1/F$) versus the reciprocal of the concentration of ANS (1/ANS) (Figure 1). There was a linear relationship between fluorescence and the inverse of the concentration of bound ANS, revealing a change in the affinity of the membrane in the presence of antibiotic with respect to control.

Table 1 shows the parameters obtained with CMP and CIP for the surface potential in the absence or presence of the antibiotics in the *S. aureus* ATCC 29213 and clinical strain *S. aureus*.

Whereas the value of F_{max} was reduced twofold and the number of binding sites decreased elevenfold, the K_d value was increased fourfold, compared to the control without antibiotic in *S. aureus* ATCC 29213 (sensitive to CIP). In clinical strain *S. aureus* (resistant to CIP) there were no significant changes in F_{max}, number of binding sites, or the K_d value. The baseline value of Ψ in the sensitive strain was −306 mV, while in the resistant strain this was −287 mV. The ΔΨ was almost seventimes higher in the sensitive strain (100 mV) than in the resistant one (15 mV). CIP, a bactericidal antibiotic, reduced this value by 33% in the sensitive strain, while the reduction in the resistant one was only 5%. Finally, CMP, a bacteriostatic antibiotic, increased the membrane potential by about 11% in the sensitive strain.

The membrane potential is an important parameter that controls various cellular processes. It is a sensitive indicator of energy status and cell viability, with membrane depolarization leading to excessive production of ROS which is an indication of an advance in cellular dysfunction and precedes many other signs of cellular injury. A reduction in the potential also provides information about the feasibility of transferring an electron "*in vivo*." In addition, the catalytic production of oxidative stress from the redox cycle is a possible mode of action of antibiotics, because it could indicate interference with the electron transport chain [20, 21].

The changes in the electric potential obtained in the present work showed alterations in the bacterial membrane of *S. aureus* in the presence of CMP and CIP. Furthermore, changes caused by antibiotics on the surface of the bacteria were demonstrated by a reduction in the number of binding sites of the fluorescent probe and an increase in the ANS dissociation constant.

Montero et al. established that CIP interacts with neutral and charged membranes at the surface level (headgroup region). They also postulated that this could be part of the mechanism of entry of the 6-fluoroquinolones through the cytoplasmic membrane [3]. Ciprofloxacin is a widely used antimicrobial agent against Gram positive and Gram negative, but there are conflicting reports about the effect of CIP on the bacterial membrane [22, 23].

There are previous results on *S. aureus*, with liposomes of *E. coli* showing interaction of ANS with a lipid bilayer and in

the presence of 6-FQs as a result of a reduction in the maximum concentration of the ANS bound to liposomes [24–27]. However, there are no comparisons reported between sensitive and resistant strains in the presence of antibiotics.

The present results demonstrated that the strains had a particular behavior in the presence of each antibiotic, an effect that was manifested by the differences obtained in the bacterial membrane potential. Moreover, on comparing the sensitive strain with the resistant one, a higher alteration in the membrane potential was observed in sensitive bacterium that was associated with the effect of the antibiotic [20, 21].

4. Conclusions

In our previous reports, we demonstrated that CIP and CMP induce oxidative stress in *S. aureus* strains, with sensitive clinical strains producing higher ROS levels than resistant ones [12–15]. The present work shows that these antibiotics had an impact on the lipid bilayer, leading to significant membrane potential changes in *S. aureus* sensitive to ciprofloxacin. These observations can be added to the mechanism of action previously described for the antibiotics investigated, with the changes generated in the lipid bilayers of *S. aureus* contributing new aspects about the action of these antibiotics on the bacterial cell.

Authors' Contribution

Paulina L. Páez and María C. Becerra contribute equally to this work.

Acknowledgments

The authors thank Dr. Gerardo Argüello (Departamento de Físicoquímica, Facultad de Ciencias Químicas, UNC, INFIQC-CONICET) for assistance with the fluorescence measurements. The authors thank Consejo Nacional de Investigaciones Científicas y Técnicas de Argentina (CONICET), Secretaría de Ciencia y Técnica de la Universidad Nacional de Córdoba (SECyT) for financial support. We thank native English speaker Dr. Paul Hobson for revision of this manuscript. Paulina L. Páez and María C. Becerra are members of the Research Career of CONICET.

References

[1] F. David, M. Hebeisen, G. Schade, E. Franco-Lara, and M. Di Berardino, "Viability and membrane potential analysis of *Bacillus megaterium* cells by impedance flow cytometry," *Biotechnology & Bioengineering*, vol. 109, no. 2, pp. 483–492, 2012.

[2] M. K. Wolf and J. Konisky, "Increased binding of a hydrophobic, photolabile probe to *Escherichia coli* inversely correlates to membrane potential but not adenosine 5'-triphosphate levels," *Journal of Bacteriology*, vol. 145, no. 1, pp. 341–347, 1981.

[3] M. T. Montero, M. Pijoan, S. Merino-Montero, T. Vinuesa, and J. Hernández-Borrell, "Interfacial membrane effects of fluoroquinolones as revealed by a combination of fluorescence binding experiments and atomic force microscopy observations," *Langmuir*, vol. 22, no. 18, pp. 7574–7578, 2006.

[4] M. G. Dinsdale, D. Lloyd, and B. Jarvis, "Yeast vitality during cider fermentation: two approaches to the measurement of membrane potential," *Journal of the Institute of Brewing*, vol. 101, no. 6, pp. 453–458, 1995.

[5] D. J. Mason, R. Allman, J. M. Stark, and D. Lloyd, "Rapid estimation of bacterial antibiotic susceptibility with flow cytometry," *Journal of Microscopy*, vol. 176, no. 1, pp. 8–16, 1994.

[6] D. Lloyd, D. J. Mason, and M. T. E. Suller, "Microbial infections," in *Cytometric Analysis of Cell Phenotype and Function*, D. A. McCarthy and M. G. Macey, Eds., pp. 2982–3213, Cambridge University Press, Cambridge, UK, 1st edition, 2001.

[7] D. Lloyd, J. C. Harris, G. A. Biagini et al., "The plasma membrane of microaerophilic protitsts: oxidative and nitrosative stress," *Microbiology*, vol. 150, no. 5, pp. 1183–1190, 2004.

[8] J. A. Scott and C. A. Rabito, "Oxygen radicals and plasma membrane potential," *Free Radical Biology and Medicine*, vol. 5, no. 4, pp. 237–246, 1988.

[9] M. Kayahara, U. Felderhoff, J. Pocock, M. N. Hughes, and H. Mehmet, "Nitric oxide (NO) and the nitrosonium cation (NO^+) reduce mitochondrial membrane potential and trigger apoptosis in neuronal PC12 cells," *Biochemical Society Transactions*, vol. 26, no. 4, p. S340, 1998.

[10] D. Lloyd, J. C. Harris, S. Maroulis et al., "Nitrosative stress induced cytotoxicity in *Giardia intestinalis*," *Journal of Applied Microbiology*, vol. 95, no. 3, pp. 576–583, 2003.

[11] M. A. Kohanski, D. J. Dwyer, B. Hayete, C. A. Lawrence, and J. J. Collins, "A common mechanism of cellular death induced by bactericidal antibiotics," *Cell*, vol. 130, no. 5, pp. 797–810, 2007.

[12] I. Albesa, M. C. Becerra, P. C. Battán, and P. L. Páez, "Oxidative stress involved in the antibacterial action of different antibiotics," *Biochemical and Biophysical Research Communications*, vol. 317, no. 2, pp. 605–609, 2004.

[13] M. C. Becerra, P. L. Páez, L. E. Laróvere, and I. Albesa, "Lipids and DNA oxidation in *Staphylococcus aureus* as a consequence of oxidative stress generated by ciprofloxacin," *Molecular and Cellular Biochemistry*, vol. 285, no. 1-2, pp. 29–34, 2006.

[14] P. L. Páez, M. C. Becerra, and I. Albesa, "Antioxidative mechanisms protect resistant strains of *Staphylococcus aureus* against ciprofloxacin oxidative damage," *Fundamental and Clinical Pharmacology*, vol. 24, no. 6, pp. 771–776, 2010.

[15] V. Aiassa, A. I. Barnes, and I. Albesa, "Resistance to ciprofloxacin by enhancement of antioxidant defenses in biofilm and planktonic *Proteus mirabilis*," *Biochemical and Biophysical Research Communications*, vol. 393, no. 1, pp. 84–88, 2010.

[16] P. L. P. Páez, M. C. Becerra, and I. Albesa, "Comparison of macromolecular oxidation by reactive oxygen species in three bacterial genera exposed to different antibiotics," *Cell Biochemistry and Biophysics*, vol. 61, no. 3, pp. 467–472, 2011.

[17] Clinical and Laboratory Standards Institute, Performance standards for antimicrobial susceptibility testing, 18th informational supplement, Clinical and Laboratory Standards Institute), p. approved standard M100-S18, Clinical and Laboratory Standards Institute, Wayne, Pennsylvania, 2008.

[18] I. Verma, A. Rohilla, and G. K. Khuller, "Alterations in macromolecular composition and cell wall integrity by ciprofloxacin in *Mycobacterium smegmatis*," *Letters in Applied Microbiology*, vol. 29, no. 2, pp. 113–117, 1999.

[19] D. E. Robertson and H. Rottenberg, "Membrane potential and surface potential in mitochondria. Fluorescence and binding

of 1-anilinonaphthalene-8-sulfonate," *The Journal of Biological Chemistry*, vol. 258, no. 18, pp. 11039–11048, 1983.

[20] N. Zamzami, T. Hirsch, B. Dallaporta, P. X. Petit, and G. Kroemer, "Mitochondrial implication in accidental and programmed cell death: apoptosis and necrosis," *Journal of Bioenergetics and Biomembranes*, vol. 29, no. 2, pp. 185–193, 1997.

[21] A. V. Gyulkhandanyan, C. J. Feeney, and P. S. Pennefather, "Modulation of mitochondrial membrane potential and reactive oxygen species production by copper in astrocytes," *Journal of Neurochemistry*, vol. 87, no. 2, pp. 448–460, 2003.

[22] A. Dalhoff, "Interaction of aminoglycosides and ciprofloxacin with bacterial membrane," in *The Influence of Antibiotics on the Host Parasite Relationship*, H. Adam, W. Hahn, and W. Opferkuch, Eds., pp. 16–27, Springer, Berlin, Germany, 1985.

[23] C. S. Lewin, B. M. A. Howard, and J. T. Smith, "Protein- and RNA-synthesis independent bactericidal activity of ciprofloxacin that involves the a subunit of DNA gyrase," *Journal of Medical Microbiology*, vol. 34, no. 1, pp. 19–22, 1991.

[24] S. Merino, J. L. Vázquez, O. Domènech et al., "Fluoroquinolone-biomembrane interaction at the DPPC/PG lipid-bilayer interface," *Langmuir*, vol. 18, no. 8, pp. 3288–3292, 2002.

[25] J. L. Vázquez, M. T. Montero, S. Merino et al., "Location and nature of the surface membrane binding site of ciprofloxacin: a fluorescence study," *Langmuir*, vol. 17, no. 4, pp. 1009–1014, 2001.

[26] A. Grancelli, A. Morros, M. E. Cabañas et al., "Interaction of 6-fluoroquinolones with dipalmitoylphosphatidylcholine monolayers and liposomes," *Langmuir*, vol. 18, pp. 9177–9182, 2002.

[27] O. Domenech, Y. F. Dufrêne, F. Van Bambeke, P. M. Tukens, and M. P. Mingeot-Leclercq, "Interactions of oritavancin, a new semi-synthetic lipoglycopeptide, with lipids extracted from *Staphylococcus aureus*," *Biochimica et Biophysica Acta*, vol. 1798, no. 10, pp. 1876–1885, 2010.